

In vitro characterization of meiotic
recombination with a special focus on
Mer3 helicase

Dissertation

der Mathematisch-Naturwissenschaftlichen Fakultät

der Eberhard Karls Universität Tübingen

zur Erlangung des Grades eines

Doktors der Naturwissenschaften

(Dr. rer. Nat.)

vorgelegt von

Magdalena Firlej

aus Bielsko-Biała, Polen

Tübingen

2022

Gedruckt mit Genehmigung der Mathematisch-Naturwissenschaftlichen
Fakultät der Eberhard Karls Universität Tübingen

Tag der mündlichen Qualifikation:	24.08.2022
Dekan:	Prof. Dr. Thilo Stehle
1. Berichterstatter:	Dr. John Weir
2. Berichterstatter:	Prof. Dr. Ralf Jansen

Summary

Sexually reproducing organisms produce haploid gametes to pass their genetic information to other organisms as a means of producing offspring. To produce gametes, organisms developed a special type of cell division - meiosis. Meiotic cell division not only reduces the number of chromosomes by half, but also creates new allele combinations via segregation of homologous chromosomes as well as chromosome recombination. Homologous recombination must be carefully regulated to assure accurate chromosome segregation. This includes the formation of connections between the chromosomes as a part of the crossover formation process. Crossovers arise as a result of the double-strand break repair and are only one of the possible break repair outcomes. Although it is not precisely known how the decision is made, we know that some proteins promote and some prevent crossover formation.

In my project, I focused on one of the crossover formation promoting proteins - the *S. cerevisiae* helicase Mer3 (HFM1 in mammals). Mer3 helicase is a member of the ZMM group of proteins that facilitates the formation of class I crossovers during meiosis. I studied the biochemical and structural characteristics of this protein and its interaction with other proteins participating in meiotic recombination. Using multiple methodological approaches, I characterized in more detail the previously described interaction with the Mlh1/Mlh2 complex. I also studied the newly discovered interaction with the recombination-regulating factors Top3 and Rmi1. Top3 and Rmi1 are a part of the Sgs1/Top3/Rmi1 complex, which acts to untangle a variety of other DNA recombination intermediates and acts against crossover formation. The results of my studies are summarized in Chapter 2, "Integrated structural study of the Mer3 helicase reveals a novel role in promoting meiotic crossovers", which is also a manuscript prepared for submission.

In Chapter 3, I explore the current knowledge about meiotic helicases, their interaction partners, and the role of regulatory modifications during meiosis I. I also focus on the molecular structure and mechanisms of these helicases.

The fourth chapter includes the manuscript published in 2020 – "Biochemical and functional characterization of a meiosis-specific Pch2/ORC AAA+ assembly". The paper includes my *in vitro* analysis, which provided biochemical insights into our knowledge about the interaction between Pch2 and the ORC complex.

During my doctorate, I also aimed to solve the Mer3 structure using different experimental techniques: crystallization and CryoEM. Although these experiments did not result in solving the structure of Mer3, I include this part of my project in my thesis together with other important preliminary data. The outcome of these experiments, due to their potential, may be the basis for future research projects.

Taken together, my results lead to a better understanding of the roles of the proteins involved in the regulation of meiotic cell division and will be a solid base for future work that can reveal the complete chain of events that happen during the meiotic division.

Zusammenfassung

Sexuell reproduzierende Organismen produzieren haploide Gameten, um ihre genetische Information an andere Organismen weiterzugeben und Nachkommen zu erzeugen. Um Gameten zu produzieren, haben Organismen eine spezielle Art der Zellteilung entwickelt - die Meiose. Die meiotische Zellteilung reduziert nicht nur die Anzahl der Chromosomen um die Hälfte, sondern schafft auch neue Allelkombinationen durch Segregation homologer Chromosomen, sowie durch Chromosomenrekombination. Die homologe Rekombination muss sorgfältig reguliert werden, um eine genaue Chromosomentrennung sicherzustellen. Dazu gehört die Bildung von Verbindungen zwischen den Chromosomen, die ein Ergebnis des Crossover-Bildungsprozesses sind. Überkreuzungen entstehen als Ergebnis der Doppelstrangbruchreparatur. Crossovers sind nur eines der möglichen Ergebnisse der Reparatur von Unterbrechungen. Obwohl nicht genau bekannt ist wie die Entscheidung getroffen wird, wissen wir, dass einige Proteine die Crossover-Bildung fördern und andere verhindern.

In meinem Projekt konzentrierte ich mich auf eines der die Crossover-Bildung fördernden Proteine – die *S. cerevisiae*-Helikase Mer3 (HFM1 bei Säugetieren). Die Mer3-Helikase ist ein Mitglied der ZMM-Proteingruppe, welche die Bildung von Klasse-I-Crossovers während der Meiose erleichtert. Ich untersuchte die biochemischen und strukturellen Eigenschaften dieses Proteins und seine Wechselwirkung mit anderen Proteinen, die an der meiotischen Rekombination beteiligt sind. Mit mehreren methodischen Ansätzen habe ich die zuvor beschriebene Interaktion mit dem Mlh1/Mlh2-Komplex näher charakterisiert. Ich habe auch die neu entdeckte Interaktion mit den rekombinationsregulierenden Faktoren Top3 und Rmi1 untersucht. Top3 und Rmi1 sind Teil des Sgs1/Top3/Rmi1-Komplexes, der eine Vielzahl anderer Zwischenprodukte der DNA-Rekombination entwirrt und der Crossover-Bildung entgegenwirkt. Die Ergebnisse meiner Studien sind in Kapitel 2 zusammengefasst, welches auch ein zur Einreichung vorbereitetes Manuskript ist. Im dritten Kapitel untersuche ich den aktuellen Wissensstand über meiotische Helikasen, ihre Interaktionspartner und die Rolle regulatorischer Modifikationen während der Meiose I. Ich fokussiere mich dabei auch auf die molekulare Struktur und die Mechanismen dieser Helikasen. Das vierte Kapitel umfasst das 2020 veröffentlichte Manuskript „Biochemical and functional characterization of a meiosis-specific Pch2/ORC AAA+ assembly“. Das Papier enthält meine In-vitro-Analyse, die biochemische Einblicke in unser Wissen über die Wechselwirkung zwischen Pch2 und dem ORC-Komplex lieferte.

Während meiner Promotion arbeitete ich auch daran die Mer3-Struktur mit verschiedenen experimentellen Techniken zu lösen: Kristallisation und CryoEM. Obwohl diese Experimente nicht zur Lösung der Struktur von Mer3 führten, beschreibe ich diesen Teil meines Projekts zusammen mit anderen wichtigen vorläufigen Daten in meiner Doktorarbeit.

Zusammengenommen führen meine Ergebnisse zu einem besseren Verständnis der Rollen der an der Regulation der meiotischen Zellteilung beteiligten Proteine und stellen eine solide Grundlage für zukünftige Arbeiten dar, welche die vollständige Kette von Ereignissen aufdecken können, die während der meiotischen Teilung stattfinden.

Acknowledgments

Here I would like to acknowledge a few of the many people who have helped me during my doctorate work and the thesis writing process.

Firstly, I would like to thank my supervisor, John Weir. John, your enthusiasm about meiosis and science in general was very infectious. The details of meiosis that you could share with me surprised me till the very last day of my work. This, combined with your empathy made you the best possible supervisor.

The second most important person was Veronika Altmannová. Without you, the project wouldn't be half as top-class as it is now. You are also one of the most honest and selfless people I have met here. I was very lucky to have you as my project partner.

Next, I would like to thank my students, Rahel Rauleder and Andreas Schäffler. Rahel was one of the most hard-working students I have ever met, but it is her kindness and optimism that we will all remember her for. She was the sunshine in the pandemic times. Andy, who was my first long-term student, was a very fun person to work with but at the same time, he always had some good ideas. While having him as my student I also gained some confidence as a scientist, which helped me during my future work.

I would also like to thank Felipe Merino and Katharina Hipp for their help with my Cryo-EM experiments. Thanks to their great experience and willingness to share their knowledge, I have learned the method that I have always wanted to learn, and I have never thought I will be able to simply use this microscope all by myself.

Of course, I would not have done as well as I did without my TAC - Oliver Weichenrieder, Ralf Jansen, and Felicity Jones. Although we only met occasionally during my TAC meetings, I always felt that you are here to support me and whenever we met you always had some great advice. I could not have chosen better.

I would also like to acknowledge a very special lab member, Dorota Rousová, who started her work as a PhD student in our group at the same time as I did, and together, we faced all the light and dark sides of the scientific world. Thank you. I cannot even imagine how it would be if we wouldn't have found each other here.

I want to thank my friends and family for all their support and believing in me (even when I did not). Having people who are cheering for you no matter what gave me the extra power to keep going.

Finally, I would like to thank my partner, Marvin. He is the person who supports me in everything I do and helped me a lot at the final stage of my thesis when I needed to push myself and put everything to paper. Thank you so much for helping me reach the finish line.

Table of Contents

1. Introduction	1
1.1. The history of meiosis	1
1.2. The power of sexual reproduction	1
1.3. Mitosis vs meiosis	1
1.4. Meiotic know-how	2
1.5. The role of the Pch2 protein in the pachytene checkpoint	3
1.6. The perfect balance in meiotic crossover formation	4
1.7. Meiotic decision making	5
1.8. Pro-crossover proteins	6
1.9. The ZMM proteins and Mer3	7
1.10. Anti-crossover proteins	8
1.11. Decision making in meiosis is highly regulated by meiotic helicases	8
1.12. Aims of this thesis	9
2. Integrated structural study of the Mer3 helicase reveals a novel role in promoting meiotic crossovers	11
Abstract	11
2.1. Introduction	12
2.2. Results	14
2.2.1. Biochemical activity of Mer3	14
2.2.2. Hybrid structural analysis of Mer3	15
2.2.3. Biophysical and structural analysis of Mer3 interaction with Mlh1 and Mlh2	17
2.2.4. Mer3 interacts with the Top3/Rmi1 complex	21
2.2.5. Mer3 interaction with Mlh1/Mlh2 is compatible with Top3/Rmi1 binding and together they are forming a 5-subunit complex	24
2.2.6. Mer3 and Sgs1 are competing for binding to the Top3/Rmi1 complex	25
2.2.7. Mer3 inhibits D-loop dissolution mediated by the Sgs1/Top3/Rmi1 complex	26
2.3. Discussion	28
2.4. Methods	32
2.4.1. Plasmids	32
2.4.2. Protein purification	32
2.4.3. Mass Photometry	37
2.4.4. DNA substrates	38
2.4.5. Electrophoretic mobility shift assays	38

2.4.6. Strand separation assays	38
2.4.7. Crosslinking Mass Spectrometry (XL-MS).....	38
2.4.8. Biacore interactions	39
2.4.9. SEC-MALS.....	39
2.4.10. AlphaFold2.....	39
2.4.11. Pull-down assays	40
2.4.12. Microscale thermophoresis (MST)	41
2.4.13. D-loop assay	41
2.4.14. Yeast strains	42
2.4.15. Yeast two-hybrid assay.....	42
2.4.16. Meiotic time course	42
2.4.17. In vivo co-immunoprecipitation	42
Acknowledgments.....	43
References.....	43
Supplementary Figures	48
Supplementary Tables.....	52
3. Unwinding during stressful times - mechanisms of helicases in meiotic recombination ...	55
Abstract	55
3.1. Introduction	56
3.2. Architecture and mechanism of nucleic acid helicases	56
3.3. Meiotic Recombination.....	57
3.4. Helicases and Meiotic Recombination.....	59
3.4.1. Formation of meiotic DSB breaks.....	59
3.4.2. Break resection.....	60
3.4.3. Presynaptic filament formation	61
3.4.4. Interhomolog bias	62
3.4.5. D-loop formation.....	64
3.4.6. Crossover decision.....	67
3.5. Summary	70
Acknowledgements.....	70
References.....	70
4. Biochemical and functional characterization of a meiosis-specific Pch2/ORC AAA+ assembly.....	83
5. Preliminary results	103

5.1. Mer3 crystallization attempts.....	103
5.2. Mer3 Cryo-EM studies	107
5.3. Mer3 interacts not only with the Top3/Rmi1 and the Mlh1/Mlh2 complex but also with Dmc1	113
5.4. Mer3 activity on DNA-RNA hybrids.....	116
5.5. Zip2/Zip4/Spo16 complex interacts with Msh4/Msh5 complex.....	117
6. Outlook.....	119
6.1. The importance of the future structural studies of the Mer3 helicase	119
6.2. Role of the zinc finger	120
6.3. Mer3 - playing solo or in a duet?	120
6.4. What about the “helicase” part in the Mer3 helicase	121
6.5. The role of phosphorylation in mediating protein-protein interaction.....	122
6.6. Partners or competitors? – the cooperativity of Mer3 binding to Mlh1/Mlh2 and Top3/Rmi1 complexes	122
6.7. Other ZMM proteins as potential players in protecting the crossover intermediate from the STR activity.....	123
6.8. The conservation of the Mer3/Top3/Rmi1 interaction in mammals	123
6.9. The importance of understanding the mechanisms in the context of fertility and cancer	124
7. Concluding remarks.....	125
Bibliography.....	127
Introduction	127
Preliminary results	135
Outlook.....	143

Figures and Tables

Figures

Figure 1.1. Meiotic division	2
Figure 1.2. Homologous recombination.....	4
Figure 2.1. Biochemical activity of Mer3.....	15
Figure 2.2. Structural analysis of Mer3	17
Figure 2.3. Biophysical and structural analysis of the interaction between Mer3 and the Mlh1/Mlh2 complex	20
Figure 2.4. Mer3 interacts with the Top3/Rmi1 complex.....	23
Figure 2.5. Mer3 interaction with Mlh1/Mlh2 is compatible with Top3/Rmi1 binding and together they are forming a 5-subunit complex.....	25
Figure 2.6. Mer3 and Sgs1 are competing for binding to the Top3/Rmi1 complex.....	27
Figure 3.1. Structural overview of helicases involved in meiotic recombination.	58
Figure 3.2. Mechanisms of nucleic acid helicases in meiosis.....	69
Figure 5.1. Biochemical domain composition of Mer3 constructs used in my experiments.....	103
Figure 5.2. Proteoplex screen graphs.....	104
Figure 5.3. Juxtaposition of two EMSA experiments using a 3' overhang as a substrate.....	104
Figure 5.4. Images of best drops from the optimization screens	106
Figure 5.5. Mer3 Cryo-EM images taken on grids frozen in selected conditions	110
Figure 5.6. Mer3 class averages	113
Figure 5.7. Mer3/Top2/Rmi1/Mlh1/Mlh1/Dmc1/Zip1 in vitro interaction experiments	115
Figure 5.8. Biochemical activity of Mer3 on DNA-DNA and DNA-RNA hybrids	117
Figure 5.9. In vitro pull-down of Msh4/Msh5 complex on ZZS complex	118

Supplementary Figures

Supplementary Figure 2.1. Biochemical activity of Mer3	48
Supplementary Figure 2.2. Structural analysis of Mer3.....	49
Supplementary Figure 2.3. Biophysical and structural analysis of the interaction between Mer3 and the Mlh1/Mlh2 complex.....	50
Supplementary Figure 2.4. Mer3 interacts with the Top3/Rmi1 complex	51
Supplementary Figure 2.5. Mer3 interaction with Mlh1/Mlh2 is compatible with Top3/Rmi1 binding and together they are forming a 5-subunit complex.....	51

Tables

Table 1.1. List of meiotic pro- or anti-crossover proteins in <i>S. cerevisiae</i> and their mammalian homologs	6
Table 3.1. General characteristics of helicases involved in meiotic recombination	66
Table 5.1. Selected conditions under which the signs of crystallization were observed.....	105
Table 5.2. List of tested crystallization conditions including protein constructs, buffer conditions, additives, and screen names.	107
Table 5.3. List of tested conditions including protein constructs, buffer conditions, additives, and blotting conditions	112

Supplementary Tables

Supplementary Table 2.1. Plasmids used in the study.....	52
Supplementary Table 2.2. Yeast strains used in the study	53
Supplementary Table 2.3. Crosslinking distances within the Mer3 structure based on the AlphaFold2 prediction	53
Supplementary Table 2.4. Crosslinking distances within the ATPase and Transducer domains of the Mlh1/Mlh2 complex structure based on the AlphaFold2 prediction	54
Supplementary Table 2.5. Crosslinking distances within the Top3/Rmi1 complex structure based on the AlphaFold2 prediction.....	54

Abbreviations

aa	amino acid
AEBSF	4-(2-aminoethyl) benzenesulfonyl fluoride hydrochloride
ATP	adenosine triphosphate
BME	β -mercaptoethanol
bp	base pair
BS3	Bis(sulfosuccinimidyl)suberat
BSA	bovine serum albumin
CO	crossover
CV	column volume
dHJ	double Holliday junction
DSB	DNA double-strand break
DSBU	disuccinimidyl dibutyric urea
D-loop	displacement loop
EDTA	ethylenediaminetetraacetic acid
EM	electron microscopy
EMSA	electrophoretic mobility shift assay
ES	expression system
GST	glutathione S-transferase
HEPES	4-(2-hydroxyethyl)1-piperazineethanesulfonic acid
IEX	ion-exchange chromatography
IPTG	isopropyl-beta-D-thiogalactopyranosid
KD	dissociation constant
LB	lysogeny broth
MALS	multi-angle light scattering
MBP	maltose-binding protein
MES	2-(N-morpholino)ethanesulfonic acid
MST	microscale thermophoresis
NCO	non-crossover
OD	optical density
ON	overnight
PAGE	polyacrylamide gel electrophoresis
PBS	phosphate-buffered saline
PEG	polyethylene glycol
RT	room temperature
SC	synaptonemal complex
SDS	sodium dodecyl sulfate
SDSA	synthesis-dependent strand annealing
SEC	size-exclusion chromatography
SPR	surface plasmon resonance
ssDNA	single-stranded DNA
Strep	streptavidin
TAE	Tris, acetic acid, EDTA buffer

TB	terrific broth
TBE	Tris, boric acid, EDTA buffer
TCEP	Tris(2-carboxyethyl)phosphine
Tris	Tris(hydroxyethyl)aminomethane
XL-MS	crosslinking mass spectrometry
Y2H	yeast two-hybrid assay
ZMM	an acronym for <u>Z</u> ip1–4, <u>M</u> sh4–5, <u>M</u> er3, Spo16
ZZS	Zip2-Zip4-Spo16 complex

1. Introduction

1.1. The history of meiosis

In 1883, the Belgian cytologist and embryologist Édouard Van Beneden observed for the very first time that the germ cells are haploid (i.e. containing only half the number of the somatic cells) and that the diploid state is restrained after the fertilization. Following this observation, August Weismann hypothesized that some alternative, reductive cell division during the sexual life cycle must exist. In 1905, Farmer and Moore introduced the term meiosis (Greek *meioun*, meaning “to make smaller”). Since then, meiosis has been extensively studied. However, many of its “mysteries” still puzzle new generations of scientists.

Meiosis reduces the chromosome count by half to ensure the same number of chromosomes in the offspring as in their parents, and - thanks to the high-frequency genetic exchange events - it contributes to the increase of genetic diversity.

1.2. The power of sexual reproduction

Due to its ability to recombine the genomes, sexual reproduction has proven to be a successful strategy of organismal adaptation to the changing environment (Bell, 1982). Genome recombination increases the genetic diversity and accelerates the evolution through the quick incorporation of advantageous mutations and the fast removal of deleterious mutations (Siller, 2001). This happens as a result of repairing double-strand breaks using the homologous chromosome as a repair template instead of the sister chromatid.

1.3. Mitosis vs meiosis

In meiosis (Figure 1.1), a single round of DNA replication is followed by two consecutive rounds of chromosome segregation. Homologous chromosomes segregate to the opposite poles at meiosis I. After that, analogously to mitosis, the sister chromatids separate to the opposite poles. While the second meiotic division resembles mitosis, the first division is unique to meiosis. One of the key differences between meiosis I and mitosis is the recombination between the homologs. During mitosis, sisters frequently undergo recombination to repair double-strand breaks with no genetic consequences. The rare cases when repair occurs between homologs hardly ever result in crossing-over. By avoiding inter-homolog repair,

meiotic cells protect themselves from loss of heterozygosity. The resulting crossover in concert with cohesive cohesin between sister chromatids provides connections (cytologically seen as chiasmata) that hold homologs together until the homologous chromosomes can be separated towards opposite ends of the cell. These links resist the pulling force of the microtubule-based spindle and allow the homologous chromosomes to orient towards opposite poles of the meiosis I spindle (Moore & Orr-Weaver, 1998). Any errors in this process, particularly failure to assure crossover formation, may result in infertility and birth defects (such as Trisomy 21) (Hassold et al., 2007). To assure a suitable crossover outcome, each intermediate state of meiotic recombination is highly controlled and regulated by a complex action of the meiotic proteins machinery.

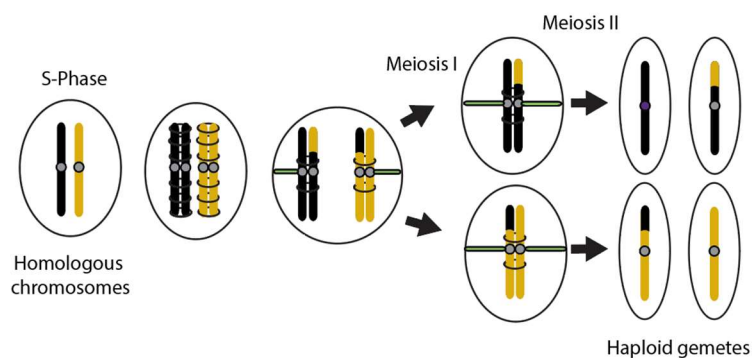


Figure 1.1. Meiotic division

1.4. Meiotic know-how

Although it is still unclear when exactly meiotic recombination (Figure 1.2) begins, one of the earliest steps is the highly controlled introduction of double-strand breaks (DSB). The DSBs are created by the endonuclease Spo11 (Keeney, 2008) and they are mainly formed at DSB hotspots, which are permissive regions where breaks are preferentially formed. Subsequently, the ends of the breaks are resected and 3' single-stranded tails are generated (average resection length in baker's yeast meiosis is ~1.1 kb, (Brick et al., 2020)). Tails are protected by the replication protein A (RPA). To locate the correct repair template to repair the breaks by homologous recombination, cells rely on recombinases Rad51 and meiosis-specific Dmc1. Recombinases are primary effectors of the "homology-searching tentacle" (Kim et al., 2010). It is not yet clear why most of the known eukaryotic organisms require two RecA recombinases homologs to assure accurate recombination during meiosis. They both may cooperate, since both proteins co-localize during meiotic recombination (Masson & West, 2001). One of the

explanations is that Dmc1 has higher tolerance of DNA mismatches than Rad51, which is likely essential for recombination between homologous chromosomes with polymorphic sequences (Borgogno et al., 2016). As a result of homology search and the ssDNA invasion on the opposite strand, a displacement loop (D-loop) is formed (Szostak et al., 1983). If the invading strand is not stabilized enough to proceed to the next stage, the break is repaired via synthesis-dependent strand annealing (SDSA). If the intermediate is stabilized (single-end invasion (SEI)) (Hunter & Kleckner, 2001), the other resected end is incorporated into the structure and a stable double Holliday junction (dHJ) is formed (Schwacha & Kleckner, 1995). The dHJ intermediate can be resolved into NCOs in a dissolution process. Dissolution is hypothesized to be an effect of Sgs1 helicase-driven inward migration of Holliday junctions and the activity of the Top3/Rmi1 complex, which decatenates the DNA structure (Bizard & Hickson, 2014). Alternatively, a dHJ intermediate can be resolved by cleavage of the dHJ to produce either COs or NCOs, depending on the cleavage at the two junctions (Allers & Lichten, 2001; Szostak et al., 1983). The Sgs1/Top3/Rmi1 complex acts to untangle not only dHJ, but also a variety of other DNA recombination intermediates (Cejka & Kowalczykowski, 2010).

If Double-Holliday junctions are resolved as crossovers, this results in the exchange of DNA sequences between homologs. The exchange of fragments together with the virtue of cohesion between sister chromatids provides physical linkage between the homologs. Cohesion along the chromosome arms is not released until anaphase I, when homologs are ready to separate to the opposite spindle poles (Klein et al., 1999; Watanabe & Nurse, 1999).

1.5. The role of the Pch2 protein in the pachytene checkpoint

Defects in the early meiotic events may lead to cell cycle arrest or even to apoptosis. The early meiotic events are monitored by a “pachytene checkpoint”, which reacts to the homolog synapsis and recombination defects (Roeder & Bailis, 2000). One of the proteins performing important functions during the cell cycle control, recombination, and chromosome morphogenesis is the widely conserved AAA+ ATPase Pch2 (for Pachytene Checkpoint 2). Pch2 is involved in diverse aspects of meiosis such as cell cycle checkpoint function, local DSB activity, CO formation, and chromosome morphogenesis (Cardoso da Silva & Vader, 2021). The recruitment of the Pch2 AAA+ ATPase to meiotic chromosomes allows it to use its activity to influence HORMA protein-dependent signaling (Rosenberg & Corbett, 2015; Vader, 2015).

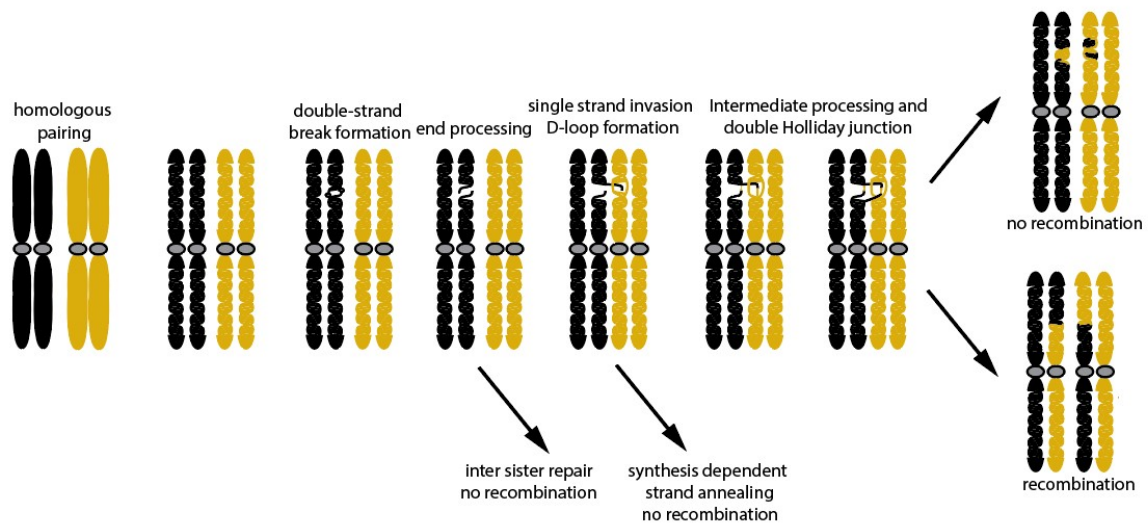


Figure 1.2. Homologous recombination

1.6. The perfect balance in meiotic crossover formation

Analysis of non-crossover and crossover products in yeast, humans and many other organisms supports the hypothesis that these products are generated by two distinct repair pathways, which do not share intermediates and require different functions (Drouaud et al., 2013; Globus & Keeney, 2012; Guillon et al., 2005; Jeffreys & May, 2004; Mancera et al., 2008; Wijnker et al., 2013). Regardless of the stochasticity of the crossing-over occurrence mechanisms, it is known that the formation of crossovers is strictly regulated (Jones & Franklin, 2006). Despite the formation of multiple DSBs on each chromosome, the final number of formed crossovers is usually kept low. In *S. cerevisiae* it's often as low as 1–2 per chromosome pair (Martini et al., 2006a).

Even though meiotic crossover frequencies vary among organisms, most organisms maintain at least one crossover per homolog pair (obligate crossover) to accurately segregate during meiosis I division (crossover assurance) (Jones & Franklin, 2006). In case more than one crossover event takes place, they tend to be distanced from each other as if the formation of one prevented the formation of another in proximity (crossover interference) (Jones & Franklin, 2006). In the case of crossover interference, there are however some exceptions to the rule. Most crossovers are sensitive to crossover interference (class I crossovers) (Guillon et al., 2005) and their occurrence depends strongly on the activity of a group of proteins termed “ZMM” (Zip1, Zip2, Zip3, Spo16, Msh4-Msh5, Mer3). However, in budding yeast, between 15% and 35% of crossovers are a result of another pathway and belong to class II

crossovers (Boddy et al., 2001; de los Santos et al., 2003). Class II crossovers do not participate in interference (de los Santos et al., 2003; Kohl & Sekelsky, 2013). They depend on double Holliday junction resolution executed by structure-specific endonucleases Mus81-Mms4, Slx1-Slx4, and Yen1 (Zakharyevich et al., 2012). Several organisms, including the fission yeast *Schizosaccharomyces pombe*, depend almost entirely on the Mus81-dependent crossover pathway. This is correlated with the absence of ZMM proteins (Hollingsworth & Brill, 2004).

Both mechanisms - crossover interference and crossover assurance - regulate the minimum and the maximum number of crossovers for every chromosome and together assure crossover homeostasis: the number of crossovers on each chromosome remains relatively constant (Cole et al., 2012; Martini et al., 2006b; Rosu et al., 2011). Regardless of our awareness of these phenomena, we still know relatively little about the details of the molecular mechanisms responsible for crossover assurance and interference. These mechanisms remain largely unclear mostly because of the complexity of studying these processes.

Each meiotic protein may have a different role and activity, which depends on many factors, including binding interaction partners, substrate binding, post-translational modifications, local environment, and many others. The complexity of the interaction network requires that each protein and each protein-protein interaction are studied both *in vivo* and *in vitro*. Only combining a variety of approaches helps to understand the studied mechanism.

1.7. Meiotic decision making

In budding yeast, during the meiotic prophase I, crossover and non-crossover processing occurs to be temporally distinct. The current model suggests that non-crossover heteroduplex products are formed with the same timing as Holliday junctions while crossovers occur later (Allers & Lichten, 2001).

Despite our limited knowledge about factors influencing DSB positioning, proteins functioning downstream of DSB formation are better characterized. Although it is not precisely known how the decision is made whether crossover or non-crossover should be formed, we know that some proteins promote, and some prevent crossover formation.

In the table below I will divide these proteins into two categories, whereas some of them fit into both categories depending on the timing and context of the protein activity (Youds & Boulton, 2011) (Table 1.1).

Pro-crossover activity		
	<i>S. cerevisiae</i>	Vertebrates
DSB end resection	Mre11, Rad50, Xrs2 (complex) Sae2 Sgs1* Exo1 Dna2	MRE11, RAD50, NBS1 (complex) CtIP BLM* EXO1 DNA2
Crossover intermediate formation	Rad51 Dmc1 Rad52 Mer3 Rad54 Msh4, Msh5 (complex) Mlh1, Mlh2 (complex) Zip2 Zip4 Spo16	RAD51 DMC1 BRCA2 HFM1 RAD54 MSH4, MSH5 (complex) MLH1, MLH2 (complex) SHOC1 TEX11 SPO16
Promote interhomolog crossing over	Zip1 Hop1 Mec1 Tel1 Mek1 Rad50	SYCP1 ATR ATM RAD50
Crossover intermediate processing	Mlh1, Mlh3 (complex) Mus81, Mms4 (complex) Yen1 Slx1, Slx4 (complex)	MLH1, MLH3 (complex) MUS81, EME1 (complex) GEN1 SLX1, SLX4/BTBD12a (complex)
Anti-crossover activity		
Double Holiday junction and D-loop dissolution	Sgs1*, Top3, Rmi1	BLM*, TOP3 α , RMI1, RMI2 RTEL1

Table 1.1. List of meiotic pro- or anti-crossover proteins in *S. cerevisiae* and their mammalian homologs

*The Sgs1 pro- and anti-crossover activity depends on the activity of its interaction partners. Sgs1 acts in a pro-crossover way in complex with Dna2 and RPA (Cejka & Kowalczykowski, 2010) or anti-crossover in complex with Top3 and Rmi1 (Kaur et al., 2015).

1.8. Pro-crossover proteins

Pro-crossover proteins act on distinct intermediate steps. In the beginning, the proteins promoting pairing and synaptonemal complex formation come into play. The synaptonemal

complex (SC) is a protein structure (synaptonemal complex-forming proteins: Ecm11, Gmc2, Red1, Zip1) formed between homologous chromosomes. It facilitates crossover formation by assuring and maintaining two homologs in proximity (Costa & Cooke, 2007; Egidio De Carvalho & Colaiácovo, 2006). Another group of pro-crossover proteins includes proteins promoting the generation of recombination intermediates. This group includes, among others Sgs1, Dna2, Exo1, the MRX complex (Mre11-Rad50-Xrs2) responsible for break resection (Gravel et al., 2008; Mimitou & Symington, 2008) and recombinases Rad51 and Dmc1, which are responsible for homology search and strand invasion into the homologous chromosome (Schwacha & Kleckner, 1995). Another group consists of proteins promoting crossovers and includes proteins Mer3, the Mlh1/Mlh2 complex, and the Msh4/Msh5 complex. These proteins are thought to be involved in the stabilization of recombination intermediates (Duroc et al., 2017; Hollingsworth et al., 1995; Ross-Macdonald & Roeder, 1994). Both Mer3, as well as the Msh4/Msh5 complex are part of the ZMM-dependent crossover formation pathway.

1.9. The ZMM proteins and Mer3

The acronym ZMM is used to name a group of meiotic proteins that together promote crossover formation. In budding yeast, most of the crossovers are formed in the ZMM proteins-dependent pathway. The ZMM group (Zip1, Zip2, Zip3, Spo16, Msh4-Msh5, Mer3) includes at least seven functionally collaborating yet evolutionarily unrelated proteins (Lynn et al., 2007). All these proteins form foci at the sites where crossover occurs. The Msh4-Msh5 complex stabilizes and preserves a meiotic bimolecular DSB repair intermediate (Snowden et al., 2004). Zip3 is a SUMO E3 ligase, which likely modulates multiple protein-protein interactions (Cheng et al., 2006; Perry et al., 2005). Zip1 localizes at the length of the synaptonemal complex during pachytene and corresponds to the transverse filament component of the SC (Sym et al., 1993).

Mer3 DExH box helicase was repeatedly characterized both *in vivo* (Duroc et al., 2017; Shen et al., 2012; Vernekar et al., 2021; K. Wang et al., 2009), and *in vitro* (Duroc et al., 2017; Jessop et al., 2006; Mazina et al., 2004; Nakagawa & Kolodner, 2002; Nakagawa & Ogawa, 1999; Vernekar et al., 2021). Mer3 is an active ATPase with a 3' to 5' directional strand separation activity (Nakagawa et al., 2001). Interestingly, the ATPase-deficient Mer3 seems to give a less defective spore viability phenotype compared to the *mer3Δ* (Nakagawa & Kolodner, 2002). This could suggest that the role of Mer3 lies in its interaction with other proteins rather than

helicase activity. To date, Mer3 has already been reported to interact with the helicase Pif1, replication factor Rfc1 (Vernekar et al., 2021), and a MutL β complex (Mlh1/Mlh2) (Duroc et al., 2017).

1.10. Anti-crossover proteins

There are various proteins known for their anti-crossover activity. Usually, they promote alternative DSB repair pathways like synthesis-dependent strand annealing, they promote using the sister chromatid as a repair template (Goldfarb & Lichten, 2010) or they assure alternative processing of recombination intermediates, e.g. non-crossover formation. One of the anti-crossover proteins in budding yeast is the Sgs1 helicase (homolog of human BLM), which acts on the Holliday junctions by suppressing the formation of multi chromatid joint molecules (de Muyt et al., 2012). Sgs1 together with Top3 and Rmi1 can dissolve Holliday junctions and thereby prevent crossover formation (Cejka et al., 2010; Fasching et al., 2015; Kaur et al., 2015; S. Tang et al., 2015). Top3/Rmi1 heterodimer catalyzes DNA single-strand passage and has been suggested to act at the end of the process of junction dissolution by resolving hemicatenanes produced earlier by the Sgs1 helicase. The Top3/Rmi1 complex has also an important, Sgs1-independent function: it ensures complete resolution of recombination intermediates and chromosome segregation by dissolving unresolvable strand entanglements that would otherwise impede intermediate resolution (Kaur et al., 2015).

1.11. Decision making in meiosis is highly regulated by meiotic helicases

Conceptually, we recognize three major stages of “decision making” in meiotic recombination:

- Placement of the double-strand break, which usually occurs within the DSB hotspots (Tock & Henderson, 2018).
- Selection between sister chromatid and the homologous chromosome for the break repair template (Humphryes & Hochwagen, 2014).
- Choosing between crossover and non-crossover as a repair outcome (Youds & Boulton, 2011).

The significance of these decisions and the severity of the consequences makes it particularly important for this complex process to be precisely regulated. Helicases play an important role in the regulation of meiosis. The ATP-driven capability of the helicases allows them to translocate along the DNA strand and dissolve the dsDNA strand or other recombination

intermediates. Moreover, interactions between helicases and other meiotic proteins can also regulate and modulate the meiotic recombination. Helicases may act as pro- or anti-crossover factors and may determine the outcome of the meiotic recombination.

1.12. Aims of this thesis

The Mer3 protein of *Saccharomyces cerevisiae* is expressed only in meiosis (Nakagawa & Ogawa, 1999). In the absence of the *mer3* gene, the distribution of crossovers is randomized (crossover interference defect) and the frequency of crossing over is reduced. Compared to the wild type, the average crossover frequency in *mer3* Δ is 2.4 times lower (Nakagawa & Ogawa, 1999). Despite the importance of Mer3 as a meiosis-specific factor in generating COs and the high level of conservation among Mer3 orthologs (Chen et al., 2005; Tanaka et al., 2006), there is little understanding of the structural organization of Mer3, its interaction with other proteins, and how the interactions facilitate meiotic recombination. In my studies, I took up the challenge of characterizing the Mer3 helicase and its role in meiotic recombination, both alone and in concert with its interaction partners.

Knowing that different substrates, post-translational modification, protein interactors, and environmental conditions may influence the properties of the protein, I have chosen an *in vitro* approach to study different aspects of Mer3 activity and to learn more about its nature. The analysis can be divided into three main aspects. Firstly, I studied the biochemical activity of Mer3 and its substrate preference. Secondly, I conducted extensive studies on the structure of Mer3, which included not only the search for the tertiary structure but also the stoichiometry of the Mer3 helicase. Finally, I studied the interaction partners of Mer3. I started with characterizing one of the known interactors – the Mlh1/Mlh2 complex. This included not only binding experiments, but also basic structural studies of the Mer3/Mlh1/Mlh2 complex. In my further experiments, I aimed to find and describe new binding partners of the Mer3 helicase. Discovering that Mer3 interacts with the Top3/Rmi1 complex resulted in the extensive characterization of the Mer3/Top3/Rmi1 complex, which included binding experiments and structural characterization. Finally, the aim was to determine whether the two interactions are compatible with each other. The results of my studies are summarized in the publication “Integrated structural study of the Mer3 helicase reveals a novel role in promoting meiotic crossovers” (Chapter 2), which soon will be submitted to bioRxiv and after that will be submitted for publication in a journal.

To supplement my experimental studies on Mer3, I also wrote a short review. In this review, I explore the current knowledge about meiotic helicases, their interaction partners, and the role of regulatory modifications during meiosis I. I also put a strong focus on the molecular structure and mechanisms of these helicases.

Apart from the leading Mer3 project, I was also involved in the collaboration with a research group at the Department of Mechanistic Cell Biology, Max Planck Institute of Molecular Physiology, Dortmund, Germany. They used *in vivo* analysis during budding yeast meiosis, coupled with *in vitro* biochemical reconstitution to investigate how Pch2 interacts with Orc1/ORC. My *in vitro* analysis provided biochemical insights into our knowledge about the interaction between Pch2 and ORC.

During my doctorate I also aimed to solve the Mer3 structure using experimental techniques: crystallization and CryoEM. Although these experiments did not result in solving the structure of Mer3, I decided to include them in my thesis together with other important preliminary results for the future scientific generations.

2. Integrated structural study of the Mer3 helicase reveals a novel role in promoting meiotic crossovers

Magdalena Firlej, Veronika Altmannová, Rahel Rauleder, Andreas Schäffler, John R. Weir
Friedrich Miescher Laboratory of the Max Planck Society, Max-Planck-Ring 9, 72076 Tübingen, Germany.

To whom correspondence should be addressed: john.weir@tuebingen.mpg.de

Author	Author position (%)	Scientific ideas (%)	Data generation (%)	Analysis & interpretation (%)	Paper writing (%)
Magdalena Firlej	1	38%	40%	38%	90%
Veronika Altmannová	1	30%	45%	40%	5%
Rahel Rauleder	2	1%	7%	0%	0%
Andreas Schäffler	3	1%	3%	2%	0%
John R. Weir	4	30%	5%	20%	5%
Paper Title	Integrated structural study of the Mer3 helicase reveals a novel role in promoting meiotic crossovers				
Status in publication process	Manuscript ready for submission				

Abstract

During meiosis I it is necessary that homologous chromosomes are linked to one another so that they can be faithfully separated. *S. cerevisiae* Mer3 (HFM1 in mammals) is a SF2 helicase and member of the ZMM group of proteins that facilitates the formation of class I crossovers during meiosis. Here we describe the biochemical activity and structural organization of Mer3. Using AlphaFold2 modeling and XL-MS we further characterize the previously described interaction with Mlh1/Mlh2. We discover that Mer3 also forms a complex with the recombination-regulating factors Top3 and Rmi1 and that this interaction is competitive with Sgs1 helicase. Using *in vitro* recombination assays, we show that Mer3 inhibits the anti-recombination activity of Sgs1/Top3/Rmi1 (STR). Thus, we provide a mechanism whereby Mer3 downregulates the anti-crossover activity of the STR complex, hence promoting the formation of crossovers during meiosis I.

2.1. Introduction

Meiotic recombination is a fundamental evolutionary process required to assure correct chromosome segregation that simultaneously contributes to the creation of new allele combinations and increasing genetic diversity. The role of homologous recombination in chromosome segregation is to provide steady connections between the homologous chromosomes during the first meiotic division. These connections are formed after double-strand breaks are introduced by Spo11 transesterase (Keeney, 2008) and the breaks are resected to 3' overhangs, which are initially bound by RPA followed by its replacement by the recombinase Rad51 and its meiosis-specific ortholog Dmc1. This leads to the formation of presynaptic filament, which mediates the homology search and strand invasion. Further, after the initial connection is formed, the double-strand break can be repaired through multiple pathways leading to either non-crossovers (NCOs) or crossovers (COs) as outcomes. Most of the non-crossovers are formed by the dissolution of unstable joint molecules (JMs) formed during the process of DSBs repair (Pâques & Haber, 1999). Crossovers are formed after the strand invasion intermediates are stabilized and the second DSB is captured forming a double Holliday junction (Schwacha & Kleckner, 1995; Szostak et al., 1983), which can then be resolved either by dissolution to produce NCOs or resolution to produce CO or NCO. In most organisms, including yeasts, plants, and mammals, the formation of crossovers during the first round of meiotic division is crucial for the correct homolog alignment and spindle assembly at metaphase I (Nicklas, 1997; Petronczki et al., 2003). There are two different meiotic crossover pathways that produce crossovers with different properties. Crossovers that exhibit interference and use pro-crossover protein complexes are referred to as class I crossovers. Crossovers that do not participate in interference are called class II crossovers (de los Santos et al., 2003; Kohl & Sekelsky, 2013).

The molecular mechanisms that are responsible for determining whether DSB will be repaired as CO or NCO have been analyzed extensively. DSBs appear in overabundance compared to the number of COs meaning that most of the DSBs are repaired as NCOs. Cells however developed a pathway to ensure that at least one CO per chromosome is formed. This pathway is to a large degree stabilized and regulated by a group of proteins called "ZMM". These proteins are required for the formation of interfering class I crossovers (Lynn et al., 2007). In budding yeast, the meiotic recombination has been extensively characterized at the molecular

level. Therefore, the proteins we are working with are *S. cerevisiae* proteins, and the mechanisms discussed further will be based on budding yeast proteins.

The *S. cerevisiae* group of ZMM proteins consists of Zip1, Zip2, Zip3, Zip4, Spo16, the Mer3 helicase, and the Msh4-Msh5 heterodimer (Lynn et al., 2007; Shinohara et al., 2008). Some are involved in the formation and stabilization of single-end invasion (SEI) intermediate (Börner et al., 2004; Hunter and Kleckner, 2001). ZMM mutants show a decrease in the formation of SEI and dHJ intermediates. In absence of ZMMs, spore viability as well as the number of COs is decreased (Börner et al., 2004; Jessop et al., 2006). ZMM proteins were also reported to downregulate the activity of Sgs1 helicase (the yeast homolog of the mammalian BLM helicase) (Jessop et al., 2006). Sgs1, together with Top3 and Rmi1 (STR complex), can dissolve D-loop structures, resulting in double-strand breaks being repaired via SDSA. Sgs1 helicase can also directly dissolve dHJs, thereby preventing CO formation (Hatkevich & Sekelsky, 2017). In meiosis, the helicase activity of Sgs1 is disposable (Ui et al., 2001). Its interaction with Top3/Rmi1 (the N-terminal region of the Sgs1 is essential for the interaction) is necessary for the regulation of CO and NCO in meiosis simultaneously, and the essential role in the dissolution of recombination intermediates is played by the activity of the Top3/Rmi1 complex (Kaur et al., 2015; Tang et al., 2015).

In vitro studies on Mer3 showed that it is an active ATPase with strand separation activity working in a 3' to 5' direction (Nakagawa et al., 2001) and that it might preferentially recognize Holliday junctions, however, it also recognizes other DNA structures (Nakagawa & Kolodner, 2002). Further *in vitro* works demonstrated that Mer3 promoted a heteroduplex extension by Rad51, that is, it enlarged and stabilized D-loops (Mazina et al., 2004). It was shown that Mer3 together with other ZMM proteins synergizes to protect nascent CO-designated recombination intermediates from dissolution by Sgs1 (Jessop et al., 2006). *In vivo* studies showed that Mer3 ATPase-deficient mutants (mer3G166D and mer3K167A) show mild spore viability defects, whereas in mer3Δ strain spore viability is strongly compromised (Nakagawa & Kolodner, 2002). This observation hints at the possibility that Mer3 may contribute to promoting crossover formation by mediating protein-protein interactions.

To date, Mer3 has been reported to interact with the helicase Pif1, replication factor Rfc1, (Vernekar et al., 2021), and a MutLβ complex (Mlh1/Mlh2) (Duroc et al., 2017). The interaction between Mer3 and MutLβ was shown to occur via the Ig-like domain of Mer3 (Duroc et al.,

2017). Removal of Mlh1 or impairing the ability of Mer3 to bind to Mlh1 leads to an increase in the length of gene conversion tracts, both in COs and in NCOs (Duroc et al., 2017).

Despite the importance of Mer3 as a meiosis-specific factor in generating COs and the high level of conservation among Mer3 orthologs (Chen et al., 2005; Tanaka et al., 2006), there is little understanding of the structural organization of Mer3, both alone and with its interaction partners.

Here we used biochemical and structural approaches to describe the activity and structural organization of Mer3. We also further characterized the Mer3 interaction with the Mlh1/Mlh2 complex. The search for novel Mer3 interactors has led us to discover that Mer3 forms a complex with Top3 and Rmi1 and that this interaction is competitive with Sgs1^{BLM} helicase (Jessop et al., 2006). We again used the biochemical and structural approach, coupled with budding yeast experiments to ascertain the role of this interaction. We show that Mer3 inhibits D-loop dissolution mediated by the Sgs1/Top3/Rmi1 complex, thus revealing a novel mechanism of crossover formation during meiosis I.

2.2. Results

2.2.1. Biochemical activity of Mer3

We set out by purifying *S. cerevisiae* (SK1 strain) full-length Mer3 through over-expression in baculovirus-infected insect cells. Using a 3-step purification we were able to produce Mer3 protein that was homogenous and free of nucleic acid contamination (Figure 2.1A, Supplementary Figure 2.1A). The stoichiometry of DNA helicases is diverse. Rec-Q helicases for example appear to exist as monomers, dimers, and hexamers (Hickson et. al 2009). Mer3 is also most similar in terms of domain organization to the spliceosome helicase Brr2, which itself contains two helicase cassettes in a single open reading frame (Pena et al., 2009). Nevertheless, using mass photometry, we detected only monomers of Mer3 in the solution (Figure 2.1B). Mer3 has been previously reported to preferentially bind to the DNA repair intermediate D-loop over other DNA substrates (Duroc et al., 2017). We repeated previous experiments using EMSA and fluorescently labeled DNA substrates (Figure 2.1C, Supplementary Figure 2.1B). While we also found that Mer3 is bound to D-loops with a high affinity (measured Kd 38+/-4.1 nM), in contrast to previous studies (Duroc et al., 2017), Mer3 could also bind to ssDNA with a similarly high affinity (measured Kd 25+/-6.2 nM). We suspect that the difference may be a result of changing the protein purification strategy compared to

some of the previous preparations. We also tested the strand displacement activity of the purified Mer3 protein (Figure 2.1D, Supplementary Figure 2.1C) and found that it had broadly similar activity to what was previously reported (Mazina et al., 2004). Even though Mer3 demonstrates the ability to unwind D-loops, it never unwinds all of the given substrates.

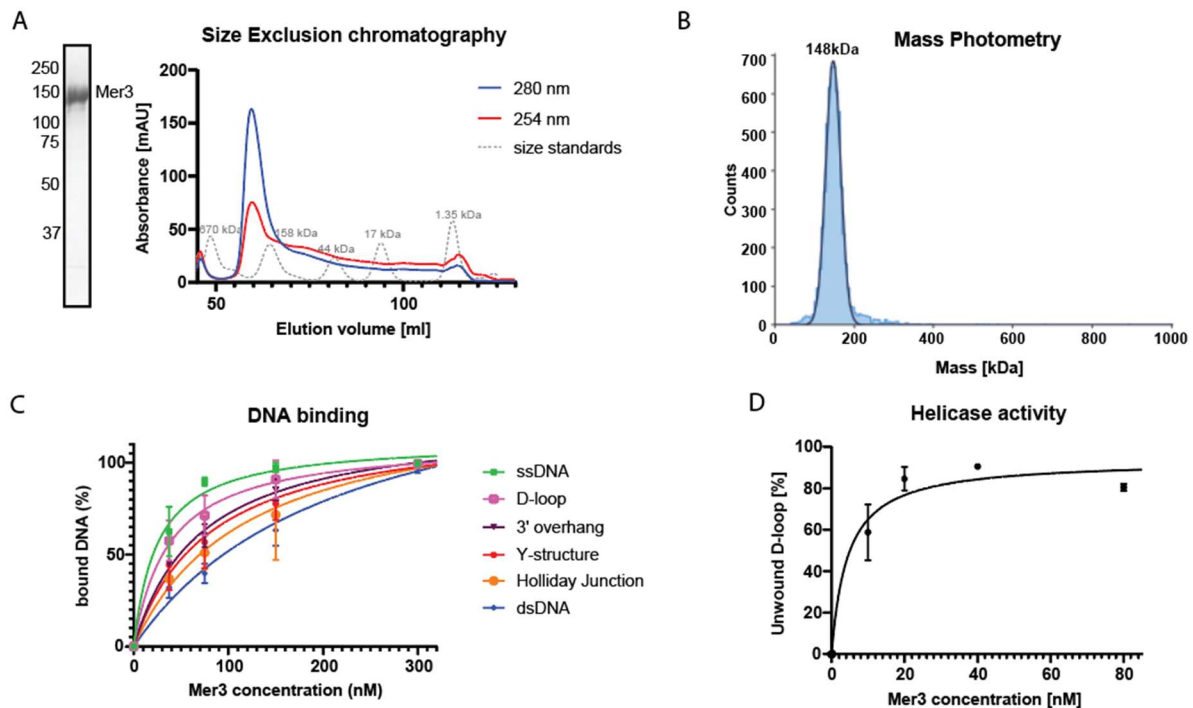


Figure 2.1. Biochemical activity of Mer3

A. Purification of Mer3 on Superdex 200 16/600 column. The relative absorbance of the complex at 280 nm and 260 nm shows that it is free of any significant nucleic acid contamination. The purified protein shows no signs of aggregation or contamination with other proteins. **B.** Mass Photometry of Mer3. Mer3 was diluted to ~30 nM and measured using a Refeyn One mass photometer as per the manufacturer's instructions. **C.** EMSAs on Mer3 binding different DNA substrates. Mer3 was titrated against 10 nM fluorescently labeled DNA substrate. The reactions were started by the addition of increasing amounts of Mer3 protein (37.5, 75, 150, and 300 nM). Error bars are the SD from three independent experiments. **D.** The strand separation assay. Mer3 was titrated against 5 nM fluorescently labeled DNA substrate. The reactions were started by the addition of increasing amounts of Mer3 protein (10, 20, 40, and 80 nM). Error bars are the SD from three independent experiments.

2.2.2. Hybrid structural analysis of Mer3

Despite extensive efforts, we were not able to crystallize a construct of Mer3 for structural studies. Instead, we made use of Mer3 models to probe the structural function. AlphaFold2 (AF2) has provided exceptionally accurate computational models of structures (Jumper et al., 2021). The AF2 model is of an overall high quality (only structured region in Figure 2.2A, full-length model in Supplementary Figure 2.2A) and to confirm the organization experimentally, we made use of crosslinking coupled to mass-spectrometry (XL-MS) (Supplementary Figure 2.2B). XL-MS on Mer3 alone showed a mix of long and short-distance crosslinks (Figure 2.2B). By modeling the crosslinks onto the Mer3 model, we surprisingly found that even when accounting for flexible loops, many of the crosslinks are not compatible with the distances

observed in the model. The XL-MS data also revealed several “self”-crosslinks that could only be compatible with the oligomerization of Mer3. Since the mass photometry results must be performed in very low protein concentration (30 nM compared to 3 μ M during crosslinking experiments), this could have had an impact on the measured stoichiometry of the Mer3 protein. We measured the crosslinked Mer3 sample using mass photometry and indeed, we could also observe the formation of bigger protein structures, possibly dimers (Supplementary Figure 2.2C). Next, we asked whether Mer3 might form a dimer in solution, but at higher concentrations. We measured its mass using size-exclusion chromatography coupled with multi-angle light scattering (SEC-MALS) (sample concentration 10 μ M). Our analysis revealed that Mer3 is indeed a dimer under these conditions (Figure 2.2C). A search for the possible dimeric structure of Mer3 leads us to the closest homology match using HHPRED, the spliceosomal helicase Brr2 (7DCO (Absmeier et al., 2015)). Brr2 is a highly unusual helicase, as it contains two complete helicase “cassettes” of which only the N-terminal cassette is active (Markus C. Wahl et. al. 2009). The Mer3 homology model built based on the Brr2 helicase however did not satisfy the not compatible crosslinks from the monomeric model. This suggests that the subunit orientation of a Mer3 dimer differs from the cassette orientation in Brr2. A credible model of the Mer3 dimer is yet to be predicted or experimentally determined. To map the possible oligomerization region, we purified Mer3 fragments lacking the N- or C-terminal region: Mer3 Δ N (122-1187), Mer3 Δ C (1-1023), and Mer3 Δ N Δ C (122-1023) (Figure 2.2D). The removed regions are predicted to be unstructured. Interestingly, both N- and C-term truncations of the Mer3 protein showed no ability to dimerize (Figure 2.2D). The self-association of Mer3 was also confirmed in the yeast two-hybrid assay. We also tested some of the truncated constructs. The construct Mer3 Δ N (122-1187) does not form dimers in yeast two-hybrid experiments indicating that the N-terminal region of Mer3 is critical for Mer3 dimerization (Figure 2.2E).

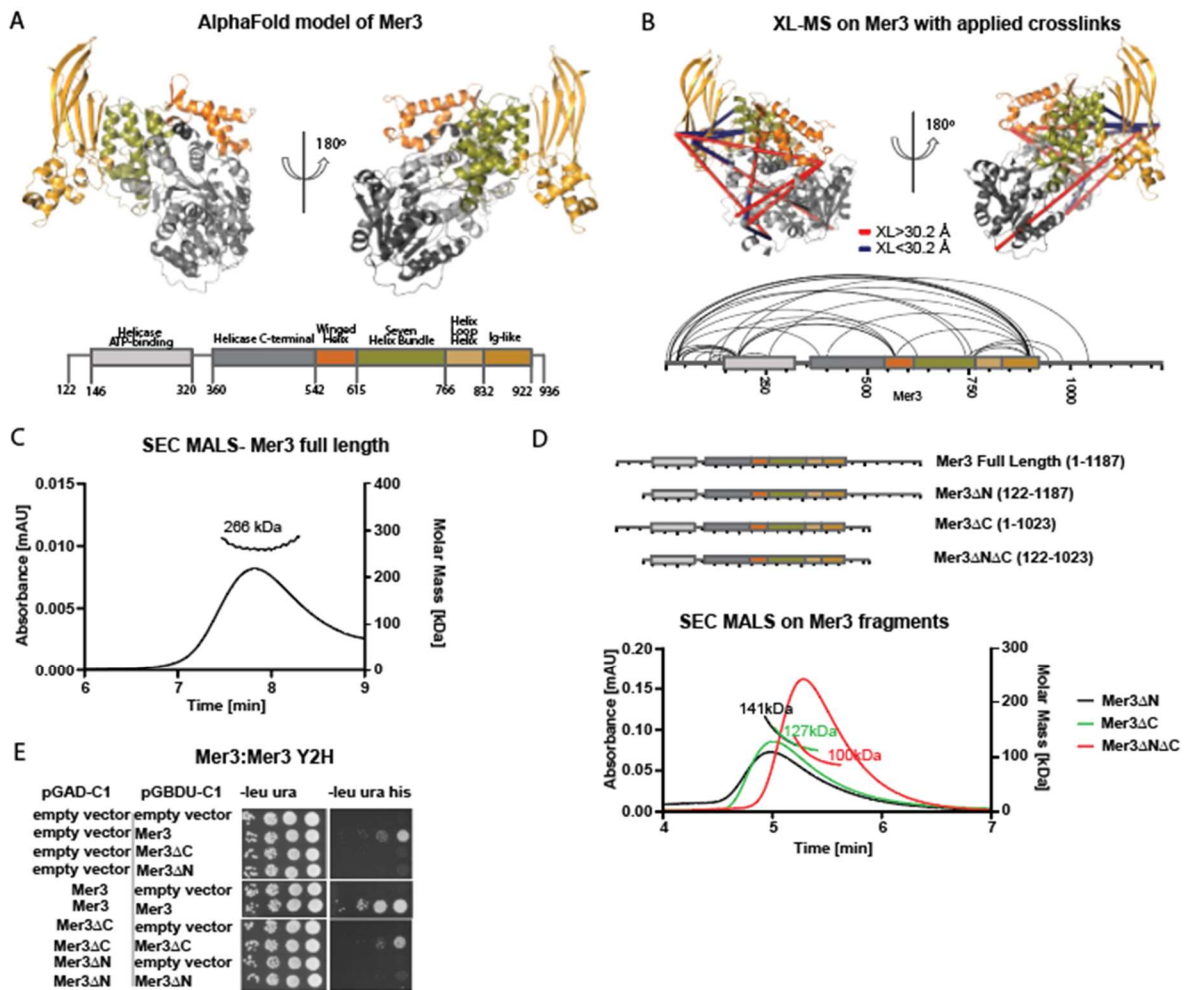


Figure 2.2. Structural analysis of Mer3

A. AlphaFold2 model of Mer3. Presented only the 122-936 fragment of the protein. The remaining fragments were unstructured. 3D Model domains are coloured according to the bar plot presented below. The complete model is presented in Supplementary Figure 2.2A. **B.** Mer3 AlphaFold model with overlaid DSBU crosslinks. Crosslinks were filtered for a match score of >135. In the model are presented non violated crosslinks (<30.2 Å; blue) and violated crosslinks (>30.2 Å; red). The complete list of crosslink lengths is included in Supplementary Table 2.3. Crosslinks are also presented on the bar plot below the model. **C.** SEC-MALS of full-length Mer3 on Superose 6 5/150 column. Measured molecular masses are indicated. **D.** SEC-MALS of Mer3 truncations on Superdex 200 5/150 column. Measured molecular masses are indicated. Bar plots represent the Mer3 truncations used in the search for the non-dimerizing Mer3 construct. Used colours are the same as in Figure 2.2A. **E.** Yeast two-hybrid experiments with Mer3 FL and selected truncations. Yeast were transformed with the pGAD-C1 and pGBDU plasmids as indicated. Cells were grown and pipetted onto non-selective (left) or selective plates (right) at four concentrations.

2.2.3. Biophysical and structural analysis of Mer3 interaction with Mlh1 and Mlh2

It was previously shown that Mer3 is bound directly to the Mlh1/Mlh2 complex and that this interaction may play a role in regulating the size of gene conversions during NCOs (Duroc et al., 2017). We purified a complex of MBP-Mlh1 and MBP-Mlh2 from insect cells, again making use of a 3-step purification to ensure that it was free of nucleic acids (Figure 2.3A, Supplementary Figure 2.3A). Both proteins were MBP tagged because purification of these proteins without the solubilization tag resulted in a much lower yield and in our experiments, we required high amounts of the protein. As a quality control, the sample was measured using

mass photometry (Figure 2.3A). The measured size of the complex corresponded to 1:1 stoichiometry.

We characterized the Mlh1/Mlh2 complex using XL-MS (Figure 2.3B) and observed that the majority of the high confidence crosslinks detected between Mlh1 and Mlh2 are broadly distributed on the sequence of the Mlh1 protein, whereas they concentrate on two distinctive locations in Mlh2. One of them is the C-terminal region of the ATPase domain (K159) and the other one is the N-terminal region of the C-terminal domain (K560). These two regions of the Mlh2 may be involved in interaction with Mlh1.

The publicly available AlphaFold2 models are currently based on monomeric proteins. To elucidate the results given by XL-MS, we endeavored to make an AF2 multimer model (Gao et al., 2022) of the Mlh1/Mlh2 heterodimer. The model prediction quality was high for the ATPase and transducer regions of both Mlh1 and Mlh2 (Predicted Aligned Error below 10 Å, pLDT score above 50) (Supplementary Figure 2.3B). Also, the orientation in relation to each other was highly ranked. The structure of the C-term domain of Mlh1 protein was also predicted to be accurate, however, the general orientation relative to the ATPase domain and the Transducer domain was low in confidence. The C-term domain of Mlh2 as well as the unstructured regions of both proteins couldn't be predicted with high confidence. We overlaid high confidence crosslinks on the Mlh1/Mlh2 model while including only ATPase and transducer domains. The crosslinks generally matched the model, since 75% of the crosslinks were shorter than 35.5 Å (Figure 2.3C). This confirmed the credibility of the Mlh1/Mlh2 model. The distance threshold was selected based on the sum of the maximal inter-residue distance that can be linked by the DSBU crosslinker, which is 28.3 Å (Merkley et al., 2014) and the Predicted Aligned Error, which in high-quality predictions should be smaller than 10 Å. The Predicted Aligned Error is an AlphaFold2 model's expected position error at residue x, when the predicted and true structures are aligned on residue y.

To characterize Mer3 and Mlh1/Mlh2 interaction, we first performed an *in vitro* pull-down assay to confirm that our purified proteins can form a complex (Figure 2.3C). However, we were not able to produce a size-exclusion chromatography stable complex. We characterized the strength of this interaction using microscale thermophoresis (MST). Measured K_d was 436+/-122 nM (Figure 2.3D). Similar results were obtained while measuring the interaction using surface plasmon resonance (SPR, Biacore). The measured K_d was 129.9 +/- 200 nM (Supplementary Figure 2.3C). Next, we determined the structural organization of the

Mer3/Mlh1/Mlh2 heterotrimeric complex using XL-MS (Figure 2.3E). Consistent with the previously reported study, we observed several high confidence crosslinks between the Mer3 Ig-like domain and both Mlh1 and Mlh2. Importantly, many crosslinks were also detected between the helicase ATP binding domain within Mer3 and both Mlh1 and Mlh2 proteins. We also investigated changes in the internal crosslinking profile of Mer3 by comparing internal crosslinks of Mer3 helicase while crosslinked alone and in the complex with Mlh1/Mlh2 (Supplementary Figure 2.3D). Some of the previously abundant crosslinks (at least two counts) disappeared (red highlight on the crosslinking network map, Figure 2.3E). This could indicate that this region becomes inaccessible after Mer3 interacts with Mlh1/Mlh2 or that some conformational change occurs. Although on the surface of the Mer3 model we see some accumulations of the crosslinks, there is no clear indication on where the Mlh1/Mlh2 complex interacts with Mer3 (Figure 2.3E, Supplementary Figure 2.3E).

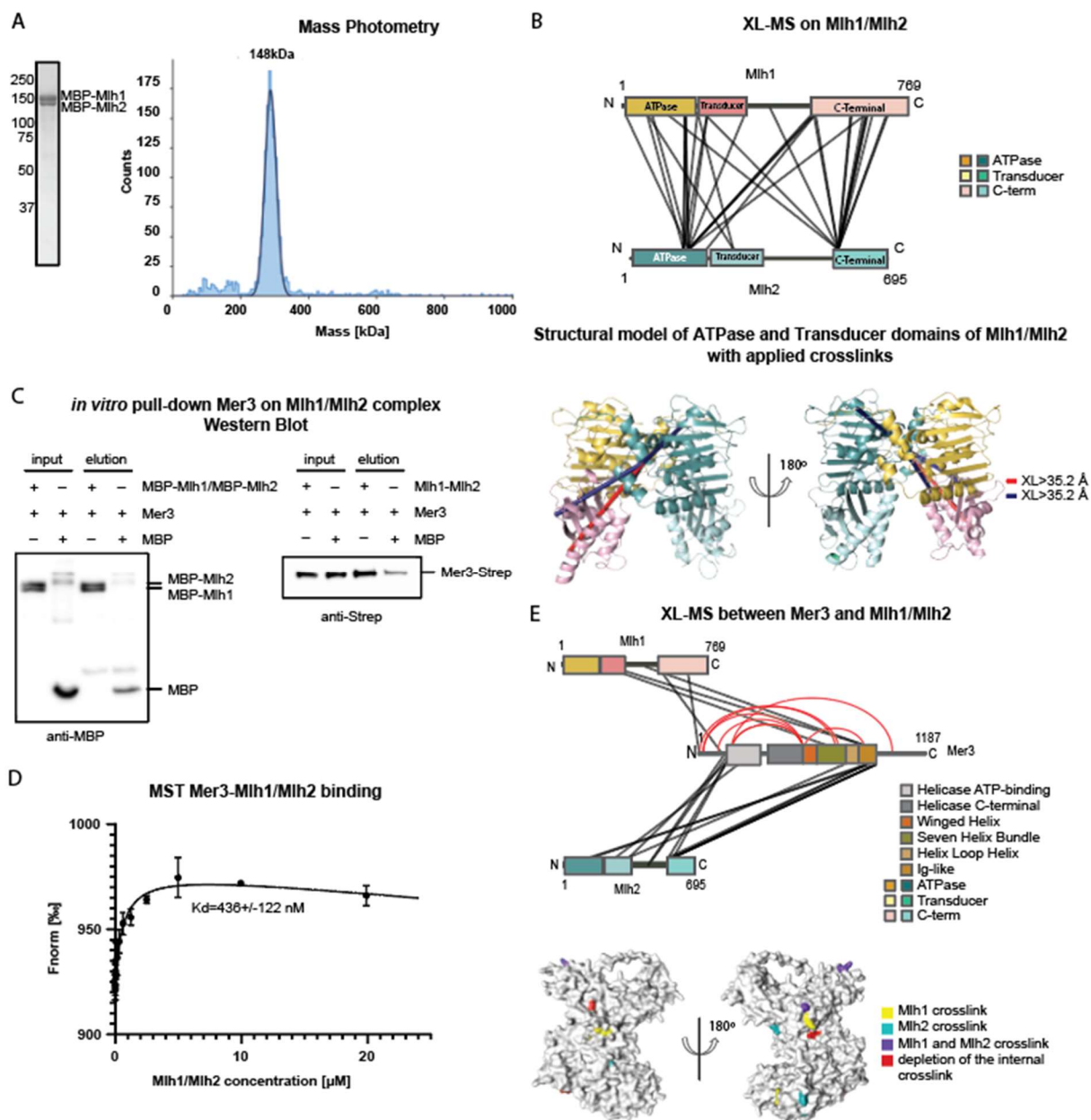


Figure 2.3. Biophysical and structural analysis of the interaction between Mer3 and the Mlh1/Mlh2 complex

A. Purification of MBP-Mlh1/MBP-Mlh2 complex on Superose 6 16/600 column (chromatogram presented in Supplementary Figure 2.3A). Mass Photometry of Mlh1/Mlh2, which was diluted to ~30 nM and measured using a Refeyen One mass photometer as per the manufacturer's instructions. **B.** XL-MS map of Mlh1/Mlh2 complex. Crosslinks were filtered for a match score of >150. Below **B.**, the AlphaFold model of ATPase and transducer domains of both Mlh1 and Mlh2 with overlaid DSBU crosslinks. On the model are presented non violated crosslinks (<35.2 Å; blue) and violated crosslinks (>35.2 Å; red). The complete list of crosslink lengths are included in Supplementary Table 2.4. Crosslinks are also presented on the bar plot below the model. **C.** *In vitro* pull-down of Mer3 on MBP-Mlh1/MBP-Mlh2 complex. Mlh1/Mlh2 complex was incubated with Strep-tagged Mer3. Anti-MBP antibody was added to the reactions, samples were incubated, and magnetic-conjugated protein G beads were added to the reactions followed by the incubation. The samples were loaded onto SDS-PAGE and analyzed by western blot. **D.** The MST Measurements on Mer3 binding to Mlh1/Mlh2. MBP-Mlh1/MBP-Mlh2 was titrated against RED-NHS labeled Mer3. Error bars are the SD from three independent experiments. **E.** XL-MS map of Mer3/Mlh1/Mlh2 complex. Crosslinks were filtered for a match score of >54. Additionally, in red, we present internal Mer3 crosslinks that are no longer detectable after crosslinking with Mlh1/Mlh2 complex. Below, we present the surface model of Mer3 with highlighted amino acids that were frequently crosslinked with Mlh1 and/or Mlh2 as well as amino acids that were no longer a subject of internal crosslinking.

2.2.4. Mer3 interacts with the Top3/Rmi1 complex

Given that in the absence of Mer3 the number of crossover defects increases and that it is Sgs1 that drastically reduces crossover frequency (Jessop et al., 2006), we decided to search for Mer3 interaction partners within the proteins involved in crossover regulation. Making use of a small-scale yeast-two-hybrid screen, we evaluated the interaction of Mer3 with several known components of the crossover pathway. Interestingly, we observed an interaction with both Rmi1 and Top3 (Figure 2.4A), which also form a complex that can interact with the Sgs1 helicase (Tang et al., 2015). To confirm that Mer3 physically interacts with the Top3/Rmi1 complex in meiosis, we performed a co-immunoprecipitation experiment from meiotic cells expressing Mer3-9xMyc and Top3-3xHA. As shown in Figure 2.4B, Mer3 co-immunoprecipitated with Top3 thus confirming that both proteins associate with one another during meiosis (Figure 2.4C).

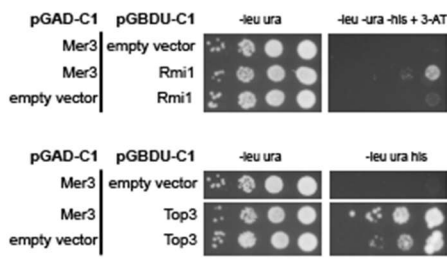
To study this interaction further, we purified Rmi1, Top3 and the Top3/Rmi1 complex from insect cells, again making use of an extensive 3-step purification to ensure that it was free of nucleic acids (Figure 2.4B). We carried out an *in vitro* pull-down assay using Strep-tagged Mer3 and either GST-Rmi1 or His-Top3 and we detected a positive interaction in both experiments (Figure 2.4D-E). To determine whether both interactions are compatible, we also carried out a pull-down using Top3/GST-Rmi1 complex. In these combinations, proteins were also interacting indicating that Mer3 interacts with the Top3/Rmi1 complex (Figure 2.4F).

We characterized the kinetics of this interaction using microscale thermophoresis (MST). The measured K_d of Mer3 binding to Top3/Rmi1 complex was 844 ± 148 nM (Figure 2.4G). Importantly, when we measured the binding for the proteins separately, the binding was weaker (K_d 2.19 ± 0.42 μ M for Top3 and K_d 1.99 ± 0.63 μ M for Rmi1; Supplementary Figure 2.4A), indicating that binding both proteins simultaneously stabilizes the interaction. Considering the high conservation of all the proteins, we decided to test whether this interaction is conserved. We studied the interaction between the human Mer3 homolog HFM1 and human TOP3 α in the yeast two-hybrid assay. In this case, no interaction was detected (Supplementary Figure 2.4B), which could suggest that this interaction is not conserved or is regulated by additional factors not present in vegetative yeast. For example, the human STR complex (BTRR complex = BLM-TOP3 α -RMI1-RMI2) consists of two Rmi1 orthologs (RMI1 and RMI2). The RMI2 protein may be required for the interaction to occur.

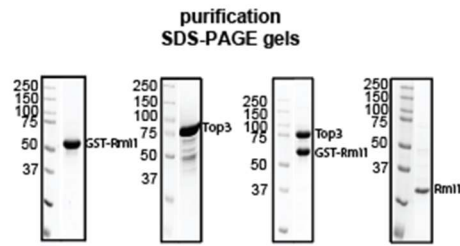
Another explanation might be the lack of certain types of post-translational modifications in the yeast system.

We used AlphaFold2 to predict the structure of the Top3/Rmi1 complex. Overall confidence in the model quality was very high (Supplementary Figure 2.4C) and the model strongly resembles the experimentally determined structure of the human TopoIII α -RMI1 complex (Bocquet et al., 2014). To evaluate the model, we used the XL-MS. 80% of the high confidence crosslinks were consistent with the model, given the maximal accepted molecule distance of 30.2 Å (distance threshold was selected based on the sum of DSBU maximal inter-residue distance restraints of 28.3 Å (Merkley et al., 2014) and the Predicted Aligned Error) (Figure 2.4H). XL-MS was also used to study the interaction between the Top3/Rmi1 complex and Mer3. We observed several high confidence crosslinks between Mer3 and both Top3 and Rmi1. Similarly, as in the case of the Mlh1/Mlh2 complex, both proteins are crosslinked with Mer3's Ig-like domain and helicase ATP-binding domain. Additionally, multiple crosslinks between Top3 and Mer3 helicase C-terminal domain were detected (Figure 2.4I). We also investigated changes in the internal crosslinking profile of Mer3 by comparing internal crosslinks of Mer3 helicase while crosslinked alone and in the complex with Top3/Rmi1 (Supplementary Figure 2.4D). We detected crosslinking pattern changes similar to the ones detected while Mer3 was crosslinked with Mlh1/Mlh2. When we examined the crosslinks accumulation on the surface of the Mer3 protein, we observed some surface accumulation of the crosslinks, which could point towards the interaction surface of Mer3 with the Top3/Rmi1 complex (Figure 2.4I and Supplementary Figure 2.4E). Knowing that interaction regions between Mer3 and the Mlh1/Mlh2 complex overlap with the interaction regions of the Top3/Rmi1 complex, we decided to investigate whether these two interactions are compatible.

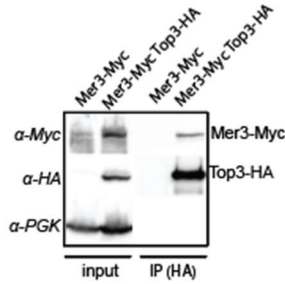
A Mer3:Rmi1 and Mer3:Top3 Y2H



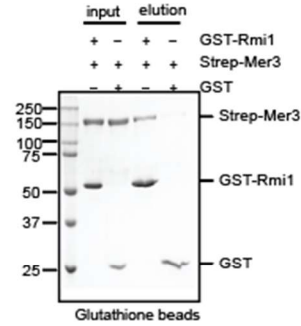
B



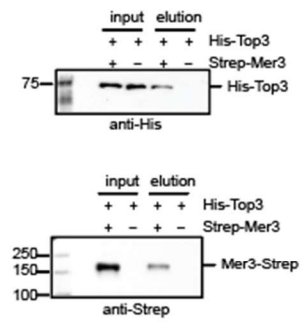
C Mer3 co-IP with Top3



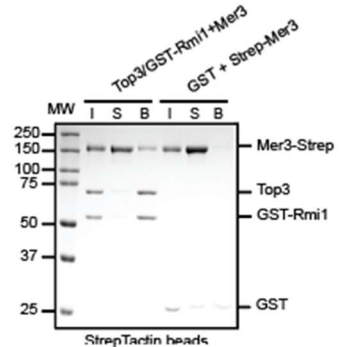
D *in vitro* pull-down Mer3 on Rmi1 SDS-PAGE gel



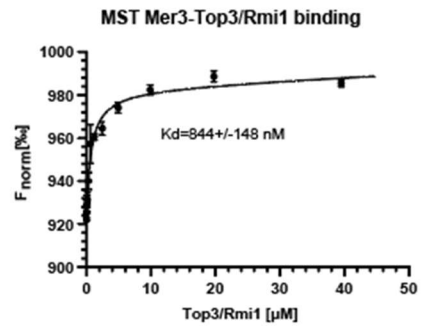
E *in vitro* pull-down Top3 on Mer3 Western Blot



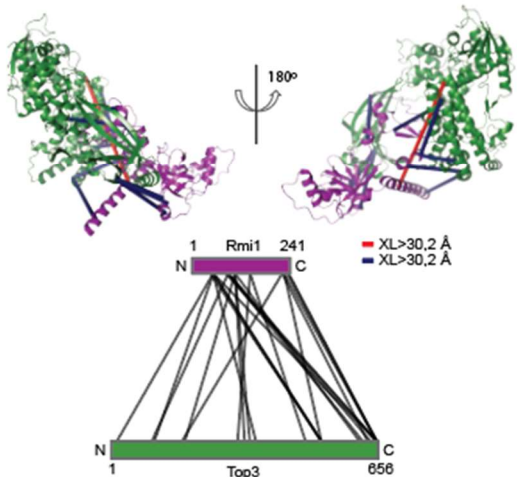
F *in vitro* pull-down Mer3 on Top3/Rmi1 SDS-PAGE gel



G



H Structural model of Top3/Rmi1 with applied crosslinks



I XL-MS between Mer3 and Top3/Rmi1

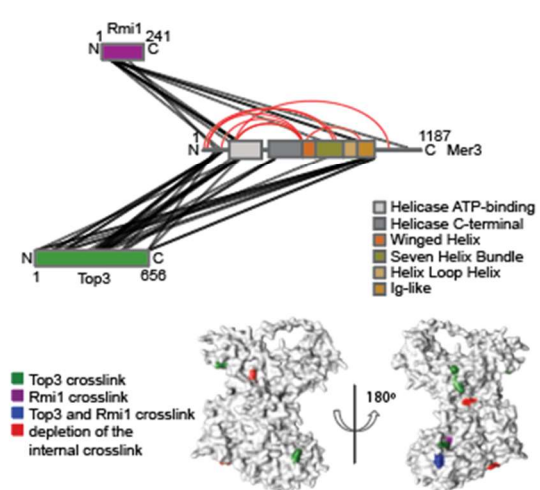


Figure 2.4. Mer3 interacts with the Top3/Rmi1 complex (The Figure description on the next page)

Figure 2.4. Mer3 interacts with the Top3/Rmi1 complex

A. Yeast two-hybrid experiments with Mer3, Top3, and Rmi1, respectively. Yeast were transformed with the pGAD-C1 (Mer3) and pGBDU (Top3 and Rmi1) plasmids as indicated. Cells were grown and pipetted onto non-selective (left) or selective plates (right) at four concentrations. **B.** Purification of GST-Rmi1, Rmi1, Top3, and Top3/GST-Rmi1 complex. **C.** Mer3 interacts with Top3 *in vivo*. Co-immunoprecipitation experiment from meiotic cells expressing Mer3-9xMyc and Top3-3xHA. Anti-HA antibody was added to the reactions, samples were incubated, and magnetic-conjugated protein G beads were added to the reactions followed by the incubation. The samples were loaded onto SDS-PAGE and analyzed by western blot. **D.** *In vitro* pull-down of Mer3 on GST-Rmi1. GST-tagged Rmi1 was incubated with Strep-tagged Mer3. Glutathione beads were then added to the samples and incubated. The proteins were eluted by boiling in SDS Laemmli buffer. The samples were loaded onto SDS-PAGE and stained by Der Blaue Jonas gel dye. **E.** *In vitro* pull-down of Top3 on Mer3. His-tagged Top3 was incubated with Strep-tagged Mer3. An anti-Strep antibody was added to the reactions and the mixtures were incubated. Finally, magnetic-conjugated protein G was added to the reactions followed by the incubation. The proteins were eluted by boiling in SDS Laemmli buffer. The samples were loaded onto SDS-PAGE and analyzed by western blot. **F.** *In vitro* pull-down of Mer3 on Top3/GST-Rmi1. GST-tagged Top3/Rmi1 was incubated with Strep-tagged Mer3. Glutathione beads were then added to the samples and incubated. The proteins were eluted by boiling in SDS Laemmli buffer. The samples were loaded onto SDS-PAGE and stained by Der Blaue Jonas gel dye. **G.** The MST Measurements of Mer3 binding to Top3/GST-Rmi1. Top3/GST-Rmi1 was titrated against RED-NHS labeled Mer3. Error bars represent the SD from three independent experiments. **H.** XL-MS map of Top3/Rmi1 complex (crosslinks were filtered for a match score of >140) and the AlphaFold model of the Top3/Rmi1 complex with overlaid DSBU crosslinks. On the model are presented non violated crosslinks (<30.2 Å; blue) and violated crosslinks (>30.2 Å; red). The complete list of crosslink lengths is included in Supplementary Table 2.5 **I.** XL-MS map of Mer3/Top3/Rmi1 complex. Crosslinks were filtered for a match score of >108. Additionally, in red are presented internal Mer3 crosslinks that are no longer detectable after crosslinking with the Top3/Rmi1 complex. Below is presented the surface model of Mer3 with highlighted amino acids that were frequently crosslinked with Top3 and/or Rmi1 as well as amino acids that were no longer a subject of internal crosslinking.

2.2.5. Mer3 interaction with Mlh1/Mlh2 is compatible with Top3/Rmi1 binding and together they are forming a 5-subunit complex

As previously described, Mer3 together with Mlh1/Mlh2 may act as regulating factors of the gene conversion size during COs and NCOs (Duroc et al., 2017). We tested whether binding Top3/Rmi1 by Mer3 is compatible with this interaction and leads to the formation of a “supercomplex” in which all five proteins could play a role in crossover formation regulation. We carried out a pull-down using purified Mer3 and Top3/GST-Rmi1 on MBP-Mlh1/MBP-Mlh2. As shown in Figure 2.5A, all proteins interacted with each other. Interestingly, the Top3/Rmi1 complex interacted with the Mlh1/Mlh2 complex also in the absence of Mer3 (Figure 2.5A), strongly indicating a potential cooperative assembly. Next, we determined the structural organization of the Mer3/Mlh1/Mlh2/Top3/Rmi1 complex using XL-MS (Figure 2.5B). The general distribution of the crosslinks between the proteins did not change, however, the number of significant crosslinks between Mer3 and Top3 was higher than between other proteins (significance of the crosslink was user-defined based on the crosslinking match score. Recommendation is above 50, but for higher certainty we increased it to 80). One of the explanations could be that formation of the complex limited the accessibility for the crosslinker because of tight protein packing within one surface area. Additionally, we also found crosslinks between Top3 and Mlh1 as well as between Rmi1 and Mlh2, consistent with our observation that Mlh1/Mlh2 directly interacts with Top3/Rmi1. When we analyzed the pattern changes in internal Mer3 crosslinks, we again detected similar

changes as the ones detected when Mer3 interacts only with the Mlh1/Mlh2 complex or only with the Top3/Rmi1 complex (Supplementary Figure 2.5A).

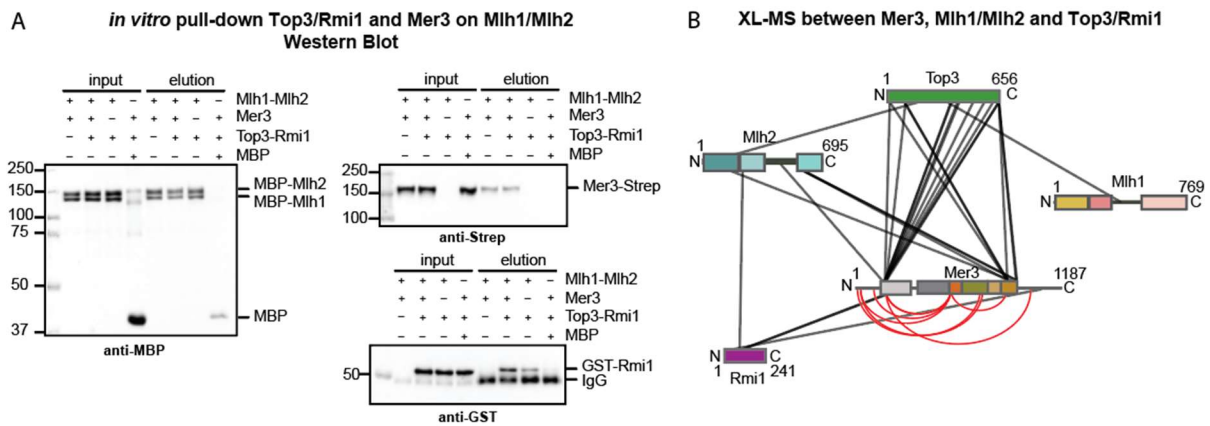


Figure 2.5. Mer3 interaction with Mlh1/Mlh2 is compatible with Top3/Rmi1 binding and together they are forming a 5-subunit complex

A. *In vitro* pull-down of Mer3 and Top3/GST-Rmi1 on MBP-Mlh1/MBP-Mlh2 complex. Mlh1/Mlh2 complex was incubated with Strep-tagged Mer3 and Top3/GST-Rmi1. Anti-MBP antibody was added to the reactions, samples were incubated, and magnetic-conjugated protein G beads were added to the reactions followed by the incubation. The samples were loaded onto SDS-PAGE and analyzed by western blot. **B.** XL-MS map of Mer3/Top3/Rmi1/Mlh1/Mlh2 complex. Crosslinks were filtered for a match score of >80.

2.2.6. Mer3 and Sgs1 are competing for binding to the Top3/Rmi1 complex

Sgs1 helicase together with the Top3/Rmi1 complex dissolves crossover intermediates and together in the complex prevents crossover formation (de Muyt et al., 2012). Abolishing the interaction however reduces the activity of both the Sgs1 and the Top3/Rmi1 complex (Harami et al., 2022). Therefore, it was important to test whether Mer3 competes with Sgs1 for the interaction with the Top3/Rmi1 complex. Preventing Sgs1 from binding to the Top3/Rmi1 complex could functionate as a protection mechanism for the pre-CO intermediates. We performed a competitive pull-down, in which we tested whether increasing amounts of Sgs1 can outcompete Mer3 bound to Top3/Rmi1. In this assay, we used only the N-terminal fragment of Sgs1 (1-605) that is known to interact with Top3/Rmi1 due to the difficulty in obtaining a high yield of full-length Sgs1 (Figure 2.6A). Results of competitive pull-down show that the increasing concentrations of N-terminal fragment of Sgs1 can outcompete Mer3 from the Mer3/Top3/Rmi1 complex, indicating that both Mer3 and Sgs1 bind the same region of Top3/Rmi1 and thereby the activity of the STR complex can be potentially modulated by Mer3 binding to Top3 /Rmi1.

2.2.7. Mer3 inhibits D-loop dissolution mediated by the Sgs1/Top3/Rmi1 complex

The Sgs1/Top3/Rmi1 complex has been shown to exhibit anti-crossover activity by negatively regulating D-loops (Fasching 2015 Mol Cell). To test if Mer3 affects D-loop dissolution by STR complex, we reconstituted D-loop formation using yeast meiosis-specific recombinase Dmc1 and RPA protein. Radioactively labeled ssDNA (90-mer) was first incubated with Dmc1 recombinase to form a presynaptic filament. After short incubation with RPA, D-loop formation was initiated by the addition of supercoiled plasmid DNA. Then, STR complex (15 nM) was added to the indicated reactions, which resulted in robust disruption of the D-loop after 10 min of incubation (30% of relative D-loop yield formed in the absence of STR). Interestingly, increasing concentrations of Mer3 were able to inhibit the D-loop dissolution by the STR complex. A 20-fold excess of Mer3 (300 nM) over Sgs1 resulted in a 70% relative yield of D-loop (compared to 30% in the absence of Mer3). We further tested if the helicase activity of Mer3 was crucial for the inhibition of D-loop dissolution by the STR complex. As shown in Figure 2.6C, the helicase-dead mutant Mer3-K167A had a similar effect on D-loop dissolution as the wild type Mer3, suggesting that the ability of Mer3 to unwind DNA is not essential for this regulatory step. Taken together, this data shows a novel and specific mechanism of crossover regulation by Mer3, independent of its helicase activity.

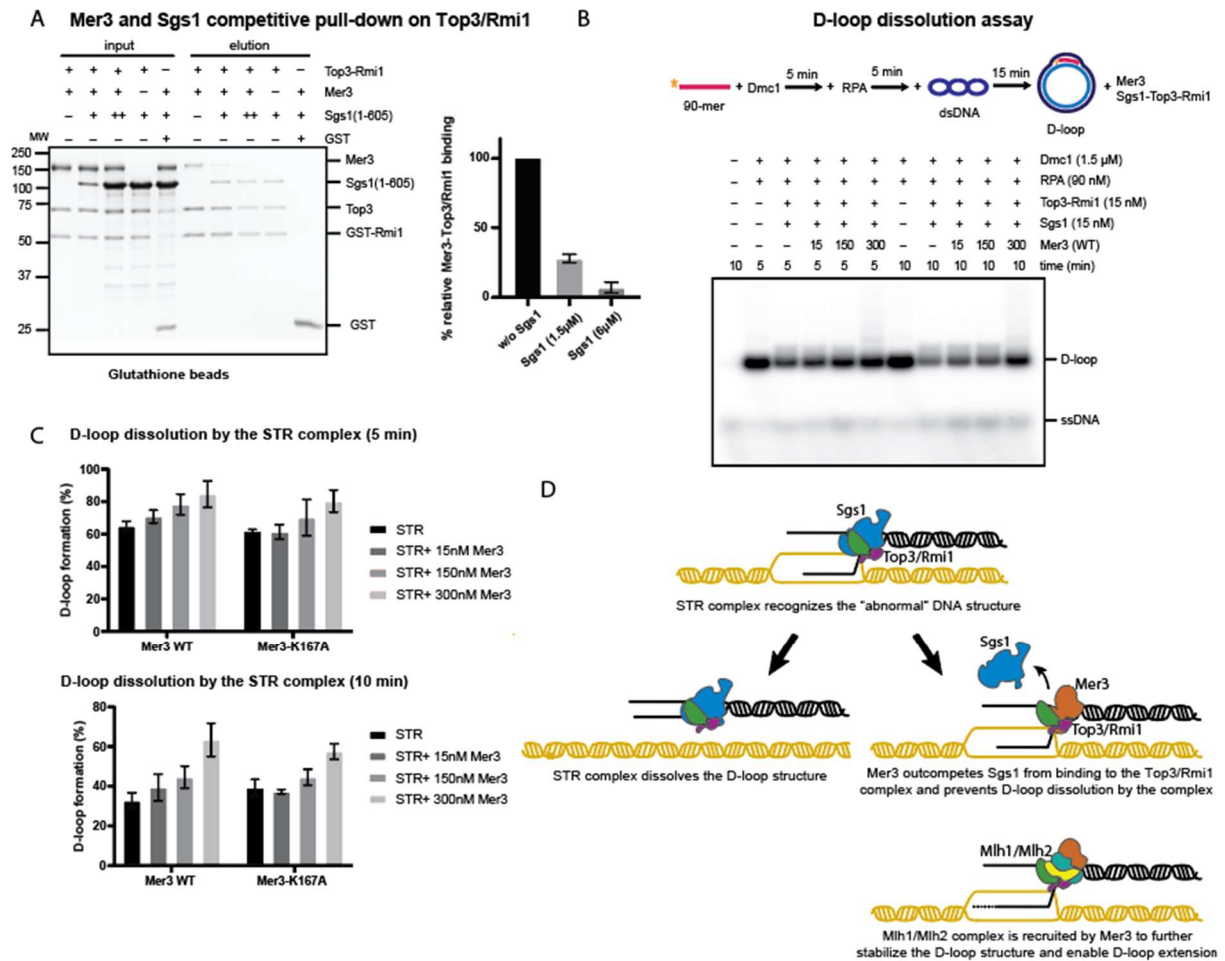


Figure 2.6. Mer3 and Sgs1 are competing for binding to the Top3/Rmi1 complex

A. For pull-down between Mer3 and Top3/Rmi1 in the presence or absence of Sgs1(1-605), GST-tagged Top3/Rmi1 was incubated with Strep-tagged Mer3, and as indicated increasing amounts of His-tagged Sgs1(1-605) were added to the reactions ($1.5 \mu M$ and $6 \mu M$). Magnetic glutathione beads ($1 \mu L$) were then added to the samples and the mixtures were incubated. The samples were loaded onto SDS-PAGE and stained by Der Blaue Jonas gel dye. The experiment was conducted in triplicate and the bands were quantified using ImageQuant TL software. Error bars represent the Standard Deviation. **B.** Radioactively labeled 90-mer ssDNA was incubated with Dmc1 protein followed by the addition of RPA. The formation of the D-loop was started by the addition of pUC19 plasmid. Sgs1, Top3/Rmi1, and the increasing amounts of Mer3 (15, 150, 300 nM) were added to the reactions. At the indicated time points, reactions were stopped. The deproteinized samples were separated in a 0.9% agarose gel. The gel was dried, exposed to a phosphor imager screen and visualized. **C.** The experiment from (B) was conducted in triplicate and the bands were quantified using ImageQuant TL software. Error bars represent the standard deviation. **D.** The cartoon visualization of our proposed model: at the time of the strand invasion STR complex attempts to dissolve the newly formed DNA structure, and the Mer3 helicase (orange) may be recruited to this site. It outcompetes the Sgs1 (blue) from the STR complex and possibly also blocks the activity of the Sgs1/Top3/Rmi1 (blue, green, and purple) complex from dissolving the DNA structures. Finally, Mer3 recruits the Mlh1/Mlh2 complex to act as a blockade that prevents D-loop extension or dissolution by Sgs1 or that stabilizes the interaction of Mer3 with Top3/Rmi1.

2.3. Discussion

Mer3 helicase was repeatedly characterized both *in vivo* (Duroc et al., 2017; Shen et al., 2012; Vernekar et al., 2021; Wang et al., 2009), and *in vitro* (Duroc et al., 2017; Jessop et al., 2006; Mazina et al., 2004; Nakagawa et al., 2001; Nakagawa & Kolodner, 2002; Vernekar et al., 2021), however, there are still many unknowns as to its function in meiosis. Mer3 is recruited to the chromosomes at early leptotene (Storlazzi et al., 2010) before chromosome alignment, yet the recruitment mechanism remains unknown. It was shown that Mer3 localization depends on Zip4 and Msh5 (Chen et al., 2005; Shen et al., 2012), nevertheless, no physical interaction was detected (neither by co-IP nor by Y2H) (Pyatnitskaya et al., 2019). Zip4 and Msh5 may be binding earlier to stabilize the early invasion intermediate and further, another factor may recruit Mer3. Mer3 binds to both sites of the resected ends of the recombination intermediate (Storlazzi et al., 1996). It might be therefore recruited by some of the proteins bound to the invading overhangs. Possible candidates are the recombinases Dmc1 and Rad51. Rad51 and Dmc1 proteins are required for the formation of joint molecules during meiotic recombination. It is known that their foci accumulate in the absence of Mer3 (Nakagawa & Ogawa, 1999). It is possible that the recruitment of Mer3 acts like a checkpoint and allows the recombinases to disassemble from the axis. Therefore, in the absence of Mer3 simply no D-loop stabilization is possible.

Our findings that Mer3 forms dimers *in vivo* and *in vitro* lead to the question what the role of dimerization is. Although it was suggested that Mer3 may be forming oligomers (Nakagawa et al., 2001), there was no experimental data that would support this hypothesis. It is not very surprising that Mer3 can form dimers considering its homology to the Brr2 helicase (the Ski2-like helicase that provides the key remodeling activity during spliceosome activation). Although the Brr2 helicase is a single polypeptide that consists of two cassettes that originated from gene duplication (Pena et al., 2009), it is possible that Mer3 also acts in a double-cassette mode as a homodimer. Only the N-terminal cassette shows helicase activity, whereas the C-terminal cassette most probably shows no significant enzymatic activity and may function as a protein-protein interaction platform (Liu et al., 2006; van Nues & Beggs, 2001). The natural question would be whether in the case of the Mer3 dimer both dimer subunits bind DNA and if both hydrolyze ATP or rather, as in the case of the Brr2, one of the subunits is fully dedicated to interactions with other proteins.

Recent studies discovered that Mer3 interacts with the Mlh1/Mlh2 complex (Duroc et al., 2017). It is predicted that Mer3 recruits Mlh1/Mlh2, which also preferentially binds D-loop structures and together they prevent overextension of recombination intermediates. Our results confirmed this interaction. Measured K_d 436+/-122 nM implies that a constitute complex is unlikely and the interaction is more likely to be transient or regulated by post-translational modifications. In our experiments, we were not able to form a stable size-exclusion complex. The affinity between Mer3 and Mlh1/Mlh2 might be stronger while proteins are bound to the DNA. It is also possible that other factors are required to stabilize the interaction. Previous studies also identified the Mer3's Ig-like domain as the region of interaction with the Mlh1/Mlh2 complex. In our XL-MS experiments, we also detected more crosslinks between Mer3 and Mlh2 than between Mer3 and Mlh1, which would support the previously published data showing that interaction with Mlh2 appeared to be stronger than the interaction with Mlh1 (Duroc et al., 2017). Another explanation could be that simply in the case of Mlh1 in complex with Mlh2 and Mer3 crosslink accessibility is very low. Interestingly, we detected crosslinks not only within the Ig-like domain but also within the Helicase ATP-binding domain, which could potentially indicate that the Mer3 interaction surface with Mlh1/Mlh2 also includes the N-terminal region of Mer3. This possibility is also supported by the change in the internal crosslinking profile of the Mer3 protein. In the presence of the Mlh1/Mlh2 complex, the distribution of the crosslinks within the two helicase domains changes and some of the crosslinks, usually located near the Helicase ATP-binding domain, disappear.

The role of the ZMM proteins in protecting nascent CO-designated recombination intermediates from dissolution mediated by the Sgs1/Top3/Rmi1 complex has been described (Jessop et al., 2006). The same studies point to an interesting correlation. In the absence of Mer3, it is Sgs1 that drastically reduces crossover frequency. Following this study, we searched for interactions within the proteins involved in crossover regulation and discovered that Mer3 interacts with both Top3 and Rmi1. Although Mer3 binds both proteins independently, the affinity measurements indicate that binding to the Top3/Rmi1 complex is stronger. Remembering that our results indicate that Mer3 forms dimers, we wondered how this relates to its interaction with Top3/Rmi1. Recent studies have also shown that the stoichiometry of the BLM-TOPIIIa-RMI1/2 complex is 2:2:2 (Hodson et al., 2022). It is therefore possible that in yeast Mer3 dimer also forms a stoichiometrically similar complex while binding to Top3/Rmi1.

To understand the role of the interaction between Mer3 and Top3/Rmi1, we studied the role of Sgs1 and Top3/Rmi1 in the regulation of NCO and CO in meiosis. Top3 and Rmi1 separately can disrupt D-loops *in vitro*, yet only as a complex can they disrupt crossover intermediates *in vivo* (Cejka & Kowalczykowski, 2010). The STR complex acts against the formation of stable CO intermediates. The studies from the human system show that disruption of the interaction between BLM and TRR complex reduces the stimulatory effect that the protein has on each other (Harami et al., 2022). BLM alone has been shown to promote both the early NCO-SDSA and the ZMM-dependent CO-only pathways (Kaur et al., 2015). Depending on the DNA-binding orientation, BLM has been shown to either disrupt the junction or to stabilize the D-loop (Harami et al., 2022). It is the TTR complex that orients the helicase towards D-loop disruption (Harami et al., 2022). In our studies, we have shown that Mer3 and Sgs1 compete for binding with the Top3/Rmi1 complex. We also show that Mer3 can prevent D-loop dissolution by the STR complex and that this role is independent of Mer3's helicase activity. Mer3's ability to hydrolyze ATP and unwind DNA, or rather the fact that this ability plays a very minor role in the functionality of the protein remains one of the biggest concerns when it comes to the role of Mer3. Although the helicase-dead mutant has a relatively mild effect on crossover formation and sporulation compared to the *mer3Δ*, the enzymatic activity of the protein is not disposable, yet shows mild spore viability defects when compared with *mer3Δ* (Nakagawa & Kolodner, 2002). It was suggested that although Mer3's binding to the D-loop is enough to stabilize them, the helicase activity might be reinforcing the stabilization (Pyatnitskaya et al., 2019). Perhaps Mer3 catalyzes partial unwinding of the D-loop until other helicases take over and thereby allows for stronger binding of the invading strand. The fact that other ZMM proteins are also involved in the D-loop stabilization (Börner et al., 2004; Jessop et al., 2006) explains why the lack of this functionality of Mer3 has just a mild effect. Discovering that the interaction between Mer3 and the Top3/Rmi1 complex is compatible with the previously described interaction with the Mlh1/Mlh2 complex raised questions about the role of such a "supercomplex" in regulating meiotic recombination. Up to date, little is known about its formation frequency. The Mlh1/Mlh2 complex is certainly recruited to the axis by Mer3 and together they perform a function of an ultimate brake that prevents overextension of the D-loop (Duroc et al., 2017). The STR activity to prevent CO formation occurs at the early stages of single-strand invasion intermediates, before the second end capture (de Muyt et al., 2012).

One of the possible chains of events is that at the time of the strand invasion, when the STR complex attempts to dissolve the newly formed DNA structure, the Mer3 helicase may be recruited. It outcompetes the Sgs1 from the STR complex. It is possible that Mer3 not only disrupts the STR complex, but also blocks the activity of Top3/Rmi1 and thereby prevents the dissolution of recombination intermediates. This would explain the previously discovered correlation between the absence of Mer3 and a decrease in the number of ZMM mediated CO events (Jessop et al., 2006). Finally, Mer3 recruits the Mlh1/Mlh2 complex. The presence of the Mlh1/Mlh2 complex may be required to act as a blockade that prevents D-loop extension or dissolution by Sgs1 or that stabilizes the interaction of Mer3 with Top3/Rmi1 making it impossible for the Top3/Rmi1 complex to disconnect and dissolve the DNA structure (Figure 2.6D).

In this manuscript we have presented the structural and biochemical analysis of the Mer3 helicase. We created a structural model using a combination of AlphaFold2 models, and XL-MS restraints. We also explored the novelty of the Mer3 dimerization. We completed a first structural analysis of Mer3 and the Mer3-Mlh1/Mlh2 complex, and we further determined the affinity of the binding. Additionally, we have identified a novel complex of Mer3 with Top3/Rmi1. We characterized the details of the structural and biochemical features of the complex. We showed that the Mer3/Top3/Rmi1 complex formation is compatible with the Mlh1/Mlh2 interaction by demonstrating the formation of a Mer3/Mlh1/Mlh2/Top3/Rmi1 “supercomplex”. Importantly we show that the interaction of Mer3 with Top3/Rmi1 is competitive with the interaction of Sgs1 helicase with Top3/Rmi1 and that the Mer3 helicase can prevent D-loop dissolution by the STR complex. To understand better the nature of this newly discovered interaction, further studies are needed. In the future, obtaining a credible model of the Mer3 dimer will help us to build the model of a Mer3 complex with the Top3/Rmi1 complex. This will allow designing point mutants of Mer3 that do not interact with Top3/Rmi1 and study the mutation's effects on meiotic recombination and meiotic progression. Simultaneously, we will continue our research to understand the function of the Mer3/Top3/Rmi1/Mlh1/Mlh2 “supercomplex” formation.

Our findings bring us a step closer to understanding the role of the Mer3 helicase in promoting ZMM-dependent crossovers. Knowing that Mer3 can prevent the dissolution of recombination intermediates may have key links to understanding why some of the intermediates are not

processed by the STR complex, indicating that Mer3 may be an essential factor in shifting the repair of the double-strand break towards crossover formation.

2.4. Methods

2.4.1. Plasmids

Sequences of *Saccharomyces cerevisiae* MER3, MLH1, MLH2, TOP3, RMI1, and SGS1 were derived from SK1 strain genomic DNA. Due to the presence of an intron in *MER3*, this was amplified as two separate fragments and Gibson-assembled. Plasmids used for protein expression were cloned as described in Altmannová et al., 2021.

Mer3, Mlh1, Mlh2, Top3, and Rmi1 were produced in the Hi-5 cell line derived from the cabbage looper *Trichoplusiani*. Mer3 was expressed as a fusion protein with a C-terminal Twin-Strep II. Mlh1/Mlh2 was expressed as a 3C HRV cleavable N-terminal MBP fusion using polycistronic vector. Rmi1 was expressed as a fusion protein with a 3C HRV cleavable N-terminal GST fusion. Top3 was expressed with a 6xHis, N-terminal 3C HRV cleavable tag. Top3/Rmi1 complex was expressed using a polycistronic vector where Rmi1 was expressed as a fusion protein with a 3C HRV cleavable N-terminal GST fusion. Bacmids for expression were cases produced in EmBacY cells and subsequently used to transfect Sf9 cells to produce baculovirus. Amplified baculovirus was used to infect Hi-5 cells in 1:100 dilution prior to 72-hour cultivation and harvest. Cells were washed with 1xPBS and always frozen in liquid nitrogen.

2.4.2. Protein purification

To purify Mer3, cells were resuspended in lysis buffer (50 mM HEPES pH 6.8, 300 mM NaCl, 5% glycerol, 0.1% Triton-X 100, 1 mM MgCl₂, 5 μM ZnCl₂, 5 mM beta-mercaptoethanol). Resuspended cells were lysed using an EmulsiFlex C3 (Avestin) in presence of Serva Protease-Inhibitor Mix and Benzonase before clearance at 130,000g at 4°C for 1h. Cleared lysate was applied on a 5 mL Strep-Tactin[®]XT column (iba) and extensively washed with lysis buffer. Mer3 constructs were eluted with a lysis buffer containing 50 mM Biotin. Eluted protein was passed through a HiTrap Heparin HP affinity column (GE Healthcare) preequilibrated with the loading buffer (50 mM HEPES pH 6.8, 300 mM NaCl, 5% glycerol, 1 mM MgCl₂, 5 μM ZnCl₂, 5 mM beta-mercaptoethanol). The proteins were eluted by increasing salt gradient to 1 M NaCl. Protein-containing elution fractions were concentrated on Vivaspin 15R, 30,000 MWCO Hydrosart

concentrators. The concentrated eluent was loaded on a Superdex 200 16/600 pre-equilibrated in SEC buffer (30 mM MES pH 6.5, 300 mM NaCl, 5% glycerol, 1 mM MgCl₂, 5 μM ZnCl₂, 1 mM TCEP). Purified protein was concentrated using Vivaspin 15R, 30,000 MWCO Hydrosart concentrators.

To purify the Mlh1/Mlh2 protein complex, cells were resuspended in lysis buffer (50 mM HEPES pH 6.8, 300 mM NaCl, 5% glycerol, 0.1% Triton-X 100, 1 mM MgCl₂, 5 mM beta-mercaptoethanol). Resuspended cells were lysed using an EmulsiFlex C3 (Avestin) in presence of Serva Protease-Inhibitor Mix and Benzonase before clearance at 130,000g at 4°C for 1h. Cleared lysate was applied on a 5 mL MBP-trap column (GE Healthcare) and extensively washed with lysis buffer. Mer3 constructs were eluted with a lysis buffer containing 1 mM Maltose. Eluted protein was passed through a HiTrap Heparin HP affinity column (GE Healthcare) pre-equilibrated with the loading buffer (50 mM HEPES pH 6.8, 300 mM NaCl, 5% glycerol, 1 mM MgCl₂, 5 mM beta-mercaptoethanol). The proteins were eluted by increasing salt gradient to 1 M NaCl. Protein-containing elution fractions were concentrated on Vivaspin 15R, 30,000 MWCO Hydrosart concentrators. The concentrated eluent was loaded on a Superdex 200 16/600 pre-equilibrated in SEC buffer (30 mM HEPES 6.8, 300 mM NaCl, 5% glycerol, 1 mM MgCl₂, 1 mM TCEP). Purified protein was concentrated using Vivaspin 15R, 30,000 MWCO Hydrosart concentrators.

Top3 was produced as an N-terminal 6xHis tag in Hi5 insect cells using the same expression conditions as described above. The cell pellet was resuspended in the lysis buffer (50 mM HEPES pH 7.5, 300 mM NaCl, 5% glycerol, 0.01% NP40, 5 mM β-mercaptoethanol, AEBSF). Resuspended cells were lysed by sonication before clearance at 35,000 rpm at 4 °C for 1 hr. Cleared lysate was loaded on a 5 mL HiTrap TALON Crude column (Cytiva) followed by a wash using 25 mL of H buffer (20 mM HEPES pH 7.5, 5% glycerol, 0.01% NP40, 1 mM β-mercaptoethanol) containing 150 mM NaCl. Top3 protein was eluted with a 50-mL gradient of 0-450 mM imidazole in an H buffer containing 150 mM NaCl. Partially purified protein was further loaded onto a 5 mL Heparin column (GE Healthcare) pre-equilibrated in H buffer containing 150 mM NaCl and eluted with an increasing salt gradient to 1 M NaCl. The fractions containing Top3 protein were then loaded onto a 6 mL ResourceS column (Cytiva) pre-equilibrated in an H buffer containing 150 mM NaCl and eluted with increasing salt gradient to 1 M NaCl. The peak fractions were concentrated on a 30 kDa MWCO Amicon concentrator and applied onto a Superose 6 10/300 column (Cytiva) pre-equilibrated in SEC buffer (20 mM

HEPES pH 7.5, 300 mM NaCl, 5% glycerol, 1 mM β -mercaptoethanol, 1 mM TCEP). The fractions containing Top3 were concentrated on a 30 kDa MWCO Amicon concentrator and stored at -80 °C in small aliquots.

Rmi1 was produced as an N-terminal GST tag in Hi5 insect cells using the same expression conditions as described above. The cell pellet was resuspended in the lysis buffer (50 mM HEPES pH 7.5, 300 mM NaCl, 5% glycerol, 0.01% NP40, 5 mM β -mercaptoethanol, AEBSEF). Resuspended cells were lysed by sonication before clearance at 35,000 rpm at 4 °C for 1 hr. Cleared lysate was loaded on a 5 mL GSTrap column (Cytiva) followed by wash using 25 mL of H buffer (20 mM HEPES pH 7.5, 5% glycerol, 0.01% NP40, 1 mM β -mercaptoethanol) containing 300 mM NaCl. The Rmi1 protein was eluted with 50 mL of H buffer containing 150 mM NaCl and 100 mM glutathione. Partially purified protein was further loaded onto a 6 mL ResourceS column (Cytiva) pre-equilibrated in H buffer containing 100 mM NaCl and eluted with increasing salt gradient to 1 M NaCl. The peak fractions were concentrated on a 30 kDa MWCO Amicon concentrator and applied onto a Superose 6 10/300 column (Cytiva) pre-equilibrated in SEC buffer (20 mM HEPES pH 7.5, 300 mM NaCl, 5% glycerol, 1 mM β -mercaptoethanol, 1 mM TCEP). The fractions containing GST-Rmi1 were concentrated on a 30 kDa MWCO Amicon concentrator and stored at -80 °C in small aliquots. To obtain untagged Rmi1, the concentrated elute fractions from ResourceS column were mixed with 3C HRV protease in a molar ratio of 50:1 and incubated overnight at 4 °C. Afterwards, the cleaved protein was loaded onto a Superdex 200 10/300 column (Cytiva) with its outlet connected to a 5 mL GSTrap column (Cytiva) pre-equilibrated in SEC buffer (20 mM HEPES pH 7.5, 300 mM NaCl, 5% glycerol, 1 mM β -mercaptoethanol, 1 mM TCEP). The fractions containing untagged Rmi1 were concentrated on a 10 kDa MWCO Amicon concentrator and stored at -80 °C in small aliquots.

To purify the Top3/Rmi1 complex, untagged Top3 and N-terminal GST-tagged Rmi1 were cloned into pBIG1a vector and expressed in Hi5 insect cells using the same expression conditions as described above. The cell pellet was resuspended in the lysis buffer (50 mM HEPES pH 7.5, 300 mM NaCl, 5% glycerol, 0.01% NP40, 5 mM β -mercaptoethanol, AEBSEF). Resuspended cells were lysed by sonication before clearance at 35,000 rpm at 4 °C for 1 hr. Cleared lysate was loaded on a 5 mL GSTrap column (Cytiva) followed by wash using 25 mL of H buffer (20 mM HEPES pH 7.5, 5% glycerol, 0.01% NP40, 1 mM β -mercaptoethanol) containing 300 mM NaCl. The Top3/Rmi1 complex was eluted with 50 mL of H buffer

containing 100 mM NaCl and 100 mM glutathione. Partially purified protein was further loaded onto a 6 mL ResourceS column (Cytiva) pre-equilibrated in H buffer containing 100 mM NaCl and eluted with an increasing salt gradient to 800 mM NaCl. The peak fractions were concentrated on a 30 kDa MWCO Amicon concentrator and applied onto a Superose 6 10/300 column (Cytiva) pre-equilibrated in SEC buffer (20 mM HEPES pH 7.5, 300 mM NaCl, 5% glycerol, 1 mM β -mercaptoethanol, 1 mM TCEP). The fractions containing the Top3/Rmi1 complex were concentrated on a 30 kDa MWCO Amicon concentrator and stored at -80 °C in small aliquots. To obtain untagged Top3/Rmi1 complex, the concentrated elute fractions from ResourceS column were mixed with 3C HRV protease in a molar ratio of 50:1 and incubated overnight at 4 °C. Afterwards, the cleaved protein was loaded onto a Superdex 200 10/300 column (Cytiva) with its outlet connected to a 5 mL GSTrap column (Cytiva) pre-equilibrated in SEC buffer (20 mM HEPES pH 7.5, 300 mM NaCl, 5% glycerol, 1 mM β -mercaptoethanol, 1 mM TCEP). The fractions containing untagged Top3/Rmi1 were concentrated on a 10 kDa MWCO Amicon concentrator and stored at -80 °C in small aliquots.

Sgs1 containing an N-terminal 6xHis-MBP tag and C-terminal 6xHis tag was produced in Hi5 cells using the similar expression conditions as described above with a minor change in using 1:300 dilution of baculovirus. The cell pellet (17 g) was resuspended in the lysis buffer (50 mM HEPES pH 7.5, 300 mM NaCl, 5% glycerol, 0.01% NP40, 5 mM β -mercaptoethanol, AEBSF, Serva protease inhibitor cocktail, and 1 mM PMSF). Resuspended cells were lysed by sonication before clearance at 35,000 rpm at 4 °C for 1 hr. Cleared lysate was loaded on a 5 mL MBPTrap column (Cytiva) followed by wash using 35 mL of H buffer (20 mM HEPES pH 7.5, 5% glycerol, 0.01% NP40, 1 mM β -mercaptoethanol) containing 300 mM NaCl. The Sgs1 protein was eluted with a 50-mL gradient of 0-20 mM maltose of H buffer containing 150 mM NaCl. To cleave off the N-terminal 6xHis-MBP tag, partially purified protein was mixed with 100 μ L 3C HRV protease (6 μ g/ μ L) and incubated overnight at 4 °C. Afterwards, the cleaved protein was loaded onto a 5 mL Heparin column (Cytiva) pre-equilibrated in H buffer containing 100 mM NaCl and eluted with an increasing salt gradient from 300 mM to 1 M NaCl. The fractions containing Sgs1 protein were concentrated on a 100 kDa MWCO Amicon concentrator and stored at -80 °C in small aliquots.

Sgs1(1-605) fragment containing N-terminal 6xHis-MBP tag was produced in *E. coli* strain BL21 STAR. Protein expression was induced by 0.2 mM IPTG at 18 °C overnight in TB media supplemented with ampicillin (100 μ g/mL). The cell pellet was resuspended in the lysis buffer

(50 mM HEPES pH 7.5, 300 mM NaCl, 5% glycerol, 0.01% NP40, 5 mM β mercaptoethanol, AEBSF, Serva protease inhibitor cocktail). Resuspended cells were lysed by sonication before clearance at 35,000 rpm at 4 °C for 1 hr. Cleared lysate was loaded on a 5 mL MBPtrap column (Cytiva) followed by the first wash using 25 mL of H buffer (20 mM HEPES pH 7.5, 5% glycerol, 0.01% NP40, 1 mM β -mercaptoethanol) containing 500 mM NaCl and the second wash using H buffer containing 150 mM NaCl. The protein was eluted with a 50 mL of H buffer containing 150 mM NaCl and 20 mM maltose. Partially purified protein was further loaded onto a 6 mL ResourceQ column (Cytiva) pre-equilibrated in H buffer containing 150 mM NaCl and eluted with increasing salt gradient to 1 M NaCl. The fractions containing Sgs1 fragment were concentrated on a 30 kDa MWCO Pierce concentrator and incubated with 3C HRV protease in a molar ratio of 50:1 overnight at 4 °C. Afterwards, the cleaved protein was applied onto a Superose 6 10/300 column (Cytiva) with its outlet connected to a 5 mL GSTRap column (Cytiva) followed by a 5 mL MBPtrap column (Cytiva). All columns were pre-equilibrated in SEC buffer (20 mM HEPES pH 7.5, 300 mM NaCl, 5% glycerol, 1 mM β -mercaptoethanol, 1 mM TCEP). The fractions containing Sgs1 protein were concentrated on a 50 kDa MWCO Amicon concentrator and stored at -80 °C in small aliquots.

Dmc1 was purified as described in Busygina et al., 2013 with minor modifications. Briefly, the plasmid expressing Dmc1 protein with N-terminus (His)₆-affinity tag (a kind gift from Lumir Krejci) was introduced into *E. coli* strain Rosetta (DE3)pLysS. Protein expression was induced by 0.5 mM IPTG at 37°C for 3 hours in LB media supplemented with ampicillin (100 μ g/mL). The cell pellet was resuspended in the lysis buffer (25 mM Tris-HCl pH 7.5, 500 mM NaCl, 10% glycerol, 0.5 mM EDTA, 0.01% NP40, 1 mM DTT, 1 mM MgCl₂, 1 mM ATP, and AEBSF). Resuspended cells were lysed by sonication before clearance at 35,000 rpm at 4 °C for 45 min. Cleared lysate was incubated with 400 μ l of Talon Resin (TaKaRa) for 1 hr at 4 °C. The beads were washed with 10 mL of buffer T (25 mM Tris-HCl pH 7.5, 10% glycerol, 0.5 mM EDTA, 0.01% NP40, 1 mM DTT) containing 150 mM NaCl followed by additional washing step with 10 mL of buffer T containing 500 mM NaCl. The protein was eluted in steps with 200 and 500 mM imidazole in buffer T containing 140 mM NaCl, 1 mM MgCl₂, and 1 mM ATP. Fractions containing Dmc1 protein were applied onto a 5-mL Heparin column (GE Healthcare) equilibrated with buffer T containing 140 mM NaCl and eluted using a 25-mL gradient of 140-1000 mM NaCl in buffer T containing 1 mM MgCl₂ and 1 mM ATP. The peak fractions were concentrated on a 30 kDa MWCO Amicon concentrator and applied onto a Superose 6 10/300

column (Cytiva) pre-equilibrated in SEC buffer (20 mM HEPES pH 7.5, 300 mM NaCl, 5% glycerol, 1 mM DTT) supplied with 1 mM MgCl₂ and 1 mM ATP. The fractions containing Dmc1 were concentrated on a 30 kDa MWCO Amicon concentrator and stored at -80 °C in small aliquots.

RPA complex was produced in *E. coli* strain C41 by co-expression of pCOLI-Twin-StrepII-Rfa1, pCDF-6xHis-Rfa2, and pRSF-6xHis-Rfa3 plasmids. Protein expression was induced by 0.5 mM IPTG at 25 °C for 3 hours in TB media supplemented with ampicillin (100 µg/mL), kanamycin (25 µg/mL), and spectinomycin (50 µg/mL). The cell pellet was resuspended in the lysis buffer (50 mM HEPES pH 7.5, 300 mM NaCl, 5% glycerol, 0.01% NP40, 5 mM β-mercaptoethanol, AEBSF). Resuspended cells were lysed by sonication before clearance at 35,000 rpm at 4 °C for 40 min. Cleared lysate was loaded on a 5 mL Strep-Tactin XT column (IBA) followed by wash using 25 mL of H buffer (20 mM HEPES pH 7.5, 5% glycerol, 0.01% NP40, 1 mM β-mercaptoethanol) containing 150 mM NaCl. The protein was eluted with a 50 mL of H buffer containing 100 mM NaCl and 50 mM biotin. Partially purified protein was further loaded onto a 5 mL Heparin column (GE Healthcare) pre-equilibrated in H buffer containing 150 mM NaCl and eluted with increasing salt gradient to 1 M NaCl. The peak fractions were concentrated on a 10 kDa MWCO Amicon concentrator and applied onto a Superose 6 10/300 column (Cytiva) pre-equilibrated in SEC buffer (20 mM HEPES pH 7.5, 300 mM NaCl, 5% glycerol, 1 mM β-mercaptoethanol, 1 mM TCEP). The fractions containing RPA complex were concentrated on a 10 kDa MWCO Amicon concentrator and stored at -80 °C in small aliquots.

2.4.3. Mass Photometry

Mass Photometry was performed in 30 mM HEPES pH 7.8, 150 mM NaCl, 5% glycerol, 1 mM MgCl₂, 1 mM TCEP. Samples were preequilibrated for 1h in the mass photometry buffer to a 3 µM concentration. Samples that were crosslinked contained 3 mM DSBU. Measurements were performed using Refeyn One mass photometer. Directly before the measurement, the sample was diluted 1:100 with the mass photometry buffer. Molecular mass was determined in Analysis software provided by the manufacturer using a NativeMark (Invitrogen) based standard curve created under the identical buffer composition.

2.4.4. DNA substrates

Fluorescently labeled DNA substrates were prepared as described previously (de Muyt et al., 2018; Ranjha et al., 2014). The sequences of all oligonucleotides were also used as in Ranjha et al., 2014.

2.4.5. Electrophoretic mobility shift assays

The binding reactions (10 μ L volume) were carried out in 25 mM HEPES pH 7.5, 0.1 μ g/ μ L BSA, 60 mM NaCl, and 10 nM fluorescently labeled DNA substrate. The reactions were started by the addition of increasing amounts of Mer3 protein (37.5, 75, 150, and 300 nM) and incubated for 20 min at 30 °C. After the addition of 2 μ L of the gel loading buffer (60% glycerol, 10 mM Tris-HCl, pH 7.4, 60 mM EDTA, 0.15% Orange G), the reaction mixtures were resolved in 0.8% agarose gel in 1x TAE buffer (40 mM Tris, 20 mM acetic acid, 1 mM EDTA, pH 7.5). The gels were scanned using Amersham Typhoon scanner (Cytiva) and quantified by ImageQuant TL software (Cytiva).

2.4.6. Strand separation assays

The strand separation assays (10 μ L volume) were carried out in 25 mM HEPES pH 7.5, 60 mM NaCl, 0.1 μ g/ μ L BSA, 1 mM MgCl₂, 1 mM ATP, 10 mM creatine phosphatase, 15 μ g/ml creatine kinase, and 5 nM fluorescently labeled DNA substrate. The reactions were started by the addition of increasing amounts of Mer3 protein (10, 20, 40, and 80 nM). After the incubation for 30 min at 30 °C the reactions were stopped with 0.5 mg/mL proteinase K and 0.1% SDS and incubated for 5 min at 37 °C. The samples were then mixed with 2 μ L of the gel loading buffer (60% glycerol, 10 mM Tris-HCl, pH 7.4, 60 mM EDTA) and separated on 10% (w/v) native polyacrylamide gel in 1xTBE buffer at a constant voltage of 110 V for 1 h at 4 °C. The gels were scanned using Amersham Typhoon scanner (Cytiva) and quantified by ImageQuant TL software (Cytiva).

2.4.7. Crosslinking Mass Spectrometry (XL-MS)

For the XL-MS analysis, proteins were diluted in 200 μ L 30 mM HEPES 6.8, 150 mM NaCl, 5% glycerol, 1 mM MgCl₂, 1 mM TCEP to the final concentration of 3 μ M, mixed with 3 μ L of DSBU (200 mM) and incubated for 1 hour at 25 °C. The reaction was stopped by adding 20 μ L of Tris pH 8.0 (1 M) and incubated for another 30 min at 25 °C. The crosslinked sample was precipitated by the addition of 4X volumes of 100% cold acetone and incubation ON at -20 °C.

Samples were analyzed as previously described (Pan, D., Musacchio, A. & Bange 2018). For interaction network visualization, XVis software was used. For the visualization of the crosslinks on the PyMol model, the PyXlinkViewer was used. Each time, different cutoff for the crosslinking credibility was selected, depending on the quality of the crosslinking data.

2.4.8. Biacore interactions

All experiments were performed at 25 °C using a Biacore X100 instrument. The CM5 chip was activated and SA-Streptag® II fusion protein was immobilized on it (Cytiva protocol Stable and oriented immobilization of SA-Strep-tag® II fusion proteins on Biacore Sensor Chip CM5). All samples were prepared in biacore buffer (30 mM MES pH 6.5, 300 mM NaCl, 5% glycerol, 1 mM MgCl₂, 5 µM ZnCl₂, 1 mM TCEP, 1% BSA, 1% CM-Dextran). Mer3 was immobilized on the chip until RU between 100 and 200 (500 nM Mer3, 45 s contact time, flow rate 10 µl/min). This biacore buffer was used as the running buffer during sample analysis. MBP-Mlh1/MBP-Mlh2 complex samples were diluted in biacore buffer to 23.4 nM; 93.8 nM; 375 nM; 1500 nM and 6000 nM concentrations and injected over the Mer3 covered surface, as well as over SA-Strep-tag surface as a background control, at a flow rate of 10 µl/min, 60 s association time, followed by the 60 s dissociation. The surface was then regenerated with 60 s injections of 3 M MgCl₂ and 30 s injections of 6 M guanidine chloride at a flow rate of 30 µl/min. Results were then processed using Biacore™ Insight Evaluation Software

2.4.9. SEC-MALS

50 µL samples at 10 µM concentration were loaded onto a Superose 6 5/150 (for the full-length protein) analytical size-exclusion column (GE Healthcare) equilibrated in SEC buffer (30 mM HEPES pH 6.8, 300 mM NaCl, 1 mM MgCl₂, 5 µM ZnCl₂, 1 mM TCEP) attached to a 1260 Infinity II LC System (Agilent). MALS was carried out using a Wyatt DAWN detector attached in line with the size-exclusion column. Mer3 fragments were analyzed on Superdex 200 5/150 column (GE Healthcare) equilibrated in SEC2 buffer (50 mM HEPES pH 7.5, 300 mM NaCl, 1 mM TCEP).

2.4.10. AlphaFold2

The monomeric model of Mer3 was generated using the ColabFold online tool (Mirdita et al., 2022). Protein complexes were generated using scripts available at <https://github.com/deepmind/alphafold>.

2.4.11. Pull-down assays

For pull-down between Top3 and Mer3, His-tagged Top3 (1.3 μM) was incubated with Strep-tagged Mer3 (0.7 μM) in the reaction buffer (25 mM HEPES pH 7.5, 5% glycerol, 50 mM NaCl, 1 mM TCEP, 0.1% Tween-20) for 20 min at 30 °C in the thermomixer (950 rpm). Anti-Strep antibody (2 μL , Abcam, ab76949) was added to the reactions and the mixtures were incubated for 1 hour at 4 °C in the thermomixer (950 rpm). Finally, 0.5 μL pre-washed magnetic-conjugated protein G beads (Dynabeads protein G, Invitrogen) were added to the reactions followed by the incubation for 1 hour at 4 °C in the thermomixer (950 rpm). Beads were washed twice with 100 μL of the reaction buffer. The proteins were eluted by boiling in 30 μL 2x SDS Laemmli buffer. The samples were loaded onto 11% SDS-PAGE and analyzed by western blot.

For pull-down between Rmi1 and Mer3, GST-tagged Rmi1 (2.5 μM) was incubated with Strep-tagged Mer3 (0.7 μM) in the reaction buffer (25 mM HEPES pH 7.5, 5% glycerol, 75 mM NaCl, 1 mM TCEP, 0.1% Tween-20) for 20 min at 30 °C in the thermomixer (950 rpm). Pre-washed glutathione beads (10 μL) were then added to the samples and the mixtures were incubated for 30 min at 7°C in the thermomixer (950 rpm). Beads were washed twice with 100 μL of the reaction buffer. The proteins were eluted by boiling in 30 μL 2x SDS Laemmli buffer. The samples were loaded onto 11% SDS-PAGE and stained by Der Blaue Jonas gel dye.

For pull-down between Mer3 and Top3/Rmi1 in the presence or absence of Sgs1(1-605), GST-tagged Top3/Rmi1 (0.8 μM) was incubated with Strep-tagged Mer3 (0.7 μg) in the reaction buffer (25 mM HEPES pH 7.5, 5% glycerol, 100 mM NaCl, 1 mM TCEP, 0.1% Tween-20) for 20 min at 30 °C in the thermomixer (950 rpm). For competition assays, increasing amounts of untagged Sgs1(1-605) were added to the reactions. Pre-washed magnetic glutathione beads (1 μL) were then added to the samples and the mixtures were incubated for 2 min at 30 °C in the thermomixer (750 rpm). Beads were washed twice with 100 μL of the reaction buffer. The proteins were eluted by boiling in 30 μL 2x SDS Laemmli buffer. The samples were loaded onto 10% SDS-PAGE and stained by Der Blaue Jonas gel dye.

For pull-down between Mlh1/Mlh2 and Mer3, MBP-tagged Mlh1/Mlh2 complex (0.13 μM) was incubated with Strep-tagged Mer3 (0.24 μM) in the reaction buffer (25 mM HEPES pH 7.5, 100 mM NaCl, 1 mM MgCl_2 , 1 mM DTT) for 20 min at 30 °C in the thermomixer (950 rpm). Anti-MBP antibody (0.5 μL , Invitrogen, PA1-989) was added to the reactions and the mixtures were incubated for 1 hour at 4 °C in the thermomixer (750 rpm). Finally, 1 μL pre-washed

magnetic-conjugated protein G beads (Dynabeads protein G, Invitrogen) were added to the reactions followed by the incubation for 1 hour at 4 °C in the thermomixer (750 rpm). Beads were washed twice with 100 µL of the reaction buffer. The proteins were eluted by boiling in 30 µL 2x SDS Laemmli buffer. The samples were loaded onto 9% SDS-PAGE and analyzed by western blot. Pull-down between Mer3, Mlh1/Mlh2 and Top3/Rmi1 complex (all 1 µg) was done using the same protocol but in reaction buffer containing 25 mM HEPES pH 7.5, 5% glycerol, 75 mM NaCl, 1 mM TCEP, 0.1% Tween-20.

2.4.12. Microscale thermophoresis (MST)

Binding affinity analysis by microscale thermophoresis was performed using the Monolith NT instrument (Nanotemper Technologies). All reactions (in triplicates) were done in the commercial MST buffer (50 mM Tris-HCl pH 7.4, 150 mM NaCl, 10 mM MgCl₂; Nanotemper Technologies) supplied with 0.05% Tween-20. Measurements were performed at 25 °C and contained a constant concentration of 45 nM RED-NHS labeled Mer3 (labeling was performed according to the manufacturer's protocol – Nanotemper Technologies) and increasing concentrations of Top3/Rmi1, Rmi1, His-Top3, or Mlh1/Mlh2, respectively. Data were analyzed by the MO. Affinity Analysis software (NanoTemper Technologies).

2.4.13. D-loop assay

The reactions (in a total volume 22 µL) were performed in D-loop reaction buffer (25 mM HEPES pH 7.5, 0.1 µg/µL BSA, 100 mM NaCl, 1 mM MgCl₂, 1 mM ATP, 10 mM creatine phosphatase, 15 µg/ml creatine kinase). Radioactively labeled 90-mer ssDNA (oWL981, 2 µM nucleotides) was incubated with Dmc1 protein (1.5 µM) for 5 min at 37 °C followed by addition of RPA (90 nM) and additional incubation for 5 min at 37 °C. The formation of D-loop was started by the addition of pUC19 plasmid (18 nM molecules). After 15 min incubation at 30 °C, Sgs1 (15 nM), Top3/Rmi1 (15 nM) and the increasing amounts of Mer3 (15, 150, 300 nM) were added to the reactions. At the indicated time points, 10.5 µL of the sample was mixed with 0.5% SDS (final) and 0.5 mg/mL proteinase K followed by incubation for 15 min at 37 °C. The deproteinized samples were separated in a 0.9% agarose gel. After electrophoresis, the gel was dried on grade 3 chromosome paper (Whatman), exposed to a phosphorimager screen, and visualized using Amersham Typhoon scanner (Cytiva). The quantification was done using ImageQuant TL software (Cytiva).

2.4.14. Yeast strains

All strains, except those used for Y2H analysis, are of the SK1 background and their genotypes are listed in Supplementary Table 2.2.

2.4.15. Yeast two-hybrid assay

Yeast genes ORFs were PCR-amplified from SK1 strain genomic DNA. MER3 was prepared by Gibson assembly of 2 PCR products eliminating MER3's intron. Human HFM1, MLH1, and TOP3a cDNA were amplified from human cDNA (a kind gift from Dingwen Su). The corresponding genes were cloned into pGAD-C1 or pGBDU-C1 vectors, respectively. The resulting plasmids were co-transformed into the *S. cerevisiae* reporter strain (yWV365) and plated onto the selective medium lacking leucine and uracil. For drop assay, 2.5 μ L from 10-fold serial dilutions of cell cultures with the initial optical density (OD₆₀₀) of 0.5 were spotted onto -Leu/-Ura (control) and -Leu/-Ura/-His plates with or without 1 mM 3-aminotriazole. Cells were grown at 30 °C for up to 4-6 days. and imaged.

2.4.16. Meiotic time course

Cells were grown overnight in liquid YPD culture at 30 °C followed by inoculation in pre-sporulation media (BYTA; 50 mM potassium phthalate, 1% yeast extract, 2% bacto-tryptone, and 1% potassium acetate) at OD₆₀₀ = 0.3 for additional 16-18 hours at 30 °C. The next morning, cells were washed twice with sporulation medium (SPO, 0.3% potassium acetate) and resuspended in sporulation medium at OD₆₀₀ = 1.9 to induce meiosis at 30 °C.

2.4.17. In vivo co-immunoprecipitation

100 mL of meiotic cultures (at 6 hours into a meiotic time course) were harvested by spinning down at 3,000 rpm for 5 min followed by a wash with 500 μ L of cold H₂O containing 1 mM PMSF. Cell pellets were resuspended in 350 μ L of ice-cold co-IP buffer (50 mM Tris-HCl pH 7.5, 150 mM NaCl, 1% Nonidet P-40, 1 mM EDTA pH 8.0, 1 mM PMSF, AEBSF, Serva protease cocktail and a cocktail of protease inhibitors that was freshly added) and glass beads. The cells were lysed using a FastPrep-24 disruptor (MP Biomedicals) (setting: 2x 40 s cycles at speed 6.0). Lysates were cleared by 2 rounds of centrifugation for 10 min at 15,000 rpm and the supernatants were transferred to a clean microcentrifuge tube after each centrifugation step. 1 μ L of antibody (anti-HA; Sigma-Aldrich H6908) was added to the samples followed by 3 hours of incubation at 4 °C. Subsequently, 25 μ L of buffer washed Dynabeads Protein G (Thermo

Fisher Scientific) was added and the samples were incubated overnight at 4 °C. The next day, Dynabeads were washed four times with 500 µL of ice-cold IP buffer. For the final wash, beads were transferred to a new microcentrifuge tube and washed 500 µL of ice-cold IP buffer without Nonidet P-40. The beads were resuspended in 55 µL of 2x SDS Laemmli buffer and incubated for 5 min at 95 °C. The samples were loaded onto a 9% SDS-polyacrylamide gel and blotted to a nitrocellulose membrane. Antibodies used were as follows: anti-PGK1 (22C5D8, Thermo Fisher Scientific, 459250, 1:1,000), anti-HA (Sigma-Aldrich H6908, 1:1,000), anti-Myc (Abcam, ab1326, 1:1,000), goat anti-rabbit IgG peroxidase conjugate (Merck, 401353), goat anti-mouse IgG peroxidase conjugate (Merck, 401215). The signal was detected using ECL Prime Western Blotting Detection Reagents (Cytiva) and visualized by a ChemiDocMP (Bio-Rad Inc).

Acknowledgments

We thank members of the Weir Lab for critical reading and input into the manuscript. IP-MS analysis was carried out in the Proteomics Facility at EMBL, Heidelberg. Thanks to Vikram Alva for advice on AlphaFold2 modeling and analysis. Thanks to Dorota Rousová for help with SEC-MALS experiments. We thank Franziska Müller and Petra Janning (MPI Molecular Physiology, Dortmund) for XL-MS experiments. Work in the Weir Lab is supported by the Max Planck Society and the German Research Foundation.

References

- Absmeier, E., Wollenhaupt, J., Mozaffari-Jovin, S., Becke, C., Lee, C. T., Preussner, M., Heyd, F., Urlaub, H., Lührmann, R., Santos, K. F., & Wahl, M. C. (2015). The large N-terminal region of the Brr2 RNA helicase guides productive spliceosome activation. *Genes and Development*, 29(24), 2576–2587. <https://doi.org/10.1101/GAD.271528.115>
- Altmannova, V., Blaha, A., Astrinidis, S., Reichle, H., & Weir, J. R. (2021). InteBac: An integrated bacterial and baculovirus expression vector suite. *Protein Science*, 30(1), 108–114. <https://doi.org/10.1002/PRO.3957>
- Bocquet, N., Bizard, A. H., Abdulrahman, W., Larsen, N. B., Faty, M., Cavadini, S., Bunker, R. D., Kowalczykowski, S. C., Cejka, P., Hickson, I. D., & Thomä, N. H. (2014). Structural and mechanistic insight into Holliday junction dissolution by Topoisomerase III α and RMI1. *Nature Structural & Molecular Biology*, 21(3), 261. <https://doi.org/10.1038/NSMB.2775>

Börner, G. V., Kleckner, N., & Hunter, N. (2004). Crossover/noncrossover differentiation, synaptonemal complex formation, and regulatory surveillance at the leptotene/zygotene transition of meiosis. *Cell*, *117*(1), 29–45. [https://doi.org/10.1016/S0092-8674\(04\)00292-2](https://doi.org/10.1016/S0092-8674(04)00292-2)

Busygina, V., Gaines, W. A., Xu, Y., Kwon, Y., Williams, G. J., Lin, S. W., Chang, H. Y., Chi, P., Wang, H. W., & Sung, P. (2013). Functional attributes of the *Saccharomyces cerevisiae* meiotic recombinase Dmc1. *DNA Repair*, *12*(9), 707–712. <https://doi.org/10.1016/J.DNAREP.2013.05.004>

Cejka, P., & Kowalczykowski, S. C. (2010). The full-length *Saccharomyces cerevisiae* Sgs1 protein is a vigorous DNA helicase that preferentially unwinds holliday junctions. *Journal of Biological Chemistry*, *285*(11), 8290–8301. <https://doi.org/10.1074/jbc.M109.083196>

Chen, C., Zhang, W., Timofejeva, L., Gerardin, Y., & Ma, H. (2005). The Arabidopsis ROCK-N-ROLLERS gene encodes a homolog of the yeast ATP-dependent DNA helicase MER3 and is required for normal meiotic crossover formation. *The Plant Journal: For Cell and Molecular Biology*, *43*(3), 321–334. <https://doi.org/10.1111/J.1365-313X.2005.02461.X>

de los Santos, T., Hunter, N., Lee, C., Larkin, B., Loidl, J., & Hollingsworth, N. M. (2003). The Mus81/Mms4 endonuclease acts independently of double-Holliday junction resolution to promote a distinct subset of crossovers during meiosis in budding yeast. *Genetics*, *164*(1), 81–94. <https://doi.org/10.1093/GENETICS/164.1.81>

de Muyt, A., Jessop, L., Kolar, E., Sourirajan, A., Chen, J., Dayani, Y., & Lichten, M. (2012). BLM helicase ortholog Sgs1 is a central regulator of meiotic recombination intermediate metabolism. *Molecular Cell*, *46*(1), 43. <https://doi.org/10.1016/J.MOLCEL.2012.02.020>

de Muyt, A., Pyatnitskaya, A., Andréani, J., Ranjha, L., Ramus, C., Laureau, R., Fernandez-Vega, A., Holoch, D., Girard, E., Govin, J., Margueron, R., Couté, Y., Cejka, P., Guérois, R., & Borde, V. (2018). A meiotic XPF–ERCC1-like complex recognizes joint molecule recombination intermediates to promote crossover formation. *Genes & Development*, *32*(3–4), 283–296. <https://doi.org/10.1101/GAD.308510.117>

Duroc, Y., Kumar, R., Ranjha, L., line Adam, C., Gué rois, R., Md Muntaz, K., Marsolier-Kergoat, M.-C., Dingli, F., Ile Laureau, R., Loew, D., Llorente, B., Charbonnier, J.-B., Cejka, P., & rie Borde, V. (2017). *Concerted action of the MutLb heterodimer and Mer3 helicase regulates the global extent of meiotic gene conversion*. <https://doi.org/10.7554/eLife.21900.001>

Gao, M., Nakajima An, D., Parks, J. M., & Skolnick, J. (2022). AF2Complex predicts direct physical interactions in multimeric proteins with deep learning. *Nature Communications* 2022 *13*:1, *13*(1), 1–13. <https://doi.org/10.1038/s41467-022-29394-2>

Harami, G. M., Pálinkás, J., Seol, Y., Kovács, Z. J., Gyimesi, M., Harami-Papp, H., Neuman, K. C., & Kovács, M. (2022). The topoisomerase III α -RMI1-RMI2 complex orients human Bloom’s syndrome helicase for efficient disruption of D-loops. *Nature Communications*, *13*(1). <https://doi.org/10.1038/s41467-022-28208-9>

Hatkevich, T., & Sekelsky, J. (2017). Bloom syndrome helicase in meiosis: Pro-crossover functions of an anti-crossover protein. *BioEssays*, *39*(9), 1700073. <https://doi.org/10.1002/BIES.201700073>

Hodson, C., Low, J. K. K., van Twest, S., Jones, S. E., Swuec, P., Murphy, V., Tsukada, K., Fawkes, M., Bythell-Douglas, R., Davies, A., Holien, J. K., O'Rourke, J. J., Parker, B. L., Glaser, A., Parker, M. W., Mackay, J. P., Blackford, A. N., Costa, A., & Deans, A. J. (2022). Mechanism of Bloom syndrome complex assembly required for double Holliday junction dissolution and genome stability. *Proceedings of the National Academy of Sciences of the United States of America*, 119(6). https://doi.org/10.1073/PNAS.2109093119/SUPPL_FILE/PNAS.2109093119.SD01.XLSX

Jessop, L., Rockmill, B., Roeder, G. S., & Lichten, M. (2006). Meiotic chromosome synapsis-promoting proteins antagonize the anti-crossover activity of *sgs1*. *PLoS Genetics*, 2(9), 1402–1412. <https://doi.org/10.1371/journal.pgen.0020155>

Jumper, J., Evans, R., Pritzel, A., Green, T., Figurnov, M., Ronneberger, O., Tunyasuvunakool, K., Bates, R., Žídek, A., Potapenko, A., Bridgland, A., Meyer, C., Kohl, S. A. A., Ballard, A. J., Cowie, A., Romera-Paredes, B., Nikolov, S., Jain, R., Adler, J., ... Hassabis, D. (2021). Highly accurate protein structure prediction with AlphaFold. *Nature* 2021 596:7873, 596(7873), 583–589. <https://doi.org/10.1038/s41586-021-03819-2>

Kaur, H., DeMuyt, A., & Lichten, M. (2015). Top3-Rmi1 DNA single-strand decatenase is integral to the formation and resolution of meiotic recombination intermediates. *Molecular Cell*, 57(4), 583–594. <https://doi.org/10.1016/j.molcel.2015.01.020>

Keeney, S. (2008). Spo11 and the Formation of DNA Double-Strand Breaks in Meiosis. *Genome Dynamics and Stability*, 2, 81–123. https://doi.org/10.1007/7050_2007_026

Kohl, K. P., & Sekelsky, J. (2013). Meiotic and Mitotic Recombination in Meiosis. *Genetics*, 194(2), 327–334. <https://doi.org/10.1534/GENETICS.113.150581>

Liu, S., Rauhut, R., Vornlocher, H. P., & Lührmann, R. (2006). The network of protein–protein interactions within the human U4/U6.U5 tri-snRNP. *RNA*, 12(7), 1418. <https://doi.org/10.1261/RNA.55406>

Lynn, A., Soucek, R., & Börner, G. V. (2007). ZMM proteins during meiosis: Crossover artists at work. In *Chromosome Research* (Vol. 15, Issue 5, pp. 591–605). <https://doi.org/10.1007/s10577-007-1150-1>

Mazina, O. M., Mazin, A. v, Nakagawa, T., Kolodner, R. D., & Kowalczykowski, S. C. (2004). *Saccharomyces cerevisiae* Mer3 Helicase Stimulates 3-5 Heteroduplex Extension by Rad51: Implications for Crossover Control in Meiotic Recombination Division of Biological Sciences Sections of Microbiology and of Molecular Rad51 and Dmc1 proteins bind to the ssDNA tails to and Cellular Biology form filamentous nucleoprotein structures that promote Center for Genetics and Development a search for homologous DNA (Hong et al junction blunt end 5-overhang, implying that the. In *Cell* (Vol. 117).

Mirdita, M., Schütze, K., Moriwaki, Y., Heo, L., Ovchinnikov, S., & Steinegger, M. (2022). ColabFold: making protein folding accessible to all. *Nature Methods* 2022, 1–4. <https://doi.org/10.1038/s41592-022-01488-1>

Nakagawa, T., Flores-Rozas, H., & Kolodner, R. D. (2001). The MER3 Helicase Involved in Meiotic Crossing Over Is Stimulated by Single-stranded DNA-binding Proteins and Unwinds DNA in the 3' to 5'

Direction. *Journal of Biological Chemistry*, 276(34), 31487–31493. <https://doi.org/10.1074/jbc.M104003200>

Nakagawa, T., & Kolodner, R. D. (2002). Saccharomyces cerevisiae Mer3 Is a DNA Helicase Involved in Meiotic Crossing Over. *Molecular and Cellular Biology*, 22(10), 3281–3291. <https://doi.org/10.1128/mcb.22.10.3281-3291.2002>

Nakagawa, T., & Ogawa, H. (1999). The Saccharomyces cerevisiae MER3 gene, encoding a novel helicase-like protein, is required for crossover control in meiosis. *The EMBO Journal*, 18(20), 5714–5723. <https://doi.org/10.1093/EMBOJ/18.20.5714>

Nicklas, R. B. (1997). How cells get the right chromosomes. *Science (New York, N.Y.)*, 275(5300). <https://doi.org/10.1126/SCIENCE.275.5300.632>

Pâques, F., & Haber, J. E. (1999). Multiple pathways of recombination induced by double-strand breaks in Saccharomyces cerevisiae. *Microbiology and Molecular Biology Reviews : MMBR*, 63(2), 349–404. <https://doi.org/10.1128/MMBR.63.2.349-404.1999>

Pena, V., Jovin, S. M., Fabrizio, P., Orłowski, J., Bujnicki, J. M., Lührmann, R., & Wahl, M. C. (2009). Common Design Principles in the Spliceosomal RNA Helicase Brr2 and in the Hel308 DNA Helicase. *Molecular Cell*, 35(4), 454–466. <https://doi.org/10.1016/j.molcel.2009.08.006>

Petronczki, M., Siomos, M. F., & Nasmyth, K. (2003). Un ménage à quatre: the molecular biology of chromosome segregation in meiosis. *Cell*, 112(4), 423–440. [https://doi.org/10.1016/S0092-8674\(03\)00083-7](https://doi.org/10.1016/S0092-8674(03)00083-7)

Pyatnitskaya, A., Borde, V., & de Muyt, A. (2019). Crossing and zipping: molecular duties of the ZMM proteins in meiosis. In *Chromosoma* (Vol. 128, Issue 3, pp. 181–198). Springer Science and Business Media Deutschland GmbH. <https://doi.org/10.1007/s00412-019-00714-8>

Ranjha, L., Anand, R., & Cejka, P. (2014). The Saccharomyces cerevisiae Mlh1-Mlh3 heterodimer is an endonuclease that preferentially binds to Holliday junctions. *The Journal of Biological Chemistry*, 289(9), 5674–5686. <https://doi.org/10.1074/JBC.M113.533810>

Schwacha, A., & Kleckner, N. (1995). Identification of double Holliday junctions as intermediates in meiotic recombination. *Cell*, 83(5), 783–791. [https://doi.org/10.1016/0092-8674\(95\)90191-4](https://doi.org/10.1016/0092-8674(95)90191-4)

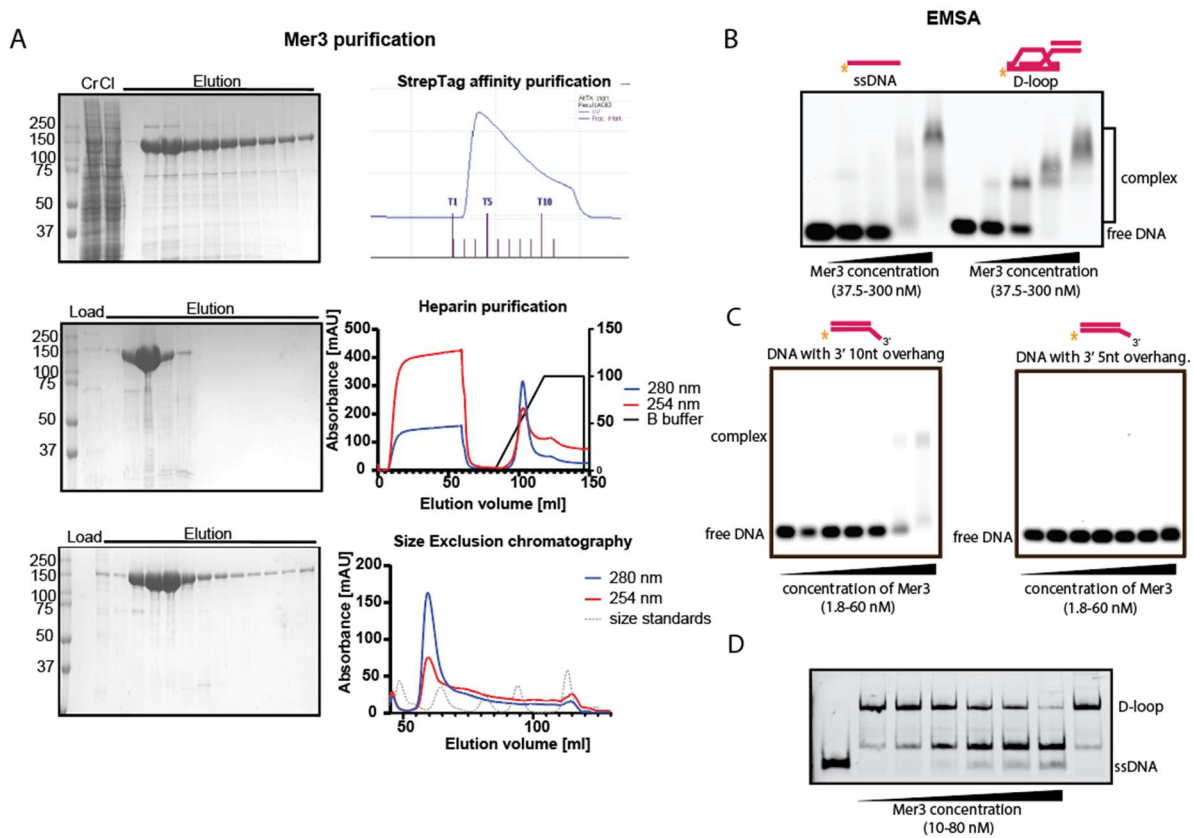
Shen, Y., Tang, D., Wang, K., Wang, M., Huang, J., Luo, W., Luo, Q., Hong, L., Li, M., & Cheng, Z. (2012). ZIP4 in homologous chromosome synapsis and crossover formation in rice meiosis. *Journal of Cell Science*, 125(11), 2581–2591. <https://doi.org/10.1242/jcs.090993>

Shinohara, M., Oh, S. D., Hunter, N., & Shinohara, A. (2008). Crossover assurance and crossover interference are distinctly regulated by the ZMM proteins during yeast meiosis. *Nature Genetics*, 40(3), 299–309. <https://doi.org/10.1038/ng.83>

Storlazzi, A., Gargano, S., Ruprich-Robert, G., Falque, M., David, M., Kleckner, N., & Zickler, D. (2010). Recombination Proteins Mediate Meiotic Spatial Chromosome Organization and Pairing. *Cell*, 141(1), 94–106. <https://doi.org/10.1016/J.CELL.2010.02.041/ATTACHMENT/48D4BE92-A714-4A50-8880-D2268EE1B6F0/MMC1>

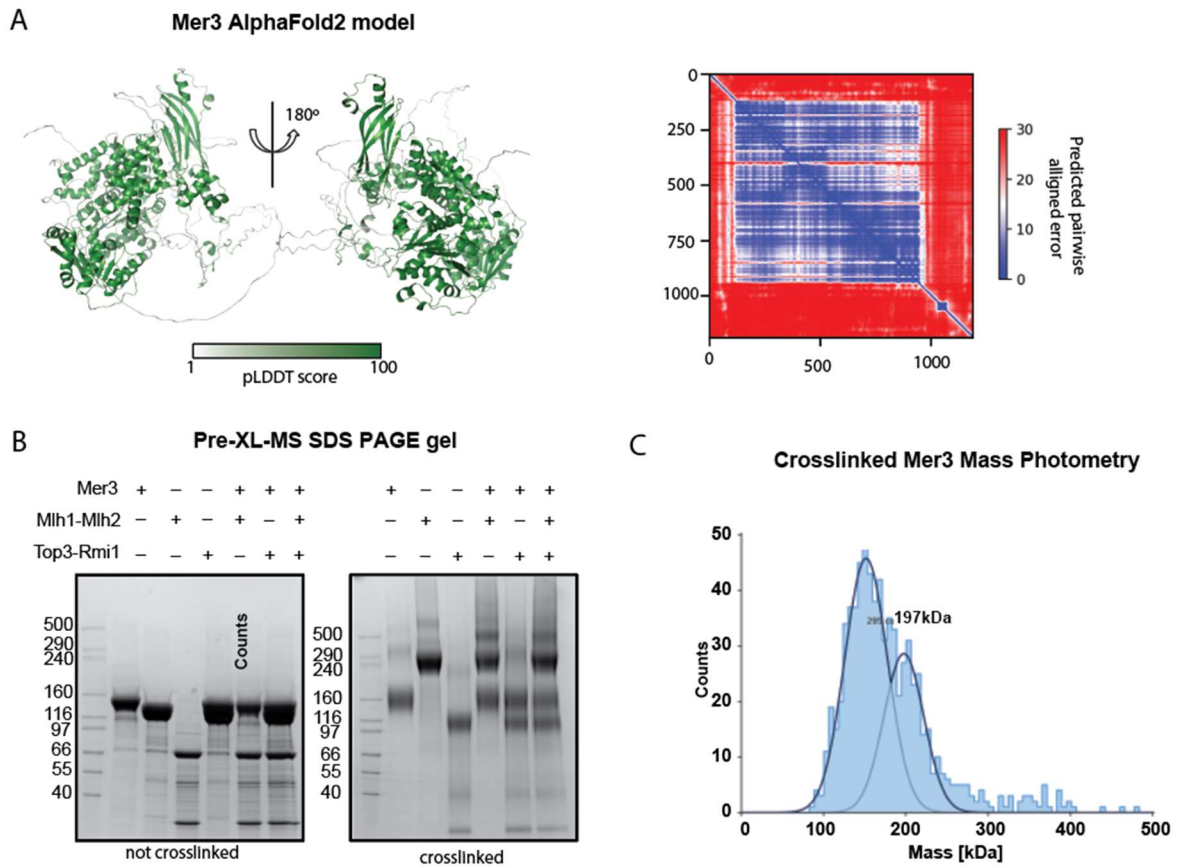
- Storlazzi, A., Xu, L., Schwacha, A., & Kleckner, N. (1996). Synaptonemal complex (SC) component Zip1 plays a role in meiotic recombination independent of SC polymerization along the chromosomes. *Proceedings of the National Academy of Sciences of the United States of America*, *93*(17), 9043–9048. <https://doi.org/10.1073/PNAS.93.17.9043>
- Szostak, J. W., Orr-Weaver, T. L., Rothstein, R. J., & Stahl, F. W. (1983). The double-strand-break repair model for recombination. *Cell*, *33*(1), 25–35. [https://doi.org/10.1016/0092-8674\(83\)90331-8](https://doi.org/10.1016/0092-8674(83)90331-8)
- Tanaka, K., Miyamoto, N., Shouguchi-Miyata, J., & Ikeda, J. E. (2006). HFM1, the human homologue of yeast Mer3, encodes a putative DNA helicase expressed specifically in germ-line cells. *DNA Sequence : The Journal of DNA Sequencing and Mapping*, *17*(3), 242–246. <https://doi.org/10.1080/10425170600805433>
- Tang, S., Wu, M. K. Y., Zhang, R., & Hunter, N. (2015). Pervasive and essential roles of the top3-rmi1 decatenase orchestrate recombination and facilitate chromosome segregation in meiosis. *Molecular Cell*, *57*(4), 607–621. <https://doi.org/10.1016/j.molcel.2015.01.021>
- Ui, A., Satoh, Y., Onoda, F., Miyajima, A., Seki, M., & Enomoto, T. (2001). The N-terminal region of Sgs1, which interacts with Top3, is required for complementation of MMS sensitivity and suppression of hyper-recombination in sgs1 disruptants. *Molecular Genetics and Genomics : MGG*, *265*(5), 837–850. <https://doi.org/10.1007/S004380100479>
- van Nues, R. W., & Beggs, J. D. (2001). Functional contacts with a range of splicing proteins suggest a central role for Brr2p in the dynamic control of the order of events in spliceosomes of *Saccharomyces cerevisiae*. *Genetics*, *157*(4), 1451–1467. <https://doi.org/10.1093/GENETICS/157.4.1451>
- Vernekar, D. V., Reginato, G., Adam, C., Ranjha, L., Dingli, F., Marsolier, M. C., Loew, D., Gue´rois, R., Llorente, B., Cejka, P., & Borde, V. (2021). The Pif1 helicase is actively inhibited during meiotic recombination which restrains gene conversion tract length. *Nucleic Acids Research*, *49*(8), 4522–4533. <https://doi.org/10.1093/nar/gkab232>
- Wang, K., Tang, D., Wang, M., Lu, J., Yu, H., Liu, J., Qian, B., Gong, Z., Wang, X., Chen, J., Gu, M., & Cheng, Z. (2009). MER3 is required for normal meiotic crossover formation, but not for presynaptic alignment in rice. *Journal of Cell Science*, *122*(12), 2055–2063. <https://doi.org/10.1242/jcs.049080>
- Wild, P., Susperregui, A., Piazza, I., Dörig, C., Oke, A., Arter, M., Yamaguchi, M., Hilditch, A. T., Vuina, K., Chan, K. C., Gromova, T., Haber, J. E., Fung, J. C., Picotti, P., & Matos, J. (2019). Network Rewiring of Homologous Recombination Enzymes during Mitotic Proliferation and Meiosis. *Molecular Cell*, *75*(4), 859-874.e4. <https://doi.org/10.1016/j.molcel.2019.06.022>

Supplementary Figures



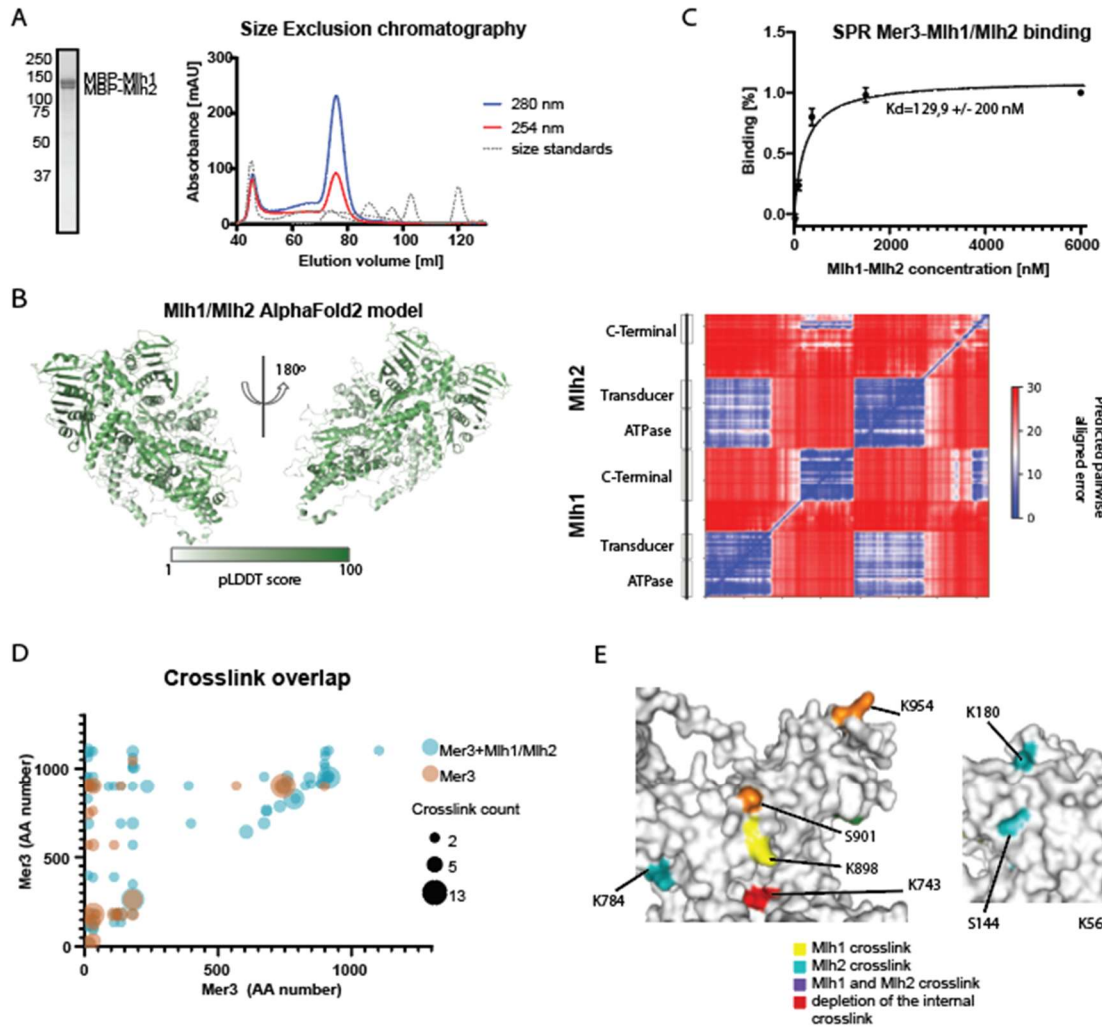
Supplementary Figure 2.1. Biochemical activity of Mer3

A. Three step purification of Mer3 using Strep-Tactin[®]XT column, HiTrap Heparin HP affinity column and Superdex 200 16/600 column. The samples were loaded onto SDS-PAGE and stained by Der Blaue Jonas gel dye. Cr = crude lysate, Cl = Cleared lysate. **B.** Example gel of EMSA from Figure 2.1C. **C.** DNA overhang binding in EMSA to determine the minimal overhang length bound by Mer3. DNA substrates were fluorescently labeled. **D.** Example image of strand separation assay from Figure 2.1D.



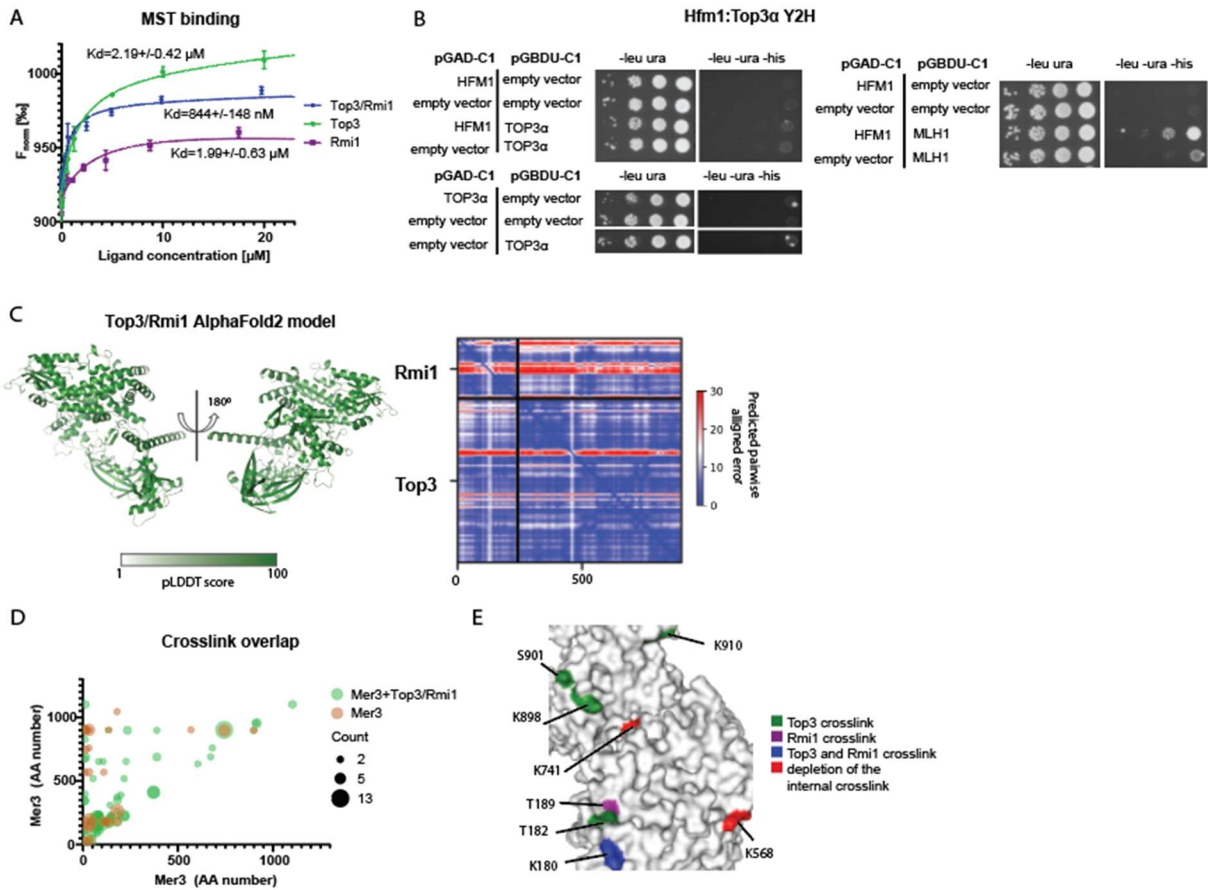
Supplementary Figure 2.2. Structural analysis of Mer3

A. AlphaFold2 model of Mer3. Model domains are coloured according to the confidence metric- pLDDT score (green represents the highest confidence regions, white - the lowest confidence regions). **B.** Control SDS-PAGE gel from XL-MS experiment. Left side represents not crosslinked proteins, right side proteins after crosslinking with DSBU. **C.** Mass Photometry on crosslinked Mer3. Mer3 was diluted to ~30 nM and measured using a Refeyn One mass photometer as per the manufacturer's instructions.



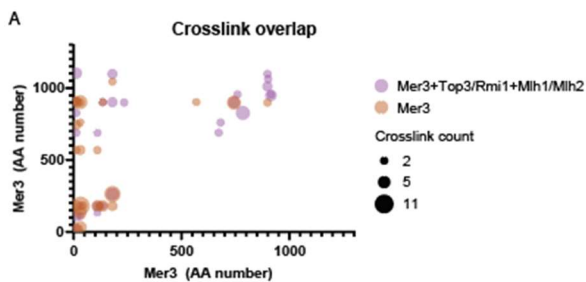
Supplementary Figure 2.3. Biophysical and structural analysis of the interaction between Mer3 and the Mlh1/Mlh2 complex

A. Size-exclusion chromatography purification step of MBP-Mlh1/MBP-Mlh2 using Superose 6 16/600 column. The samples were loaded onto SDS-PAGE and stained by Der Blaue Jonas gel dye. **B.** AlphaFold2 model of the Mlh1/Mlh2 complex. Model domains are coloured according to the confidence metric-pLDDT score (green represents the highest confidence regions, white -the lowest confidence regions). **C.** The SPR Measurements on Mer3 binding to Mlh1/Mlh2. MBP-Mlh1/MBP-Mlh2 was injected onto the Mer3 coated CM5 chip. Error bars are the SD from three independent experiments. **D.** The bubble chart representing the overlap between the internal crosslinks of Mer3 and while it is interacting with the Mlh1/Mlh2 complex. **E.** Partial surface of the Mer3 model. The Mer3 AA, which were often crosslinked with Mlh1 (yellow), Mlh2 (blue) or both (purple) are highlighted. In red, the AA that are no longer crosslinked within the Mer3 structure (Supplementary Figure 2.3D) are highlighted.



Supplementary Figure 2.4. Mer3 interacts with the Top3/Rmi1 complex

A. The MST Measurements on Mer3 binding to Top3/GST-Rmi1 compared with Top3 and Rmi1 alone. Top3, Rmi1 and Top3/GST-Rmi1 were titrated against RED-NHS labeled Mer3. Error bars are the SD from three independent experiments. **B.** Yeast two-hybrid experiments to test the interactions between the human HFM1 and TOP3α, or MLH1, respectively. Yeast were transformed with the pGAD-C1 and pGBDU plasmids as indicated. Cells were grown and pipetted onto non-selective (left) or selective plates (right) at three concentrations. **C.** AlphaFold2 model of the Top3/Rmi1 complex. Model domains are coloured according to the confidence metric- pLDDT score (green represents the highest confidence regions, white - the lowest confidence regions). **D.** The bubble chart representing the overlap between the internal crosslinks of Mer3 and while it is interacting with the Top3/Rmi1 complex. **E.** Partial surface of the Mer3 model. The Mer3 AA, which were often crosslinked with Top3 (green), Rmi1 (purple) or both (blue) are highlighted. In red the AA that are no longer crosslinked within the Mer3 structure (Supplementary Figure 2.4D) are highlighted.



Supplementary Figure 2.5. Mer3 interaction with Mlh1/Mlh2 is compatible with Top3/Rmi1 binding and together they are forming a 5-subunit complex

A. The bubble chart representing the overlap between the internal crosslinks of Mer3 and while it is interacting with the Top3/Rmi1 and Mlh1/Mlh2 complex simultaneously.

Supplementary Tables

Plasmid ID	Description	Reference
pWL413	pLIB-Mer3-Strep	This study
pWL522	pCOLI-Strep-Rfa1	This study
pWL526	pCDF-6xHis-Rfa2	This study
pWL527	pRSF-6xHis-Rfa3	This study
pWL746	pET11c-Dmc1	Lumir Krejci
pWL808	pLIB-GST-Rmi1	This study
pWL812	pLIB-6xHis-Top3	This study
pWL856	pBIG1a-Top3/GST-Rmi1	This study
pWL993	pBIG1a-6xHis-MBP-Mlh1 6xHis-MBP-Mlh2	This study
pWL1016	pLIB-6xHis-MBP-Sgs1-6xHis	This study
pWL1097	pLIB-Mer3(K167A)-Strep	This study
pWL1897	pCOLI-6xHis-Sgs1(1-605)	This study
pWL1565	pGAD-C1	This study
pWL1564	pGBDU-C1	This study
pWL1700	pGAD-C1-Mer3	This study
pWL1716	pGBDU-C1-Mer3	This study
pWL1713	pGAD-C1-Mer3(1-1023)	This study
pWL1712	pGBDU-C1-Mer3(1-1023)	This study
pWL1826	pGAD-C1-Mer3(122-1187)	This study
pWL1827	pGBDU-C1-Mer3(122-1187)	This study
pWL1696	pGBDU-C1-Top3	This study
pWL1695	pGBDU-C1-Rmi1	This study
pWL1656	pGAD-C1-HFM1	This study
pWL1800	pGBDU-C1-TOP3 α	This study
pWL1823	pGBDU-C1-MLH1	This study

Supplementary Table 2.1. Plasmids used in the study

Strain	Genotype	Source
yWL365	MATa, ura3-52, leu2-3, his3, trp1, gal4del, gal80del, GAL2-ADE2, LYS2::GAL1-HIS3, met2::GAL7-lacZ	Gerben Vader
yWL430	MAT a ho::LYS2 ura3 leu2::hisG trp1::hisG his3::hisG MER3-9xMyc::KanMX4 MAT alpha ho::LYS2 ura3 leu2::hisG trp1::hisG his3::hisG MER3-9xMyc::KanMX4	This study
yWL444	MAT a ho::LYS2 ura3 leu2::hisG trp1::hisG his3::hisG MER3-9xMyc::KanMX4 Top3-3HA::hphNTI MAT alpha ho::LYS2 ura3 leu2::hisG trp1::hisG his3::hisG MER3-9xMyc::KanMX4 Top3-3HA::hphNTI	This study
yWL452	MAT a ho::LYS2 ura3 leu2::hisG trp1::hisG his3::hisG MER3-9xMyc::KanMX4 MAT alpha ho::LYS2 ura3 leu2::hisG trp1::hisG his3::hisG MER3-9xMyc::KanMX4 Δ sgs1::natNT2	This study

Supplementary Table 2.2. Yeast strains used in the study

Chain 1	Residue 1	Chain 2	Residue 2	C α to C α distance
Mer3	759	Mer3	921	9.4
Mer3	129	Mer3	180	10.7
Mer3	180	Mer3	263	13.1
Mer3	135	Mer3	180	20.3
Mer3	137	Mer3	180	20.3
Mer3	743	Mer3	898	21.4
Mer3	759	Mer3	898	23
Mer3	256	Mer3	898	25.6
Mer3	743	Mer3	901	27.7
Mer3	759	Mer3	946	33.1
Mer3	759	Mer3	948	36.7
Mer3	180	Mer3	624	38.9
Mer3	759	Mer3	980	39.3
Mer3	180	Mer3	568	40.1
Mer3	182	Mer3	568	40.4
Mer3	898	Mer3	982	52.3
Mer3	180	Mer3	901	52.3
Mer3	135	Mer3	901	58.8
Mer3	568	Mer3	901	64.9
Mer3	398	Mer3	898	74.2
Mer3	180	Mer3	1044	80.4
Mer3	180	Mer3	982	84.5

Supplementary Table 2.3. Crosslinking distances within the Mer3 structure based on the AlphaFold2 prediction

Chain 1	Residue 1	Chain 2	Residue 2	C α to C α distance
Mlh1	6	Mlh2	159	28.1
Mlh1	231	Mlh2	159	33
Mlh1	172	Mlh2	159	35.4
Mlh1	333	Mlh2	159	40.4

Supplementary Table 2.4. Crosslinking distances within the ATPase and Transducer domains of the Mlh1/Mlh2 complex structure based on the AlphaFold2 prediction

Chain 1	Residue 1	Chain 2	Residue 2	C α to C α distance
Rmi1	143	Top3	478	13.9
Rmi1	89	Top3	638	17.8
Rmi1	53	Top3	517	22.1
Rmi1	106	Top3	328	23.5
Rmi1	143	Top3	311	23.8
Rmi1	106	Top3	611	24.4
Rmi1	89	Top3	653	24.7
Rmi1	52	Top3	517	25.6
Rmi1	227	Top3	653	26.1
Rmi1	83	Top3	653	26.6
Rmi1	235	Top3	653	30
Rmi1	89	Top3	619	30.1
Rmi1	227	Top3	517	31.6
Rmi1	46	Top3	517	32.2
Rmi1	106	Top3	341	32.4
Rmi1	106	Top3	181	32.5
Rmi1	238	Top3	653	32.8
Rmi1	222	Top3	631	42.5
Rmi1	89	Top3	100	49.8
Rmi1	52	Top3	653	56.1
Rmi1	222	Top3	174	57.2
Rmi1	52	Top3	356	73.2
Rmi1	52	Top3	14	89
Rmi1	53	Top3	106	94.6

Supplementary Table 2.5. Crosslinking distances within the Top3/Rmi1 complex structure based on the AlphaFold2 prediction

3. Unwinding during stressful times - mechanisms of helicases in meiotic recombination

Magdalena Firlej and John R. Weir*

Structural Biochemistry of Meiosis Group, Friedrich Miescher Laboratory of the Max Planck Society, Max Planck Ring 9, 72076 Tuebingen, Germany

Author	Author position (%)	Scientific ideas (%)	Data generation (%)	Analysis & interpretation (%)	Paper writing (%)
Magdalena Firlej	1	50%	-	-	50%
John Weir	1	50%	-	-	50%
Paper Title		Unwinding during stressful times - mechanisms of helicases in meiotic recombination			
Status in publication process		Accepted			

Abstract

Successful meiosis I requires that homologous chromosomes be correctly linked before they are segregated. In most organisms this physical linkage is achieved through the generation of crossovers between the homologs. Meiotic recombination co-opts and modifies the canonical homologous recombination pathway to successfully generate crossovers. One of the central components of this pathway are a number of conserved DNA helicases. Helicases couple nucleic acid binding to nucleotide hydrolysis and use this activity to modify DNA or protein-DNA substrates. During meiosis I it is necessary for the cell to modulate the canonical DNA repair pathways in order to facilitate the generation of interhomolog crossovers. Many of these meiotic modulations take place in pathways involving DNA helicases, or with a meiosis specific helicase. This short review explores what is currently understood about these helicases, their interaction partners, and the role of regulatory modifications during meiosis I. We focus in particular on the molecular structure and mechanisms of these helicases.

3.1. Introduction

“If a man insisted always on being serious, and never allowed himself a bit of fun or relaxation, he would go mad or become unstable without knowing it.” - Herodotus

The connection between relaxation and stability holds true not just for our general wellbeing, but specifically for our genomes. Helicases, proteinaceous machines that connect nucleic acid binding, translocation, and/or unwinding to ATP hydrolysis, play a myriad of roles in genome stability. Indeed, several helicases have key roles as anti-recombination factors, thus maintaining genome integrity. During meiosis I, however, most species require recombination in order to link homologous chromosomes and thus ensure their faithful segregation during anaphase I, ultimately producing viable gametes. As such meiosis I is an intricate dance between pro- and anti-recombination factors. Here we make a whistle stop tour of eight helicases (Figure 3.1) that have specific roles during meiotic recombination, examine them from a structural biochemical perspective, and briefly discuss their meiosis specific interactions and modifications, and, where possible, the implications for human health and disease.

3.2. Architecture and mechanism of nucleic acid helicases

Helicases all make use of a number of RecA like domains that couple nucleic acid binding to ATP hydrolysis. These RecA-like domains may be part of an intramolecular arrangement (usually two RecA-like domains) or an intermolecular arrangement (frequently six RecA-like domains arranged as a hexameric ring) (Singleton et al., 2007). All of the helicases we focus on through this review consist of two RecA-like domains (RecA1 and RecA2) decorated with a number of accessory domains and belong to either Superfamily 1 (SF1) or Superfamily 2 (SF2 helicases). In this review not all the “helicases” here unwind dsDNA. Many are nucleic acid translocases that do not have unwinding capability. While the RecA-like domains are highly similar, the diverse accessory domains alter the substrate binding and interaction network of each helicase. Here, we mostly focus on the factors from the budding yeast *S. cerevisiae*, but also integrate data from other organisms to try to present a more comprehensive picture.

3.3. Meiotic Recombination

Our understanding of meiotic recombination was described elsewhere (Hunter, 2015). Briefly, meiotic recombination is initiated through the introduction of programmed double strand DNA breaks (DSBs). Break formation is catalysed by the meiosis specific topoisomerase Spo11 (Keeney, 2008; Keeney et al., 1997). Break sites are initially resected by the nuclease activity of Mre11, with further resection by Exo1 (Szankasi & Smith, 1995) and Dna2 (Budd et al., 2000) (see below). Single-stranded DNA (ssDNA) is then coated by the general recombinase Rad51, and also by the meiosis specific recombinase Dmc1 to form presynaptic filaments nucleated by Rad51, but with filaments of Dmc1 on the 3' end, thus ensuring the dominance of Dmc1 in meiosis (Brown & Bishop, 2014). Once a presynaptic filament successfully invades a homologous sequence, the complementary strand is displaced forming a "D-loop", the first and most unstable form of joint molecule (JM) (Schwacha & Kleckner, 1994). A number of factors either act to extend, stabilise, or dissolve these nascent D-loops which give rise to more stable JMs such as single end invasions (SEIs) and double Holliday junctions (dHJs) (Hunter & Kleckner, 2001; Schwacha & Kleckner, 1995). Biased endonucleases then resolve these Holliday junctions into crossovers or non-crossovers (Allers & Lichten, 2001; Cannavo et al., 2020; Hunter & Kleckner, 2001; Kulkarni et al., 2020).

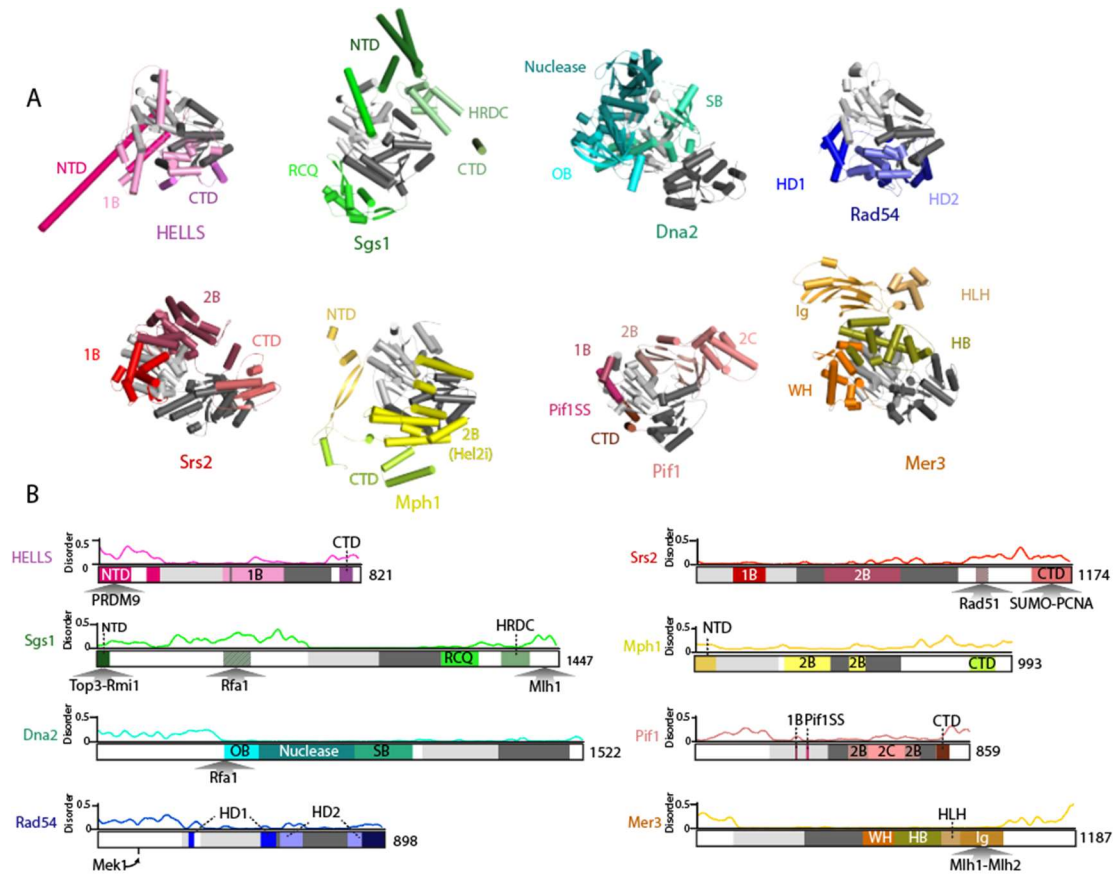


Figure 3.1. Structural overview of helicases involved in meiotic recombination.

A. Predicted structures of eight helicases central to meiotic recombination. Predicted structures of each helicase were downloaded from the publicly available AlphaFold database (<https://www.alphafold.ebi.ac.uk/>). Regions where the pLDDT score was <37 were hidden and the structures superimposed on one another using SMM and the RecA1 domain as a common reference. While crystal structures exist for many, or parts, of the helicases shown here, we have used AlphaFold predictions for a fair comparison. RecA1 shown in light grey, and RecA2 in dark grey. Domain annotations are according to previous publications. (Hu et al., 2021) (Pif1 (Lu et al., 2018), Mph1; based on RIG-1 (Luo et al., 2011)**B.** Domain cartoons of helicases, coloured as in A). Disordered plot is based on fIDPnn server (<http://biomine.cs.vcu.edu/servers/fIDPnn/>), and is shown above the domain cartoon. RecA1 shown in light grey, and RecA2 in dark grey. Unstructured regions, or regions with low pLDDT score are shown in white. Interactions and modifications are shown below the domain cartoon. Note that while the Rfa1 interaction region for Sgs1 is known (Hegnauer et al., 2012), this region of Sgs1 is predicted to be unstructured.

3.4. Helicases and Meiotic Recombination

3.4.1. Formation of meiotic DSB breaks

The formation of Spo11 mediated double-strand DNA breaks is an event that is tightly regulated. One element of spatial regulation of DSBs is connected to the enrichment of H3K4^{me3} marks (Acquaviva et al., 2013; Sommermeyer et al., 2013). In many organisms, including budding yeast, H3K4^{me3} marks transcriptional start sites. In other organisms, including humans, an additional protein, PRDM9, deposits H3K4^{me3} and H3K27^{me3} at sequence specific regions of the genome (Baudat et al., 2010). PRDM9 consists of N-terminal methyltransferase domains, and a C-terminal array of zinc fingers (reviewed in (Baudat et al., 2013)). The function of PRDM9 is regulated by additional cofactors for example the helicase HELLS (Imai et al., 2020; Spruce et al., 2020).

HELLS helicase

HELLS (also known as Lsh or PASG) is a SF2 family helicase (Flaus et al., 2006), and was originally identified as being involved in regulating DNA methylation at repeat elements throughout the mouse genome (Dennis et al., 2001). While HELLS^{-/-} mice are non-viable, analysis of fetal ovarian tissue revealed that while germ cells are present, there is a failure of chromosomes to undergo synapsis during meiosis I (De La Fuente et al., 2006).

Recently HELLS was shown to interact directly with PRDM9 forming a complex both *in vivo* (Spruce et al., 2020), and *in vitro* (from Y2H experiments, (Imai et al., 2020)). The N-terminus of HELLS contains a coiled-coil domain, not found in other helicases (Figure 3.1), and this domain is required for interaction with PRDM9 (Imai et al., 2020). Taken together a model has been proposed whereby the PRDM9-HELLS “pioneer” complex moves nucleosomes away from PRDM9 binding sites, thus facilitating PRDM9 DNA binding and subsequent site-specific DSB formation by the Spo11 complex (Imai et al., 2020; Spruce et al., 2020) (Figure 3.2A).

Interestingly, purifications of recombinant HELLS out of bacteria showed low ATPase and chromatin remodelling activity *in vitro* (Burrage et al., 2012). Similarly to PRDM9, CDCA7 is a Zn²⁺-finger protein that binds to HELLS and *in vitro* promotes robust chromatin remodelling by HELLS (Jenness et al., 2018). Currently, it is not clear whether CDCA7 and PRDM9 bind to the same site, or whether PRDM9 stimulates HELLS activity.

In male mice, PRDM9 binding sites are extensively methylated (Brick et al., 2018). The recruitment of HELLS and PRDM9 is required for the formation of these methylation marks

(Imai et al., 2020). The role of both 5-hydroxymethylcytosine (5hmC) and 5-methylcytosine (5mC) in meiosis is unclear, however, HELLS could also play a role in the generation of these marks, since Tet proteins (that generate 5hmC (Ito et al., 2011)) have been shown to associate with HELLS (Jia et al., 2017).

3.4.2. Break resection

Following the formation of Spo11 mediated double-strand DNA breaks, the breaks are resected to generate ssDNA (reviewed in (Cejka & Symington, 2021)). At nascent breaks both the endo- and exo-nuclease activity of Mre11 (in complex with Rad50 and Xrs2^{NBS1} as the MRX^{MRN} complex) removes both Spo11 from the 5' end and generates initial 3' ssDNA. Subsequently, longer 3' ssDNA is generated by the exonuclease activity of Exo1 (Szankasi & Smith, 1995) and Dna2 (Budd et al., 2000). ssDNA is initially bound by the RPA complex (in yeast containing the proteins Rfa1, Rfa2 and Rfa3) which protects it from further degradation and formation of secondary structures (H. Chen et al., 2013; Deng et al., 2015), and helps to "funnel" ssDNA to the downstream pathways (Fanning et al., 2006).

Sgs1^{BLM} and Dna2 in break resection

Dna2 contains both a nuclease domain (Budd et al., 2000), and a C-terminal helicase domain (Bae & Seo, 2000), an organisation which is conserved in evolution (Bae et al., 1998). Our current understanding is that the helicase activity of Dna2 is required for Okazaki fragment processing and recombination (Zheng et al., 2020). Sgs1^{BLM} is involved in dissolving both D-loops and dHJs (reviewed in (Gupta & Schmidt, 2020), see below) but in addition the direct binding of Sgs1 to Dna2 facilitates the nuclease activity in the latter providing a parallel resection pathway to Exo1 (Figure 3.2B) (Gravel et al., 2008; Mimitou & Symington, 2008; Sturzenegger et al., 2014; Zhu et al., 2008). Likewise, Dna2 has been shown to stimulate Sgs1 activity, independent of Dna2 helicase and nuclease activities (Kasaciunaite et al., 2019; Xue et al., 2019) whereas the CtIP (Sae2 in yeast) stimulates the motor activity of Dna2 reconstituted end resection almost an order of magnitude more efficient (Ceppi et al., 2020). In budding yeast Exo1 is apparently the dominant end resection pathway (Mimitou et al., 2017; Zakharyevich et al., 2010), whereas DNA2 in mammalian meiotic DSB resection might be particularly important in, since *Exo1^{-/-}* mice do not show resection defects in spermatocytes (Paiano et al., 2020). Mutations in human *DNA2* gene have been associated with the primordial dwarfism disorder Seckel syndrome (specifically Seckel Syndrome 8 OMIM 615807)

in which fertility defects, specifically repeated miscarriages, were observed (Shaheen et al., 2014).

3.4.3. Presynaptic filament formation

Srs2

Srs2 is an ATP dependent 3' to 5' helicase that binds to Rad51 via amino acids 875-910 (Colavito et al., 2009). The C-terminus of Srs2 serves as an interaction region for SUMOylated PCNA as well as the target of post-translational modification (such as SUMOylation) (Armstrong et al., 2012; Pfander et al., 2005) (Figure 3.1B). The SIM (SUMO-interacting motif) has been shown to be involved in interaction with SUMOylated PCNA (Armstrong et al., 2012; Kolesar et al., 2012; Papouli et al., 2005; Pfander et al., 2005). The SIM in Srs2 may be of particular importance in meiosis given the recently described pervasive role of SUMOylation during meiotic recombination (Bhagwat et al., 2021). The ortholog of Srs2 in mammals is unclear. A potential functional analog of Srs2 is RTEL1, a member of the XPD helicase family (Barber et al., 2008). Mutations in RTEL1 have been associated with several diseases such as Hoyeraal-Hreidarsson syndrome, a severe form of the bone-marrow failure and cancer predisposition disorder, and dyskeratosis congenita (Vannier et al., 2014), and RTEL1 was shown to dissolve D-loops *in vitro* and limit crossover formation *in vivo* (Youds et al., 2010).

The formation of presynaptic filaments is antagonised by the helicase Srs2^{RTEL1} through disrupting Rad51 filaments (Krejci et al., 2003; Veaute et al., 2003). The mechanism of Rad51 removal by Srs2 is dependent on the translocase activity of Srs2 (Kaniecki et al., 2017; Krejci et al., 2003). There is also direct interaction between Srs2 and Rad51, which stimulates Rad51 ATPase activity and causes filaments to disassemble (Antony et al., 2009), but this is thought to play a less prominent role as shown both *in vitro* (Kaniecki et al., 2017) and *in vivo*, by ectopic recombination assays, crossover to non-crossover ratio assessment and BIR assays (Elango et al., 2017; Jenkins et al., 2019). During meiosis this activity of Srs2 is antagonised, since Dmc1 filaments are resistant to Srs2 (Crickard, Kaniecki, Kwon, Sung, & Greene, 2018) (Figure 3.2C). Given the similarity between Dmc1 and Rad51 it will be intriguing to understand how Srs2 distinguishes between Dmc1 and Rad51, and whether additional modifications play a role in these interactions in meiosis.

Rad54 (I)

Rad54 and its homolog Rdh54^{RAD54B} are members of Snf2/Swi2 family of SF2 helicases. Rad54 is a highly processive translocase that forms multimers on DNA, possibly in the form of rings (Amitani et al., 2006). Rad54 interacts directly with Rad51 via its N-terminus (Clever et al., 1997; Raschle et al., 2004). Budding yeast *rad54Δ rdh54Δ* double mutants are completely defective in meiosis, showing 1.6% spore viability, compared to 53% viability for *rad54Δ* and 82% for *rdh54Δ* single mutants (Shinohara et al., 1997). One possibility is that Rdh54^{RAD54B} preferentially associates with the meiosis specific Dmc1 (Dresser et al., 1997) (whereas Rad54 interacts with Rad51). Mammalian RAD54B however, while involved in DNA repair, does not seem to function as Rdh54 in meiosis (Wesoly et al., 2006). *In vitro* Rad54 enhances the strand invasion activity of Rad51, and it can also remodel chromatinized DNA, which is stimulated by Rad51 presynaptic filaments (Petukhova et al., 1998). It is assumed that the homology search by Rad51 is also enhanced by interaction with Rad54 (Crickard et al., 2020; Kowalczykowski, 2015).

During meiosis Hed1 associates with Rad51 and blocks the interaction with Rad54 (Busygina et al., 2008). Indeed, the association of Hed1 with Rad51 on presynaptic filaments *in vitro* is very stable, and only unbinds when the filament is disassembled (Crickard, Kaniecki, Kwon, Sung, Lisby, et al., 2018). In contrast Hed1 does not bind to the meiosis specific Rad51 homolog Dmc1. Rad51 is required for meiosis, but its strand-exchange activity is not, thus leading to the conclusion that Rad51 is a structural accessory factor during meiosis (Cloud et al., 2012). Taken together, Hed1 presumably functions to promote the specific functional association of Rad54 with Dmc1 during meiosis.

3.4.4. Interhomolog bias

HR during meiosis could either use the sister chromatid or the homologous chromosome as a template. Indeed, the sister chromatid is proximal to the break site and identical in sequence making it a perfect template. Nevertheless, meiotic recombination requires that the homologous chromosome is used as a template (reviewed (Lao & Hunter, 2010)) This process, known as interhomolog bias, is apparently regulated at several levels. (Reviewed in (Humphryes & Hochwagen, 2014)). Here we will look at the roles of two helicases, Rad54 and Mph1 in facilitating interhomolog bias.

Rad54 (II)

Mek1 is a S/K kinase that is activated through the ATM/ATR dependent phosphorylation of the axial protein Hop1 (Carballo et al., 2008; Niu et al., 2005; Penedos et al., 2015). Mek1 phosphorylates both Rad54 (Niu et al., 2009) and Hed1 (Callender et al., 2016). Phosphorylation of Rad54 T132 inhibits its activity, which impairs DNA repair (Niu et al., 2009) (Figure 3.2D). Hed1, a meiotic co-factor, binds specifically to Rad51 and prevents its association with Rad54 (Busygina et al., 2008). Phosphorylation of Hed1 by Mek1 leads to the increased protein stability of Hed1 thus further suppressing Rad51 activity (Callender et al., 2016). Taken together the model suggests DNA repair proximal to the break site, i.e. using the sister chromatid as a template, is inhibited, and thus repair is directed to the distal homolog. However, Hed1 has no effect on the Dmc1-Rad54 interaction (Busygina et al., 2008), so there is likely a more complex network of interactions (Lao et al., 2013). Nevertheless, in yeast the principal “signaller” of IH bias is Mek1 kinase, since specific inhibition of *mek1-as* gives rise to a WT ratio of interhomolog and intersister crossovers (Terentyev et al., 2010).

Mph1^{FANCM}

Mph1 is a SF2 type helicase that belongs to the FANCM family of helicases. FANCM has been implicated in Fanconi anaemia disorder, a syndrome characterised by cancer predisposition, developmental disorder, and bone marrow failure (Whitby, 2010). Most of the sequence similarity between Mph1 and FANCM is within the N-terminal helicase domain (Figure 3.1B). Budding yeast Mph1 lacks the C-terminal ERCC4 nuclease domain found in other FANCM family members, (except *S. pombe* Fml1). Likewise most FANCM family members have a double helix-hairpin-helix ((HhH)₂) domain, C-terminal to the ERCC4 domain, and was previously thought to be absent from Mph1. The AlphaFold2 prediction of Mph1 shows that there is very likely to be a (HhH)₂ like-domain present (Figure 3.1A, yellow). In other FANCM family members the (HhH)₂ domain facilitates protein-protein interactions.

In meiosis Mph1^{FANCM} has two important functions. One is to limit crossover formation, shown in both fission yeast and plants (Crismani et al., 2012; Lorenz et al., 2012). In fission yeast it was shown that Fml1 (Mph1 homologue) dissociates the D-loops, the loss of which leading to a decrease in non-crossovers arising from SDSA (Lorenz et al., 2012). In plants, FANCM mutants show a three-fold higher number of crossovers via a pathway that is independent of the ZMM pathway (see below for a description of ZMM proteins) (Crismani et al., 2012). In

both plants and fission yeast these results are consistent with the observation in somatic cells that one function of Mph1^{FANCM} is to dissolve D-loops (Prakash et al., 2009).

The second, recently reported function of Mph1, is in facilitating interhomolog bias (Sandhu et al., 2020). Mph1 has been reported to limit inter-sister joint molecule formation, thereby favouring repair from the homolog (Figure 3.2E). Consistent with this idea is that *mph1* mutants become more sensitive to reduced DSB number, presumably because too few DNA repair intermediates are being funnelled to the interhomolog pathway, and are thus repaired from the sister (Sandhu et al., 2020). Consistent with the meiotic functions of Mph1^{FANCM} described here, FANCM mutants in humans cause both spermatogenic and premature ovarian failure (Fouquet et al., 2017; Kasak et al., 2018).

3.4.5. D-loop formation

Mer3^{HFM1}

Mer3^{HFM1} is a SF2 DExH box helicase, with an extended C-terminal domain (Figure 3.1B). Mer3^{HFM1} is the only meiosis specific helicase. Orthologs of Mer3 have been clearly identified in plants and mammals (C. Chen et al., 2005; Tanaka et al., 2006). In humans, heterozygotic mutations in HFM1 lead to primary ovarian insufficiency (J. Wang et al., 2014). *In vitro* studies on Mer3 showed that it is an active ATPase with strand separation activity working a 3' to 5' direction (Nakagawa et al., 2001) and that it might preferentially recognise Holliday junctions (Nakagawa & Kolodner, 2002b), though it is unclear how this might promote crossovers.

Further *in vitro* work demonstrated that Mer3 facilitated a heteroduplex extension by Rad51, that is, it enlarged and stabilised D-loops, stabilising this crossover intermediate (Figure 3.2F) (Mazina et al., 2004). In a back-to-back paper (Börner et al., 2004) identified Mer3 as being one of the “ZMM” proteins that facilitate type I crossover formation (together with Zip1, Zip2, Zip3, Msh4 and Msh5). Taken together this, and previous work, identifies Mer3 as an active helicase that is still part of a larger protein interaction network.

Interestingly, ATPase deficient Mer3 gave rather mild spore viability defects when compared with *mer3Δ* (Nakagawa & Kolodner, 2002a). While the effect of some residual helicase activity remains a possibility, this observation hinted at the idea that the critical role of Mer3 might lie in mediating protein:protein interactions. Beyond the concept of the “ZMM” group of proteins, the first indications of the intermolecular interactions have been recently determined. An IP-MS study on Mlh1 identified Mer3 as a potential interactor, via the Ig-like

domain of Mer3 (Duroc et al., 2017). Deletion of Mlh1 or non-Mlh1 binding Mer3 mutant leads to an increase in the length of gene conversion tracts, both in crossovers (COs) and in non-crossovers (NCOs) (Figure 3.2F). The interactions between Mlh1/Mlh2 and Pif1 (see below) don't fully explain the strong meiotic crossover effect of *mer3Δ*, since *mlh2Δ* does not have an effect on crossover formation (T. F. Wang et al., 1999), and Structurally, Mer3 is remarkably similar to the spliceosome RNA helicase Brr2 (Figure 3.1). Brr2 contains two helicase "cassettes" where the second cassette has lost catalytic activity, thus functioning as a dimer (Absmeier et al., 2016). Furthermore, Brr2 has multiple protein-protein interactions that change as the spliceosome matures. We are then left with some intriguing questions. Might Mer3 also function on a template that contains RNA? RNA transcripts have been shown to have an important role in homologous recombination (Keskin et al., 2014). Does Mer3 function as a dimer? Can Mer3 be regulated by additional protein-protein interactions in addition to Mlh1/Mlh2? The last question has recently been answered with the discovery of the interaction with another helicase; Pif1.

Pif1

Pif1 is a SF1b helicase that is widely conserved throughout eukaryotes. Within the helicase domain there are several insertions. In RecA-1 there is a strand-separating 1B domain, which is thought to be stabilised by the characteristic Pif1 signature sequence (Pif1SS), (Byrd & Raney, 2017). RecA-2 is interrupted with the 2B insertion, which folds into an SH3 domain, which usually mediates protein-protein interactions (Li, 2005).

One role of Pif1 is in the regulation of telomerase, removing it from telomeres and thus regulating their length. Pif1 also removes telomerase from DSB sites, preventing the aberrant addition of telomeric DNA (Schulz & Zakian, 1994). Indeed, Pif1 is phosphorylated by Rad53 in response to DNA damage on residues in the C-terminus (T763 and T766), which prevents the recruitment of telomerase at break sites (Makovets & Blackburn, 2009). Pif1 was also found to have a role in break induced replication (BIR), and that Pif1 had a highly stimulatory effect on Pol δ activity. During BIR Pif1 migrates D-loop bubbles to mediate conservative DNA synthesis by Pol δ (Chung et al., 2010; Wilson et al., 2013). Pif1 interacts with the replication machinery by binding through its C-terminus to the sliding clamp PCNA (Buzovetsky et al., 2017).

IP-MS on Mer3 found both Mlh1-Mlh2 (as previously described) but also the PCNA clamp loader Rfc1 (Vernekar et al., 2021). *Mlh2Δ* gives rise to longer gene conversion tracts during

meiosis (Duroc et al., 2017), an effect that is rescued when using a Pif1 mutant that cannot enter the nucleus (Vernekar et al., 2021), suggesting that Mlh1-Mlh2 may prevent Pif1 from migrating D-loop bubbles, as it does in BIR (Chung et al., 2010; Wilson et al., 2013). In an elegant *in vitro* experiment, it was confirmed that the inhibitory effect on Pif1 indeed required not only Mlh1-Mlh2, but also Mer3, which thus limits the size of gene conversion tracts (Vernekar et al., 2021) (Figure 3.2G). While the exact nature of the inhibitory effect on Pif1 remains to be elucidated, a possibility is that both Pif1 and Mer3/Mlh1-2 compete for the same binding site on PCNA. With Pif1 being recruited but also inhibited during meiosis, why should it be recruited at all? Vernekar *et al.* proposed that the helicase activity of Pif1 could be a safeguard, in case Pol δ were to encounter secondary structure DNA elements that could block DNA repair.

Name	Functional orthologs from human (% similarity)	Molecular mass (residues)	Directionality	Direct binding partners	Meiosis specific post translational modifications
HELLS (mouse)	-	95.1kDa (821 a.a.)		PRDM9	-
Dna2	DNA2 (37%)	171.7 kDa (1,522 a.a.)		Rfa1	-
Sgs1	BLM (40%)	163.8 kDa (1,447 a.a.)	3'→5'	Top3, Rmi1, Rfa1	SUMO (6 sites) ¹ CDK and Cdk5 phosphorylation (Grigaitis et al., 2020)
Rad54	RAD54 (53%)	101.8 kDa (898 a.a.)	Bidirectional translocase on dsDNA	Rad51	pT132 (Niu et al., 2009)
Srs2	RTEL1 (20%)	134.3 kDa (1,174 a.a.)	3'→5'	PCNA, Rad51, Sgs1	SUMO (4 sites) ¹
Mph1	FANCM (23.5%)	114.0 kDa (993 a.a.)	3'→5'	-	-
Pif1	PIF1 (38%)	97.7 kDa (859 a.a.)	5'→3'	PCNA, Pol δ	SUMO (4 sites) ¹
Mer3	HFM1 (37.5%)	135 kDa (1,187 a.a.)	3'→5'	Mlh1, Mlh2, Rfc1, Pif1	SUMO (11 sites) ¹

Table 3.1. General characteristics of helicases involved in meiotic recombination

3.4.6. Crossover decision

Sgs1

Sgs1 carries out a number of functions in meiosis. Firstly, Sgs1, together with Top3 and Rmi1 (known as STR complex), can dissolve nascent D-loop structures, resulting in these DNA breaks being repaired via SDSA. Secondly, Sgs1 helicase can directly dissolve dHJs, resulting in NCOs rather than COs (Figure 3.2H). Finally, and somewhat counterintuitively, Sgs1 is required for the normal distribution of meiotic COs (Hatkevich & Sekelsky, 2017; Holloway et al., 2010). This observation is likely connected to the role of Sgs1 in preventing aberrant inter-sister recombination during meiosis (Jessop et al., 2006; Oh et al., 2007), thus creating an available “pool” of ssDNA ends that can be subsequently captured by the ZMM group of proteins (Hatkevich & Sekelsky, 2017).

While humans have five RecQ helicases, the functional ortholog of Sgs1 in meiosis is Bloom Helicase (BLM). BLM is named after a multifaceted disease, Bloom’s Syndrome, where the common feature is loss-of-function mutations in BLM. Bloom’s Syndrome patients show growth deficiency, photosensitivity, immune deficiency, insulin resistance, and an increased risk of early onset of cancer or multiple cancers (Cunniff et al., 2017). Bloom Syndrome like disorders are also caused by mutations in TOP3A, RMI1 and RMI2 (Hudson et al., 2016; Martin et al., 2018), reflecting the fact that these proteins work together in a complex, known as Bloom Syndrome Complex (BTRR) in mammals (Bythell-Douglas & Deans, 2021).

The interaction of Sgs1^{BLM} with Top3^{TOP3A} is conserved through eukaryotes (Ahmad & Stewart, 2005; Bennett et al., 2000). While the helicase activity of Sgs1^{BLM} is required for most of its functions (Bernstein et al., 2009), even the helicase defective form of Sgs1^{BLM} can stimulate the decatenation activity of Top3^{TOP3A} (Cejka et al., 2012). Both the helicase activity of Sgs1 and Top3-Rmi1 are essential for the resolution of meiotic recombination intermediates (Kaur et al., 2015; Tang et al., 2015).

Rmi1 contains an OB-fold and in mammals there are two Rmi proteins RMI1 and RMI2). The mammalian RMI1-2 complex binds to FANCM (Deans & West, 2009), it is unclear if this interaction is conserved in yeast. During meiosis ZMM proteins must presumably act to downregulate Sgs1^{BLM} activity (Jessop et al., 2006; Oh et al., 2007), yet to date there have been no reports of direct interactions between Sgs1^{BLM} and the ZMM proteins despite in-depth time-resolved proteomic studies (Wild et al., 2019).

In budding yeast, resolution of dHJs is temporally controlled through the polo kinase Cdc5, which initiates crossovers with pachytene exit (Allers & Lichten, 2001; Clyne et al., 2003). In a breakthrough study the Matos laboratory has provided a detailed mechanistic explanation for the temporal regulation of crossover formation through the phosphorylation of Sgs1 (Grigaitis et al., 2020). Sgs1 is phosphorylated by CDK on up to nine consensus sites, including within the Top3/Rmi1 and Rfa1 interaction regions and the helicase domain. CDK phosphorylations stimulate the helicase activity of Sgs1 by increasing the processivity and unwinding velocity. CDK phosphorylations also serve as priming phosphorylations for Cdc5^{PLK}, which hyperphosphorylates Sgs1^{BLM}, presumably leading to downregulation of the helicase activity. As such the activation of Cdc5 provides a time window in which to allow crossovers to occur. Consistent with this argument is the observation that Cdc5^{PLK} phosphorylation of the structure selective endonuclease Mus81-Mms4 enhances DNA cleavage (Matos et al., 2011), although this is complicated by the fact that Sgs1 is also required for class-I (Mus81-Mms4 independent) crossovers (Zakharyevich et al., 2010).

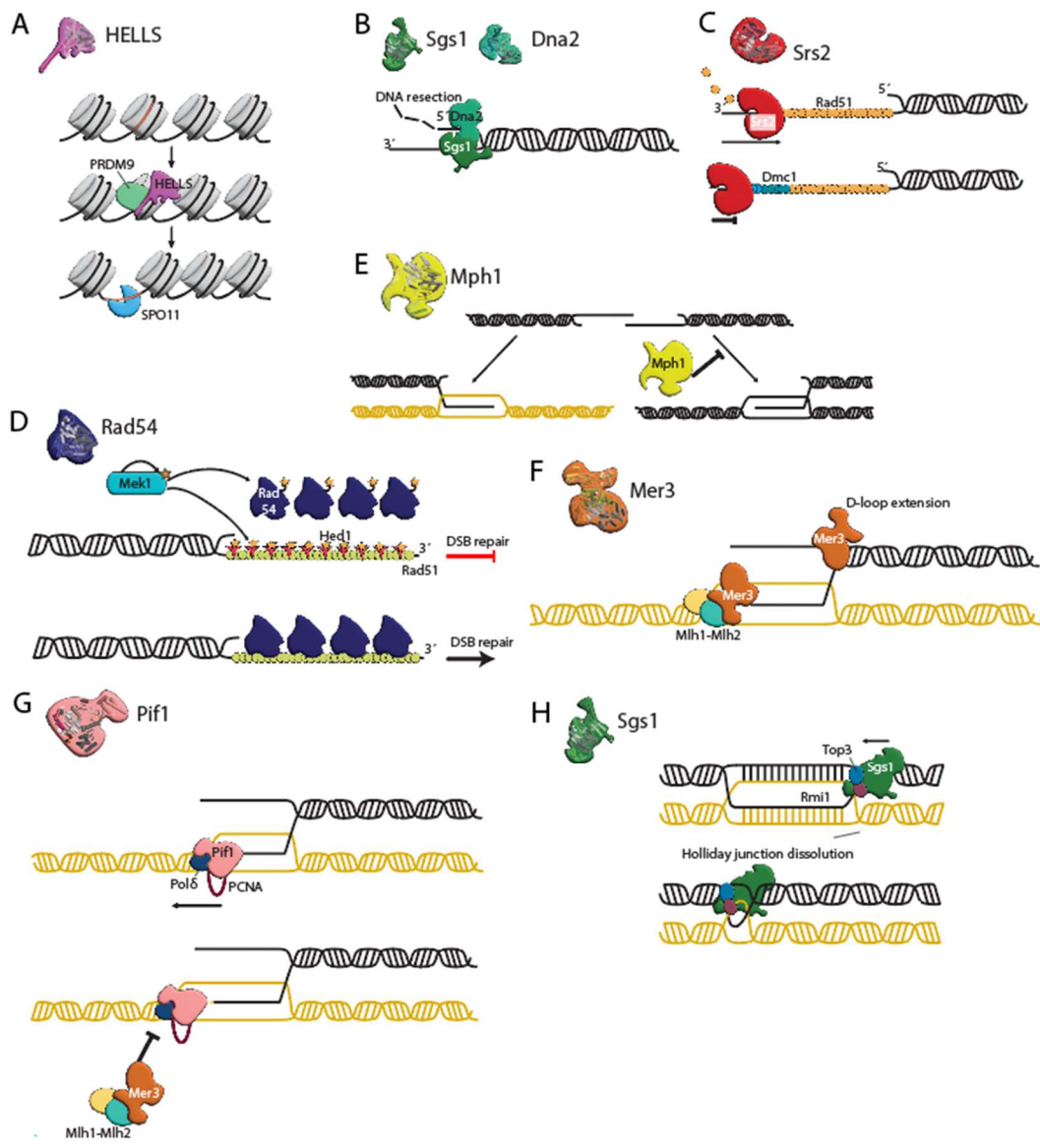


Figure 3.2. Mechanisms of nucleic acid helicases in meiosis

A. Mechanism of HELLs helicase. PRDM9 (green) binds to specific DNA sequences. HELLs (purple) is brought to these sites via direct binding to PRDM9 and moves nucleosomes away from the PRDM9 DNA sequence (red), enabling cleavage by SPO11 (blue). **B.** Sgs1 and Dna2 in DSB resection. The nuclease region of Dna2 (cyan) is a complementary pathway in break resection to Exo1. The nuclease activity of Dna2 is stimulated by Sgs1 (green). **C.** Srs2-mediated disruption of presynaptic filaments. Srs2 (red) down regulates HR by removing Rad51 (yellow) from presynaptic filaments. Dmc1 (blue) on presynaptic filaments is refractory to Srs2 activity, thus stimulating HR in meiosis. **D.** Rad54 on presynaptic filaments. During meiosis Rad54 (dark blue) can be phosphorylated by Mek1 kinase (light blue), which also targets the Rad54 cofactor Hed1 (red). The combination of these phosphorylations prevents Rad54 from catalysing the invasion of DNA duplexes by the presynaptic filament, and therefore downregulates DNA repair. **E.** Mph1 and interhomolog bias. In yeast, Mph1 antagonises intersister recombination (right) thereby favouring recombination from the homolog (left). **F.** Mer3 acting on nascent D-loops. Mer3 regulates D-loop extension and facilitates the formation of SEIs. Mer3 also interacts with Mlh1/Mlh2, which may form a block on the extension of D-loops, limiting the size of gene conversion tracts. **G.** Pif1, Pol δ and PCNA. The helicase Pif1 stimulates the polymerase activity of Pol δ together with PCNA. In the context of recombination intermediates this activity is antagonised by the Mer3/Mlh1/Mlh2 complex, which acts to limit the size of gene conversion tracts. **H.** Sgs1, Top3, Rmi1 form a complex (STR), which dissolves a variety of HR intermediates. Here the helicase activity of Sgs1 is being shown working on a double Holliday junction.

3.5. Summary

With the exception of Mer3/HFM1 none of the helicases above are unique to meiosis. Yet through a combination of meiosis-specific interaction partners and post-translational modifications the activity of many helicases are modulated to facilitate the goal of meiosis I, namely the successful generation of crossover recombination events between homologous chromosomes. Genetic and proteomic studies continue to generate new interaction partners and modifications for these helicases. Recent breakthroughs in protein structure prediction have given the community access to what are likely to prove high-quality models of these helicases and their binding partners. Additional hybrid structural biological approaches combined with multi-component biochemical reconstitution experiments and separation of function mutations will provide us with both details of these interactions and their potential physiological function.

Acknowledgements

We thank Gerben Vader, Elisabeth Weir, and members of the Weir Laboratory for input and critical reading of the manuscript. Work in the Weir Lab is funded by the Max Planck Society, and by the German Research Foundation (WE 6513/2-1). We would also like to take the opportunity to apologise to those scientists whose excellent work we were unable to include here due to space constraints.

References

- Absmeier, E., Santos, K. F., & Wahl, M. C. (2016). Functions and regulation of the Brr2 RNA helicase during splicing. *Cell Cycle*, *15*(24), 3362–3377. <https://doi.org/10.1080/15384101.2016.1249549>
- Acquaviva, L., Székvolgyi, L., Dichtl, B., Dichtl, B. S., André, C. de L. R. S., Nicolas, A., & Géli, V. (2013). The COMPASS Subunit Spp1 Links Histone Methylation to Initiation of Meiotic Recombination. *Science*, *339*(6116), 215–218. <https://doi.org/10.1126/science.1225739>
- Ahmad, F., & Stewart, E. (2005). The N-terminal region of the *Schizosaccharomyces pombe* RecQ helicase, Rqh1p, physically interacts with Topoisomerase III and is required for Rqh1p function. *Molecular Genetics and Genomics: MGG*, *273*(1), 102–114. <https://doi.org/10.1007/s00438-005-1111-3>
- Allers, T., & Lichten, M. (2001). Differential timing and control of noncrossover and crossover recombination during meiosis. *Cell*, *106*(1), 47–57. [https://doi.org/10.1016/s0092-8674\(01\)00416-0](https://doi.org/10.1016/s0092-8674(01)00416-0)

- Amitani, I., Baskin, R. J., & Kowalczykowski, S. C. (2006). Visualization of Rad54, a chromatin remodeling protein, translocating on single DNA molecules. *Molecular Cell*, *23*(1), 143–148. <https://doi.org/10.1016/j.molcel.2006.05.009>
- Antony, E., Tomko, E. J., Xiao, Q., Krejci, L., Lohman, T. M., & Ellenberger, T. (2009). Srs2 disassembles Rad51 filaments by a protein-protein interaction triggering ATP turnover and dissociation of Rad51 from DNA. *Molecular Cell*, *35*(1), 105–115. <https://doi.org/10.1016/j.molcel.2009.05.026>
- Armstrong, A. A., Mohideen, F., & Lima, C. D. (2012). Recognition of SUMO-modified PCNA requires tandem receptor motifs in Srs2. *Nature*, *483*(7387), 59–63. <https://doi.org/10.1038/nature10883>
- Bae, S.-H., Choi, E., Lee, K.-H., Park, J. S., Lee, S.-H., & Seo, Y.-S. (1998). Dna2 of *Saccharomyces cerevisiae* Possesses a Single-stranded DNA-specific Endonuclease Activity That Is Able to Act on Double-stranded DNA in the Presence of ATP*. *The Journal of Biological Chemistry*, *273*(41), 26880–26890. <https://doi.org/10.1074/jbc.273.41.26880>
- Bae, S.-H., & Seo, Y.-S. (2000). Characterization of the Enzymatic Properties of the Yeast Dna2 Helicase/Endonuclease Suggests a New Model for Okazaki Fragment Processing *. *The Journal of Biological Chemistry*, *275*(48), 38022–38031. <https://doi.org/10.1074/jbc.M006513200>
- Barber, L. J., Youds, J. L., Ward, J. D., McIlwraith, M. J., O’Neil, N. J., Petalcorin, M. I. R., Martin, J. S., Collis, S. J., Cantor, S. B., Auclair, M., Tissenbaum, H., West, S. C., Rose, A. M., & Boulton, S. J. (2008). RTEL1 maintains genomic stability by suppressing homologous recombination. *Cell*, *135*(2), 261–271. <https://doi.org/10.1016/j.cell.2008.08.016>
- Baudat, F., Buard, J., Grey, C., Fledel-Alon, A., Ober, C., Przeworski, M., Coop, G., & de Massy, B. (2010). PRDM9 is a major determinant of meiotic recombination hotspots in humans and mice. *Science*, *327*(5967), 836–840. <https://doi.org/10.1126/science.1183439>
- Baudat, F., Imai, Y., & de Massy, B. (2013). Meiotic recombination in mammals: localization and regulation. *Nature Reviews. Genetics*, *14*(11), 794–806. <https://doi.org/10.1038/nrg3573>
- Bennett, R. J., Noirot-Gros, M.-F., & Wang, J. C. (2000). Interaction between Yeast Sgs1 Helicase and DNA Topoisomerase III *. *The Journal of Biological Chemistry*, *275*(35), 26898–26905. [https://doi.org/10.1016/S0021-9258\(19\)61459-6](https://doi.org/10.1016/S0021-9258(19)61459-6)
- Bernstein, K. A., Shor, E., Sunjevaric, I., Fumasoni, M., Burgess, R. C., Foiani, M., Brnzei, D., & Rothstein, R. (2009). Sgs1 function in the repair of DNA replication intermediates is separable from its role in homologous recombinational repair. *The EMBO Journal*, *28*(7), 915–925. <https://doi.org/10.1038/emboj.2009.28>
- Bhagwat, N. R., Owens, S. N., Ito, M., Boinapalli, J. V., Poa, P., Ditzel, A., Koppurapu, S., Mahalawat, M., Davies, O. R., Collins, S. R., Johnson, J. R., Krogan, N. J., & Hunter, N. (2021). SUMO is a pervasive regulator of meiosis. *eLife*, *10*, e57720. <https://doi.org/10.7554/eLife.57720>
- Börner, G. V., Kleckner, N., & Hunter, N. (2004). Crossover/noncrossover differentiation, synaptonemal complex formation, and regulatory surveillance at the leptotene/zygotene transition of meiosis. *Cell*, *117*(1), 29–45. [https://doi.org/10.1016/s0092-8674\(04\)00292-2](https://doi.org/10.1016/s0092-8674(04)00292-2)

- Brick, K., Thibault-Sennett, S., Smagulova, F., Lam, K.-W. G., Pu, Y., Pratto, F., Camerini-Otero, R. D., & Petukhova, G. V. (2018). Extensive sex differences at the initiation of genetic recombination. *Nature*, *561*(7723), 338–342. <https://doi.org/10.1038/s41586-018-0492-5>
- Brown, M. S., & Bishop, D. K. (2014). DNA strand exchange and RecA homologs in meiosis. *Cold Spring Harbor Perspectives in Biology*, *7*(1), a016659. <https://doi.org/10.1101/cshperspect.a016659>
- Budd, M. E., Choe, W.-C., & Campbell, J. L. (2000). The Nuclease Activity of the Yeast Dna2 Protein, Which Is Related to the RecB-like Nucleases, Is Essential in Vivo *. *The Journal of Biological Chemistry*, *275*(22), 16518–16529. <https://doi.org/10.1074/jbc.M909511199>
- Burrage, J., Termanis, A., Geissner, A., Myant, K., Gordon, K., & Stancheva, I. (2012). The SNF2 family ATPase LSH promotes phosphorylation of H2AX and efficient repair of DNA double-strand breaks in mammalian cells. *Journal of Cell Science*, *125*(Pt 22), 5524–5534. <https://doi.org/10.1242/jcs.111252>
- Busygina, V., Sehorn, M. G., Shi, I. Y., Tsubouchi, H., Roeder, G. S., & Sung, P. (2008). Hed1 regulates Rad51-mediated recombination via a novel mechanism. *Genes & Development*, *22*(6), 786–795. <https://doi.org/10.1101/gad.1638708>
- Buzovetsky, O., Kwon, Y., Pham, N. T., Kim, C., Ira, G., Sung, P., & Xiong, Y. (2017). Role of the Pif1-PCNA Complex in Pol δ -Dependent Strand Displacement DNA Synthesis and Break-Induced Replication. *Cell Reports*, *21*(7), 1707–1714. <https://doi.org/10.1016/j.celrep.2017.10.079>
- Byrd, A. K., & Raney, K. D. (2017). Structure and function of Pif1 helicase. *Biochemical Society Transactions*, *45*(5), 1159–1171. <https://doi.org/10.1042/BST20170096>
- Bythell-Douglas, R., & Deans, A. J. (2021). A Structural Guide to the Bloom Syndrome Complex. *Structure*, *29*(2), 99–113. <https://doi.org/10.1016/j.str.2020.11.020>
- Callender, T. L., Laureau, R., Wan, L., Chen, X., Sandhu, R., Laljee, S., Zhou, S., Suhandynata, R. T., Prugar, E., Gaines, W. A., Kwon, Y., Börner, G. V., Nicolas, A., Neiman, A. M., & Hollingsworth, N. M. (2016). Mek1 Down Regulates Rad51 Activity during Yeast Meiosis by Phosphorylation of Hed1. *PLoS Genetics*, *12*(8), e1006226. <https://doi.org/10.1371/journal.pgen.1006226>
- Cannavo, E., Sanchez, A., Anand, R., Ranjha, L., Hugener, J., Adam, C., Acharya, A., Weyland, N., Aran-Guiu, X., Charbonnier, J.-B., Hoffmann, E. R., Borde, V., Matos, J., & Cejka, P. (2020). Regulation of the MLH1-MLH3 endonuclease in meiosis. *Nature*, *586*(7830), 618–622. <https://doi.org/10.1038/s41586-020-2592-2>
- Carballo, J. A., Johnson, A. L., Sedgwick, S. G., & Cha, R. S. (2008). Phosphorylation of the Axial Element Protein Hop1 by Mec1/Tel1 Ensures Meiotic Interhomolog Recombination. *Cell*, *132*(5), 758–770. <https://doi.org/10.1016/j.cell.2008.01.035>
- Cejka, P., Plank, J. L., Dombrowski, C. C., & Kowalczykowski, S. C. (2012). Decatenation of DNA by the *S. cerevisiae* Sgs1-Top3-Rmi1 and RPA complex: a mechanism for disentangling chromosomes. *Molecular Cell*, *47*(6), 886–896. <https://doi.org/10.1016/j.molcel.2012.06.032>
- Cejka, P., & Symington, L. S. (2021). DNA End Resection: Mechanism and Control. *Annual Review of Genetics*, *55*, 285–307. <https://doi.org/10.1146/annurev-genet-071719-020312>

- Ceppi, I., Howard, S. M., Kasaciunaite, K., Pinto, C., Anand, R., Seidel, R., & Cejka, P. (2020). CtIP promotes the motor activity of DNA2 to accelerate long-range DNA end resection. *Proceedings of the National Academy of Sciences of the United States of America*, *117*(16), 8859–8869. <https://doi.org/10.1073/pnas.2001165117>
- Chen, C., Zhang, W., Timofejeva, L., Gerardin, Y., & Ma, H. (2005). The Arabidopsis ROCK-N-ROLLERS gene encodes a homolog of the yeast ATP-dependent DNA helicase MER3 and is required for normal meiotic crossover formation. *The Plant Journal: For Cell and Molecular Biology*, *43*(3), 321–334. <https://doi.org/10.1111/j.1365-313X.2005.02461.x>
- Chen, H., Lisby, M., & Symington, L. S. (2013). RPA coordinates DNA end resection and prevents formation of DNA hairpins. *Molecular Cell*, *50*(4), 589–600. <https://doi.org/10.1016/j.molcel.2013.04.032>
- Chung, W.-H., Zhu, Z., Papusha, A., Malkova, A., & Ira, G. (2010). Defective resection at DNA double-strand breaks leads to de novo telomere formation and enhances gene targeting. *PLoS Genetics*, *6*(5), e1000948. <https://doi.org/10.1371/journal.pgen.1000948>
- Clever, B., Interthal, H., Schmuckli-Maurer, J., King, J., Sigrist, M., & Heyer, W. D. (1997). Recombinational repair in yeast: functional interactions between Rad51 and Rad54 proteins. *The EMBO Journal*, *16*(9), 2535–2544. <https://doi.org/10.1093/emboj/16.9.2535>
- Cloud, V., Chan, Y.-L., Grubb, J., Budke, B., & Bishop, D. K. (2012). Rad51 Is an Accessory Factor for Dmc1-Mediated Joint Molecule Formation During Meiosis. *Science*, *337*(6099), 1222–1225. <https://doi.org/10.1126/science.1219379>
- Clyne, R. K., Katis, V. L., Jessop, L., Benjamin, K. R., Herskowitz, I., Lichten, M., & Nasmyth, K. (2003). Polo-like kinase Cdc5 promotes chiasmata formation and cosegregation of sister centromeres at meiosis I. *Nature Cell Biology*, *5*(5), 480–485. <https://doi.org/10.1038/ncb977>
- Colavito, S., Macris-Kiss, M., Seong, C., Gleeson, O., Greene, E. C., Klein, H. L., Krejci, L., & Sung, P. (2009). Functional significance of the Rad51-Srs2 complex in Rad51 presynaptic filament disruption. *Nucleic Acids Research*, *37*(20), 6754–6764. <https://doi.org/10.1093/nar/gkp748>
- Crickard, J. B., Kaniecki, K., Kwon, Y., Sung, P., & Greene, E. C. (2018). Meiosis-specific recombinase Dmc1 is a potent inhibitor of the Srs2 antirecombinase. *Proceedings of the National Academy of Sciences of the United States of America*, *115*(43), E10041–E10048. <https://doi.org/10.1073/pnas.1810457115>
- Crickard, J. B., Kaniecki, K., Kwon, Y., Sung, P., Lisby, M., & Greene, E. C. (2018). Regulation of Hed1 and Rad54 binding during maturation of the meiosis-specific presynaptic complex. *The EMBO Journal*, *37*(7), e98728. <https://doi.org/10.15252/embj.201798728>
- Crickard, J. B., Moevus, C. J., Kwon, Y., Sung, P., & Greene, E. C. (2020). Rad54 Drives ATP Hydrolysis-Dependent DNA Sequence Alignment during Homologous Recombination. *Cell*, *181*(6), 1380–1394.e18. <https://doi.org/10.1016/j.cell.2020.04.056>

- Crismani, W., Girard, C., Froger, N., Pradillo, M., Santos, J. L., Chelysheva, L., Copenhaver, G. P., Horlow, C., & Mercier, R. (2012). FANCM limits meiotic crossovers. *Science*, *336*(6088), 1588–1590. <https://doi.org/10.1126/science.1220381>
- Cunniff, C., Bassetti, J. A., & Ellis, N. A. (2017). Bloom's Syndrome: Clinical Spectrum, Molecular Pathogenesis, and Cancer Predisposition. *Molecular Syndromology*, *8*(1), 4–23. <https://doi.org/10.1159/000452082>
- Deans, A. J., & West, S. C. (2009). FANCM connects the genome instability disorders Bloom's Syndrome and Fanconi Anemia. *Molecular Cell*, *36*(6), 943–953. <https://doi.org/10.1016/j.molcel.2009.12.006>
- De La Fuente, R., Baumann, C., Fan, T., Schmidtman, A., Dobrinski, I., & Muegge, K. (2006). Lsh is required for meiotic chromosome synapsis and retrotransposon silencing in female germ cells. *Nature Cell Biology*, *8*(12), 1448–1454. <https://doi.org/10.1038/ncb1513>
- Deng, S. K., Yin, Y., Petes, T. D., & Symington, L. S. (2015). Mre11-Sae2 and RPA Collaborate to Prevent Palindromic Gene Amplification. *Molecular Cell*, *60*(3), 500–508. <https://doi.org/10.1016/j.molcel.2015.09.027>
- Dennis, K., Fan, T., Geiman, T., Yan, Q., & Muegge, K. (2001). Lsh, a member of the SNF2 family, is required for genome-wide methylation. *Genes & Development*, *15*(22), 2940–2944. <https://doi.org/10.1101/gad.929101>
- Dresser, M. E., Ewing, D. J., Conrad, M. N., Dominguez, A. M., Barstead, R., Jiang, H., & Kodadek, T. (1997). DMC1 functions in a *Saccharomyces cerevisiae* meiotic pathway that is largely independent of the RAD51 pathway. *Genetics*, *147*(2), 533–544. <https://doi.org/10.1093/genetics/147.2.533>
- Duroc, Y., Kumar, R., Ranjha, L., Adam, C., Guérois, R., Md Muntaz, K., Marsolier-Kergoat, M.-C., Dingli, F., Laureau, R., Loew, D., Llorente, B., Charbonnier, J.-B., Cejka, P., & Borde, V. (2017). Concerted action of the MutL β heterodimer and Mer3 helicase regulates the global extent of meiotic gene conversion. *eLife*, *6*. <https://doi.org/10.7554/eLife.21900>
- Elango, R., Sheng, Z., Jackson, J., DeCata, J., Ibrahim, Y., Pham, N. T., Liang, D. H., Sakofsky, C. J., Vindigni, A., Lobachev, K. S., Ira, G., & Malkova, A. (2017). Break-induced replication promotes formation of lethal joint molecules dissolved by Srs2. *Nature Communications*, *8*(1), 1790. <https://doi.org/10.1038/s41467-017-01987-2>
- Fanning, E., Klimovich, V., & Nager, A. R. (2006). A dynamic model for replication protein A (RPA) function in DNA processing pathways. *Nucleic Acids Research*, *34*(15), 4126–4137. <https://doi.org/10.1093/nar/gkl550>
- Flaus, A., Martin, D. M. A., Barton, G. J., & Owen-Hughes, T. (2006). Identification of multiple distinct Snf2 subfamilies with conserved structural motifs. *Nucleic Acids Research*, *34*(10), 2887–2905. <https://doi.org/10.1093/nar/gkl295>
- Fouquet, B., Pawlikowska, P., Caburet, S., Guigon, C., Mäkinen, M., Tanner, L., Hietala, M., Urbanska, K., Bellutti, L., Legois, B., Bessieres, B., Gougeon, A., Benachi, A., Livera, G., Rosselli, F., Veitia, R. A., &

- Misrahi, M. (2017). A homozygous FANCM mutation underlies a familial case of non-syndromic primary ovarian insufficiency. *eLife*, *6*. <https://doi.org/10.7554/eLife.30490>
- Gravel, S., Chapman, J. R., Magill, C., & Jackson, S. P. (2008). DNA helicases Sgs1 and BLM promote DNA double-strand break resection. *Genes & Development*, *22*(20), 2767–2772. <https://doi.org/10.1101/gad.503108>
- Grigaitis, R., Ranjha, L., Wild, P., Kasaciunaite, K., Ceppi, I., Kissling, V., Henggeler, A., Susperregui, A., Peter, M., Seidel, R., Cejka, P., & Matos, J. (2020). Phosphorylation of the RecQ Helicase Sgs1/BLM Controls Its DNA Unwinding Activity during Meiosis and Mitosis. *Developmental Cell*, *53*(6), 706–723.e5. <https://doi.org/10.1016/j.devcel.2020.05.016>
- Gupta, S. V., & Schmidt, K. H. (2020). Maintenance of Yeast Genome Integrity by RecQ Family DNA Helicases. *Genes*, *11*(2). <https://doi.org/10.3390/genes11020205>
- Hatkevich, T., & Sekelsky, J. (2017). Bloom syndrome helicase in meiosis: Pro-crossover functions of an anti-crossover protein. *BioEssays: News and Reviews in Molecular, Cellular and Developmental Biology*, *39*(9). <https://doi.org/10.1002/bies.201700073>
- Hegnauer, A. M., Hustedt, N., Shimada, K., Pike, B. L., Vogel, M., Amsler, P., Rubin, S. M., van Leeuwen, F., Guénolé, A., van Attikum, H., Thomä, N. H., & Gasser, S. M. (2012). An N-terminal acidic region of Sgs1 interacts with Rpa70 and recruits Rad53 kinase to stalled forks. *The EMBO Journal*, *31*(18), 3768–3783. <https://doi.org/10.1038/emboj.2012.195>
- Holloway, J. K., Morelli, M. A., Borst, P. L., & Cohen, P. E. (2010). Mammalian BLM helicase is critical for integrating multiple pathways of meiotic recombination. *The Journal of Cell Biology*, *188*(6), 779–789. <https://doi.org/10.1083/jcb.200909048>
- Hudson, D. F., Amor, D. J., Boys, A., Butler, K., Williams, L., Zhang, T., & Kalitsis, P. (2016). Loss of RMI2 Increases Genome Instability and Causes a Bloom-Like Syndrome. *PLoS Genetics*, *12*(12), e1006483. <https://doi.org/10.1371/journal.pgen.1006483>
- Hu, G., Katuwawala, A., Wang, K., Wu, Z., Ghadermarzi, S., Gao, J., & Kurgan, L. (2021). fIDPnn: Accurate intrinsic disorder prediction with putative propensities of disorder functions. *Nature Communications*, *12*(1), 4438. <https://doi.org/10.1038/s41467-021-24773-7>
- Humphries, N., & Hochwagen, A. (2014). A non-sister act: Recombination template choice during meiosis. *Experimental Cell Research*, *329*(1), 53–60. <https://doi.org/10.1016/j.yexcr.2014.08.024>
- Hunter, N. (2015). Meiotic Recombination: The Essence of Heredity. *Cold Spring Harbor Perspectives in Biology*, *7*(12). <https://doi.org/10.1101/cshperspect.a016618>
- Hunter, N., & Kleckner, N. (2001). The single-end invasion: an asymmetric intermediate at the double-strand break to double-holliday junction transition of meiotic recombination. *Cell*, *106*(1), 59–70. [https://doi.org/10.1016/s0092-8674\(01\)00430-5](https://doi.org/10.1016/s0092-8674(01)00430-5)
- Imai, Y., Biot, M., Clément, J. A., Teragaki, M., Urbach, S., Robert, T., Baudat, F., Grey, C., & de Massy, B. (2020). PRDM9 activity depends on HELLS and promotes local 5-hydroxymethylcytosine enrichment. *eLife*, *9*. <https://doi.org/10.7554/eLife.57117>

- Ito, S., Shen, L., Dai, Q., Wu, S. C., Collins, L. B., Swenberg, J. A., He, C., & Zhang, Y. (2011). Tet proteins can convert 5-methylcytosine to 5-formylcytosine and 5-carboxylcytosine. *Science*, *333*(6047), 1300–1303. <https://doi.org/10.1126/science.1210597>
- Jenkins, S. S., Gore, S., Guo, X., Liu, J., Ede, C., Veaute, X., Jinks-Robertson, S., Kowalczykowski, S. C., & Heyer, W.-D. (2019). Role of the Srs2-Rad51 Interaction Domain in Crossover Control in *Saccharomyces cerevisiae*. *Genetics*, *212*(4), 1133–1145. <https://doi.org/10.1534/genetics.119.302337>
- Jeness, C., Giunta, S., Müller, M. M., Kimura, H., Muir, T. W., & Funabiki, H. (2018). HELLS and CDCA7 comprise a bipartite nucleosome remodeling complex defective in ICF syndrome. *Proceedings of the National Academy of Sciences of the United States of America*, *115*(5), E876–E885. <https://doi.org/10.1073/pnas.1717509115>
- Jessop, L., Rockmill, B., Roeder, G. S., & Lichten, M. (2006). Meiotic chromosome synapsis-promoting proteins antagonize the anti-crossover activity of sgs1. *PLoS Genetics*, *2*(9), e155. <https://doi.org/10.1371/journal.pgen.0020155>
- Jia, J., Shi, Y., Chen, L., Lai, W., Yan, B., Jiang, Y., Xiao, D., Xi, S., Cao, Y., Liu, S., Cheng, Y., & Tao, Y. (2017). Decrease in Lymphoid Specific Helicase and 5-hydroxymethylcytosine Is Associated with Metastasis and Genome Instability. *Theranostics*, *7*(16), 3920–3932. <https://doi.org/10.7150/thno.21389>
- Kaniecki, K., De Tullio, L., Gibb, B., Kwon, Y., Sung, P., & Greene, E. C. (2017). Dissociation of Rad51 Presynaptic Complexes and Heteroduplex DNA Joints by Tandem Assemblies of Srs2. *Cell Reports*, *21*(11), 3166–3177. <https://doi.org/10.1016/j.celrep.2017.11.047>
- Kasaciunaite, K., Fettes, F., Levikova, M., Daldrop, P., Anand, R., Cejka, P., & Seidel, R. (2019). Competing interaction partners modulate the activity of Sgs1 helicase during DNA end resection. *The EMBO Journal*, *38*(13), e101516. <https://doi.org/10.15252/embj.2019101516>
- Kasak, L., Punab, M., Nagirnaja, L., Grigorova, M., Minajeva, A., Lopes, A. M., Punab, A. M., Aston, K. I., Carvalho, F., Laasik, E., Smith, L. B., GEMINI Consortium, Conrad, D. F., & Laan, M. (2018). Bi-allelic Recessive Loss-of-Function Variants in FANCM Cause Non-obstructive Azoospermia. *American Journal of Human Genetics*, *103*(2), 200–212. <https://doi.org/10.1016/j.ajhg.2018.07.005>
- Kaur, H., De Muyt, A., & Lichten, M. (2015). Top3-Rmi1 DNA Single-Strand Decatenase Is Integral to the Formation and Resolution of Meiotic Recombination Intermediates. *Molecular Cell*, *57*(4). <https://doi.org/10.1016/j.molcel.2015.01.020>
- Keeney, S. (2008). Spo11 and the Formation of DNA Double-Strand Breaks in Meiosis. *Genome Dynamics and Stability*, *2*, 81–123. https://doi.org/10.1007/7050_2007_026
- Keeney, S., Giroux, C. N., & Kleckner, N. (1997). Meiosis-specific DNA double-strand breaks are catalyzed by Spo11, a member of a widely conserved protein family. *Cell*, *88*(3), 375–384. [https://doi.org/10.1016/s0092-8674\(00\)81876-0](https://doi.org/10.1016/s0092-8674(00)81876-0)

- Keskin, H., Shen, Y., Huang, F., Patel, M., Yang, T., Ashley, K., Mazin, A. V., & Storici, F. (2014). Transcript-RNA-templated DNA recombination and repair. *Nature*, *515*(7527), 436–439. <https://doi.org/10.1038/nature13682>
- Kolesar, P., Sarangi, P., Altmannova, V., Zhao, X., & Krejci, L. (2012). Dual roles of the SUMO-interacting motif in the regulation of Srs2 sumoylation. *Nucleic Acids Research*, *40*(16), 7831–7843. <https://doi.org/10.1093/nar/gks484>
- Kowalczykowski, S. C. (2015). An Overview of the Molecular Mechanisms of Recombinational DNA Repair. *Cold Spring Harbor Perspectives in Biology*, *7*(11). <https://doi.org/10.1101/cshperspect.a016410>
- Krejci, L., Van Komen, S., Li, Y., Villemain, J., Reddy, M. S., Klein, H., Ellenberger, T., & Sung, P. (2003). DNA helicase Srs2 disrupts the Rad51 presynaptic filament. *Nature*, *423*(6937), 305–309. <https://doi.org/10.1038/nature01577>
- Kulkarni, D. S., Owens, S. N., Honda, M., Ito, M., Yang, Y., Corrigan, M. W., Chen, L., Quan, A. L., & Hunter, N. (2020). PCNA activates the MutLγ endonuclease to promote meiotic crossing over. *Nature*, *586*(7830), 623–627. <https://doi.org/10.1038/s41586-020-2645-6>
- Lao, J. P., Cloud, V., Huang, C.-C., Grubb, J., Thacker, D., Lee, C.-Y., Dresser, M. E., Hunter, N., & Bishop, D. K. (2013). Meiotic crossover control by concerted action of Rad51-Dmc1 in homolog template bias and robust homeostatic regulation. *PLoS Genetics*, *9*(12), e1003978. <https://doi.org/10.1371/journal.pgen.1003978>
- Lao, J. P., & Hunter, N. (2010). Trying to avoid your sister. *PLoS Biology*, *8*(10), e1000519. <https://doi.org/10.1371/journal.pbio.1000519>
- Li, S. S.-C. (2005). Specificity and versatility of SH3 and other proline-recognition domains: structural basis and implications for cellular signal transduction. *Biochemical Journal*, *390*(Pt 3), 641–653. <https://doi.org/10.1042/BJ20050411>
- Lorenz, A., Osman, F., Sun, W., Nandi, S., Steinacher, R., & Whitby, M. C. (2012). The fission yeast FANCM ortholog directs non-crossover recombination during meiosis. *Science*, *336*(6088), 1585–1588. <https://doi.org/10.1126/science.1220111>
- Lu, K.-Y., Chen, W.-F., Rety, S., Liu, N.-N., Wu, W.-Q., Dai, Y.-X., Li, D., Ma, H.-Y., Dou, S.-X., & Xi, X.-G. (2018). Insights into the structural and mechanistic basis of multifunctional *S. cerevisiae* Pif1p helicase. *Nucleic Acids Research*, *46*(3), 1486–1500. <https://doi.org/10.1093/nar/gkx1217>
- Luo, D., Ding, S. C., Vela, A., Kohlway, A., Lindenbach, B. D., & Pyle, A. M. (2011). Structural insights into RNA recognition by RIG-I. *Cell*, *147*(2), 409–422. <https://doi.org/10.1016/j.cell.2011.09.023>
- Makovets, S., & Blackburn, E. H. (2009). DNA damage signalling prevents deleterious telomere addition at DNA breaks. *Nature Cell Biology*, *11*(11), 1383–1386. <https://doi.org/10.1038/ncb1985>
- Martin, C.-A., Sarlós, K., Logan, C. V., Thakur, R. S., Parry, D. A., Bizard, A. H., Leitch, A., Cleal, L., Ali, N. S., Al-Owain, M. A., Allen, W., Altmüller, J., Aza-Carmona, M., Barakat, B. A. Y., Barraza-García, J., Begtrup, A., Bogliolo, M., Cho, M. T., Cruz-Rojo, J., ... Jackson, A. P. (2018). Mutations in TOP3A Cause

- a Bloom Syndrome-like Disorder. *American Journal of Human Genetics*, 103(2), 221–231. <https://doi.org/10.1016/j.ajhg.2018.07.001>
- Matos, J., Blanco, M. G., Maslen, S., Skehel, J. M., & West, S. C. (2011). Regulatory control of the resolution of DNA recombination intermediates during meiosis and mitosis. *Cell*, 147(1), 158–172. <https://doi.org/10.1016/j.cell.2011.08.032>
- Mazina, O. M., Mazin, A. V., Nakagawa, T., Kolodner, R. D., & Kowalczykowski, S. C. (2004). *Saccharomyces cerevisiae* Mer3 Helicase Stimulates 3'–5' Heteroduplex Extension by Rad51. *Cell*, 117(1), 47–56. [https://doi.org/10.1016/s0092-8674\(04\)00294-6](https://doi.org/10.1016/s0092-8674(04)00294-6)
- Mimitou, E. P., & Symington, L. S. (2008). Sae2, Exo1 and Sgs1 collaborate in DNA double-strand break processing. *Nature*, 455(7214), 770–774. <https://doi.org/10.1038/nature07312>
- Mimitou, E. P., Yamada, S., & Keeney, S. (2017). A global view of meiotic double-strand break end resection. *Science*, 355(6320), 40–45. <https://doi.org/10.1126/science.aak9704>
- Nakagawa, T., Flores-Rozas, H., & Kolodner, R. D. (2001). The MER3 Helicase Involved in Meiotic Crossing Over Is Stimulated by Single-stranded DNA-binding Proteins and Unwinds DNA in the 3' to 5' Direction. *The Journal of Biological Chemistry*, 276(34), 31487–31493. <https://doi.org/10.1074/jbc.M104003200>
- Nakagawa, T., & Kolodner, R. D. (2002a). *Saccharomyces cerevisiae* Mer3 is a DNA helicase involved in meiotic crossing over. *Molecular and Cellular Biology*, 22(10), 3281–3291. <https://doi.org/10.1128/mcb.22.10.3281-3291.2002>
- Nakagawa, T., & Kolodner, R. D. (2002b). The MER3 DNA helicase catalyzes the unwinding of holliday junctions. *The Journal of Biological Chemistry*, 277(31), 28019–28024. <https://doi.org/10.1074/jbc.M204165200>
- Niu, H., Wan, L., Baumgartner, B., Schaefer, D., Loidl, J., & Hollingsworth, N. M. (2005). Partner choice during meiosis is regulated by Hop1-promoted dimerization of Mek1. *Molecular Biology of the Cell*, 16(12), 5804–5818. <https://www.molbiolcell.org/doi/abs/10.1091/mbc.E05-05-0465>
- Niu, H., Wan, L., Busygina, V., Kwon, Y., Allen, J. A., Li, X., Kunz, R. C., Kubota, K., Wang, B., Sung, P., Shokat, K. M., Gygi, S. P., & Hollingsworth, N. M. (2009). Regulation of meiotic recombination via Mek1-mediated Rad54 phosphorylation. *Molecular Cell*, 36(3), 393–404. <https://doi.org/10.1016/j.molcel.2009.09.029>
- Oh, S. D., Lao, J. P., Hwang, P. Y.-H., Taylor, A. F., Smith, G. R., & Hunter, N. (2007). BLM ortholog, Sgs1, prevents aberrant crossing-over by suppressing formation of multichromatid joint molecules. *Cell*, 130(2), 259–272. <https://doi.org/10.1016/j.cell.2007.05.035>
- Paiano, J., Wu, W., Yamada, S., Sciascia, N., Callen, E., Paola Cotrim, A., Deshpande, R. A., Maman, Y., Day, A., Paull, T. T., & Nussenzweig, A. (2020). ATM and PRDM9 regulate SPO11-bound recombination intermediates during meiosis. *Nature Communications*, 11(1), 857. <https://doi.org/10.1038/s41467-020-14654-w>

- Papouli, E., Chen, S., Davies, A. A., Huttner, D., Krejci, L., Sung, P., & Ulrich, H. D. (2005). Crosstalk between SUMO and ubiquitin on PCNA is mediated by recruitment of the helicase Srs2p. *Molecular Cell*, *19*(1), 123–133. <https://doi.org/10.1016/j.molcel.2005.06.001>
- Penedos, A., Johnson, A. L., Strong, E., Goldman, A. S., Carballo, J. A., & Cha, R. S. (2015). Essential and Checkpoint Functions of Budding Yeast ATM and ATR during Meiotic Prophase Are Facilitated by Differential Phosphorylation of a Meiotic Adaptor Protein, Hop1. *PLoS One*, *10*(7), e0134297. <https://doi.org/10.1371/journal.pone.0134297>
- Petukhova, G., Stratton, S., & Sung, P. (1998). Catalysis of homologous DNA pairing by yeast Rad51 and Rad54 proteins. *Nature*, *393*(6680), 91–94. <https://doi.org/10.1038/30037>
- Pfander, B., Moldovan, G.-L., Sacher, M., Hoegge, C., & Jentsch, S. (2005). SUMO-modified PCNA recruits Srs2 to prevent recombination during S phase. *Nature*, *436*(7049), 428–433. <https://doi.org/10.1038/nature03665>
- Prakash, R., Satory, D., Dray, E., Papusha, A., Scheller, J., Kramer, W., Krejci, L., Klein, H., Haber, J. E., Sung, P., & Ira, G. (2009). Yeast Mph1 helicase dissociates Rad51-made D-loops: implications for crossover control in mitotic recombination. *Genes & Development*, *23*(1), 67–79. <https://doi.org/10.1101/gad.1737809>
- Raschle, M., Van Komen, S., Chi, P., Ellenberger, T., & Sung, P. (2004). Multiple interactions with the Rad51 recombinase govern the homologous recombination function of Rad54. *The Journal of Biological Chemistry*, *279*(50), 51973–51980. <https://doi.org/10.1074/jbc.M410101200>
- Sandhu, R., Monge Neria, F., Monge Neria, J., Chen, X., Hollingsworth, N. M., & Börner, G. V. (2020). DNA Helicase Mph1FANCM Ensures Meiotic Recombination between Parental Chromosomes by Dissociating Precocious Displacement Loops. *Developmental Cell*, *53*(4), 458–472.e5. <https://doi.org/10.1016/j.devcel.2020.04.010>
- Schulz, V. P., & Zakian, V. A. (1994). The *Saccharomyces* PIF1 DNA helicase inhibits telomere elongation and de novo telomere formation. *Cell*, *76*(1), 145–155. [https://doi.org/10.1016/0092-8674\(94\)90179-1](https://doi.org/10.1016/0092-8674(94)90179-1)
- Schwacha, A., & Kleckner, N. (1994). Identification of joint molecules that form frequently between homologs but rarely between sister chromatids during yeast meiosis. *Cell*, *76*(1), 51–63. [https://doi.org/10.1016/0092-8674\(94\)90172-4](https://doi.org/10.1016/0092-8674(94)90172-4)
- Schwacha, A., & Kleckner, N. (1995). Identification of double Holliday junctions as intermediates in meiotic recombination. *Cell*, *83*(5), 783–791. [https://doi.org/10.1016/0092-8674\(95\)90191-4](https://doi.org/10.1016/0092-8674(95)90191-4)
- Shaheen, R., Faqeih, E., Ansari, S., Abdel-Salam, G., Al-Hassnan, Z. N., Al-Shidi, T., Alomar, R., Sogaty, S., & Alkuraya, F. S. (2014). Genomic analysis of primordial dwarfism reveals novel disease genes. *Genome Research*, *24*(2), 291–299. <https://doi.org/10.1101/gr.160572.113>
- Shinohara, M., Shita-Yamaguchi, E., Buerstedde, J. M., Shinagawa, H., Ogawa, H., & Shinohara, A. (1997). Characterization of the roles of the *Saccharomyces cerevisiae* RAD54 gene and a homologue of

RAD54, RDH54/TID1, in mitosis and meiosis. *Genetics*, 147(4), 1545–1556. <https://doi.org/10.1093/genetics/147.4.1545>

Singleton, M. R., Dillingham, M. S., & Wigley, D. B. (2007). Structure and mechanism of helicases and nucleic acid translocases. *Annual Review of Biochemistry*, 76, 23–50. <https://doi.org/10.1146/annurev.biochem.76.052305.115300>

Sommermeier, V., Béneut, C., Chaplais, E., Serrentino, M. E., & Borde, V. (2013). Spp1, a Member of the Set1 Complex, Promotes Meiotic DSB Formation in Promoters by Tethering Histone H3K4 Methylation Sites to Chromosome Axes. *Molecular Cell*, 49(1), 43–54. <https://doi.org/10.1016/j.molcel.2012.11.008>

Spruce, C., Dlamini, S., Ananda, G., Bronkema, N., Tian, H., Paigen, K., Carter, G. W., & Baker, C. L. (2020). HELLS and PRDM9 form a pioneer complex to open chromatin at meiotic recombination hot spots. *Genes & Development*, 34(5-6), 398–412. <https://doi.org/10.1101/gad.333542.119>

Sturzenegger, A., Burdova, K., Kanagaraj, R., Levikova, M., Pinto, C., Cejka, P., & Janscak, P. (2014). DNA2 cooperates with the WRN and BLM RecQ helicases to mediate long-range DNA end resection in human cells. *The Journal of Biological Chemistry*, 289(39), 27314–27326. <https://doi.org/10.1074/jbc.M114.578823>

Szankasi, P., & Smith, G. R. (1995). A role for exonuclease I from *S. pombe* in mutation avoidance and mismatch correction. *Science*, 267(5201), 1166–1169. <https://doi.org/10.1126/science.7855597>

Tanaka, K., Miyamoto, N., Shouguchi-Miyata, J., & Ikeda, J.-E. (2006). HFM1, the human homologue of yeast Mer3, encodes a putative DNA helicase expressed specifically in germ-line cells. *DNA Sequence: The Journal of DNA Sequencing and Mapping*, 17(3), 242–246. <https://doi.org/10.1080/10425170600805433>

Tang, S., Wu, M. K. Y., Zhang, R., & Hunter, N. (2015). Pervasive and Essential Roles of the Top3-Rmi1 Decatenase Orchestrate Recombination and Facilitate Chromosome Segregation in Meiosis. *Molecular Cell*, 57(4). <https://doi.org/10.1016/j.molcel.2015.01.021>

Terentyev, Y., Johnson, R., Neale, M. J., Khisroon, M., Bishop-Bailey, A., & Goldman, A. S. H. (2010). Evidence that MEK1 positively promotes interhomologue double-strand break repair. *Nucleic Acids Research*, 38(13), 4349–4360. <https://doi.org/10.1093/nar/gkq137>

Vannier, J.-B., Sarek, G., & Boulton, S. J. (2014). RTEL1: functions of a disease-associated helicase. *Trends in Cell Biology*, 24(7), 416–425. <https://doi.org/10.1016/j.tcb.2014.01.004>

Veaute, X., Jeusset, J., Soustelle, C., Kowalczykowski, S. C., Le Cam, E., & Fabre, F. (2003). The Srs2 helicase prevents recombination by disrupting Rad51 nucleoprotein filaments. *Nature*, 423(6937), 309–312. <https://doi.org/10.1038/nature01585>

Vernekar, D. V., Reginato, G., Adam, C., Ranjha, L., Dingli, F., Marsolier, M.-C., Loew, D., Guérois, R., Llorente, B., Cejka, P., & Borde, V. (2021). The Pif1 helicase is actively inhibited during meiotic recombination which restrains gene conversion tract length. *Nucleic Acids Research*, 49(8), 4522–4533. <https://doi.org/10.1093/nar/gkab232>

- Wang, J., Zhang, W., Jiang, H., Wu, B.-L., & Primary Ovarian Insufficiency Collaboration. (2014). Mutations in HFM1 in recessive primary ovarian insufficiency. *The New England Journal of Medicine*, 370(10), 972–974. <https://doi.org/10.1056/NEJMc1310150>
- Wang, T. F., Kleckner, N., & Hunter, N. (1999). Functional specificity of MutL homologs in yeast: evidence for three Mlh1-based heterocomplexes with distinct roles during meiosis in recombination and mismatch correction. *Proceedings of the National Academy of Sciences of the United States of America*, 96(24), 13914–13919. <https://doi.org/10.1073/pnas.96.24.13914>
- Wesoly, J., Agarwal, S., Sigurdsson, S., Bussen, W., Van Komen, S., Qin, J., van Steeg, H., van Benthem, J., Wassenaar, E., Baarends, W. M., Ghazvini, M., Tafel, A. A., Heath, H., Galjart, N., Essers, J., Grootegoed, J. A., Arnheim, N., Bezzubova, O., Buerstedde, J.-M., ... Kanaar, R. (2006). Differential contributions of mammalian Rad54 paralogs to recombination, DNA damage repair, and meiosis. *Molecular and Cellular Biology*, 26(3), 976–989. <https://doi.org/10.1128/MCB.26.3.976-989.2006>
- Whitby, M. C. (2010). The FANCM family of DNA helicases/translocases. *DNA Repair*, 9(3), 224–236. <https://doi.org/10.1016/j.dnarep.2009.12.012>
- Wild, P., Susperregui, A., Piazza, I., Dörig, C., Oke, A., Arter, M., Yamaguchi, M., Hilditch, A. T., Vuina, K., Chan, K. C., Gromova, T., Haber, J. E., Fung, J. C., Picotti, P., & Matos, J. (2019). Network Rewiring of Homologous Recombination Enzymes during Mitotic Proliferation and Meiosis. *Molecular Cell*, 75(4), 859–874.e4. <https://doi.org/10.1016/j.molcel.2019.06.022>
- Wilson, M. A., Kwon, Y., Xu, Y., Chung, W.-H., Chi, P., Niu, H., Mayle, R., Chen, X., Malkova, A., Sung, P., & Ira, G. (2013). Pif1 helicase and Pol δ promote recombination-coupled DNA synthesis via bubble migration. *Nature*, 502(7471), 393–396. <https://doi.org/10.1038/nature12585>
- Xue, C., Wang, W., Crickard, J. B., Moevus, C. J., Kwon, Y., Sung, P., & Greene, E. C. (2019). Regulatory control of Sgs1 and Dna2 during eukaryotic DNA end resection. *Proceedings of the National Academy of Sciences of the United States of America*, 116(13), 6091–6100. <https://doi.org/10.1073/pnas.1819276116>
- Youds, J. L., Mets, D. G., McIlwraith, M. J., Martin, J. S., Ward, J. D., O'Neil, N. J., Rose, A. M., West, S. C., Meyer, B. J., & Boulton, S. J. (2010). RTEL-1 enforces meiotic crossover interference and homeostasis. *Science*, 327(5970), 1254–1258. <https://doi.org/10.1126/science.1183112>
- Zakharyevich, K., Ma, Y., Tang, S., Hwang, P. Y.-H., Boiteux, S., & Hunter, N. (2010). Temporally and biochemically distinct activities of Exo1 during meiosis: double-strand break resection and resolution of double Holliday junctions. *Molecular Cell*, 40(6), 1001–1015. <https://doi.org/10.1016/j.molcel.2010.11.032>
- Zheng, L., Meng, Y., Campbell, J. L., & Shen, B. (2020). Multiple roles of DNA2 nuclease/helicase in DNA metabolism, genome stability and human diseases. *Nucleic Acids Research*, 48(1), 16–35. <https://doi.org/10.1093/nar/gkz1101>
- Zhu, Z., Chung, W.-H., Shim, E. Y., Lee, S. E., & Ira, G. (2008). Sgs1 helicase and two nucleases Dna2 and Exo1 resect DNA double-strand break ends. *Cell*, 134(6), 981–994. <https://doi.org/10.1016/j.cell.2008.08.037>



4. Biochemical and functional characterization of a meiosis-specific Pch2/ORC AAA+ assembly

María Ascensión Villar-Fernández^{1,2}, Richard Cardoso da Silva¹, Magdalena Firlej³, Dongqing Pan¹, Elisabeth Weir¹, Annika Sarembe¹, Vivek B Raina^{1,2}, Tanja Bange¹, John R Weir^{1,3}, Gerben Vader¹

Author	Author position (%)	Scientific ideas (%)	Data generation (%)	Analysis & interpretation (%)	Paper writing (%)
Magdalena Firlej	3%	10%	5%	5%	5%
Other authors		90%	95%	95%	95%
Paper Title	Biochemical and functional characterization of a meiosis-specific Pch2/ORC AAA+ assembly				
Status in publication process	Published				

Pch2 is a meiosis-specific AAA+ protein that controls several important chromosomal processes. We previously demonstrated that Orc1, a subunit of the ORC, functionally interacts with budding yeast Pch2. The ORC (Orc1-6) AAA+ complex loads the AAA+ MCM helicase to origins of replication, but whether and how ORC collaborates with Pch2 remains unclear. Here, we show that a Pch2 hexamer directly associates with ORC during the meiotic G2/prophase. Biochemical analysis suggests that Pch2 uses its non-enzymatic NH₂-terminal domain and AAA+ core and likely engages the interface of ORC that also binds to Cdc6, a factor crucial for ORC-MCM binding. Canonical ORC function requires association with origins, but we show here that despite causing efficient removal of Orc1 from origins, nuclear depletion of Orc2 and Orc5 does not trigger Pch2/Orc1-like meiotic phenotypes. This suggests that the function for Orc1/Pch2 in meiosis can be executed without efficient association of ORC with origins of replication. In conclusion, we uncover distinct functionalities for Orc1/ORC that drive the establishment of a non-canonical, meiosis-specific AAA+ assembly with Pch2.

DOI [10.26508/lsa.201900630](https://doi.org/10.26508/lsa.201900630) | Received 18 December 2019 | Revised 13 August 2020 | Accepted 13 August 2020 | Published online 21 August 2020

Introduction

Meiosis is a specialized cell division program that produces haploid gametes that are required for sexual reproduction. Ploidy reduction requires several meiosis-specific events, which occur in the context of a highly orchestrated meiotic program (Petronczki et al, 2003). During the meiotic G2/prophase, Spo11-dependent DNA double-strand breaks (DSBs) are repaired via homologous recombination (Lam & Keeney, 2015). DSB formation and recombination are essential for meiosis, but errors that occur during these events endanger genome stability of the developing gametes (Sasaki et al, 2010).

Pch2 (known as TRIP13 in mammals) is an AAA+ protein that controls multiple aspects of meiotic homologous recombination and checkpoint signaling (San-Segundo & Roeder, 1999; Bhalla & Dernburg, 2005; Li & Schimenti, 2007; Borner et al, 2008; Joshi et al, 2009; Roig et al, 2010; Vader et al, 2011; Vader, 2015). AAA+ proteins are ATPases that, via cycles of nucleotide binding and hydrolysis, can undergo conformational changes to influence a wide range of client molecules (reviewed in Hanson and Whiteheart [2005]). A characteristic of AAA+ proteins is their ability to assemble into ring-shaped homo- or hetero-hexamers, often mediated through interactions between AAA+ domains. Pch2 forms homo-hexamers and uses its enzymatic activity to remodel (and affect the function of clients) (Chen et al, 2014; Ye et al, 2015; Ye et al, 2017; Alfieri et al, 2018). HORMA domain-containing proteins are confirmed Pch2 clients, and many, if not all, functions ascribed to Pch2 can be explained by its enzymatic activity toward HORMA proteins (Vader, 2015).

Because recruitment of Pch2 to chromosomes is associated with (at least some) Pch2 functions, it is imperative to understand how Pch2 is recruited to meiotic chromosomes and whether adaptor proteins are required to facilitate specific functions of this AAA+ protein. In addition to its global role in controlling meiotic recombination, Pch2 is needed to prevent inappropriate DSB formation and recombination within the repetitive ribosomal DNA (rDNA) array of budding yeast (San-Segundo & Roeder, 1999; Vader et al, 2011). In line with a role for Pch2 in promoting rDNA stability, Pch2 is enriched within the nucleolus, the nuclear compartment where the rDNA resides. This rDNA-specific recruitment and function of Pch2 requires Orc1 (Vader et al, 2011), raising the interesting possibility that Orc1 could fulfill a meiosis-specific role by interacting with a meiosis-specific AAA+ protein complex.

Orc1 is a component of the origin recognition complex (ORC), a central mediator of several key chromosomal processes. The ORC is a hetero-hexameric protein complex composed of Orc1 through Orc6, wherein Orc1-5 are AAA+ proteins, and Orc6 shows no structural similarity with the rest of ORC components (reviewed in

Bell and Kaguni [2013] and Bell and Labib [2016]). A key role for the ORC in the chromosome metabolism lies in its function in the initiation of the eukaryotic DNA replication. The ORC binds to origins of replication, which in budding yeast are defined by a specific DNA sequence. Such sequence specificity seems to be absent in *Schizosaccharomyces pombe* and metazoans, in which origins of replication are predominantly determined by the chromatin structure, epigenetic marks, and specifically, the presence of a nucleosome-free region (Peng et al, 2015; Prioleau & MacAlpine, 2016). At origins, interaction of Orc1-6 with Cdc6, another AAA+ protein, through typical AAA+-to-AAA+ interactions, creates a hexameric ORC-Cdc6 assembly. ORC-Cdc6 (with the help of additional proteins) drives the localized, chromosomal recruitment of the AAA+ MCM helicase (Bell & Labib, 2016). The MCM helicase forms the basis of the replication complex and as such is key to initiate DNA replication. This canonical MCM loader function of the ORC occurs at origins of replication during the G1 phase of the cell cycle and is essential for DNA replication.

In addition to the role of the ORC in DNA replication, the ORC executes several other chromosomal functions during the mitotic cell cycle. In budding yeast, the ORC is required for transcriptional gene silencing at the cryptic mating-type loci and at telomeres (Foss et al, 1993; Loo et al, 1995; Fox et al, 1997). At the mating loci, the ORC recruits Sir1, a silencing factor, via a direct association between Sir1 and Orc1 (Triolo & Sternglanz, 1996; Hou et al, 2005). Furthermore, the budding yeast ORC is also involved in regulating sister chromatid cohesion (Suter et al, 2004; Shimada & Gasser, 2007). Importantly, all these roles of the ORC are associated with binding of the ORC to origins of replication, which has led to a model wherein the ORC functions as a structural “loading platform” for specific interacting proteins which subsequently allows for the establishment of localized chromosomal activities at origins of replication (Bell & Labib, 2016).

Here, we use *in vivo* analysis during budding yeast meiosis, coupled to *in vitro* biochemical reconstitution to investigate how Pch2 interacts with Orc1/ORC. We find that Pch2 directly engages the entire ORC in the meiotic G2/prophase, in a manner that is consistent with an AAA+ to client/adaptor relationship. Surprisingly, we find that depletion of Orc2 or Orc5 does not trigger phenotypes that are associated with Pch2 function at rDNA. These findings are in contrast to earlier depletion studies, using hypomorphic alleles of Orc1, which revealed a key contribution for Orc1 to Pch2 function (Vader et al, 2011). Our *in vitro* analysis provides biochemical insights into the interaction between Pch2 and ORC. Chemical cross-linking combined with mass spectrometry (XL-MS), coupled to biochemical characterization, shows that the ORC-Pch2 interaction is distinct from the well-established interaction between ORC and MCM. In contrast to the ORC-MCM assembly, the ORC-Pch2 assembly does not require Cdc6. Our data suggest that Orc1 plays a key role in the interaction between ORC and Pch2, which is in agreement with the key role of Orc1 in mediating the function of Pch2 in maintaining rDNA stability. As a whole, our data point to the existence of a distinct function for Orc1/ORC during meiosis, during which it interacts with Pch2.

Results

Pch2 functionally interacts with Orc1 to protect rDNA border regions from instability during meiosis (Vader et al, 2011), and we aimed to

further understand the interaction between these two AAA+ proteins. We first investigated how this interaction depended on Pch2 hexamer formation and ATP hydrolysis activity *in vivo*. We used an ATP hydrolysis mutant within the Walker B domain of Pch2 (*pch2-E399Q*) (Fig 1A), which is unable to support rDNA-associated DSB protection (Vader et al, 2011). In other AAA+ enzymes, mutating this critical residue in the Walker B domain prevents efficient ATP hydrolysis and stalls the stereotypical catalytic cycle of AAA+ enzymes. This often leads to stabilized interactions between AAA+ proteins and their clients and/or adaptors. Equivalent mutants in other AAA+ enzymes have been used to trap enzyme-client and/or enzyme-adaptor interactions (Hanson & Whiteheart, 2005; Ritz et al, 2011). We detected an increased interaction between Pch2 and Orc1 in meiotic cells expressing Pch2-E399Q as compared with cells expressing wild-type Pch2 (Figs 1B and S1A). We also detected a robust interaction between Orc1 and Pch2 in lysates where DNA was degraded (Fig S1B and C), excluding potential indirect association mediated by DNA present in our co-immunoprecipitation assays. We next investigated a different mutant Pch2 allele, which carried a mutation within the Walker A motif (K320R). Mutations in residues located within this motif have been shown to reduce ATP binding (Hanson & Whiteheart, 2005). When we probed the interaction between Pch2 and Orc1, Orc1-TAP failed to co-immunoprecipitate Pch2-K320R (Fig 1A and C). Considering that mutations in the Walker A motif lead to monomerization of Pch2 *in vivo* (Herruzo et al, 2016), our data suggest that the efficient interaction between Pch2 and Orc1 relies on ATP binding and Pch2 hexamer formation. As a whole, these experiments indicate that Pch2 interacts with Orc1 in a manner that is consistent with a stereotypical AAA+/client and/or adaptor interaction.

Many, if not all, functions ascribed to Orc1 involve its assembly into the six-component ORC (consisting of Orc1-6) (Bell & Labib, 2016). We therefore tested whether in addition to Orc1, other subunits of the ORC also interacted with Pch2. We used the *pch2-E399Q* allele to stabilize *in vivo* interactions. Our co-immunoprecipitation (co-IP) assays revealed that TAP-tagged versions of Orc2/Orc5 (Fig S1A) co-immunoprecipitated with Pch2 during the meiotic G2/prophase (Fig 1D and E). Similarly, we could pulldown 3xFlag-tagged Pch2-E399Q with Orc2 using an α -Orc2 antibody (Fig 1F). Furthermore, an unbiased mass spectrometric analysis of the Pch2-E399Q interactome identified Orc5 in addition to Orc1, indicating that Pch2 interacts with multiple ORC subunits (VB Raina and G Vader, unpublished observations). Altogether, we conclude that in addition to Orc1, Pch2 can *in vivo* associate with other subunits of the ORC during the meiotic G2/prophase. We consistently observed a strong association between Pch2 and Orc1 relative to the other subunits tested in our comparative *in vivo* co-IP experiments (Fig 1E), which together with other data (XL-MS, co-IP assays, pulldowns and functional analysis; see below) suggest that Orc1 might be a central interactor of Pch2.

Our *in vivo* analysis demonstrated that Pch2 associates with Orc1/ORC, and we sought to test whether this association is direct. For this, we expressed and purified budding yeast Pch2 (carrying an NH₂-terminal His-MBP tag) through a baculovirus-based protein expression system. As judged by size exclusion chromatography (SEC), purified Pch2 assembled into an apparent hexamer (predicted size ~636 kD), with a minor fraction that appears to be monomeric (size of ~106 kD for His-MBP-Pch2) (Fig 2A). We confirmed the

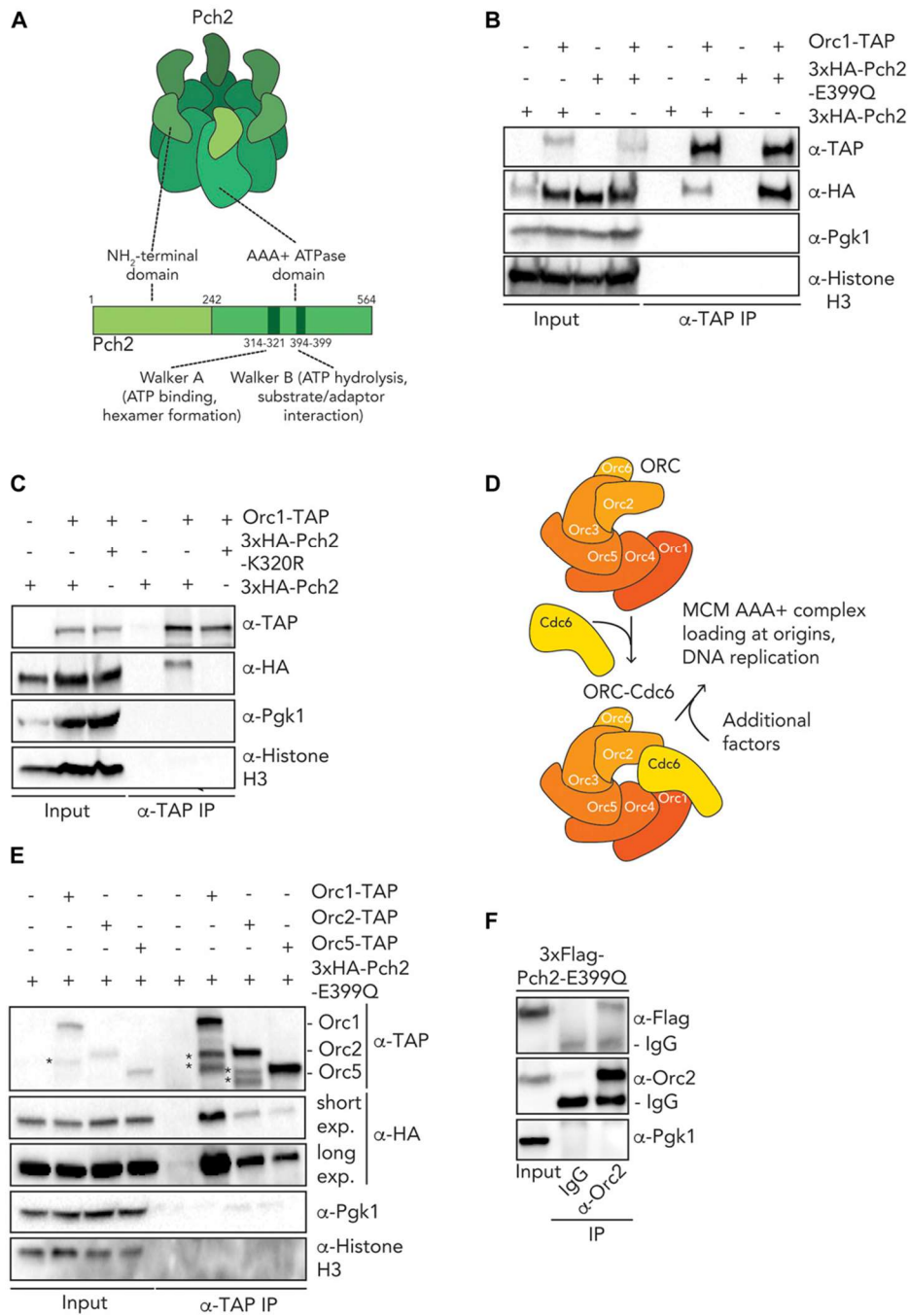


Figure 1. In vivo characterization of ORC-Pch2.

(A) Schematic of hexameric Pch2 AAA+ assembly, with domains organization of Pch2. (B) Co-immunoprecipitation (co-IP) of wild-type Pch2 and Pch2-E399Q with Orc1-TAP (via α-TAP-IP) during the meiotic prophase (5 h into meiotic program). (C) co-IP of wild-type Pch2 and Pch2-K320R with Orc1-TAP (via α-TAP-IP) during the meiotic prophase (5 h into meiotic program). (D) Schematic of the Orc1-6/AAA+ complex and its canonical role with the Cdc6 AAA+ protein (and additional factors) in MCM/AAA+ complex loading and DNA replication. (E) co-IP of Pch2-E399Q with Orc1-TAP, Orc2-TAP, and Orc5-TAP during the meiotic prophase (5 h into meiotic program) (via α-TAP-IP). For α-HA, short and long exposures are shown. * indicate degradation products of either Orc1-TAP or Orc2-TAP. (F) co-IP of Pch2-E399Q with Orc2 (via α-Orc2 IP). Isotype IgG IP was used as negative control.

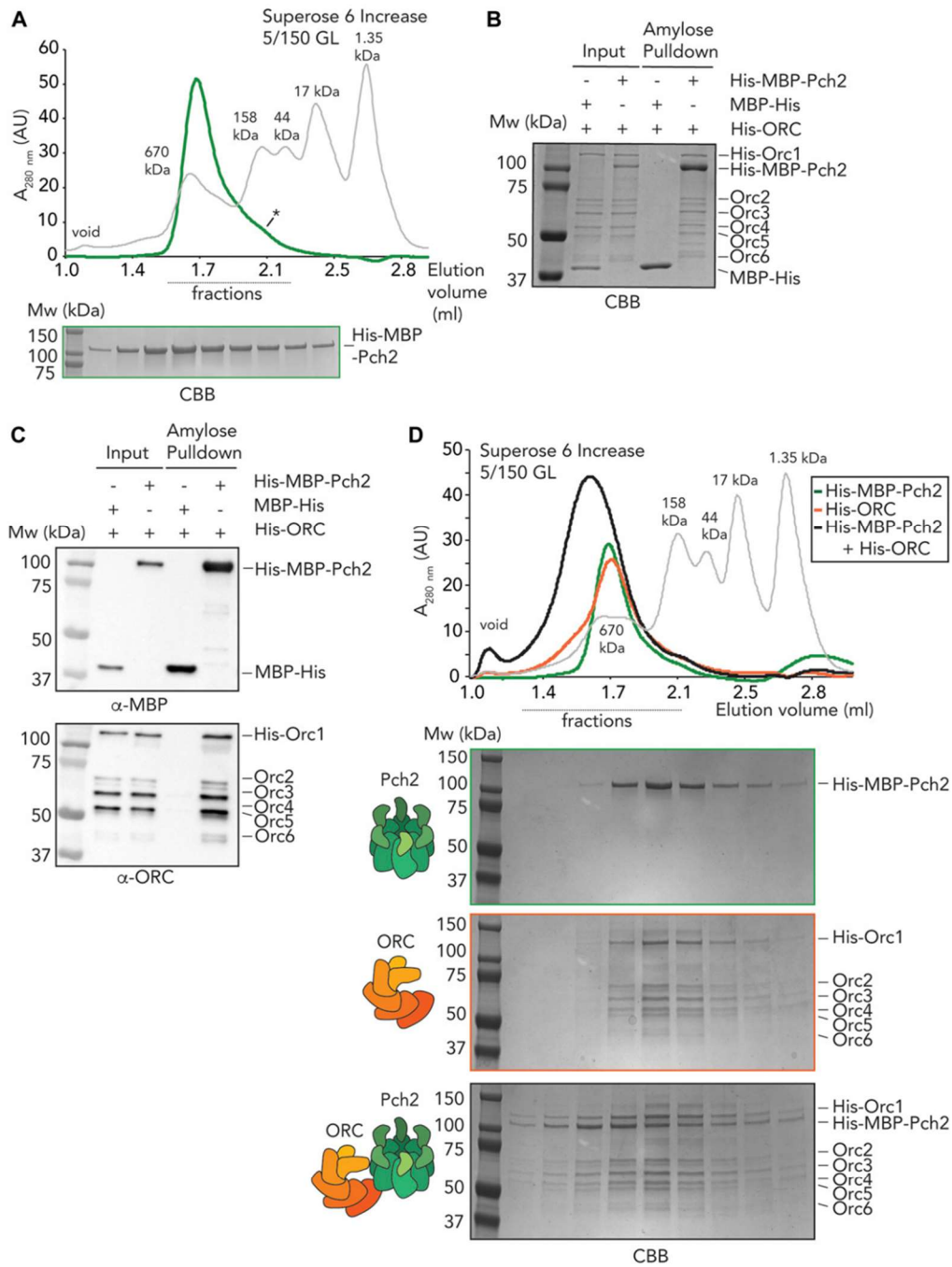


Figure 2. In vitro reconstitution of the origin recognition complex (ORC)-Pch2 complex.

(A) Size exclusion chromatography of His-MBP-Pch2 purified from insect cells. Coomassie Brilliant Blue (CBB) staining of peak fractions (dotted line) run on SDS-PAGE gel. * indicates likely monomeric fraction of His-MBP-Pch2. AU, arbitrary units. (B, C) Amylose-based pull-down of the ORC (His-Orc1-6 and His-ORC) purified from insect cells, with His-MBP-Pch2. (B) CBB staining, (C) Western blot analysis using α -MBP and α -ORC (which recognizes all six ORC subunits). (D) Size exclusion chromatography of His-ORC (His-MBP-Pch2) assembly. CBB staining of peak fractions (dotted line) run on SDS-PAGE gel. AU, arbitrary units.

functionality of our affinity-purified Pch2 by demonstrating a direct interaction with its substrate Hop1, as previously described (Chen et al, 2014) (Fig S2A). We note that performing the pulldown between Pch2 and Hop1 in the presence of ATP or a slow-hydrolysable form of ATP (ATP- γ S) did not alter the binding behavior (Fig S2B), in contrast to what has been observed (Chen et al, 2014) and would be expected based on the AAA+ catalytic cycle. We do not currently know the basis of this difference, but we speculate that the purification of Pch2 from insect cells (as opposed to purification from budding yeast [Chen et al, 2014]) might yield a Pch2 hexamer that is not properly activated potentially because of lack of certain (yeast-specific) posttranslational modifications. Under such conditions, impairing ATP hydrolysis is not expected to influence interactions.

We next tested whether Pch2 directly interacted with the ORC. For this, we used either the ORC purified from insect cells, as described here (i.e., Orc1-6, with Orc1 carrying a His tag; total size ~414 kD) (see Fig S3A and B) or ORC (i.e., Orc1-6, with Orc1 carrying a CBP tag) purified from α -factor-arrested vegetative budding yeast cells, as described (e.g., see Yeeles et al [2015]) (see below). We confirmed the presence of all ORC subunits in the insect cell-purified ORC by mass spectrometry (MS) (Fig S3C), and the composition of the insect cell-purified ORC was comparable with the budding yeast-purified ORC (Fig S3D). We did observe that in the case of purification from insect cells, the Orc6 subunit of the ORC migrated as a double band (Fig S3D), suggesting that a fraction of Orc6 might be phosphorylated, as described (Nguyen et al, 2001; Weinreich et al, 2001). Indeed, treatment of the insect cell-purified ORC with λ -phosphatase caused a collapse of the double band into a single Orc6 band (Fig S3E).

Using solid-phase pulldown experiments, we found that Pch2 is able to interact with the entire ORC (i.e., Orc1-6), irrespective of the source of the ORC (i.e., insect cells [Fig 2B and C] or budding yeast [Fig S3G]). The dephosphorylated ORC also interacted with Pch2, showing that the phospho-status of Orc6 did not affect interaction with Pch2 (Fig S3F). These experiments demonstrate that these AAA+ proteins indeed interact directly. Next, we asked whether this interaction could also be reconstituted in solution. SEC analysis confirmed that the ORC and Pch2 form a complex in solution, as judged by a reduced retention volume (which is indicative of a larger and/or more elongated complex) when combined, as compared with the elution profiles of Pch2 or ORC individually (Fig 2D). We suggest that the ORC and Pch2 interact with each other in an ORC (Orc1-6 hexamer) to Pch2 (hexamer) fashion, yielding what would be a complex of ~1 MD. We finally tested the effect of nucleotides on binding between Pch2 and ORC. As we observed with regard to the interaction between Pch2 and Hop1, addition of ATP (or ADP, or nonhydrolysable analogs) did not affect binding behavior between Pch2 and ORC (Fig S3H). Because we did observe differences in the interaction between Pch2 and Orc1 in the meiotic G2/prophase (Fig 1B and C), we again speculate that these different behaviors can be attributed to differential Pch2 ATPase activity levels present in our *in vitro* preparations as compared with *in vivo* conditions. Taken together, these experiments demonstrate that Pch2 directly interacts with the ORC, and as such reveal a novel direct interaction partner of Pch2 during the meiotic G2/prophase.

We next focused on understanding how Pch2 associates with the ORC. Associations between AAA+ proteins typically rely on interdomain

AAA+ interactions (Hanson & Whiteheart, 2005). For example, inter-domain AAA+ contacts between individual ORC subunits establish the hexameric ORC formation (Bell & Kaguni, 2013; Bell & Labib, 2016). Alternatively, many hexameric AAA+ ATPases (including TRIP13, the mammalian homolog of Pch2 [Alfieri et al, 2018; Ye et al, 2017]) associate with clients/adaptors via an initial engagement using their NTDs (as is the case for the interaction between Pch2/TRIP13 and HORMA domain proteins) and, subsequently, show interactions mediated through AAA+ core/client binding (Hanson & Whiteheart, 2005). We thus set out to investigate the contributions of the NTD and AAA+ domains of Pch2 to ORC association. We first tested whether the NTD of Pch2 was involved in Pch2-ORC assembly. For this, we used Y2H analysis to show that Pch2 lacking its NTD (amino acids 2–242) was unable to interact with Orc1 (Fig 3A and B). We next purified Pch2 lacking the NTD (His-MBP-Pch2-243-564) from insect cells. By SEC, we observed that this Pch2 protein eluted at an apparent size that indicated a more extended shape or less organized assembly as compared with full-length Pch2 (Fig S4A). These findings imply a role for the NTD in stabilizing and/or maintaining Pch2 into a stable, well-ordered hexamer (see also above). Importantly, the ability of purified Pch2-243-564 to interact with the ORC was abolished, further demonstrating an important contribution of the NTD of Pch2 in directing interaction with the ORC (Fig 3C). Finally, we investigated the interaction between Pch2 and Orc1 in the meiotic G2/prophase by expressing an identical truncated version of Pch2 (3xFlag-Pch2-243-564). This truncated version of Pch2 was impaired in its ability to interact with Orc1 (Fig 3D), similar to what was observed using Y2H and *in vitro* interaction studies, pointing to a crucial contribution of the NTD of Pch2 to establish binding with the ORC. The residual interaction of Pch2-243-564 with Orc1 in the meiotic G2/prophase might indicate that under physiological conditions, Pch2 lacking its NTD retains a certain degree of affinity toward ORC (Fig 3D). Pch2 protects rDNA array borders (i.e., the ~1–10 outermost rDNA repeats and ~50 kb of single-copy flanking sequences) against meiotic DSB formation ([Vader et al, 2011], and Fig 3E). In agreement with an important role of the NTD of Pch2 in mediating Pch2 function (and Orc1/ORC association) during the meiotic G2/prophase, we found that cells expressing 3xFlag-Pch2-243-564 (Fig 3F) exhibited rDNA border-associated DSB formation, as is observed in *pch2* Δ cells (Fig 3G).

We next used chemical cross-linking coupled to mass spectrometry (XL-MS) to build a more comprehensive understanding of the association between Pch2 and ORC. XL-MS can provide information on inter- and intramolecular interactions that can yield useful insights into assembly principles of complex protein preparations. Using an experimental pipeline based on an MS-cleavable chemical cross-linker (DSBU, disuccinimidyl dibutyric urea, also known as BuUrBu) (Pan et al, 2018) (Fig 4A), we cross-linked purified Pch2 (His-MBP-Pch2) and ORC (His-Orc1-6) (Fig 4B) and after processing and MS analysis, identified cross-linked peptides (for cross-links, see Tables S1 and S2). (Note that DSBU is able to cross-link lysine, serine, and threonine residues.) We validated the quality of our XL-MS dataset by analyzing (intramolecular) cross-linked peptides within the MBP moiety present in our Pch2 preparation (see the Materials and Methods section for more detailed information). After applying a stringent cut off analysis by setting a false-discovery rate (FDR) of 2% (Pan et al, 2018), we obtained a total of 313 nonredundant cross-links out of a total of

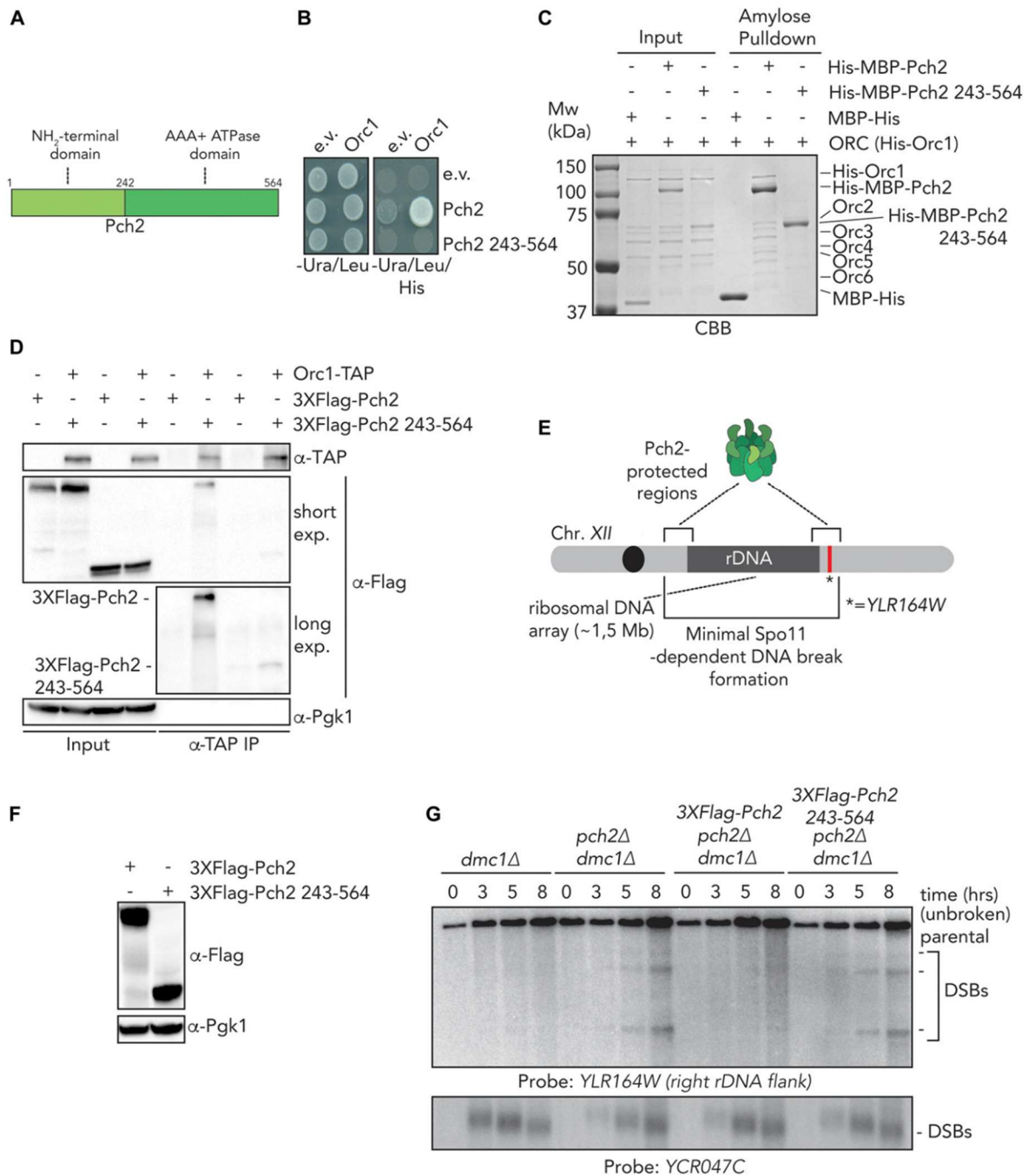


Figure 3. The NH₂-terminal domain (NTD) of Pch2 is required for ORC-Pch2 formation.
(A) Schematic of Pch2 domain organization. **(B)** Yeast two-hybrid analysis between Orc1 and Pch2 (full-length Pch2, and AAA+ ATPase domain [Pch2-243-564]).
(C) Amylose-based pull-down of His-ORC (His-Orc1-6) purified from insect cells, with His-MBP-Pch2 or His-MBP-Pch2-243-564. Coomassie Brilliant Blue (CBB) staining.
(D) Co-immunoprecipitation of 3XFlag-Pch2 and 3XFlag-Pch2 243-564 with Orc1-TAP (via α-TAP-IP) during the meiotic prophase (4 h into meiotic program). For α-Flag, short and long exposures are shown. α-Pgk1 is used as a loading control. **(E)** Schematic of the role of Pch2 in controlling Spo11-dependent DNA double-strand break (DSB) formation within the flanking regions of the budding yeast ribosomal DNA array located on chromosome XII. * indicates location of YLR164W locus, where DSB formation is

721 cross-linked peptides identified by MeroX (Fig 4C and Table S2). We used these nonredundant cross-links to generate cross-link network maps for the ORC–Pch2 assembly by using xVis (<https://xvis.genzentrum.lmu.de>) (Grimm et al, 2015). These 313 cross-links consist of 121 intermolecular cross-links (i.e., cross-links between peptides originating from two different proteins) and 192 intramolecular cross-links (i.e., cross-links between peptides originating from a single protein). We identified 96 Pch2–Pch2 cross-links (Fig 4C, red lines on Pch2 schematic, Fig S5 and Table S2). Importantly, because Pch2 forms a homo-hexamer, we cannot distinguish whether Pch2–Pch2–cross-linked peptides originate from intra- or intermolecular cross-linked peptides. We observed 77 cross-links between ORC subunits (i.e., inter-ORC cross-links) (Fig 4C, represented by blue lines. See also Fig S5A and B and Table S2). When comparing cross-link abundance between individual ORC subunits with a published cryo-EM structure of the ORC to model the position of each subunit (Fig 4F; based on structure protein data bank (PDB) 5v8f; [Yuan et al, 2017]), we noted that neighboring subunits often displayed the most abundant cross-links (e.g., Orc1/Orc2, Orc2/Orc3 and Orc3/Orc5; see Table S2). However, several observed cross-links span considerable distance when based on the ORC structure we used for analysis (PDB 5v8f; [Yuan et al, 2017]), arguing for significant levels of flexibility within our ORC preparation. Of note, our ORC is devoid of Cdc6, not associated with origin DNA, and also not bound to MCM–Cdt1, contrary to the reported structure (Yuan et al, 2017), which conceivably could affect complex topology. Furthermore, we cannot exclude that Pch2 leads to structural rearrangements of the ORC upon binding. A significant fraction of the cross-links (42 of 96; 44%) consisted of cross-links between peptides from the noncatalytic NH₂-terminal domain (NTD, amino acids 1–242) and the COOH-terminal AAA+ domain of Pch2 (amino acids 243–564) (Figs 4C and S5C). Because we cannot distinguish between inter- or intramolecular cross-links with respect to hexamer Pch2-derived peptides (see also above), these cross-linked peptides could be a reflection of (i) a close proximity between the NTD and AAA+ domain within a single Pch2 polypeptide or of (ii) an association between the NTD of one Pch2 monomer and the AAA+ domain of an adjacent (or potentially more distally localized, depending on domain flexibility) AAA+ module, from a distinct Pch2 monomer. With regard to these observations, we noted that in biochemical purifications, mutational disruption of the NTD of Pch2 influenced the apparent formation of stable/properly assembled Pch2 hexamers (Fig S4A), indeed hinting at a contribution of the NTD of Pch2 to the stable hexamerization of Pch2's AAA+ core. We also identified 21 inter-ORC–Pch2 cross-links (Figure 4C–F; black lines). Several observations are of note when considering these cross-links. First, we found cross-links that contain Pch2 peptides from both its enzymatic AAA+ core (12 out of 21; 57%) and its noncatalytic NTD (9 of 21; 43%) (see also Fig S5D and E). We interpret this to indicate that Pch2 makes extensive contacts with the ORC, whereby both its enzymatic core and its NTD come in close proximity to the

ORC. The observation that both Pch2's AAA+ core and NTD seem to be engaged in ORC binding is consistent with a similar scenario in which Pch2 binds to the ORC in an AAA+/client and/or adaptor-type engagement, as also indicated by our *in vivo* analysis (see above, Fig 1). The efficiency of such a binding mode is expected to rely on the hexameric state of Pch2. These results are in agreement with our *in vivo* observations using ATPase mutants (Fig 1). The largest fraction of the total Pch2–ORC cross-links is established between Pch2 and Orc1 (6 of 21; 29%). Orc1 is the largest subunit of the Orc1–6 complex, which might influence the distribution of the observed cross-links. However, the observed cross-links between Pch2 and Orc1 are all derived from a narrow region within Orc1 (spanning amino acids 551–615) located within the AAA+ ATPase core of Orc1. Thus, we interpret this enrichment for Orc1-derived cross-links to indicate that when associated with the ORC, Pch2 resides in close proximity to the Orc1 subunit. Combined with our *in vivo* observations, in which we consistently found Orc1 as the most robust factor associating with Pch2 (Fig 1), these findings suggest that Orc1 constitutes a major interaction hub for Pch2 within the ORC.

In addition to Orc1, Orc2 also forms a number of cross-links with Pch2 (Orc1/Orc2 together forms 10 of 21 cross-links; 48%). We noted that Orc1/Orc2 is neighboring the position that is occupied by Cdc6 when it is engaged with the ORC (Yuan et al, 2017). Cdc6 is not present in our preparations, leaving this space unoccupied. We thus speculate that Pch2 might use the vacated Cdc6-binding position to establish its interaction with the ORC. We attempted to map the 21 inter-ORC–Pch2 cross-links onto an ORC structure (PDB 5v8f [Yuan et al, 2017], Fig 4F; cross-linked residues are marked by a black dot). Because of the absence of regions of the ORC within the used structure, we were unable to map several of the ORC–Pch2 cross-links (i.e., cross-links with Orc2, Orc5, and Orc6; please refer to Fig 4D). Mapping of observed cross-links showed a distribution of residues across a large surface of the ORC, suggesting that Pch2 is in close proximity with a large region of the ORC when engaged. When we analyzed the position of these residues in a structure containing Cdc6, we noted that three cross-linked residues within Orc1 (K612, T614, and S615) were located in a position that is shielded by Cdc6 when bound to it, according to the ORC–Cdc6–Cdt1–MCM complex structure (PDB 5v8f [Yuan et al, 2017]). This finding reiterates the idea that Pch2 uses a binding mode that might involve binding interfaces within Orc1/ORC that is also involved in Cdc6 engagement during the G1 phase of the cell cycle. These data suggest that Pch2–ORC association can occur in the absence of Cdc6, and we performed *in vivo* several experiments to reinforce this premise. Pch2 expression is induced during the meiotic S-phase and G2/prophase, whereas Cdc6 availability is restricted to the G1 phase (Drury et al, 2000), also in the meiotic program (Phizicky et al, 2018). This mutually exclusive expression pattern already suggests that Pch2–ORC should not depend on Cdc6. We used a meiosis-specific null allele of *CDC6* (*cdc6-mn*) (Hochwagen et al, 2005) which interferes with premeiotic DNA replication (Fig S6A), to investigate if

interrogated. (f) Western blot analysis of meiotic time-course samples of yeast strains expressing wild-type 3xFlag–Pch2 and 3xFlag–Pch2 243–564 as used in (A). (3xFlag–PCH2 *pch2Δ dmc1Δ* and 3xFlag–*pch2 243–564 pch2Δ dmc1Δ*). (g) Southern blot analysis of YLR164W locus (right ribosomal DNA flank; chromosome XII) and YCR047C locus (control DSB region; chromosome III), in *dmc1Δ*, *pch2Δ dmc1Δ*, 3xFlag–PCH2 *pch2Δ dmc1Δ*, and 3xFlag–*pch2 243–564 pch2Δ dmc1Δ* background. *dmc1Δ* is a DSB repair deficient mutant used to detect accumulation of meiotic DSBs.

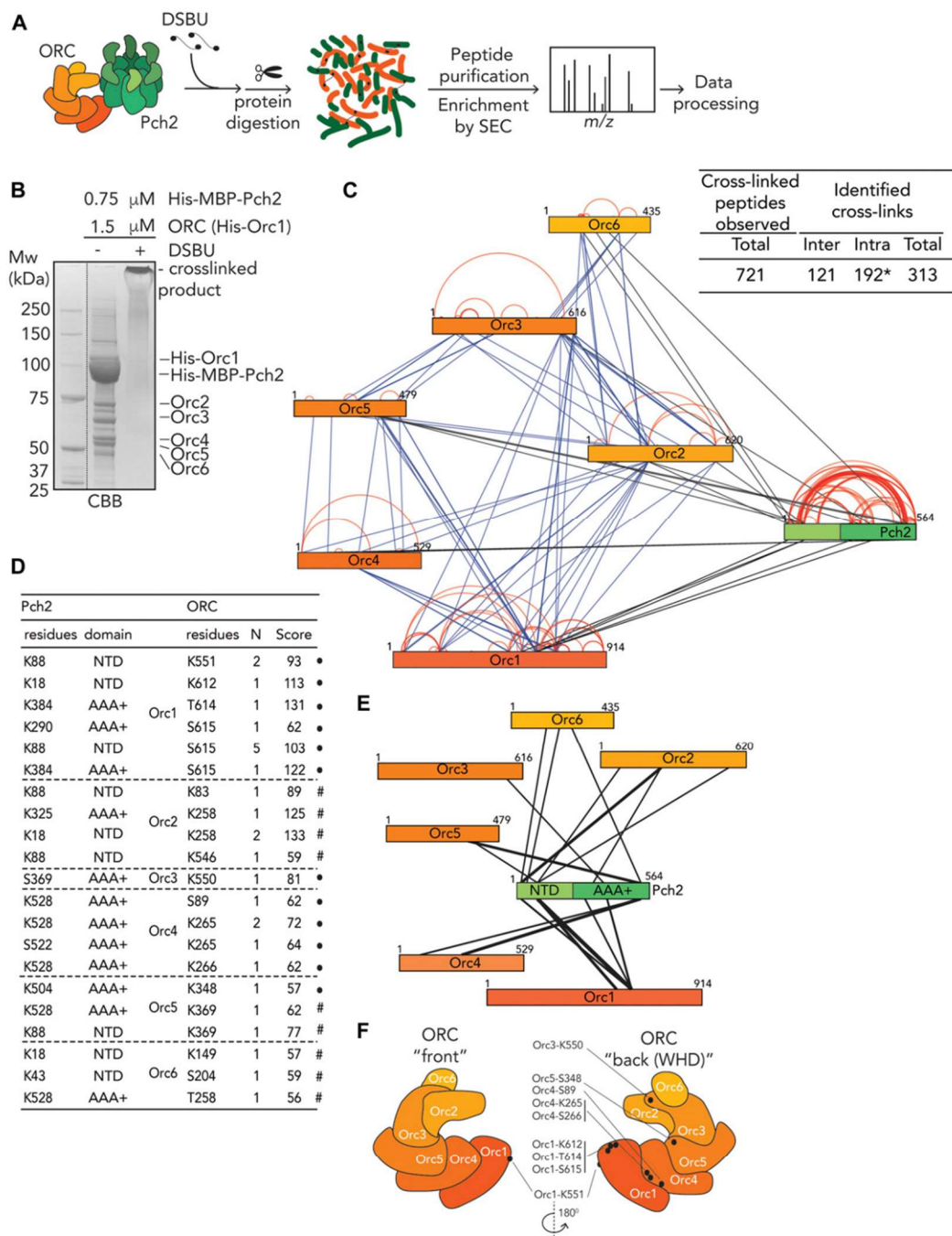


Figure 4. Cross-linking mass spectrometric analysis of origin recognition complex (ORC)-Pch2 complex assembly.

(A) Schematic of DSBU-based cross-linking mass spectrometry (XL-MS) experimental pipeline. (B) Coomassie Brilliant Blue (CBB) staining of DSBU-cross-linked Pch2-ORC. (C) Right panel: Table indicating total cross-linked peptides and derived nonredundant (inter- and intramolecular) cross-links with a false discovery rate of 2%. * indicates that intramolecular cross-link peptides include 96 Pch2-Pch2 cross-links, which can be derived from inter- or intramolecular Pch2-Pch2 cross-links. Left panel: Schematic indicating all identified nonredundant cross-links. Blue: inter-ORC, red: intra-ORC and intra-Pch2, black: inter-ORC-Pch2. Network plots were generated using *x/vis*. (D) Table showing inter-ORC-Pch2 cross-links. Indicated are residues in Pch2, and ORC subunits, domain of Pch2 involved (NTD: 1-242, AAA+: 243-564). N

depletion of Cdc6 influenced Pch2–ORC binding and function. (Note that in the *cdc6-mn* background, despite a failure to undergo bulk DNA replication [which indicates an efficient functional depletion], meiotic progression is unaffected and cells initiate DSB formation in a meiotic G2/prophase-like state [Hochwagen et al, 2005; Blitzblau et al, 2012].) As expected from our in vitro analysis, the interaction between Pch2 and Orc1 in the *cdc6-mn* background was similar to the binding observed in *CDC6* cells (Fig S6B), indicating that ORC–Pch2 assembly occurs under conditions of Cdc6 depletion. Similarly, Cdc6 depletion (via *cdc6-mn*) did not trigger a Pch2-like phenotype at rDNA borders, as judged by the analysis of meiotic DSB formation at the right rDNA flank (*YLR164W*) (Fig S6C). *pch2Δcdc6-mn* efficiently formed DSBs within the right rDNA flank (Fig S6C), demonstrating that bulk (Cdc6-dependent) DNA replication does not impact DSB formation in these regions, also in cells lacking Pch2.

Based on our earlier in vivo and in vitro results, we surmised that the NTD of Pch2 plays important roles in establishing the interaction between Pch2 and ORC. We aimed to further dissect this interaction. Based on Pch2 amino acid sequence conservation and secondary structure predictions (see Fig S7A for sequence alignments and placement of truncations), we performed Y2H analyses using a series of COOH-truncated fragments of Pch2. These analyses revealed that the NTD of Pch2 (consisting of amino acids 2–242) is sufficient to establish the interaction with Orc1 (Fig 5A). Further truncations of the NTD identified a minimal fragment of Pch2 (containing amino acids 2–144) sufficient for the interaction between Pch2 and Orc1 (Fig 5A, represented as a red dotted box). The behavior of this fragment is in agreement with our XL-MS analysis, which identified several cross-links between Pch2 and ORC subunits that consisted of Pch2 peptides that are located within this region of the NTD (K88, K18, K43; Fig 4D and E and Table S2). We attempted to express corresponding Pch2 NTD fragments in meiosis but often observed that these fragments were poorly expressed. This precluded us from performing in vivo interaction studies using these fragments. To further test a role for the NTD of Pch2 in mediating interaction with the ORC, we expressed recombinant NTD fragments. Similar to our in vivo observations, many recombinantly produced fragments were poorly expressed or aggregated under purifying conditions. We managed to express and purify the minimal NH₂-terminal fragment of Pch2 (His–MBP–Pch2-2–144) that was sufficient for Orc1 interaction in our Y2H analysis. SEC analysis suggested that this fragment exists as a monomer (expected size ~59 kD), which is in agreement with the crucial role AAA+ domains play in mediating hexamerization of AAA+ complexes (Fig 5B). This fragment was capable to interact with the ORC (Fig 5C and D). We noted however that this interaction is much weaker than the interaction with the full-length Pch2. This could indicate additional binding interfaces between Pch2 and ORC that lie outside of this domain (as suggested by the observation of additional

cross-links containing peptides from regions outside of the NTD of Pch2, and by the residual in vivo interaction we observed between Pch2–ΔNTD and Orc1; see above). Alternatively, this could indicate that hexamer formation of Pch2 (driven by AAA+/AAA+ interactions) is essential to increase the local effective concentration of the NTD. This would contribute to efficient binding between Pch2 and ORC. The latter interpretation is in agreement with our observation that the in vivo interaction between Pch2 and Orc1 is severely diminished in cells expressing a Pch2 Walker A domain mutant, which is expected to disrupt ATP binding and hexamerization (Herruzo et al, 2016) (Fig 1C). Altogether, these data strongly imply that the association of Pch2 with ORC constitutes a meiosis-specific assembly of two AAA+ protein complexes, which is dictated by unique interaction characteristics.

Canonical ORC function in yeast depends on ORC integrity and association with origins of replication (Foss et al, 1993; Loo et al, 1995; Fox et al, 1997; Suter et al, 2004; Shimada & Gasser, 2007). Our in vivo and in vitro analyses indicated that Pch2 interacts with the entire ORC. Pch2 is required to prevent rDNA-associated meiotic DSB formation (Vader et al, 2011). Inactivating Orc1 (via a temperature-sensitive allele of *ORC1*, *orc1-161*) triggers a similar rDNA-associated DSB formation as observed in cells lacking Pch2 (Vader et al, 2011). This rDNA-associated phenotype seen in the *orc1-161* background is exposed under conditions that are permissive for mitotic and meiotic DNA replication (i.e., they manifest at a permissive temperature of 23°C) (Vader et al, 2011), demonstrating a particular sensitivity of Pch2-associated phenotypes for Orc1 functionality. We sought to address whether a similar relationship existed between Pch2 and other ORC subunits. ORC subunits are essential for cell viability, and we used the “anchor-away” method (Haruki et al, 2008), which has been used to efficiently deplete chromosomal factors in budding yeast meiosis (Vincenten et al, 2015; Subramanian et al, 2016, 2019; Alfieri et al, 2018; Heldrich et al, 2020) to inactivate selected ORC subunits (Fig 6A). Mitotically proliferating cells that carry FRB-tagged versions of *ORC2* or *ORC5* (*orc2-FRB* and *orc5-FRB*) exhibited a strong growth defect when grown in the presence of rapamycin (Fig 6B), demonstrating efficient nuclear depletion. Because of technical reasons, we were unable to generate a functional *orc1-FRB* allele. To investigate the efficacy and timing of functional depletion, we used flow cytometry to query DNA replication in logarithmically growing cultures after treatment with rapamycin. In the *orc2-FRB* and *orc5-FRB* backgrounds, addition of rapamycin induced DNA replication to cease (as judged by an accumulation of 2C-containing cells) within 180 min of treatment, with the first effects detectable after 90 min (Fig 6C). In addition, we confirmed nuclear depletion during meiosis via chromatin immunoprecipitation coupled to quantitative PCR (ChIP-qPCR) analysis on *orc2-FRB* cells (see below, Figs 6H and S9A and B). These experiments indicate a rapid

indicates how often cross-links were identified. MeroX score is indicated. ● indicates cross-linked ORC residues that are mapped into cartoon representation of the ORC structure in (F). # indicates cross-links that fall in regions of ORC subunits that are not present in the used ORC structure. (E) Schematic indicating identified nonredundant inter-Pch2–ORC cross-links. The line thickness corresponds to the number of cross-links, as shown in (D). (F) Cartoon depiction of ORC organization, based on structure PDB 5v8f; (Yuan et al, 2017). “Back” and “front” are relative to winged helix domain (WHD) orientation, as indicated. Black dots represent ORC cross-linked residues in our XL-MS analysis. Note that because of a lack of regions in the structure used to generate the ORC schematic representation, not all cross-links are represented (see also text).

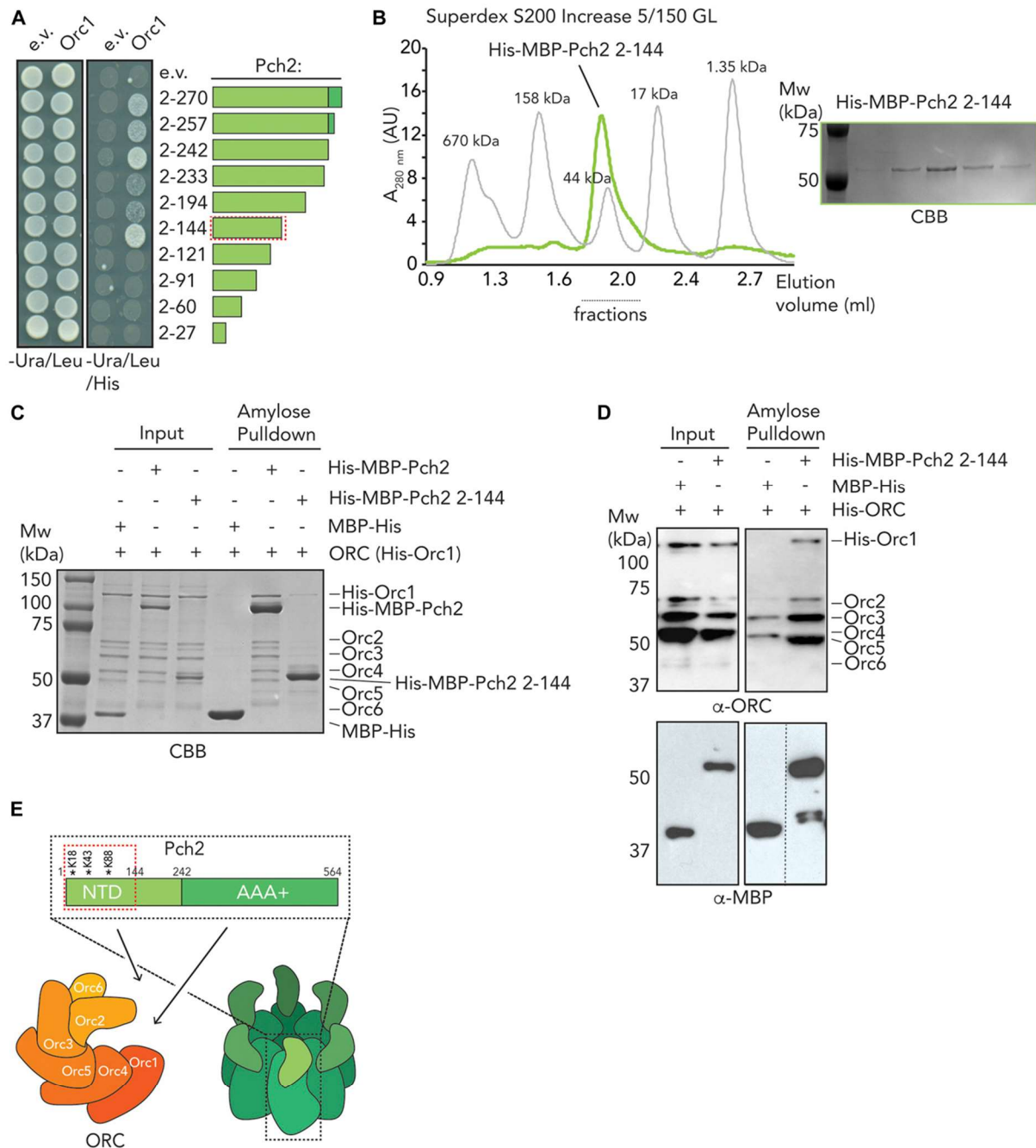


Figure 5. Dissection of the role of the NTD of Pch2 in origin recognition complex (ORC) association. (A) Yeast two-hybrid analysis between Orc1 and NH₂-terminal fragments of Pch2 (2-270, 2-257, 2-242, 2-233, 2-194, 2-144, 2-121, 2-91, 2-60, 2-27). Red-dotted box indicates the minimal fragment of Pch2 that showed interaction with Orc1. (B) Size exclusion chromatography of His-MBP-Pch2-2-144 purified from insect cells; Coomassie Brilliant Blue (CBB) staining of the peak fractions (dotted line). AU, arbitrary units. (C) Amylose-based pull-down of the ORC (His-Orc1-6) purified from insect cells, with His-MBP-Pch2 or His-MBP-Pch2-2-144; Coomassie Brilliant Blue staining. (D) Amylose-based pull-down of the ORC (His-Orc1-6) purified from insect cells, with His-MBP-Pch2 or His-MBP-Pch2-2-144; Western blot analysis using α -MBP and α -ORC. (E) Schematic of interaction mode between the ORC and Pch2. Red-dotted box indicates the NH₂-terminal 2-144 region of Pch2's NTD. Cross-linked residues within the Pch2-2-144 region are indicated with *.

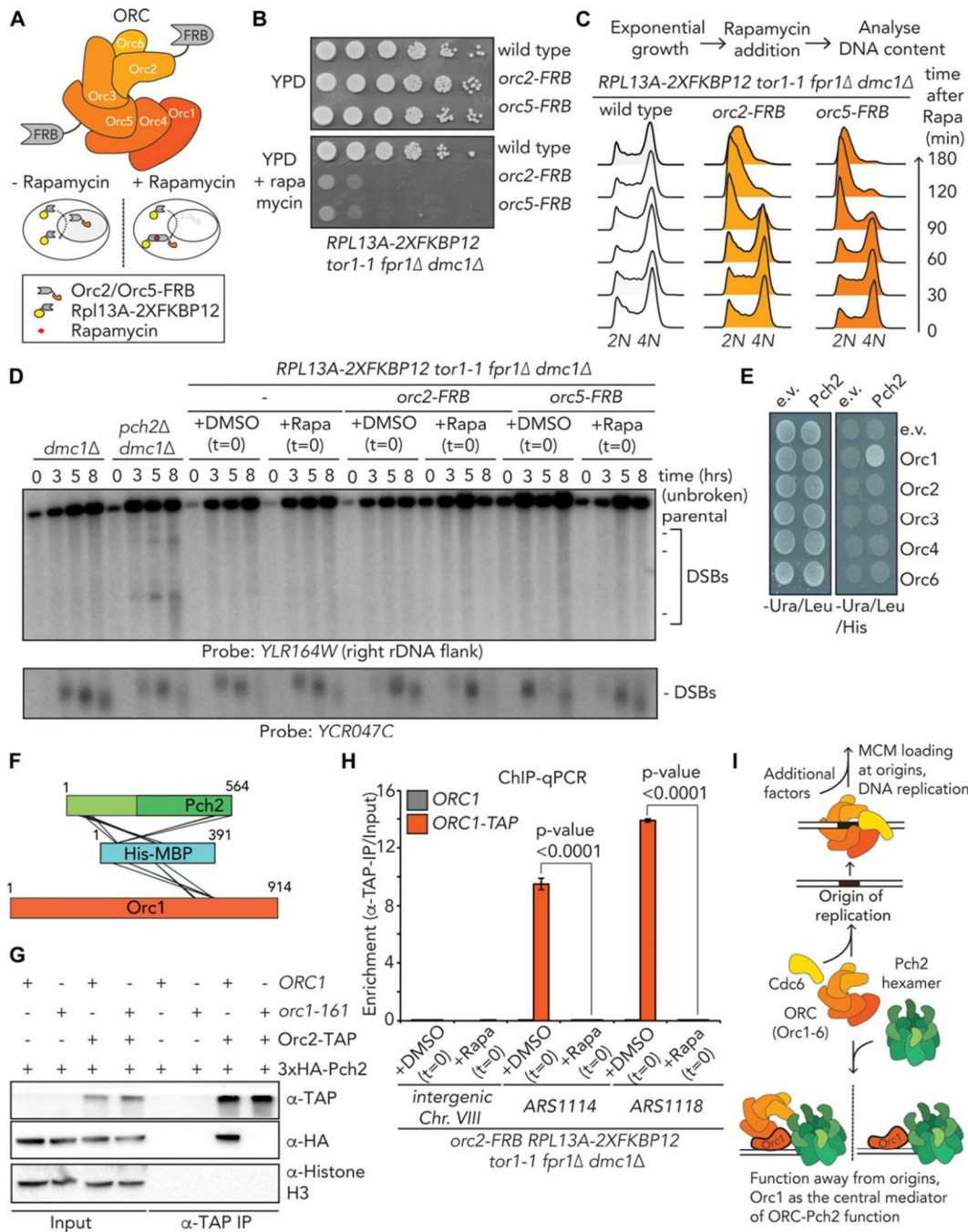


Figure 6. Functional in vivo analysis of origin recognition complex (ORC)-Pch2. (A) Schematic of the ORC assembly and rapamycin-based anchor-away method. (B) 10-fold serial dilution spotting assay for anchor-away strains (untagged, *orc2-FRB* and *orc5-FRB*). Strains are grown on YP-dextrose (YPD) or YPD + rapamycin (1 μ g/ml). (C) Flow cytometry analysis of efficiency of *orc2-FRB* and *orc5-FRB* nuclear depletion. Cells were treated as indicated, with rapamycin (1 μ g/ml) at $t = 0$. (D) Southern blot analysis of *YLR164W* locus (right ribosomal DNA flank; chromosome *XII*) and *YCR047C* locus (control double-strand break [DSB] region; chromosome *III*). *dmc1 Δ* is a DSB repair deficient mutant that is used to detect accumulation of meiotic DSBs. Rapamycin (1 μ g/ml) or DMSO was added at indicated $t = 0$. Samples were taken at indicated time points after meiotic induction. (E) Yeast two-hybrid analysis between

functional depletion of Orc2 and Orc5. We used these *ORC* alleles to investigate rDNA-associated DSB formation (by probing meiotic DSB formation at the right rDNA flank; *YLR164W* [Vader et al, 2011]). Meiotic progression was normal under these conditions because meiotic DSB formation at a control locus (*YCR047C*; chromosome III) occurred normally (Fig 6D), and premeiotic DNA replication timing appeared unaffected under this treatment regimen. MCM association with origins of replication (the critical *ORC*-dependent step during DNA replication) occurs before induction into the meiotic program (and thus rapamycin exposure in our experimental setup) (Phizicky et al, 2018), and therefore, nuclear depletion of the *ORC* in this regimen is not expected to interfere with efficient premeiotic DNA replication. In contrast to what is observed in cells lacking Pch2 or in cells expressing *orc1-161* (Vader et al, 2011), rapamycin-induced depletion of Orc2 or Orc5 did not trigger an increase in rDNA-associated DSB formation (Fig 6D). Although we cannot exclude the possibility that Orc2/5 are incompletely depleted from the nucleus under the used conditions. The viability effects (Fig 6B), the timing of the observed effects on DNA replication of Orc2/5 depletion during vegetative growth (i.e., within 90–180 min; Fig 6C), and our ChIP-qPCR analysis (see below and Figs 6H and S9A and B) suggest that in our meiotic experiments (which include rapamycin treatments for 8 h), Orc2/5 are functionally depleted from the nucleus. Of note, experiments in which cells were exposed to longer periods of rapamycin treatment by adding the drug in premeiotic cultures (i.e., 3 h before initiation of meiotic cultures) also did not reveal an effect of Orc2/Orc5 depletion on rDNA-associated DNA break formation, despite the appearance of (mild) premeiotic DNA replication defects (unpublished observations, MA Villar-Fernández and G Vader). We conclude that under regimens that trigger clear replication defects in mitosis, we do not observe Pch2-like phenotypes in cells expressing depletion alleles of *ORC2* and *ORC5*. This is in striking contrast to phenotypes observed in cells expressing *orc1-161* under conditions (i.e., permissive temperature) where DNA replication is still supported in mitosis and meiosis, and Pch2-like phenotypes are exposed at the rDNA (Vader et al, 2011). These data suggest a specific reliance of Pch2 on Orc1 function that is not shared by Orc2 and Orc5, and together with several other observations (see below), point to Orc1 as a central functional interacting partner of Pch2. Orc1 was identified as an interactor of Pch2 via a Y2H screen (Vader et al, 2011), and when comparing Pch2 co-IP efficiencies of Orc1, Orc2, and Orc5, we consistently find the strongest interaction with Orc1 (Fig 1E). Our XL-MS analysis also hints at a crucial role for Orc1 as a Pch2 interactor (see above). We analyzed pair-wise interactions between individual *ORC* subunits (Orc1-4, and Orc6; Orc5 was not queried for technical reasons) and Pch2 using Y2H. We confirmed the interaction between Orc1 and Pch2, as reported earlier (Vader et al, 2011), but did not observe an interaction between Pch2 and Orc2-4 or Orc6 in this experimental

setup (Fig 6E). In addition, we analyzed our XL-MS dataset for intermolecular cross-links containing peptides from the MBP moiety (that is NH₂-terminally fused to Pch2 in His-MBP-Pch2). This revealed, in addition to 17 intermolecular cross-links between MBP and Pch2 (which are expected because these two polypeptides are covalently linked), 6 MBP-Orc1 intermolecular cross-links (Fig 6F and Table S2). In contrast, we observed no cross-links between MBP and other *ORC* subunits. Because efficient cross-linking depends on a proximity of ~12 Å between Cα's of cross-linked amino acids (Pan et al, 2018), these data argue that Orc1 is in close vicinity of MBP (and, by extension, Pch2). Together, these findings strengthen the idea that Orc1 plays a crucial role in mediating the *ORC*-Pch2 assembly. This predicts that the absence of Orc1 should lead to a decreased association between Pch2 and other *ORC* components. To test this premise, we probed the interaction between Pch2 and Orc2/Orc5 in the presence of a temperature-sensitive allele of *ORC1* (*orc1-161*). Indeed, Orc2 and Orc5 showed a decreased ability to immunoprecipitate Pch2 under such conditions, demonstrating that Orc1 is crucial in mediating the interaction between the *ORC* and Pch2 (Figs 6G and S8A). By contrast, the interaction between Orc1 and Pch2 was not affected by the nuclear depletion of Orc2 (in *orc2-FRB*-expressing cells) (Fig S8B).

The *ORC* function is closely linked to its association with origins of replication, and impairing *ORC* integrity (e.g., by removing one of its subunits) is expected to trigger its efficient removal from origins of replication. Because our data suggest that depletion of Orc2/Orc5 is not associated with Pch2-like phenotypes, one possibility is that efficient binding of Orc1/*ORC* to origins is not required for this function. We therefore tested the association of the *ORC* with origins of replication under the condition of nuclear depletion of Orc2. By performing chromatin immunoprecipitation coupled to quantitative PCR (ChIP-qPCR) of Orc1-TAP in cells expressing Orc2-FRB, we observed, upon the addition of rapamycin, a near-complete loss of Orc1 from selected euchromatic origins of replication (*ARS1114*, *ARS1118*, and *ARS1116*) in *orc2-FRB* cells (Figs 6H and S9A, see also Table S3). We also analyzed the effect of Orc2-FRB nuclear depletion on the association of Orc1 with the *ARS* localized at the rDNA (*ARS1216.5*). Although the loss of Orc1 from this rDNA origin was less dramatic than the effect that was seen at euchromatic origins, Orc1 binding at *ARS1216.5* was also significantly diminished upon rapamycin addition (Fig S9B). These results again underscore the nuclear depletion of Orc2 via the anchor-away method. In addition, because under identical treatment conditions, we do not observe rDNA-associated DSB formation (Fig 6D), these data argue that efficient binding of Orc1/*ORC* to origins is not strictly required for the function of Orc1/Pch2 in locally suppressing DSBs during the meiotic G2/prophase. In agreement with this, analysis of the chromosomal association of Pch2 (through immunofluorescence analysis of spread meiotic chromosomes) using identical depletion conditions showed that Pch2 localization was not significantly affected in

Pch2 and Orc1, Orc2, Orc3, Orc4, and Orc6. (F) Schematic indicating inter-MBP-Pch2 and inter-MBP-Orc1 nonredundant cross-links. (G) Co-immunoprecipitation assay of Pch2-E399Q with Orc2-TAP in *ORC1* or *orc1-161* backgrounds (via α -TAP-IP) during the meiotic prophase (4 h into meiotic program). Experiments were performed at 23°C. (H) TAP-based ChIP-qPCR in *ORC1* and *ORC1-TAP* expressing *orc2-FRB* anchor-away strains. Rapamycin (1 μ g/ml) or DMSO was added at t = 0, and samples were taken at t = 4 h. Primers that amplify intergenic *Chr. VIII* (control locus), *ARS1114*, and *ARS1118* were used. Experimental data are the average of three biological replicates. SEM is indicated. Significance was calculated using an unpaired t test, and P-values are indicated. (I) Model depicting the origin-independent function of Pch2-Orc1/*ORC* in local meiotic DSB control.

response to Orc2 or Orc5 depletion from the nucleus (nor specifically from the nucleolar/rDNA region) (Fig S9C–F).

Altogether, our data suggest that *in vivo*, Pch2 interacts with the entire ORC, with Orc1 being an important mediator of this interaction. Our findings suggest that Orc1 is a crucial functional mediator of Pch2's role at rDNA borders and argue that this function is executed away from origins of DNA replication and does not *per se* require Orc2/Orc5. We propose that during the meiotic G2/prophase, Orc1/ORC is repurposed and interacts with Pch2 in a biochemical and functional manner that is uniquely distinct from its well-documented roles at origins of replication (Fig 6I).

Discussion

Pch2 is an important regulator of meiosis, and it uses its enzymatic activity to influence the chromosomal association of its clients. Up until now, HORMA domain-containing proteins were the only known direct interaction partners of Pch2/TRIP13 (Chen et al, 2014; Ye et al, 2015). Here, we demonstrate the direct association of Pch2 with a multi-protein complex essential for DNA replication (ORC). The canonical role for the ORC lies in forming the loading platform for the MCM replicative helicase (Bell & Kaguni, 2013; Bell & Labib, 2016), while it is also involved in gene silencing and sister chromatid cohesion (Foss et al, 1993; Loo et al, 1995; Fox et al, 1997; Suter et al, 2004; Shimada & Gasser, 2007). All these functions rely on association of the ORC with defined genomic regions, called origins of replication.

Our data reveal several biochemical characteristics about the ORC–Pch2 assembly and suggest that Pch2 uses an AAA+ /client and/or adaptor binding mode toward the ORC: (i) binding is increased in a mutant that stalls ATP hydrolysis (Fig 1B), (ii) hexamerization is required for efficient interaction (Fig 1C), and (iii) the nonenzymatic NTD of Pch2 plays a crucial role in mediating the interaction between Pch2 and ORC (Figs 3 and 5). In ORC–Cdc6, binding of a monomer of the Cdc6 AAA+ protein to the five other AAA+–like ORC proteins (Orc1–5) establishes the functional ring-shaped ORC hexamer (i.e., a Cdc6–Orc1–5 hexamer), which, in this composition, is proficient in loading the MCM AAA+ hexamer (Bell & Kaguni, 2013; Bell & Labib, 2016) (Fig 1D). An intriguing possibility regarding the association between Pch2 and ORC was that a monomer of Pch2 AAA+ protein could, in lieu of Cdc6, establish a complex with Orc1–5 (i.e., a 1:5 Pch2/Orc1–5 hexamer). However, we do not find evidence supporting such a binding mode. First, when we reconstituted the ORC–Pch2 complex, we observed that the pool of Pch2 that elutes at the expected size of a Pch2 hexamer interacts with the ORC (as judged by SEC analysis; Fig 2D). Second, the non-AAA+ domain of Pch2 (i.e., its NTD) provides a key contribution to the efficient binding of Pch2 to ORC (Figs 3–5). This would not be expected if a 1:5 Pch2/ORC (Orc1–5) would be established via binding principles that are similar to Cdc6–ORC, wherein AAA+/AAA+ interactions are the main driver of complex formation. Third, a Walker A domain Pch2 mutant that is expected to form a monomer (Herruzo et al, 2016) (Fig 1C) fails to interact with the ORC *in vivo*. Although we cannot formally exclude the existence of a 1:6 Pch2/ORC complex that binds to a hexamer of Pch2 (in a manner analogous to a 1:6 Cdc6–ORC

[Orc1–6]: hexameric MCM assembly), we interpret our experiments to indicate that the ORC (Orc1–6) is complexed with a hexamer of Pch2. In addition, we also show that Pch2–ORC assembly does not require Cdc6 (or any other accessory factors). During the meiotic program, expression of Pch2 is induced during the S-phase and peaks during the G2/prophase, when the ORC is not complexed with Cdc6 (Drury et al, 2000; Phizicky et al, 2018). In line with a temporal separation of Pch2- and Cdc6-bound ORC, we found evidence from *in vitro* reconstitution that Pch2 might (partially) engage the binding pocket that in ORC–Cdc6 is occupied by Cdc6.

Could the ORC be considered a client or an adaptor of Pch2? We believe that the most parsimonious explanation of our current analysis (combined with our earlier observations, which revealed that Orc1 is required for the nucleolar localization and function of Pch2 [Vader et al, 2011]), is that Orc1 plays an adaptor-like role, and as such acts as a recruiter of Pch2. The only known Pch2/TRIP13 adaptor is p31comet, a HORMA domain-containing factor that is required for the recognition of Mad2 during spindle assembly checkpoint signaling. p31comet is likely not conserved in budding yeast (Vleugel et al, 2012; van Hooff et al, 2017). We speculate that the ORC might have evolved adaptor functions for Pch2 in budding yeast meiosis.

However, in contrast to the role of the ORC as a chromosomal loader of MCM, our data imply that such a loading function for Pch2 is fundamentally different. Our ORC depletion experiments suggest that the loading role of Orc1 can be executed under conditions where ORC integrity is compromised (i.e., by nuclear depletion of Orc2 or Orc5), which is associated with a significant dissociation of Orc1 from origins of replication. This implies that the role of Pch2 (and by extension Orc1) should be executed away from origins of replication. In agreement with such a model, we recently reported genome-wide localization experiments of Pch2 during the meiotic G2/prophase, which revealed distinct binding patterns (which depend on Orc1) but no significant association of Pch2 with origins of replication (Cardoso da Silva et al, 2020).

How can we explain the role of Orc1 in directing Pch2 function, even under conditions where depletion of other ORC subunits compromises ORC integrity and origin association? A possibility is that *in vivo*, Orc1 could exist in two distinct pools: one where it is complexed with Orc2–6 (i.e., ORC) and the other where it exists as a monomer. Conceivably, Pch2 could interact with both pools. Such a model would be in agreement with our observation that *in vivo*, Orc1 exhibits a strong association with Pch2 (Fig 1E). If Orc1 is the factor that provides the needed functionality to Pch2 (whether complexed with ORC or not), inactivating other ORC components (such as Orc2/Orc5) would not *per se* trigger Pch2-like phenotypes. In such a scenario, the other non-Orc1 subunits of the ORC (Orc2–6) could be considered as piggybacking along with Orc1 and would not play any active role in Pch2 action. However, there may be subtle or additional roles for the non-Orc1 subunits for the ORC, which are not exposed in our current experimental approaches, for example, in aiding in binding affinity or activation of Pch2. In any case, our findings point to a noncanonical role for Orc1/ORC in mediating the function of Pch2 during the meiotic G2/prophase.

Based on these observations and following a model in which Orc1 is crucial to recruit Pch2 to the defined chromosomal regions, Orc1 should contain a chromosome-binding activity that is required for recruitment of Pch2. Indeed, Orc1 contains a nucleosome-binding

module (a bromo-adjacent homology [BAH] domain) (Callebaut et al, 1999; Yang & Xu, 2013), whose deletion mildly affects DNA replication (Müller, 2010). We have previously shown that this domain is required for the rDNA-associated role of Pch2 (Vader et al, 2011). Recent work has further demonstrated a role for the BAH domain of Orc1 in rDNA-associated protection against meiotic DSB activity (De Ioannes, 2019). Interestingly, our recent analysis of Pch2 chromosomal localization revealed that the BAH domain of Orc1 provides a crucial contribution to the proper recruitment of Pch2 to meiotic chromosomes (Cardoso da Silva et al, 2020). Taken together, these findings highlight the importance of this domain for meiosis-specific functions of Orc1/ORC, in connection to Pch2.

In conclusion, we have used a combination of *in vivo* and *in vitro* analyses to reveal the establishment of a meiosis-specific AAA+ assembly between ORC and Pch2. Our findings broaden the list of known ORC interactors by revealing a novel direct binding partner of the ORC (i.e., Pch2). Similarly, we also uncover a hitherto unknown direct association partner for Pch2 besides the already described HORMA domain-containing proteins. We propose that the function of ORC/Pch2 is executed away from origins of replication and strongly relies on Orc1 (Fig 6). We suggest that Orc1/ORC is important in mediating the recruitment of Pch2 to chromosomes, where it can act on its client protein Hop1 to control DSB activity. In the future, it will be interesting to establish the dynamic interplay between Pch2, Hop1, and Orc1/ORC.

By establishing an *in vitro* reconstituted assembly of Pch2 and ORC combined with *in vivo* analysis, we have shed light on an interaction between Pch2 and an AAA+ adaptor-like protein complex. Our experiments reveal characteristics of this assembly and highlight certain plasticity in the ability of the ORC to interact with distinct AAA+ proteins. Understanding the biochemical, structural, and functional connections between these two ATPases in more detail will be an avenue for future research.

Materials and Methods

Yeast strains

All strains, except those used for yeast two-hybrid analysis and ORC purification, are of the SK1 background. See Supplemental Data 1 for a description of genotypes of strains used per experiment.

Yeast two-hybrid analysis

Pch2 (full-length and different truncations/mutants) and Orc1-Orc6 were cloned in the pGBDU-C1 or pGAD-C1 vectors. The resulting bait and prey plasmids were transformed into a yeast two-hybrid reporter strain (yGV864). Yeast two-hybrid (Y2H) spot assay was performed by spotting 5 μ l of cultures at an optical density at 600 nm (OD600) of 0.5 onto -Ura-Leu plates (control) and -Ura-Leu-His (selective plate) and grown for 2–4 d.

Yeast viability assays

For spotting assays, anchor-away strains were grown on YP-glycerol plates overnight at 30°C, transferred to YP-dextrose (YPD) plates,

and further grown overnight at 30°C. Cells were then inoculated into 15 ml YPD culture and incubated overnight at 23°C and 180 rotations/minute (rpm) shaking. The following morning, cells were diluted to a final OD600 of 0.4 and grown for 4 h at 30°C and 180 rpm shaking. Then, 5 ml of cells were harvested at 90g for 3 min, washed in 1 ml H₂O, and resuspended in 500 μ l H₂O. And then, 10 μ l of 10-fold serial dilutions were prepared and spotted on YPD plates with or without 1 μ g/ml rapamycin. Growth at 30°C was monitored for the following 2–4 d.

Meiotic induction

Cells were patched from glycerol stocks onto YP-glycerol plates and grown overnight. Patched cells were transferred to YPD and further grown overnight. Cells were cultured in liquid YPD at 23°C overnight and diluted at OD600 0.3 into presporulation media (BYTA; phthalate-buffered yeast extract, tryptone, and acetate). Cells were grown in BYTA for 16–18 h at 30°C, washed twice in water, and resuspended in sporulation media (0.3% KAc) at OD600 1.9 to induce meiosis. Sporulation cultures were grown at 30°C (except for experiments involving temperature-sensitive strains, where strains were grown at the permissive temperature [23°C]). For time courses in which the anchor-away system was used, rapamycin (1 μ g/ml) or DMSO was added at $t = 0$ h (in sporulation media). Time courses were conducted, and samples for flow cytometry and Western or Southern blots were taken at different time points. For Western blot analysis, samples were taken after 0, 3, and 4 or 5 h, whereas for FACS and Southern blot analysis, samples were typically taken after 0, 3, 5, and 8 h.

Flow cytometry

Flow cytometry was used to assess synchronous passage through the meiotic program (as judged by duplication of the genomic content) and was performed as described (Vader et al, 2011). For analysis of rapamycin-induced phenotype, mitotic cultures were grown to saturation and diluted to OD600 1.0, and rapamycin was added. Samples for flow cytometry were taken at the indicated time points. A total of 10,000 cells were counted for each sample.

Western blot analysis

For Western blot analysis, protein lysates from yeast meiotic cultures were prepared using trichloroacetic acid (TCA) precipitation and run on 8% or 10% SDS gels, transferred for 90 min at 300 mA, and blotted with the selected primary/secondary antibodies, as described (Vader et al, 2011).

Southern blot analysis

For Southern blot assay, DNA from meiotic samples was prepared as described (Vader et al, 2011). DNA was digested with *HindIII* (to detect DSBs at the control YCR047C hot spot) or *ApaI* (to monitor DSBs in the region of interest: right rDNA flank; YLR164W), followed by gel electrophoresis, blotting of the membranes, and radioactive (³²P) hybridization using probes specific for YCR047C (chromosome III; 209,361–201,030) or YLR164W (chromosome XII; 493,432–493,932)

(for detection of DSBs in the hot spot control region or rDNA, respectively) (Vader et al, 2011). DSB signals were monitored by exposing an X-ray film to the membranes and further developed using a Typhoon Trio scanner (GE Healthcare) after 1 wk of exposure.

In vivo co-IP

For IP assays, 100 ml meiotic cultures at OD₆₀₀ 1.9 were grown, harvested after 4.5 h (G₂/prophase; unless otherwise indicated), washed with cold H₂O, and snap frozen. Acid-washed glass beads were then added, together with 300 μ l of ice-cold IP buffer (50 mM Tris-HCl pH 7.5, 150 mM NaCl, 1% Triton X-100, 1 mM EDTA pH 8.0, with protease inhibitors), and the cells broken with a Fastprep disruptor (FastPrep-24; MP Biomedicals) by two 45-s cycles on speed 6. The lysate was subsequently spun 3 min at 200g and the supernatant transferred to a falcon tube. The lysate was next sonicated for 25 cycles (30 s on/30 s off), in high power range, using a Bioruptor (Bioruptor-Plus sonication device; Diagenode), and then spun down 20 min at 20,000g. Supernatant was transferred to a new microcentrifuge tube, and 50 μ l of input was taken. For α -Flag/HA/TAP-based IPs, 1 μ l of antibody (α -Flag-M2 antibody; Sigma-Aldrich/ α -HA; BioLegend/ α -TAP; Thermo Fisher Scientific) was added to the lysate and rotated for 3 h. After the incubation step, 30 μ l of Dynabeads protein G (Invitrogen, Thermo Fisher Scientific) was added and rotated overnight at 4°C. For α -Orc2-based IPs, lysate was precleared with 10 μ l of Dynabeads protein G for 1 h at 4°C. Lysate was then incubated with 2 μ l of α -V5 (IgG isotype control; Invitrogen) or 11 μ l of α -Orc2 (Santa Cruz Biotechnology) for 3 h at 4°C, followed by 3-h incubation with 25 μ l of Dynabeads protein G. Suspensions were washed four times with ~500 μ l of ice-cold IP buffer. In the last wash, beads were transferred to a new microcentrifuge tube. Then, 55 μ l of loading buffer was added, boiled at 95°C, and run in an SDS gel. The inputs followed a TCA precipitation step. Briefly, 10% TCA was added and incubated for 30 min on ice. Pellets were then washed with ice-cold acetone, spun, and dried on ice, and further resuspended in TCA resuspension buffer (50 mM Tris-HCl 7.5, 6 M urea). After incubating for 30 min on ice, pellets were dissolved by pipetting and vortexing. Finally, 10 μ l of loading buffer was added, and samples were boiled at 95°C and run in an SDS gel together with the IP samples. Note that for the experiments shown in Fig 3D, 50 ml of sporulation culture, instead of 100 ml, was collected to perform the IP protocol. For Fig S1B and C, DNA was digested by addition of 20 U Benzonase (Sigma-Aldrich) to half of a 200 ml sample before cell lysis, and co-IPs were performed essentially as described. A fraction of the total lysate was used to isolate DNA using TRIzol (Thermo Fisher Scientific), according to manufacturer's protocol. DNA was analyzed using standard DNA PAGE.

Expression and purification of recombinant proteins in insect cells

Full-length Pch2 and its truncated versions were purified from insect cells. Specifically, fragments containing the coding sequences of Pch2 or its truncations, derived from codon-optimized cDNA, were subcloned into a pLIB-His-MBP vector (kind gift of Andrea Musacchio [Max Planck Institute of Molecular Physiology],

derived from pLIB [Weissmann et al, 2016]), and further integrated into EMBacY cells via Tn7 transposition. Positive clones were identified by blue/white screening and subsequently transfected into Sf9 cells to produce baculovirus (according to previously described methods) (Trowitzsch et al, 2010; Wilde et al, 2014). Baculovirus was amplified three times in Sf9 cells and used to infect Tnao38 cells for protein production. Tnao38 cells infected with the corresponding baculovirus (at a 1:10 dilution of virus to culture) were grown for 48 h, and pellets from 2 liter cultures were harvested. Cell pellets were resuspended in lysis buffer (50 mM HEPES pH 8.0, 300 mM NaCl, 5 mM imidazole, 5% glycerol, 5 mM β -mercaptoethanol, 1 mM MgCl₂, Benzonase, supplemented with SERVA protease inhibitor mix SERVA and cComplete mini, and EDTA-free protease inhibitor cocktail tablets Sigma-Aldrich) and lysed by sonication (Branson Sonifier 450). Sonicated cells were cleared by centrifugation 1 h at 100,000g (4°C) and the supernatant filtered. Clear lysate was immediately passed through a 5-ml TALON Superflow cartridge (Takara Bio). After extensive washing with buffer A (50 mM HEPES pH 8.0, 300 mM NaCl, 5 mM imidazole, 5% glycerol, 5 mM β -mercaptoethanol, and 1 mM MgCl₂) and wash buffer (50 mM HEPES pH 8.0, 1 M NaCl, 5 mM imidazole, 5% glycerol, 5 mM β -mercaptoethanol, and 1 mM MgCl₂), protein was eluted with a gradient between buffer A and buffer B (50 mM HEPES pH 8.0, 300 mM NaCl, 400 mM imidazole, 5% glycerol, 5 mM β -mercaptoethanol, and 1 mM MgCl₂). The presence of protein was monitored by UV280 nm. Those fractions containing the protein of interest were pooled and incubated 30 min at 4°C with pre-equilibrated amylose resin (New England Biolabs) and eluted with elution buffer (30 mM HEPES pH 8.0, 500 mM NaCl, 3% glycerol, 2 mM TCEP, 1 mM MgCl₂, and 20 mM maltose). The eluted protein was concentrated using an Amicon-Ultra-15 centrifugal filter (MWCO 30 kD) (Merck Millipore), spun down 15 min in a benchtop centrifuge (4°C), and subsequently purified by SEC, by loading onto a Superose 6 Increase 10/300 GL (GE Healthcare) previously equilibrated in gel filtration buffer (30 mM HEPES pH 8.0, 500 mM NaCl, 3% glycerol, 2 mM TCEP, and 1 mM MgCl₂). The peak fractions were analyzed by SDS-PAGE, and those fractions corresponding to the protein of interest were collected and concentrated using a 30K Amicon-Ultra-4 centrifugal filter (in the presence of protease inhibitors). The concentrated protein was snap frozen in liquid N₂ and stored at -80°C until further use. Note that for purification of His-MBP-Pch2-243-564, buffers were adjusted to pH 7.6 instead of pH 8.0.

The His-tagged ORC was purified from insect cells. The multiple subunits of the ORC were cloned using the biGbac method described in Weissmann et al (2016). Briefly, the coding sequences of the individual ORC subunits (Orc1, Orc2, Orc3, Orc4, Orc5, and Orc6) were cloned into pLIB vectors, with the particularity that Orc1 coding sequence was subcloned into a pLIB vector containing a 6xHis tag. pLIB vectors of His-Orc1, Orc2, and Orc3 were subsequently cloned into a pBIG1a vector, whereas the pLIB vectors of Orc4, Orc5, and Orc6 were assembled into a pBIG1b construct. pBIG1a and pBIG1b constructs were used to transform EMBacY cells by Tn7 transposition, and the positive clones were used to generate baculovirus by transfection to Sf9 cells. After 4-d amplification of the baculoviruses, the supernatant of both viruses containing His-Orc1-3 and Orc4-Orc6, respectively, were used for protein expression. A 3 liter culture of Tnao38 cells was coinfecting with the

two baculoviruses and 48 h post-infection, cells were harvested by centrifugation, washed once with PBS, and snap frozen. Cell pellets were resuspended in lysis buffer (50 mM HEPES 7.5, 300 mM KCl, 1 mM MgCl₂, 10% glycerol, 5 mM β-mercaptoethanol, 5 mM imidazole, Benzonase, protease inhibitors SERVA protease inhibitor mix and cOMplete mini, and EDTA-free protease inhibitor cocktail) and lysed by sonication. Lysed cells were harvested by ultracentrifugation 1 h at 100,000g (4°C), and the supernatant was filtered and precipitated with 20% (NH₄)₂SO₄ on ice for ~45 min and recentrifuged. Clear lysate was affinity-purified by incubating it with cOMplete His-tag purification resin (Roche) for 2 h (4°C). After extensive washing with a 5–15 mM imidazole gradient in buffer A (50 mM HEPES–KOH 7.5, 300 mM KCl, 1 mM MgCl₂, 10% glycerol, and 5 mM β-mercaptoethanol), protein was eluted with elution buffer (buffer A supplemented with 300 mM imidazole). The eluted protein complex was concentrated using a 30K Amicon-Ultra-15 centrifugal filter, spun down 15 min at 20,000g in a benchtop centrifuge (4°C), and loaded onto a Superose 6 Increase 10/300 GL column (GE Healthcare), previously equilibrated in gel filtration buffer (30 mM HEPES pH 7.5, 300 mM KCl, 5% glycerol, 1 mM MgCl₂, and 2 mM TCEP). Fractions were analyzed by SDS–PAGE, and those fractions containing His–ORC were concentrated using a 30 kD MWCO concentrator and flash-frozen in liquid N₂.

Expression and purification of ORC from budding yeast cells

The ORC was purified from budding yeast (yGV3358) essentially as described by the Diffley laboratory (Yeeles et al, 2015). The ORC that was directly concentrated on calmodulin beads was used for ORC-based pulldowns.

Expression and purification of Hop1

Hop1 was purified from bacterial cells. Briefly, the coding sequence of Hop1 was subcloned into a pET28a vector for expression of recombinant NH₂-terminally polyhistidine-tagged Hop1 (6xHis–Hop1). For protein expression, BL21 RIPL cells were transformed with the resulting vector and further used to inoculate 11 L of LB media, supplemented with kanamycin and chloramphenicol. Cultures were grown at 37°C with vigorous shaking until OD₆₀₀ ~ 0.6–0.8. Protein expression was induced by addition of 0.25 mM IPTG overnight at 18°C. Cells were harvested by centrifugation at 400g for 15 min and the pellet washed with PBS and immediately snap frozen. For protein purification, cell pellets were resuspended in buffer A (50 mM HEPES, pH 7.5, 300 mM NaCl, 5 mM imidazole, 10% glycerol, 0.05% Tween-20, and 5 mM β-mercaptoethanol) supplemented with Benzonase and protease inhibitors (1 mM PMSF and SERVA protease inhibitor mix). Cells were lysed using a microfluidizer (Microfluidizer M-110S; Microfluidics Corporation), centrifuged at 100,000g, 4°C for 1 h, and the lysate filtered. The clear lysate was first passed through a 5-ml TALON column (GE Healthcare). After extensive washing, protein was eluted with an imidazole gradient between buffer A and buffer B (buffer A supplemented with 400 mM imidazole). Eluate was pooled, diluted 2:1 in buffer A without NaCl and imidazole, and subsequently loaded into a heparin column (HiTrap Heparin 16/10; GE Healthcare), previously equilibrated with buffer C (20 mM HEPES, pH 7.5, 150 mM NaCl, 5 mM MgCl₂, 10% glycerol, and 5 mM β-mercaptoethanol). Protein was further eluted in a gradient between buffers C and D

(buffer C with 1 M NaCl), and fractions pooled and concentrated using a 30K Amicon-Ultra-15 centrifugal filter. Concentrated protein was spun down 15 min in a benchtop centrifuge (4°C) and immediately loaded onto a HiLoad 16/600 Superdex 200 column (GE Healthcare), pre-equilibrated in gel filtration buffer consisting of 20 mM HEPES pH 7.5, 300 mM NaCl, 5 mM MgCl₂, 5% glycerol, and 2 mM β-mercaptoethanol. Fractions were analyzed by SDS–PAGE, and those fractions containing 6xHis–Hop1 were concentrated with an Amicon-Ultra-15 concentrator (MWCO 30 kD), snap frozen, and kept at –80°C until further use.

In vitro pulldown assays

For pulldown between His–Hop1 and His–MBP–Pch2, 7.5 μl of amylose beads (New England BioLabs), preblocked with 5% BSA, were incubated with 6 μM His–MBP or 1 μM His–MBP–Pch2 (assuming a hexamer of Pch2) for 1 h on ice in a final volume of 30 μl pulldown buffer (50 mM Tris pH 7.5, 50 mM NaCl, 10 mM imidazole, 10 mM β-mercaptoethanol, 0.1% Tween-20, and 1 mM MgCl₂) supplemented with 200 μM ATP or 200 μM ATPγS when specified. Beads were then washed once with 100 μl pulldown buffer, and 6 μM Hop1 was added. As input, 6% of the final volume was taken. This reaction was incubated for 90 min on ice and next washed once with wash buffer (50 mM Tris pH 7.5, 200 mM NaCl, 10 mM imidazole, 10 mM β-mercaptoethanol, 0.5% Triton X-100 and 1 mM MgCl₂). Then, 20 μl loading buffer was added, samples boiled at 95°C, and supernatant transferred to a new microcentrifuge tube. Samples were analyzed by SDS–PAGE and stained with Coomassie Brilliant Blue (CBB).

For pulldowns between His–MBP–Pch2 and His–ORC, 5 μl of 5% BSA preblocked amylose beads were incubated with 6 μM His–MBP or 1 μM His–MBP–Pch2 (assuming a hexamer of Pch2) for 1 h on ice in a 30 μl final volume of pulldown buffer (30 mM HEPES pH 7.5, 150 mM NaCl, 10 mM imidazole, 10 mM β-mercaptoethanol, 0.1% Tween-20, and 10 mM MgCl₂). The pulldown reactions were washed twice with 200 μl of pulldown buffer, and 1 μM ORC was added. As input, 10% of the final volume was taken. This reaction was incubated for 90 min on ice and washed twice with 200 μl wash buffer containing 30 mM HEPES pH 7.5, 200 mM NaCl, 10 mM imidazole, 10 mM β-mercaptoethanol, 10% Triton X-100, and 10 mM MgCl₂. Inputs were diluted with pulldown buffer up to 10 μl, and then loading buffer was added. For the pulldown reactions, 20 μl of loading buffer was added. Samples were boiled at 95°C, and supernatant from pulldown reactions transferred to a new microcentrifuge tube. Samples were analyzed by SDS–PAGE and stained with CBB. Alternatively, the input/pulldown samples were analyzed by Western blotting as follows: half of the input/pulldown reactions were run on SDS–PAGE gel, transferred at 300 mA for 90 min and probed overnight with α-MBP (1:10,000; New England BioLabs) or α-ORC (1:1,000, kind gift of Stephen Bell), and subsequently developed using the corresponding secondary antibody. For pulldown with dephosphorylated His–ORC, 3 μM of His–ORC was dephosphorylated by λ-phosphatase treatment at 4°C overnight (see below) in a total volume of 30 μl. Then, 10 μl was taken and incubated with either 1 μM of His–MBP–Pch2 or 6 μM of His–MBP in pulldown buffer, and pulldown was performed similarly as described above.

Pulldowns with Pch2 fragments (His-MBP-Pch2-2-144/His-MBP-Pch2-243-564) were performed similarly, except that 6 μM of His-MBP-Pch2-2-144 was used (due to formation of monomer instead of hexamer in this fragment. See the Results section for further details). Note that for pulldown with His-MBP-Pch2-2-144 and His-ORC analyzed by Western blot, we used a twofold excess of His-MBP-Pch2-2-144 fragment as compared with the pulldown analyzed by CBB. Western blotting was performed similarly as detailed above, probing with α -MBP (New England BioLabs) or α -ORC (kind gift of Stephen Bell, MIT).

For pulldowns with the ORC purified from budding yeast, the ORC bound to calmodulin beads was transferred into a 1.5-ml reaction tube (40 μl of the beads solution/condition) and washed with pulldown buffer: (30 mM HEPES pH 7.5, 200 mM NaCl, 10 mM β -mercaptoethanol, 0.1% Tryton, and 2 mM CaCl_2 [supplemented or not with 1 mM MgCl_2]) with or without nucleotides (ADP, AppNHP, and ATP γ S [50 μM] or ATP [50 μM]). His-MBP (1 μl of the MBP solution [300 μM stock]) or His-MBP-Pch2 (1 μM of the protein solution [40 μM , assuming a Pch2 hexamer]) was added for 1 h on ice. Then, 8 μl of the sample was taken as input. Inputs were diluted with pulldown buffer up to 20 μl , and then 5 \times SDS loading buffer was added. The pulldown reactions were washed twice with 200 μl of pulldown buffer, briefly spun down, and supernatant removed. And then, 20 μl of 2.5 \times SDS loading buffer was added. Samples were boiled at 95 $^\circ\text{C}$, and supernatant from pulldown reactions transferred to a new 0.5-ml microfuge tube. Samples were analyzed by SDS-PAGE and stained with CBB.

Lambda phosphatase treatment of purified His-ORC

For dephosphorylation of His-ORC purified from insect cells, 2 μM of His-ORC were incubated with λ -phosphatase (1:5, λ -phosphatase: His-ORC) in a total volume of 30 μl in a buffer containing 30 mM HEPES pH 7.5, 300 mM KCl, 5% glycerol, and 2 mM TCEP. The dephosphorylation reaction was supplemented with 10 mM MnCl_2 and incubated for 1 h at room temperature or overnight at 4 $^\circ\text{C}$. Then, 5 \times SDS loading buffer was added, and samples were analyzed by SDS-PAGE followed by CBB staining.

Analytical SEC

Analytical SEC was performed on a Superose 6 5/150 GL column (GE Healthcare) connected to an AKTAmicro FPLC system (GE Healthcare). Proteins (1 μM His-MBP-Pch2, 3 μM His-ORC) were mixed in a total volume of 50 μl , incubated 2 h on ice, and spun down for 15 min at 20,000g in a benchtop centrifuge (4 $^\circ\text{C}$) before injection. All samples were eluted under isocratic conditions at 4 $^\circ\text{C}$ in SEC buffer containing 30 mM HEPES pH 7.5, 150 mM NaCl, 3% glycerol, 1 mM MgCl_2 , and 2 mM TCEP, at a flow rate of 0.1 ml/min. Fractions (100 μl) were collected, and 20 μl were analyzed by SDS-PAGE and CBB staining.

For SEC profiles represented in Figs 2A, 5B, S3A, and S4A, the purified proteins were run as described above. Briefly, purified His-MBP-Pch2 (2 μM), His-MBP-Pch2-2-144 (6 μM), or His-ORC (6 μM) or His-MBP-Pch2-243-564 (2 μM) were diluted in SEC buffer (30 mM HEPES pH 7.5, 150 mM NaCl, 3% glycerol, 2 mM TCEP, and 1 mM MgCl_2) up to a volume of 50 μl , spun down 15 min at 20,000g (4 $^\circ\text{C}$),

and immediately loaded into a Superose 6 Increase 5/150 GL column (for His-MBP-Pch2 and His-ORC) or into a Superdex 200 5/150 GL (for His-MBP-Pch2-2-144).

Cross-linking mass spectrometry

Cross-linking mass spectrometry (XL-MS) was performed as described (Pan et al, 2018). Briefly, 0.75 μM of His-MBP-Pch2 was mixed with 1.5 μM of His-ORC complex in 200 μl of buffer (30 mM HEPES pH 7.5, 150 mM NaCl, and 2 mM TCEP) and incubated at 4 $^\circ\text{C}$ for 90 min. DSBU (disuccinimidyl dibutyric urea—also known as BuUrBu-, Alinda Chemical Limited) was added to a final concentration of 3 mM and incubated at 25 $^\circ\text{C}$ for 1 h. The reaction was stopped by adding Tris-HCl pH 8.0 to a final concentration of 100 mM and incubated at 25 $^\circ\text{C}$ for an additional 30 min. Then, 10 μl of protein sample was taken before and after adding the cross-linker for analysis by SDS-PAGE. SDS-PAGE gel was stained with CBB. Cross-linked protein complexes were precipitated by adding 4 volumes of cold acetone (-20 $^\circ\text{C}$ overnight) and centrifuged 5 min at 20,000g, and the pellet was dried at room temperature. Protein pellets were denatured in denaturation reduction solution (8 M urea and 1 mM DTT) for 30 min at 25 $^\circ\text{C}$. Cysteine residues were alkylated by adding 5.5 mM chloroacetamide and incubating for 20 min at 25 $^\circ\text{C}$. ABC buffer (20 mM ammonium bicarbonate pH 8.0) was added to reduce the final concentration of urea to 4M. Sample was digested by Lys-C (2 μg) at 25 $^\circ\text{C}$ for 3 h, followed by overnight Trypsin (1 μg) digestion in buffer containing 100 mM Tris-HCl pH 8.5, and 1 mM CaCl_2 at 25 $^\circ\text{C}$. The digestion was stopped by adding TFA to a final concentration of 0.2%.

Resulting peptides after digestion were run in three independent SEC runs on a Superdex Peptide 3.2/300 column (GE Healthcare) connected to an AKTAmicro FPLC system (GE Healthcare). SEC runs were performed at a flow rate of 0.1 ml/min in buffer containing 30% acetonitrile and 0.1% formic acid. And 100 μl fractions were collected, and the same fractions from the three SEC runs were pooled, dried, and submitted to liquid chromatography-mass spectrometry/mass spectrometry analysis.

The liquid chromatography-mass spectrometry/mass spectrometry analysis was performed as previously reported using an UltiMate 3000 RSLC nano system and a Q-Exactive Plus mass spectrometer (Thermo Fisher Scientific) (Pan et al, 2018). Peptides were dissolved in water containing 0.1% TFA and were separated on the UltiMate 3000 RSLC nano system (precolumn: C18, Acclaim PepMap, 300 μm \times 5 mm, 5 μm , 100 \AA , separation column: C18, Acclaim PepMap, 75 μm \times 500 mm, 2 μm , 100 \AA ; Thermo Fisher Scientific). After loading the sample on the precolumn, a multistep gradient from 5–40% B (90 min), 40–60% B (5 min), and 60–95% B (5 min) was used with a flow rate of 300 nl/min; solvent A: water + 0.1% formic acid; solvent B: acetonitrile + 0.1% formic acid. Data were acquired using the Q-Exactive Plus mass spectrometer in data-dependent MS/MS mode. For full-scan MS, we used a mass range of m/z 300–1,800, resolution of $R = 140,000$ at m/z 200, one microscan using an automated gain control (AGC) target of 3×10^6 , and a maximum injection time of 50 ms. Then, we acquired up to 10 HCD MS/MS scans of the most intense at least doubly charged ions (resolution 17,500, AGC target 1×10^5 , injection time 100 ms, isolation window 4.0 m/z , normalized collision energy 25.0, intensity threshold 2×10^4 , dynamic exclusion 20.0 s). All spectra were recorded in profile mode.

Raw data from the Q-Exactive Plus mass spectrometer were converted to Mascot generic file format. Program MeroX (version 1.6.6.6) was used for cross-link identification (Gotze et al, 2015). Combined MS data in Mascot generic file format and the protein sequences in FASTA format were loaded on the program, and MS spectra matching cross-linked peptides were identified. In the settings of MeroX, the precursor precision and the fragment ion precision were changed to 10.0 and 20.0 ppm, respectively. RISE mode was used, and the maximum missing ions was set to 1. MeroX estimates the FDR by comparison of the distribution of the cross-link candidates found using provided protein sequences and the distribution of the candidates found from decoy search using shuffled sequences. A 2% FDR was used as the cutoff to exclude the candidates with lower MeroX scores. The results of cross-link data were exported in comma-separated value format. Cross-link network maps were generated using the xVis website (<https://xvis.genzentrum.lmu.de>) (Grimm et al, 2015). Validation of the datasets was performed by identifying 13 intra-MBP cross-links and using a published crystal structure of MBP (PDB 1FQB, [Duan et al, 2001]) to map Ca-Ca distances between identified cross-linked amino acids. The average Ca-Ca was 14.41 Å, which is in good agreement with the Ca-Ca distance (12 Å) which the cross-linked state of DSBU is able to facilitate (Table S2).

Chromatin IP-qPCR

For ChIP experiments, 100 ml SPO cultures (OD600 of 1.9) were harvested 4 h after entering meiosis. Cultures were cross-linked with 1% methanol-free formaldehyde (FA) for 15 min at room temperature. Cross-linking was quenched with 125 mM glycine. After a wash with ice-cold TBS, cells were snap frozen and stored at -80°C. Cells were resuspended in 600 µl of TAP ChIP buffer (25 mM Tris-HCl pH 8.0, 150 mM NaCl, 0.1% NP-40, and 1 mM EDTA, pH 8.0) supplemented with EDTA-free protease inhibitors (Roche), 1 mM PMSF, 1× SERVA protease inhibitor mix (SERVA), and 1 mM sodium orthovanadate, and broken with glass beads using a bead beater (FastPrep-24; MP Biomedicals) (two times 60 s, speed 6, incubated on ice for 5 min in between runs). Chromatin was sheared by sonication using a Bioruptor UCD 200 (Diagenode) (settings: 25 cycles of 30 s on/off, high power at 4°C). Lysates were centrifuged at 16,000g for 10 min at 4°C. Input samples were taken. Then, 550 µl of cell lysates was preincubated with 1 µg of anti-TAP (Thermo Fisher Scientific) for 3 h at 4°C before overnight incubation under rotation with magnetic Dynabeads protein-G (Invitrogen). Beads were washed four times with buffer containing detergent and another time with the same buffer without detergent. Reverse cross-linking, proteinase-K, and RNase-A treatments and final purifications and elution were performed with ChIP and input samples as previously described in Blitzblau and Hochwagen (2013). For the rDNA-specific ChIP experiment shown in Fig S9B, chromatin was extracted as above and IP was performed with the following modifications: cells were resuspended in FA buffer (50 mM HEPES-KOH, pH 7.5, 140 mM NaCl, 1 mM EDTA, 1% Triton X-100, 0.1% sodium deoxycholate, and protease and phosphatase inhibitors). Suspension was then incubated with 30 µl IgG Sepharose (GE Healthcare) for 3 h at 4°C. Beads were twice washed with FA buffer, twice with FA buffer containing 500 mM NaCl, and twice

with Tris/EDTA (TE) buffer. Reverse cross-linking, proteinase-K and RNase-A treatments, and final purifications and elution were performed as above. ChIP and input samples were quantified by qRT-PCR on a 7500 fast real-time PCR machine (Applied Biosystems). The experiment shown on Fig 6H was performed using the CFX-Connect real-time PCR detection system (Bio-Rad). The percentage of ChIP relative to input was calculated for the target loci as well as for the negative controls. The enrichment was calculated using the ΔC_t method: $1/(2^{\Delta C_t - C_{t\text{control}}})$.

Primers that were used amplify for qRT-PCR were as follows:

Intergenic chromosome VIII-forward: 5'-GCTGCATTCCACCACGTC-3'
Intergenic chromosome VIII-reverse: 5'-GCATTTAACACGGCCACCA-3'
PPR1-forward: 5'-AGAACGTCATCTCCGGAATCT-3'
PPR1-reverse: 5'-TGGGCACGATGAGAGAAAGT-3'
ARS1116-forward: 5'-AAGCTTTTCATCCCAGCAGA-3'
ARS1116-reverse: 5'-TTTTGTGCTGTTGTCGATTCA-3'
ARS1118-forward: 5'-CCCTGATTGGAGTGATTTTC-3'
ARS1118-reverse: 5'-GGACCGTCTGAAGAGGTGAA-3'
ARS1114-forward: 5'-TGAGCGTTTCTTTAGAT-3'
ARS1114-reverse: 5'-GCAATTGTTCCATTTTCTCC-3'
5S-forward: 5'-TGCGGCCAIAICTACCAGAAA-3'
5S reverse: 5'-CACCTGAGTTTCGCGTATGG-3'
ARS1216.5-forward: 5'-CACCACTCTACCAATAACGG-3'
ARS1216.5-reverse: 5'-AAAGGTGCGGAAATGGCTGA-3'

Primer efficiencies (calculated using standard procedures) were as follows: *Intergenic chromosome VIII* = 1.889, *PPR1* = 1.998, *ARS1116* = 1.991, *ARS1118* = 1.995, *ARS1114* = 1.943, *5S* = 2.008, *ARS1216.5* = 1.951.

Chromosome spreads

Chromosome spreads and quantification of 3XHA-Pch2 in *orc2-FRB* or *orc5-FRB* backgrounds (nucleolus and non-nucleolar) were performed as described in Cardoso da Silva et al (2020). Chromosome synapsis was detected using an antibody against Gmc2 (kind gift of Amy MacQueen, Wesleyan University) (Voelkel-Meiman et al, 2019).

Supplementary Information

Supplementary Information is available at <https://doi.org/10.26508/lsa.201900630>.

Acknowledgements

This work was financially supported by the European Research Council (Starting Grant URDNA, agreement nr. 638197, to G. Vader), a CAPES-Humboldt fellowship from the Alexander von Humboldt Foundation (agreement nr. 99999.000021/2016-04, to R. Cardoso da Silva) and the Max Planck Society. We thank Andrea Musacchio (Max Planck Institute of Molecular Physiology, Dortmund, Germany) for ongoing support and for sharing unpublished reagents. We thank Andreas Brockmeyer and Franziska Müller (Max Planck Institute of Molecular Physiology, Dortmund, Germany) for technical and computational assistance in preparation of the XL-MS dataset. We thank

Jolien van Hooff, Geert Kops (Hubrecht Institute, Utrecht, The Netherlands), and Berend Snel (Utrecht University, Utrecht, The Netherlands) for help with sequence alignments. We thank Stephen Bell (MIT, Cambridge, USA), Christoph Kurat, Allison McClure, John Diffley (Francis Crick Institute, UK), and Amy MacQueen (Wesleyan University, USA) for sharing reagents and protocols. We thank Andreas Hochwagen (New York University, New York, USA), Adèle Marston (Wellcome Centre for Cell Biology, Edinburgh, UK), Hannah Blitzblau (Novogy, Cambridge, USA), and Arnaud Rondelet (Max Planck Institute of Molecular Physiology, Dortmund, Germany) for comments on the manuscript. We thank members of the Vader and Bird groups (Max Planck Institute of Molecular Physiology, Dortmund, Germany) for helpful discussions and comments on the manuscript.

Author Contributions

MA Villar-Fernández: conceptualization, formal analysis, investigation, and methodology.

R Cardoso da Silva: conceptualization, funding acquisition, investigation, and methodology.

M Firlej: investigation.

D Pan: formal analysis, investigation, and methodology.

E Weir: investigation and methodology.

A Sarembe: investigation and methodology.

VB Raina: investigation.

T Bange: formal analysis.

JR Weir: conceptualization, investigation, and methodology.

G Vader: conceptualization, formal analysis, supervision, funding acquisition, investigation, visualization, methodology, project administration, and writing—original draft, review, and editing.

Conflict of Interest Statement

The authors declare that they have no conflict of interest.

References

- Alfieri C, Chang L, Barford D (2018) Mechanism for remodelling of the cell cycle checkpoint protein MAD2 by the ATPase TRIP13. *Nature* 559: 274–278. doi:10.1038/s41586-018-0281-1
- Bell SP, Kaguni JM (2013) Helicase loading at chromosomal origins of replication. *Cold Spring Harb Perspect Biol* 5: a010124. doi:10.1101/cshperspect.a010124
- Bell SP, Labib K (2016) Chromosome duplication in *Saccharomyces cerevisiae*. *Genetics* 203: 1027–1067. doi:10.1534/genetics.115.186452
- Bhalla N, Dernburg AF (2005) A conserved checkpoint monitors meiotic chromosome synapsis in *Caenorhabditis elegans*. *Science* 310: 1683–1686. doi:10.1126/science.1117468
- Blitzblau HG, Chan CS, Hochwagen A, Bell SP (2012) Separation of DNA replication from the assembly of break-competent meiotic chromosomes. *PLoS Genet* 8: e1002643. doi:10.1371/journal.pgen.1002643
- Blitzblau HG, Hochwagen A (2013) ATR/Mec1 prevents lethal meiotic recombination initiation on partially replicated chromosomes in budding yeast. *Elife* 2: e00844. doi:10.7554/elife.00844
- Borner GV, Barot A, Kleckner N (2008) Yeast Pch2 promotes domain axis organization, timely recombination progression, and arrest of defective recombinosomes during meiosis. *Proc Natl Acad Sci U S A* 105: 3327–3332. doi:10.1073/pnas.0711864105

Callebaut I, Courvalin JC, Mornon JP (1999) The BAH (bromo-adjacent homology) domain: A link between DNA methylation, replication and transcriptional regulation. *FEBS Lett* 446: 189–193. doi:10.1016/s0014-5793(99)00132-5

Cardoso da Silva R, Villar-Fernandez MA, Vader G (2020) Active transcription and Orc1 drive chromatin association of the AAA+ ATPase Pch2 during meiotic G2/prophase. *PLoS Genet* 16: e1008905. doi:10.1371/journal.pgen.1008905

Chen C, Jomaa A, Ortega J, Alani EE (2014) Pch2 is a hexameric ring ATPase that remodels the chromosome axis protein Hop1. *Proc Natl Acad Sci U S A* 111: E44–E53. doi:10.1073/pnas.1310755111

De Ioannes P, Leon VA, Kuang Z, Wang M, Boeke JD, Hochwagen A, Armache KJ (2019) Structure and function of the Orc1 BAH-nucleosome complex. *Nat Commun* 10: 2894. doi:10.1038/s41467-019-10609-y

Drury LS, Perkins G, Diffley JF (2000) The cyclin-dependent kinase Cdc28p regulates distinct modes of Cdc6p proteolysis during the budding yeast cell cycle. *Curr Biol* 10: 231–240. doi:10.1016/s0960-9822(00)00355-9

Duan X, Hall JA, Nikaido H, Quijcho FA (2001) Crystal structures of the maltodextrin/maltose-binding protein complexed with reduced oligosaccharides: Flexibility of tertiary structure and ligand binding. *J Mol Biol* 306: 1115–1126. doi:10.1006/jmbi.2001.4456

Foss M, McNally FJ, Laurenson P, Rine J (1993) Origin recognition complex (ORC) in transcriptional silencing and DNA replication in *S. cerevisiae*. *Science* 262: 1838–1844. doi:10.1126/science.8266071

Fox CA, Ehrenhofer-Murray AE, Loo S, Rine J (1997) The origin recognition complex, SIR1, and the S phase requirement for silencing. *Science* 276: 1547–1551. doi:10.1126/science.276.5318.1547

Gotze M, Pettelkau J, Fritzsche R, Ihling CH, Schafer M, Sinz A (2015) Automated assignment of MS/MS cleavable cross-links in protein 3D-structure analysis. *J Am Soc Mass Spectrom* 26: 83–97. doi:10.1007/s13361-014-1001-1

Grimm M, Zimniak T, Kahraman A, Herzog F (2015) xVis: A web server for the schematic visualization and interpretation of crosslink-derived spatial restraints. *Nucleic Acids Res* 43: W362–W369. doi:10.1093/nar/gkv463

Hanson PI, Whiteheart SW (2005) AAA+ proteins: Have engine, will work. *Nat Rev Mol Cell Biol* 6: 519–529. doi:10.1038/nrm1684

Haruki H, Nishikawa J, Laemmli UK (2008) The anchor-away technique: Rapid, conditional establishment of yeast mutant phenotypes. *Mol Cell* 31: 925–932. doi:10.1016/j.molcel.2008.07.020

Heldrich J, Sun X, Vale-Silva LA, Markowitz TE, Hochwagen A (2020) Topoisomerases modulate the timing of meiotic DNA breakage and chromosome morphogenesis in *Saccharomyces cerevisiae*. *Genetics* 215: 59–73. doi:10.1534/genetics.120.303060

Herruzo E, Ontoso D, Gonzalez-Arranz S, Caverio S, Lechuga A, San-Segundo PA (2016) The Pch2 AAA+ ATPase promotes phosphorylation of the Hop1 meiotic checkpoint adaptor in response to synaptonemal complex defects. *Nucleic Acids Res* 44: 7722–7741. doi:10.1093/nar/gkw506

Hochwagen A, Tham WH, Brar GA, Amon A (2005) The FK506 binding protein Fpr3 counteracts protein phosphatase 1 to maintain meiotic recombination checkpoint activity. *Cell* 122: 861–873. doi:10.1016/j.cell.2005.07.010

Hou Z, Bernstein DA, Fox CA, Keck JL (2005) Structural basis of the Sir1-origin recognition complex interaction in transcriptional silencing. *Proc Natl Acad Sci U S A* 102: 8489–8494. doi:10.1073/pnas.0503525102

Joshi N, Barot A, Jamison C, Borner GV (2009) Pch2 links chromosome axis remodeling at future crossover sites and crossover distribution during yeast meiosis. *PLoS Genet* 5: e1000557. doi:10.1371/journal.pgen.1000557

- Lam I, Keeney S (2015) Mechanism and regulation of meiotic recombination initiation. *Cold Spring Harb Perspect Biol* 7: a016634. doi:10.1101/cshperspect.a016634
- Li XC, Schimenti JC (2007) Mouse pachytene checkpoint 2 (trip13) is required for completing meiotic recombination but not synapsis. *PLoS Genet* 3: e130. doi:10.1371/journal.pgen.0030130
- Loo S, Fox CA, Rine J, Kobayashi R, Stillman B, Bell S (1995) The origin recognition complex in silencing, cell cycle progression, and DNA replication. *Mol Biol Cell* 6: 741–756. doi:10.1091/mbc.6.6.741
- Müller P, Park S, Shor E, Huebert DJ, Warren CL, Ansari AZ, Weinreich M, Eaton ML, MacAlpine DM, Fox CA (2010) The conserved bromo-adjacent homology domain of yeast Orc1 functions in the selection of DNA replication origins within chromatin. *Genes Dev* 24: 1418–1433. doi:10.1101/gad.1906410
- Nguyen VQ, Co C, Li JJ (2001) Cyclin-dependent kinases prevent DNA replication through multiple mechanisms. *Nature* 411: 1068–1073. doi:10.1038/35082600
- Pan D, Brockmeyer A, Mueller F, Musacchio A, Bange T (2018) Simplified protocol for cross-linking mass spectrometry using the MS-cleavable cross-linker DSBU with efficient cross-link identification. *Anal Chem* 90: 10990–10999. doi:10.1021/acs.analchem.8b02593
- Peng C, Luo H, Zhang X, Gao F (2015) Recent advances in the genome-wide study of DNA replication origins in yeast. *Front Microbiol* 6: 117. doi:10.3389/fmicb.2015.00117
- Petronczki M, Siomos MF, Nasmyth K (2003) Un ménage à quatre: The molecular biology of chromosome segregation in meiosis. *Cell* 112: 423–440. doi:10.1016/s0092-8674(03)00083-7
- Phizicky DV, Berchowitz LE, Bell SP (2018) Multiple kinases inhibit origin licensing and helicase activation to ensure reductive cell division during meiosis. *Elife* 7: e33309. doi:10.7554/elife.33309
- Prioleau MN, MacAlpine DM (2016) DNA replication origins—where do we begin? *Genes Dev* 30: 1683–1697. doi:10.1101/gad.285114.116
- Ritz D, Vuk M, Kirchner P, Bug M, Schutz S, Hayer A, Bremer S, Lusk C, Baloh RH, Lee H, et al (2011) Endolysosomal sorting of ubiquitylated caveolin-1 is regulated by VCP and UBXD1 and impaired by VCP disease mutations. *Nat Cell Biol* 13: 1116–1123. doi:10.1038/ncb2301
- Roig I, Dowdle JA, Toth A, de Rooij DG, Jasin M, Keeney S (2010) Mouse TRIP13/PCH2 is required for recombination and normal higher-order chromosome structure during meiosis. *PLoS Genet* 6: e1001062. doi:10.1371/journal.pgen.1001062
- San-Segundo PA, Roeder GS (1999) Pch2 links chromatin silencing to meiotic checkpoint control. *Cell* 97: 313–324. doi:10.1016/s0092-8674(00)80741-2
- Sasaki M, Lange J, Keeney S (2010) Genome destabilization by homologous recombination in the germ line. *Nat Rev Mol Cell Biol* 11: 182–195. doi:10.1038/nrm2849
- Shimada K, Gasser SM (2007) The origin recognition complex functions in sister-chromatid cohesion in *Saccharomyces cerevisiae*. *Cell* 128: 85–99. doi:10.1016/j.cell.2006.11.045
- Subramanian VV, MacQueen AJ, Vader G, Shinohara M, Sanchez A, Borde V, Shinohara A, Hochwagen A (2016) Chromosome synapsis alleviates Mek1-dependent suppression of meiotic DNA repair. *PLoS Biol* 14: e1002369. doi:10.1371/journal.pbio.1002369
- Subramanian VV, Zhu X, Markowitz TE, Vale-Silva LA, San-Segundo PA, Hollingsworth NM, Keeney S, Hochwagen A (2019) Persistent DNA-break potential near telomeres increases initiation of meiotic recombination on short chromosomes. *Nat Commun* 10: 970. doi:10.1038/s41467-019-08875-x
- Suter B, Tong A, Chang M, Yu L, Brown GW, Boone C, Rine J (2004) The origin recognition complex links replication, sister chromatid cohesion and transcriptional silencing in *Saccharomyces cerevisiae*. *Genetics* 167: 579–591. doi:10.1534/genetics.103.024851
- Triolo T, Sternglanz R (1996) Role of interactions between the origin recognition complex and SIR1 in transcriptional silencing. *Nature* 381: 251–253. doi:10.1038/381251a0
- Trowitzsch S, Bieniossek C, Nie Y, Garzoni F, Berger I (2010) New baculovirus expression tools for recombinant protein complex production. *J Struct Biol* 172: 45–54. doi:10.1016/j.jsb.2010.02.010
- Vader G (2015) Pch2(TRIP13): Controlling cell division through regulation of HORMA domains. *Chromosoma* 124: 333–339. doi:10.1007/s00412-015-0516-y
- Vader G, Blitzblau HG, Tame MA, Falk JE, Curtin L, Hochwagen A (2011) Protection of repetitive DNA borders from self-induced meiotic instability. *Nature* 477: 115–119. doi:10.1038/nature10331
- van Hooff JJ, Tromer E, van Wijk LM, Snel B, Kops GJ (2017) Evolutionary dynamics of the kinetochore network in eukaryotes as revealed by comparative genomics. *EMBO Rep* 18: 1559–1571. doi:10.15252/embr.201744102
- Vincenten N, Kuhl LM, Lam I, Oke A, Kerr AR, Hochwagen A, Fung J, Keeney S, Vader G, Marston AL (2015) The kinetochore prevents centromere-proximal crossover recombination during meiosis. *Elife* 4: e100850. doi:10.7554/elife.10850
- Vleugel M, Hoogendoorn E, Snel B, Kops GJ (2012) Evolution and function of the mitotic checkpoint. *Dev Cell* 23: 239–250. doi:10.1016/j.devcel.2012.06.013
- Voelkel-Meiman K, Cheng SY, Parziale M, Morehouse SJ, Feil A, Davies OR, de Muyt A, Borde V, MacQueen AJ (2019) Crossover recombination and synapsis are linked by adjacent regions within the N terminus of the Zip1 synaptonemal complex protein. *PLoS Genet* 15: e1008201. doi:10.1371/journal.pgen.1008201
- Weinreich M, Liang C, Chen HH, Stillman B (2001) Binding of cyclin-dependent kinases to ORC and Cdc6p regulates the chromosome replication cycle. *Proc Natl Acad Sci U S A* 98: 11211–11217. doi:10.1073/pnas.201387198
- Weissmann F, Petzold G, VanderLinden R, Huis In 't Veld PJ, Brown NG, Lampert F, Westermann S, Stark H, Schulman BA, Peters JM (2016) biGBac enables rapid gene assembly for the expression of large multisubunit protein complexes. *Proc Natl Acad Sci U S A* 113: E2564–E2569. doi:10.1073/pnas.1604935113
- Wilde M, Klausberger M, Palmberger D, Ernst W, Grabherr R (2014) Tnao38, high five and Sf9: Evaluation of host-virus interactions in three different insect cell lines: Baculovirus production and recombinant protein expression. *Biotechnol Lett* 36: 743–749. doi:10.1007/s10529-013-1429-6
- Yang N, Xu RM (2013) Structure and function of the BAH domain in chromatin biology. *Crit Rev Biochem Mol Biol* 48: 211–221. doi:10.3109/10409238.2012.742035
- Ye Q, Kim DH, Dereli I, Rosenberg SC, Hagemann G, Herzog F, Toth A, Cleveland DW, Corbett KD (2017) The AAA+ ATPase TRIP13 remodels HORMA domains through N-terminal engagement and unfolding. *EMBO J* 36: 2419–2434. doi:10.15252/embj.201797291
- Ye Q, Rosenberg SC, Moeller A, Speir JA, Su TY, Corbett KD (2015) TRIP13 is a protein-remodeling AAA+ ATPase that catalyzes MAD2 conformation switching. *Elife* 4: e07367. doi:10.7554/elife.07367
- Yeeles JT, Deegan TD, Janska A, Early A, Diffley JF (2015) Regulated eukaryotic DNA replication origin firing with purified proteins. *Nature* 519: 431–435. doi:10.1038/nature14285
- Yuan Z, Riera A, Bai L, Sun J, Nandi S, Spanos C, Chen ZA, Barbon M, Rappsilber J, Stillman B, et al (2017) Structural basis of Mcm2-7 replicative helicase loading by ORC-Cdc6 and Cdt1. *Nat Struct Mol Biol* 24: 316–324. doi:10.1038/nsmb.3372



License: This article is available under a Creative Commons License (Attribution 4.0 International, as described at <https://creativecommons.org/licenses/by/4.0/>).

5. Preliminary results

This chapter contains a summary of the experiments conducted during my doctorate work that could be an important source of information for future experiments. A big part of the experimental work consists of structural studies of Mer3, however, I am also including some of the protein-protein interaction studies as well as some new hints on Mer3 activity.

5.1. Mer3 crystallization attempts

Although we expected that Mer3 crystallization would not be such an impossible task, considering that proteins with similar folds were already crystallized before (Absmeier et al., 2017), none of my crystallization attempts resulted in the formation of diffraction quality crystals that could be measured and result in 3D structure.

For the crystallization, Mer3 constructs purified both from bacteria and insect cells were used (Figure 5.1). I decided to use both expression systems because both have their advantages and disadvantages. The insect cell system might improve the protein folding, however, introduced post-translational modifications may be a heterogeneity source and disrupt crystal formation.

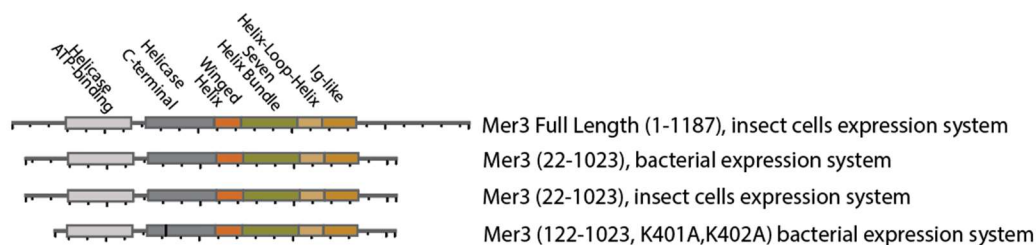


Figure 5.1. Biochemical domain composition of Mer3 constructs used in my experiments

First attempts to crystallize full-length Mer3 resulted only in the formation of precipitate. No signs of crystallization were observed. In further experiments, I have used a slightly shorter construct with a truncated unstructured C-terminal region and partially truncated N-terminal region (22-1023) (Figure 5.1), purified from bacteria and from the insect cells. The N-terminal region of Mer3 is very sensitive to truncations. At that time all shorter constructs that I have tested were not soluble, possibly due to the compromised structure. This time, also the buffer in which the protein was purified was improved based on the results from the Proteoplex screen. Proteoplex is a method, used to optimize the stability, homogeneity, and solubility of protein complexes by the sparse-matrix screening of their thermal unfolding behavior in the

presence of various buffers and small molecules (Chari et al., 2015). In this method, the increase of the unfolding temperature is selected as a stability increase marker. The first performed screen included a variety of buffers. Although none of the buffers drastically increased the stability of the protein, in MES pH 6.5 the temperature was slightly higher, therefore I used it in my further experiments instead of HEPES 7.0 (Figure 5.2A). The second round of the Proteoplex screen that included a variety of possible buffer additives indicated also strong stabilization effects of DNA fragments (Figure 5.2B).

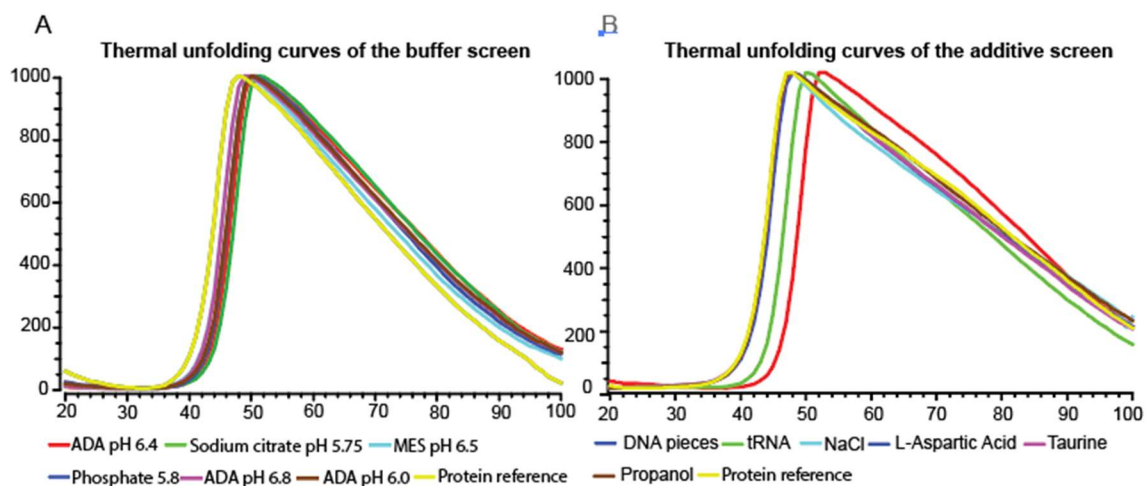


Figure 5.2. Proteoplex screen graphs

The graphs are representing the thermal unfolding curves of the A. Buffer screen and B. additive screen. The higher unfolding temperature indicates the higher stability of the protein in the tested condition.

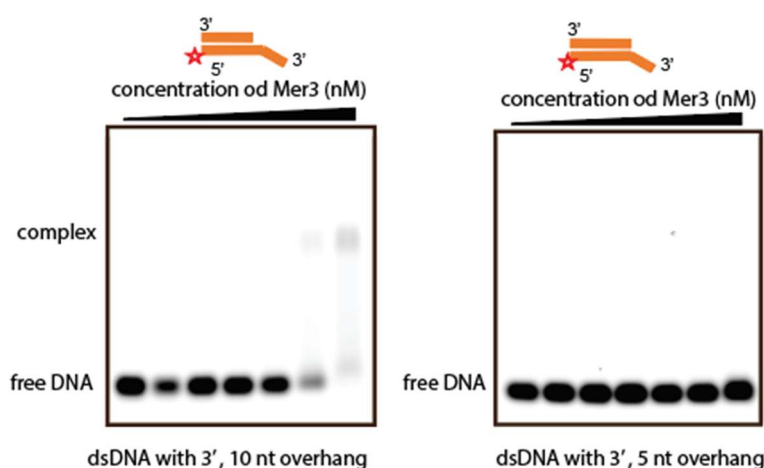


Figure 5.3. Juxtaposition of two EMSA experiments using a 3' overhang as a substrate

The left gel shows binding of the 10 nt long overhang to Mer3, whereas the right gel shows a lack of binding of the 5 nt long overhang.

To optimize the Mer3 construct for crystallization, I used a combination of limited proteolysis and structure prediction tools. This allowed me to remove the unstructured N- and C-terminal regions without disrupting the folded regions. I also introduced two mutations within one of the loops. These actions were intended to increase the structural stability of Mer3. Mer3 (122-1023, K401A, K402A) (Figure 5.1) as the resulting construct was purified and used in crystallization screens, which were performed by Jerome Basquin at the Research Department Structural Cell Biology at Max Planck Institute of Biochemistry, Martinsried. This time in some of the conditions, both with and without DNA addition, we could observe the formation of crystalline-like structures (conditions and images listed in Table 5.1).






				
0.2 M Ammonium chloride, 10 mM MES pH 6.0, 20% PEG 6000, 20 °C	0.2 M Magnesium chloride, 0.1 M MES pH 6.0, 20% PEG 6000, 4 °C	0.1 M Bis-Tris pH 5.5, 1 M Ammonium Sulfate, 4 °C	DNA, 50 mM MES pH 6.0, 0.2 M Lithium Sulfate, 40% PEG 3350, 20 °C	DNA, 50 mM Tris pH 8.0, 0.2 M Magnesium chloride, 30% PEG 3350, 4 °C

Table 5.1. Selected conditions under which the signs of crystallization were observed

Based on the condition's similarities between drops in which I could observe some crystallization, I selected two buffering conditions 50 mM MES pH 6.0 and 50 mM Tris pH 8.0 as well as two precipitation agents (20% PEG 6000 and 30% PEG 3350). In my optimization screens (additives: DNA overhang, ADP; selected buffer variables MES 5.8-6.3 and TRIS 8-8.2; selected precipitant variables: PEG 6000 13-21% or PEG 3350 24-32%) I could observe the formation of some crystalline-like dust, however, no crystals were formed (Figure 5.4A). In another screen, apart from adjusting the crystallization buffer conditions, I decided to test more DNA substrates. One of them was a 7 nt ssDNA, which, as tested, binds to Mer3. Some normally mobile domains might assemble on the DNA, which could stabilize the Mer3 structure in one conformation. Concurrently, the substrate needs to be only long enough to

completely fit inside the protein molecule, thereby not disrupting the crystal lattice formation. Another new substrate was very similar to the previously used overhang, however, it also contained a single nucleotide alanine overhang on the 5' end, which potentially could enable the DNA stacking and help with Mer3 organization in a crystal lattice. The buffer conditions were further adjusted (selected buffer variables MES 5.5-5.7 and TRIS 7.6-8.2; selected precipitant variables: PEG 6000 12-23% or PEG 3350 25-37%). This did not improve crystallization and again gave similar results as in the previous optimization screen. I decided to use the crystalline dust from the previous screen for nucleation source in a so-called "seeding" experiment. The crystalline "dust" was smashed using Seed Beads (Hampton Research) and added to the protein contained drop to help the crystals grow on preexisting microcrystals. I selected constant buffer conditions - MES buffer pH 5.6 and precipitation agent gradient (PEG 6000 19-22%). The seeding stock was serially diluted. This time hanging drops plate was used and instead of the room temperature, which was my standard in previous experiments, I set up the plates at 4 °C. Although I have observed the formation of some crystal-like structures (Figure 5.4B), they were too small to fish and measure. No additive condition changes resulted in crystallization improvement. One of the possible explanations why Mer3 did not crystallize was its ability to dimerize, which we discovered in later experiments. As such, we might have had a mixture of monomers and dimers. Thus, finding a way to stabilize Mer3 in a dimer-only state could increase the sample homogeneity and allow it to crystallize. The fact that Mer3 can dimerize, and as a dimer it is almost 300 kDa large can be used to our advantage - Mer3 is a perfect candidate for structure determination using Cryo-EM. Hence, I have decided to move towards this method to study the structure of Mer3.

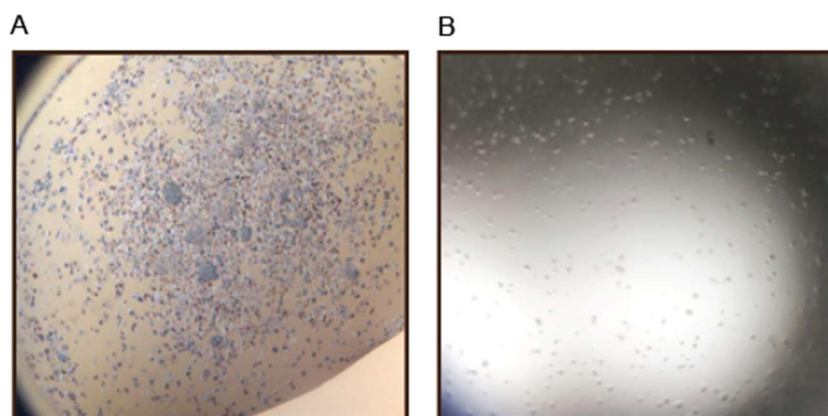


Figure 5.4. Images of best drops from the optimization screens

A. MES buffer pH 5.6, PEG 6000 21%, 20 °C **B.** MES buffer pH 5.6, PEG 6000 21%, seeding, 4 °C

Mer3	Protein concentration and buffer conditions	Additives	Screen
Full length	6.1 mg/ml, Buffer 30 mM HEPES pH 7.0, 1 mM MgCl ₂ , 5% glycerol, 300 mM NaCl, 1 mM TCEP	none	Classics Classics II PEGs PEGs II Morpheus JCSG+
22-1023 <i>E. coli</i> purified	4.7 mg/ml, Buffer 30 mM MES pH 6.5, 1 mM MgCl ₂ , 5% glycerol, 300 mM NaCl, 1 mM TCEP	15 nt dsDNA with a 10 nt ssDNA overhang and ADP in the molar ratio 1:1.2:1.5 (Mer3:DNA:ADP)	Classics Classics II PEGs PEGs II Morpheus
22-1023 <i>E. coli</i> purified	4.7 mg/ml, Buffer 30 mM MES pH 6.5, 1 mM MgCl ₂ , 5% glycerol, 300 mM NaCl, 1 mM TCEP	15 nt dsDNA with a 10 nt ssDNA overhang and AMPpNp in the molar ratio 1:1.2:1.5 (Mer3:DNA:AMPpNp)	Classics Classics II PEGs PEGs II Morpheus
22-1023 Insect cells purified	8.5 mg/ml, Buffer 30 mM MES pH 6.5, 1 mM MgCl ₂ , 5% glycerol, 300 mM NaCl, 1 mM TCEP	15 nt dsDNA with a 10 nt ssDNA overhang and ADP in the molar ratio 1:1.2:1.5 (Mer3:DNA:ADP)	Classics Classics II PEGs PEGs II Morpheus JCSG+ PACT

Table 5.2. List of tested crystallization conditions including protein constructs, buffer conditions, additives, and screen names.

5.2. Mer3 Cryo-EM studies

Given numerous possibilities brought by the in-house CryoEM microscope facility, I decided to use this method to study the structure of Mer3. Using Cryo-EM allows to ask more complex and courageous questions than crystallization experiments. Since here we are not limited by sample homogeneity, we could attempt imaging Mer3 bound to more complex substrates (D-loop) and plan future experiments to image not only Mer3 alone but also as a complex with other proteins. Knowing already that Mer3 may dimerize Cryo-EM also could help to group

the particles and separate monomers from dimers (or the Mer3-DNA complex from free protein molecules). Another advantage of using Cryo-EM is that the presence of unstructured regions does not impede the experiment. Knowing that the unstructured regions of Mer3 seem to be important for protein dimerization using Cryo-EM could help us understand how they participate in the dimerization.

First, I attempted to visualize the unmodified protein, without any additives using the Mer3(22-1023) construct, purified from bacteria (Figure 5.1). In this case, however, the protein was always aggregated. Since the previous Proteoplex screen indicated the stabilizing effects of DNA binding, I decided to bind Mer3 to the DNA and visualize the DNA-protein complex. As a DNA substrate, I used two different substrates: 3'overhang and D-loop. Unlike in crystallization, the size and flexibility of the DNA are not limiting factors. The Mer3-DNA complex was size-exclusion purified, therefore the molar quantities of the protein and DNA should be comparable. Surprisingly, on the grids, I could only see the DNA and some very small protein particles that were most probably "ruptured" pieces of Mer3 (Figure 5.5A). To further stabilize the protein, I used BS3 (an amine-to-amine crosslinker with a spacer arm length of 11.4 Å) after Mer3 was bound to the DNA. Although I could see some improvement (Figure 5.5B), most of the protein was still damaged. In my next experiment, I used a different construct (Mer3(122-1023)-K401A, K402A) and changed the crosslinking method. This time I crosslinked Mer3 bound to the DNA using glutaraldehyde. To assure high quality of crosslinking, I attempted to mildly crosslink the sample using the gradient fixation (GraFix) method (Stark, 2010). As a crosslinker, I used glutaraldehyde, which can link both proteins and DNA, thus stabilize the Mer3-DNA complex (glycerol gradient 5-25%, max. glutaraldehyde concentration 0.02%). Such sample, however, was strongly compromised and aggregated (possibly over-crosslinked). In another attempt, I increased the glycerol gradient density (glycerol gradient 10-30%, max. glutaraldehyde concentration 0.02%). This time protein molecules visible on the grids looked much better, I could see many C-shaped particles (Figure 5.6D), although this time the DNA disappeared. I decided to collect a small data set to generate 2D classes and see if the protein is structured (Figure 5.6A). It seems that during freezing many particles lost their primary 3D structure (many elongated classes, many different protein shapes). Also, the crosslinking captured many dimeric particles of Mer3 (see: Chapter 2, Supplementary Figure 2.2C). It seemed that despite the expected stabilizing effect of DNA in solution, freezing Mer3 in complex with DNA rather disturbs than helps to stabilize Mer3 on

the grid. Thus, I decided to repeat a simple grid preparation using full-length Mer3 purified from insect cells. Protein was purified only on affinity columns (StrepTactin column + Heparin column) with the omission of size-exclusion, which based on my observations has a negative effect on the protein stability while freezing. I also excluded the freezing step after purification. This time protein molecules on the grids appeared intact. Collected 2D classes from this screen looked better than the previous ones, however, still it seems that the freezing conditions of the Cryo-grids have a negative impact on the stability of Mer3. For this reason, particles collected from the grid could not be used for the 3D reconstruction (Figure 5.6B). To improve the freezing, one of the possible approaches is to add some detergents to the sample. I used octyl glucoside as well as different detergents offered with the Cryo-EM VitroEase™ Buffer Screening Kit. Despite using much higher protein concentration and low detergent concentration, all grids looked empty.

Although I was not able to collect any high-quality images, I believe that with more attempts it could be possible to visualize Mer3 using Cryo-EM and determine the 3D structure. My suggestions for future experiments are the following:

- To achieve higher sample quality, purified Mer3 should not be aliquoted and flash frozen.
- It is important to use the SEC buffer without glycerol. The presence of glycerol drastically reduces image resolution, which is crucial considering that Mer3 is a small protein for Cryo-EM standards. If it forms a dimer, it would be as big as 270 kDa, however, on the grids, I could only observe monomers. This might be a side effect of freezing since the used sample is at the concentration at which Mer3 already dimerizes. Crosslinking preserves dimerization during the freezing process.
- Mer3 purification in low salt and without glycerol often results in a much lower yield than usual (purifying Mer3 in 100 mM NaCl results in up to 10 times lower yield than when purified in 300 mM NaCl).

For future experiments, one of the yet untested sample treatment conditions is crosslinking Mer3 without any DNA before purifying it on size-exclusion to obtain a more homogeneous sample. This could be followed by concentrating the protein to much higher concentrations, which could allow testing again different detergents. I would also recommend trying lower detergent concentrations. What must be kept in mind is that some fraction of Mer3 forms dimers, hence it will be important to keep track of the crosslinked protein size by using mass

photometry. Another important aspect to consider is that so far, the presence of DNA had a very strange effect on the sample. Instead of structured molecules, I could only observe small protein fragments (black dots). It could imply that the presence of DNA for a yet unknown reason destabilizes the protein. If future attempts to freeze Mer3 with the DNA will also be unsuccessful, the alternative solution to structurally study Mer3-DNA complex could be rotary shadowing using electron microscopy. The resolution of images obtained by rotary shadowing is very low. Data obtained by using this method can rather be used as a guideline to how the protein binds to the DNA than to solve the structure. This however, coupled with CryoEM data, could be enough to study DNA binding by Mer3. After collecting a high-quality dataset, solving the structure should be possible with the help of our high-quality AlphaFold2 model. This in turn would enable further work on the Mer3 model in a complex with other proteins. Learning about the interaction surfaces between Mer3 and other proteins would allow us to design separation of function mutants of Mer3. A Mer3 mutant that does not interact with Top3/Rmi1 could be used to study the role of this interaction *in vivo*.

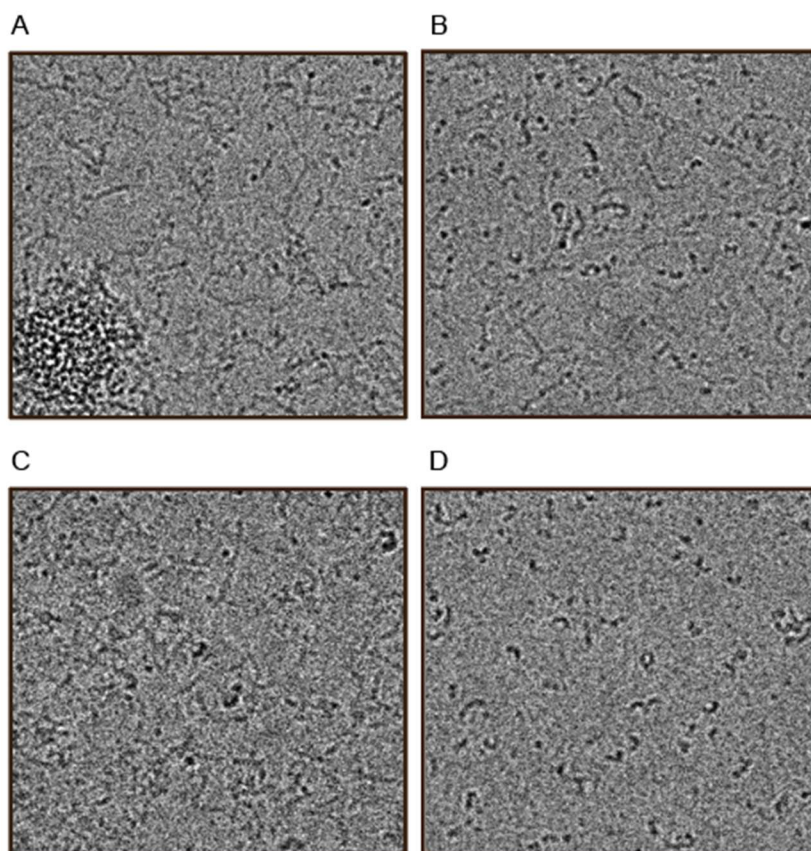


Figure 5.5. Mer3 Cryo-EM images taken on grids frozen in selected conditions

All samples were applied on glow discharged (PELCO easiGlow, TED Paella) copper grids (Quantifoil R1.2/1.3 100 Holey Carbon, Cu 300 mesh, Quantifoil) and blotted using Vitrobot (FEI, Thermo Scientific)

Mer3	Concentration and buffer conditions	Additives	Blotting conditions	Result
511	1.2 mg/ml, 0.8 mg/ml, 0.6 mg/ml Buffer: 30 mM MES pH 6.5, 1 mM MgCl ₂ , 200 mM NaCl, 1 mM TCEP	DNA overhang	100% humidity 4 °C, 3 µl sample, 4 s waiting time, 5 s blotting time, -1 blot force	Mostly protein aggregates and DNA fragments
511	2.3 mg/ml, 1.15 mg/ml, 0.5 mg/ml Buffer: 30 mM MES pH 6.5, 1 mM MgCl ₂ , 200 mM NaCl, 1 mM TCEP	D-loop	100% humidity, 4 °C, 3 µl and 4 µl sample, 5 s blotting time, -1 blot force	Mostly protein aggregates and DNA fragments (Figure 5.5A)
511	10 mg/ml, 2 mg/ml, 1 mg/ml Buffer: 30 mM MES pH 6.5, 1 mM MgCl ₂ , 200 mM NaCl, 1 mM TCEP	D-loop+ BS3	80% humidity, 20 °C, 4 µl sample, 5 s blotting time, -1 blot force	Fewer aggregates, some protein molecules not broken, still excess of the DNA (Figure 5.5B)
1111	5 mg/ml, 3.75 mg/ml, 2.5 mg/ml, 1.6 mg/ml Buffer: 30 mM MES pH 6.5, 1 mM MgCl ₂ , 200 mM NaCl, 1 mM TCEP	D-loop+ glutaraldehyde (crosslinking in glycerol gradient 5-25%, max glutaraldehyde concentration 0.02%)	90% humidity, 4 °C, 5 µl and 4 µl sample, 3.5 s blotting time, -3 blot force	Very little protein molecules compared to the DNA molecules, many aggregates (Figure 5.5C)

Mer3	Concentration and buffer conditions	Additives	Blotting conditions	Result
1111	3.75 mg/ml, 1.75 mg/ml, 1 mg/ml, 0.5 mg/ml, Buffer: 30 mM MES pH 6.5, 1 mM MgCl ₂ , 200 mM NaCl, 1 mM TCEP	D-loop+ glutaraldehyde (crosslinking in glycerol gradient 10-30%, max glutaraldehyde concentration 0.02%)	100% humidity, 4 °C, 4 µl sample, 2.5 s blotting time, -3 blot force	Much less DNA, protein molecules seem to be complete; small data set was collected (Figure 5.6A). Many molecules were crosslinked as dimers, but DNA wasn't bound. Possibly impossible to crosslink DNA to Mer3 without it getting damaged during the freezing process. (Figure 5.5D)
413	0.2 mg/ml Purified heparin only Buffer: 30 mM MES pH 6.5, 1 mM MgCl ₂ , 200 mM NaCl, 1 mM TCEP	none	100% humidity, 4 °C, 4 µl sample, 2.5 s blotting time, -1 blot force	Molecules looked good, small dataset collected (Figure 5.6B)
413	1.7 mg/ml, 0.85 mg/ml, 0.43 mg/ml, 0.21 mg/ml Purified heparin only Buffer: 30 mM MES pH 6.5, 1 mM MgCl ₂ , 200 mM NaCl, 1 mM TCEP	(0.1%) octyl glucoside	100% humidity, 4 °C, 4 µl sample, 5 s blotting time, -1 blot force	No protein molecules visible
413	1.7 mg/ml Purified on heparin only Buffer: 30 mM MES pH 6.5, 1 mM MgCl ₂ , 200 mM NaCl, 1 mM TCEP	0.04% CTAB 0.7% CHAPS 0.05% FOM 0.007% Tween-20™ 0.2% β-OG 0.25% DM	100% humidity, 4 °C, 4 µl sample, 5 s blotting time, -1 blot force	No protein molecules visible

Table 5.3. List of tested conditions including protein constructs, buffer conditions, additives, and blotting conditions



Figure 5.6. Mer3 class averages

5.3. Mer3 interacts not only with the Top3/Rmi1 and the Mlh1/Mlh2 complex but also with Dmc1

In Chapter 2, I have included the analysis of Mer3 interaction with the Top3/Rmi1 complex as well as with the Mlh1/Mlh2 complex. In the discussion (Chapter 2.3), I'm also mentioning that one of the protein factors recruiting Mer3 to the axis might be one of the meiotic recombinases Rad51 or Dmc1. Veronika Altmannová has detected a direct interaction between Mer3 and Dmc1 using an *in vitro* pull-down assay and the meiotic IP-MS. Zip1 could be another interaction partner of Mer3. It was detected in our meiotic IP-MS, in which the Zip1 protein was detected together with the Mer3 protein. Zip1 is a synaptonemal complex protein required for meiotic chromosome synapsis (Sym et al., 1993).

I was curious if any of these protein-protein relations are compatible with my previously described interactions and if Dmc1 and/or Zip1 might interact with the Mer3/Top3/Rmi1/Mlh1/Mlh2 complex. It could not be tested by conducting an *in vitro* pull-

down because of the overlapping fusion tags (I could not select any affinity beads). Although the formation of a size-exclusion stable complex between Mer3 and the Mlh1/Mlh2 complex as well as between Mer3 and the Top3/Rmi1 complex could not be observed, I decided to test the interaction in the presence of Dmc1 and Zip1(1-348) (Zip1 N-terminal fragment was the only one that could be purified in high quantity). If these two proteins interact with the complex, we should see a shift on size-exclusion. When we look at the chromatograms only and compare the profiles of proteins run separately and together, we do not see much difference between the chromatograms of proteins run separately and overlapping chromatograms of the proteins mixed all together. When we look at the gels, we can see that Dmc1 (Figure 5.7D, blue) was eluted basically in all elution fractions, which is not very surprising since Dmc1 can form multimers. As a result, we wouldn't be able to see a shift if it interacts with other proteins (it also elutes in all fractions while run with other proteins, Figure 5.7D, black). However, after analyzing the gels from other proteins we can see that Mer3 (Figure 5.7A, orange), Mlh1/Mlh2 (Figure 5.7C, yellow), and Top3 (Figure 5.7B.1, grey) eluted much earlier than when they are run alone compared to when they run all together (Figure 5.7A, B.1, C, black). Interestingly we could not observe any shift in the case of the Rmi1 protein (Figure 5.7B.1, grey vs black). Also, no change in the elution profile of Zip1(1-348) was detected (Figure 5.7E, green vs black), indicating that Zip1 most likely doesn't interact with any of the selected proteins (or at least the purified fragment 1-348 does not).

This experiment directs us towards the further investigation of the role of Dmc1 in recruiting Mer3 to the axis as well as in mediating its interaction with Top3/Rmi1 and Mlh1/Mlh2. Since the experiment was conducted only once, we cannot conclude much from it. Nevertheless, it is worth remembering that Dmc1 might be one of the stabilizing factors in Mer3's functionality and interaction with other proteins.

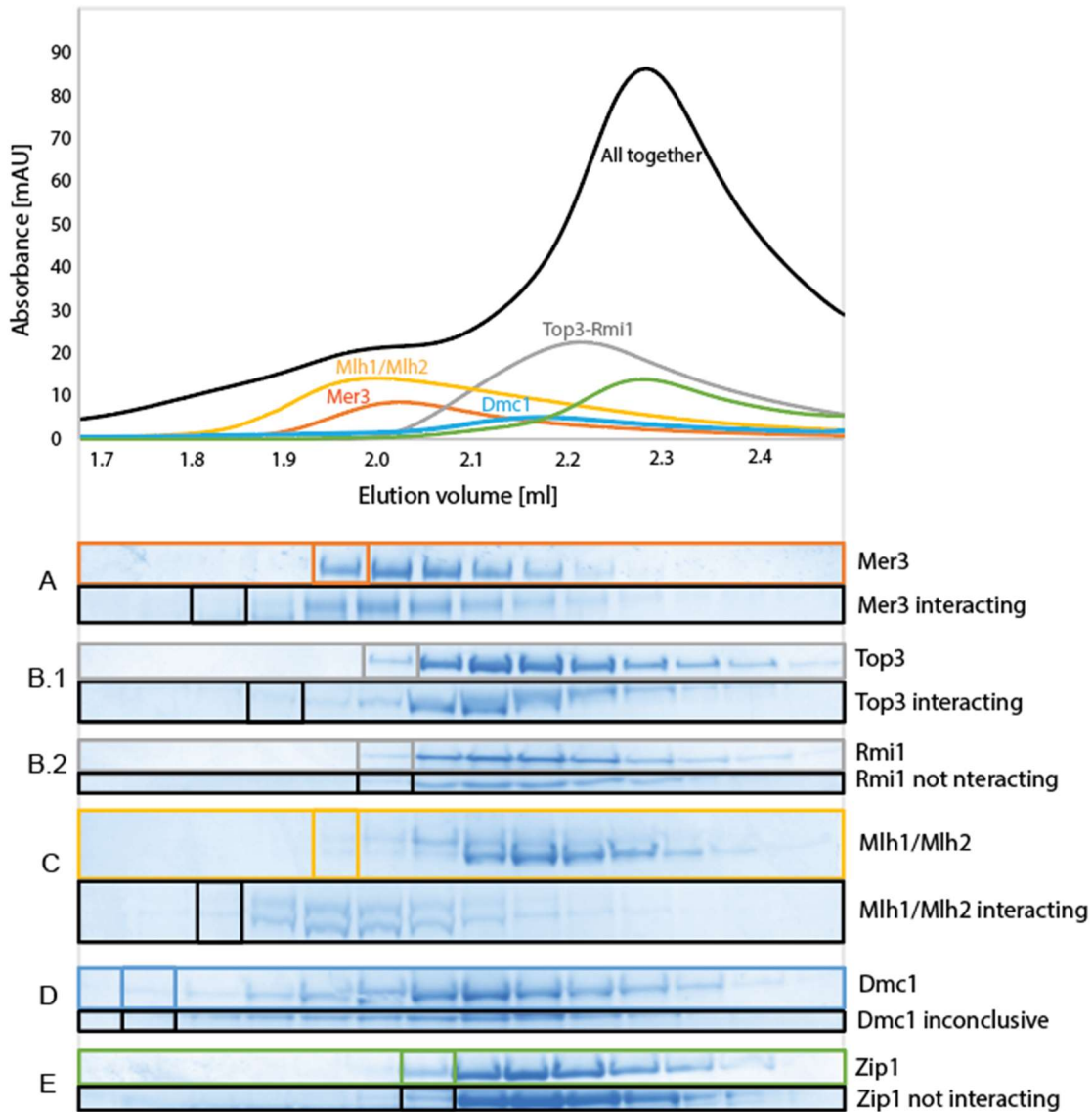


Figure 5.7. Mer3/Top2/Rmi1/Mlh1/Mlh1/Dmc1/Zip1 in vitro interaction experiments

Analytical size-exclusion chromatography (SEC). Analytical SEC was performed using Superose 6 5/150 GL column (GE Healthcare) in a buffer containing 30 mM HEPES pH 6.8, 150 mM NaCl, 5% glycerol, 1 mM TCEP, 1 mM MgCl₂. Protein elution was monitored at 280 nm. Fractions were subsequently analyzed by SDS-PAGE and Blauer Jonas staining. To detect complex formation, proteins were mixed at 5 μ M concentration in 50 μ L and incubated on ice for over night prior to SEC analysis.

The top chromatogram represents SEC profiles of each protein (protein complexes) alone and all proteins mixed. SDS-PAGE gels below contain identical fractions from the SEC purification for every protein alone as well as the gel fragment corresponding to the protein run on SEC together with other proteins. In each case, the top gel fragment corresponds to the single protein run and the bottom gel fragment corresponds to the protein run with other proteins.

5.4. Mer3 activity on DNA-RNA hybrids

Another experimental branch that was not extensively studied is the activity of Mer3 on alternative substrates other than DNA. Mer3 helicase is structurally very similar to many other Ski2-like helicases (Brr2, Hel308), some of which are RNA helicases (Brr2, Slh1) (Absmeier et al., 2017; Pena et al., 2009). Multiple independent studies have shown that RNA-DNA hybrids function as transient intermediates during double-strand break repair. DNA-RNA hybrids may facilitate DSB repair by providing RNA as a template, recruiting recombination factors, or regulating DSB ends resection (D'Alessandro et al., 2018; Keskin et al., 2014; Lu et al., 2018; Mazina et al., 2017; Ohle et al., 2016; Yasuhara et al., 2018). Although the function of DNA-RNA hybrids was less explored in meiosis, the recent study (Yang et al., 2021) suggests that meiotic RNA-DNA hybrids play an active role in efficient homologous recombination. Mer3 helicase could potentially be involved in the process of removing the RNA from the DNA strand, thus preventing its accumulation on the recombination sites. Importantly, the same study has shown that in the absence of Dmc1 (meiosis-specific DNA recombinase, which according to our data interacts with Mer3) DNA-RNA hybrids accumulate.

In my preliminary experiments, I have discovered that Mer3 not only binds DNA-RNA hybrids, but can also unwind them (Figure 5.8), although the unwinding activity on DNA-RNA hybrids is lower than the unwinding activity on DNA-DNA hybrids. In my experiments, I used the DNA-RNA hybrid in which the overhang was DNA based, and the shorter strand was RNA based. It would be interesting to see if the helicase and binding activity of Mer3 would be different if the overhang strand was RNA made. Another possible experiment would be to compare the activity of other helicases to see if Mer3's activity on the DNA-RNA hybrids is Mer3-specific. If yes, finding a mutant that unwinds dsDNA but not DNA-RNA and studying mutation's effect *in vitro* could give us some insight into the role of Mer3 and DNA-RNA hybrids in meiosis. It would be interesting to see whether Mer3 and DNA-RNA hybrids colocalize and if the absence of Mer3 impacts the abundance of the hybrids (RNA-DNA hybrids can be specifically detected by the S9.6 antibody (Boguslawski et al., 1986)). Future experiments including single-molecule studies would be required, in order to compare the processivity of Mer3 on dsDNA and DNA-RNA hybrids. The scope of such experiments would potentially help to uncover the new role of Mer3 helicase in meiotic recombination.

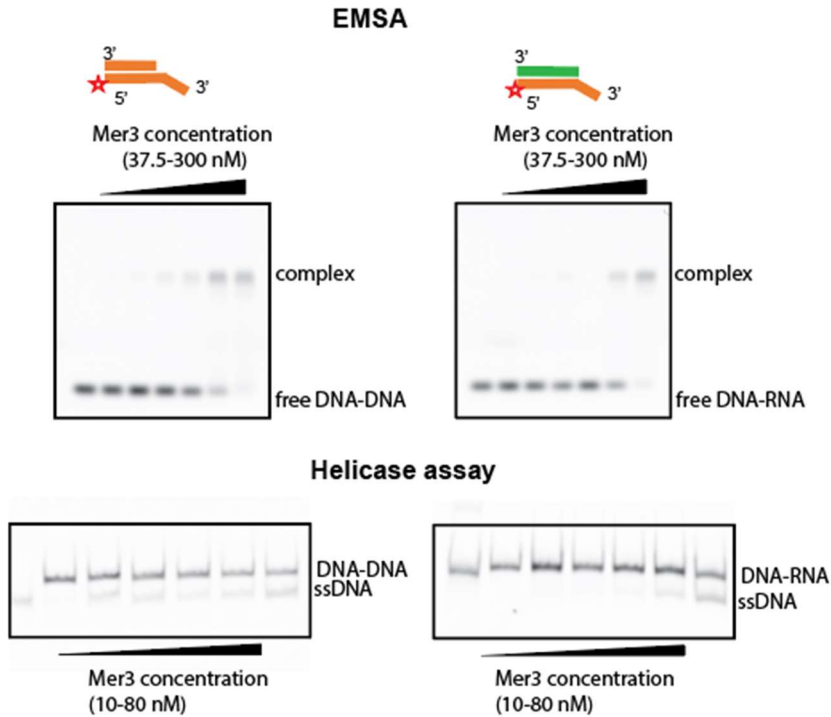


Figure 5.8. Biochemical activity of Mer3 on DNA-DNA and DNA-RNA hybrids
 Top panel: EMSAs comparing Mer3 DNA binding ability. Bottom panel: strand displacement assay comparing the ability to unwind DNA-DNA and DNA-RNA hybrids.

5.5. Zip2/Zip4/Spo16 complex interacts with Msh4/Msh5 complex

Despite Mer3 helicase being my main experimental focus, I also engaged myself in searching for interactions between other proteins involved in the meiotic recombination regulation. One of the reported interactions *in vivo* was the interaction between Msh4/Msh5, a complex that stabilizes dHJs (Snowden et al., 2004), and the ZYS complex (Zip2, Zip4, and Spo16). The ZYS complex has less well-defined functions, but is known to be required for crossover formation and may direct recombination intermediates towards crossovers (de Muyt et al., 2018). Physical interaction between Msh5 and Zip4 was detected in a yeast two-hybrid assay. It was proposed that the interaction between Msh4/Msh5 and ZYS complex may coordinate the activities of the Zip2-Zip4-Spo16 and Msh4-Msh5 complexes on the branched DNA structure to convert D-loops into highly stable recombination intermediates.

In my experiments, I investigated this possible interaction by *in vitro* pull-down assay using the purified Msh4/Msh5 complex as well as the purified ZYS complex. I have observed Msh4/5 forming a complex with the ZYS complex and the interaction seemed to be ATP independent (Figure 5.9).

This interaction, similarly to the starting point of my Mer3 interaction with Mlh1/Mlh2, was not yet extensively studied *in vitro* and could potentially be a good target for structural studies as well as a good base for building even bigger protein complexes. It is expected that Zip4 facilitates multiple protein-protein interactions, however, the role of the ZZS complex is not yet fully understood and taking a similar experimental path to the one I took for Mer3 interaction with Mlh1/Mlh2 could again result in broadening our understanding of the meiotic recombination machinery.

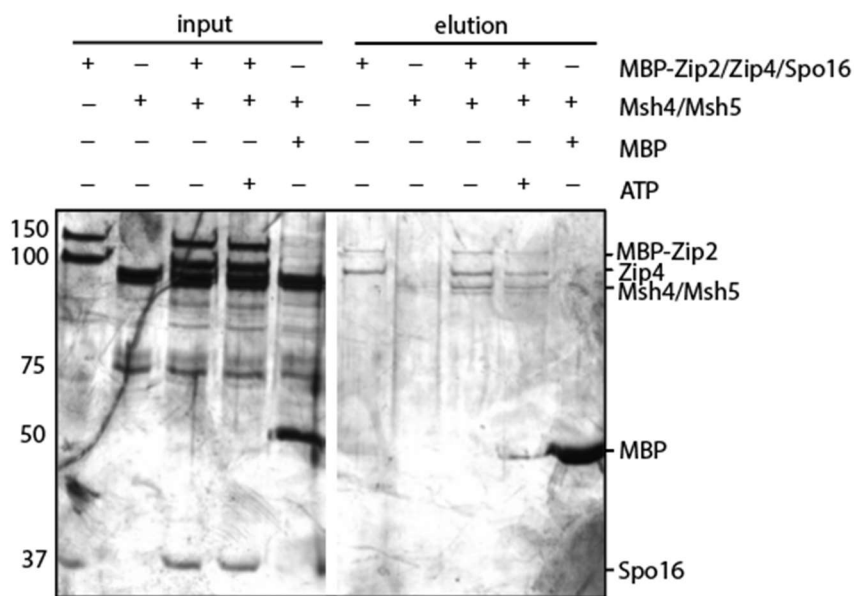


Figure 5.9. *In vitro* pull-down of Msh4/Msh5 complex on ZZS complex
Msh4/Msh5 complex was pulled on the ZZS complex bound to the amylose beads. Silver stained SDS-PAGE gel.

6. Outlook

Presented Chapter 2 and Chapter 4 include the results of my experiments that are part of paper manuscripts. Chapter 3 contained my review paper, and Chapter 5 consisted of the summary of the additional preliminary results. Thematically, my results are not directly connected, therefore they were discussed independently within each chapter. However, all of my studies share a common ground, since they were focused on proteins involved in the regulation and execution of processes that take place during the first meiotic division, especially during homologous recombination.

6.1. The importance of the future structural studies of the Mer3 helicase

One of the key parts of my project was to determine the 3D structure of Mer3. The experimental approach, which included crystallization and Cryo-EM did not result in structure determination. The computational structure provided by AlphaFold2 structure prediction did indeed predict with high confidence the structure of all Mer3 domains, however, it could not predict the structure of the unstructured N and C terminal regions and how they are oriented or interact with the structured “core”. Based on the SEC-MALS and yeast two-hybrid experiments, we know that Mer3 can dimerize and that the unstructured regions are required for the dimerization. Obtaining the experimental structural data could help us to understand how Mer3 dimerizes and provide insights as to what role that plays in the function of Mer3 in meiosis.

Another important aspect of structural studies involves imaging the protein complexes, especially the Mer3/Top3/Rmi1 complex.

Better structural knowledge about the interaction between Mer3 and Top3/Rmi1 could enable us to design a non-interacting separation-of-function Mer3 mutant that can be further characterized *in vivo*. This would help us to better understand the biological significance of Mer3 interaction with the Top3/Rmi1 complex. We designed and purified noninteracting Mer3 mutants based on the surface sequence conservation. Some of these mutations resulted in a complete loss of protein stability. The remaining mutants that were stable and showed decreased ability to interact with the Top3/Rmi1 complex also partially lost their helicase activity and therefore were not suitable for separation-of-function experiments.

Finding a fully active mutant that is defective only in Top3-Rmi1 interaction would allow us to study the *in vivo* effect that the lack of Mer3 interaction with Top3/Rmi1 has on crossover formation and spore viability in yeast cells, and potentially also in other organisms.

6.2. Role of the zinc finger

Mer3 has a predicted C4-type zinc finger (characterized by 4 cysteine residues coordinating zinc) within the unstructured C-terminal region, which is conserved among the other Mer3 homologs. Despite our extensive studies, its function remains unknown. Our experiments show that it is not required for the ability to bind or unwind DNA (unpresented data). Also, up to date, the zinc finger did not show to be relevant in any of the known interactions with other proteins. Since many zinc fingers help to direct the protein to the specific DNA sequence, it may help Mer3 to localize in specific chromosome locations. However, until now, there is no data available to support this hypothesis. To test the role of the zinc finger we could study the influence of Mer3 Δ Zn *in vivo*. Even if it does not show any strong phenotype (e.g. decrease in spore viability) it could influence Mer3's interactome. Also, more extensive *in vitro* studies could be very informative (e.g. single-molecule experiments).

6.3. Mer3 - playing solo or in a duet?

Although it was suggested that Mer3 may be forming oligomers (Nakagawa et al., 2001), there was no experimental data that would support this hypothesis. Our experiments have shown that Mer3 helicase does indeed dimerize (SEC-MALS, XL-MS, XL-MS coupled with the mass photometry, yeast two-hybrid assay, crosslinking coupled with Cryo-EM).

It is not very surprising that Mer3 can form dimers considering its homology to the Brr2 helicase. The Brr2 helicase is a Ski2-like helicase, which provides the key remodeling activity during spliceosome activation. Although the Brr2 helicase is a single polypeptide that consists of two cassettes that originated from gene duplication (Pena et al., 2009), it is possible that Mer3 also acts in a double-helicase mode as a homodimer. Only the N-terminal cassette of Brr2 shows helicase activity, whereas the C-terminal cassette most probably shows no significant enzymatic activity and may function as a protein-protein interaction platform (Liu et al., 2006; van Nues & Beggs, 2001). The natural question would be whether in the case of the Mer3 dimer both dimer subunits bind DNA and if both hydrolyze ATP or rather, as in the case of the Brr2, one of the subunits is fully dedicated to interactions with other proteins.

The most burning question is in which state - monomeric or dimeric - Mer3 functions during meiosis, especially while it interacts with other proteins. One of the possible scenarios is that Mer3 only interacts in either a dimeric or monomeric state. The monomer-dimer transition could be regulated by e.g. phosphorylation. Depending on the phosphorylation state, Mer3 could form a monomer or a dimer, thus regulating the interaction of Mer3 with other proteins. It is also possible that while dimerizing, Mer3 enables other proteins to dimerize or form a complex.

Since our results indicated that Mer3 forms dimers, we wondered how this fits with the interaction with Top3/Rmi1. Recent studies have shown that the stoichiometry of the BLM-TOPIIIa-RMI1/2 complex is 2:2:2 (Hodson et al., 2022). Therefore, it is possible that in yeast Mer3 dimer also forms a similar complex while binding to Top3/Rmi1. To study the stoichiometry of the Mer3/Top3/Rmi1 complex (knowing that the interaction is relatively weak or driven by specific post-translational modifications), the future experiments will most likely need to be coupled with crosslinking. Using SEC-MALS or Cryo-EM might help to reveal the complex organization. Furthermore, the improvement of the Mer3 dimer structure prediction using the AlphaFold2 should help to predict the model structure of the Mer3/Top3/Rmi1 complex.

6.4. What about the “helicase” part in the Mer3 helicase

Another remaining enigma is the activity of Mer3. Mer3's ability to hydrolyze ATP and unwind DNA, or rather the fact that these activities play a very minor role in the functionality of the protein remains one of the biggest concerns when it comes to the role of Mer3. The helicase-dead mutant has a relatively mild effect on crossover formation and sporulation compared to the mer3 Δ . The enzymatic activity-deficient mutant shows only mild spore viability defects (Nakagawa & Kolodner, 2002).

The diversity of functions that can be carried by enzymes possessing helicase activity is not limited to the ability to unwind the DNA strand. We still know too little about the activity of Mer3 to tell which of the functions the helicase activity of Mer3 has. It may be one of the helicases that translocate along with the DNA and mediate or disrupt the protein-protein interactions. It would be interesting to study the effect of Mer3-interacting partners on Mer3 processivity and general activity on the DNA strand. To do that, a single-molecule experiment using for example magnetic tweezers will be needed. Understanding the role of the conserved

ATPase and helicase activity in Mer3 could help us understand the dynamics of Mer3 during crossover formation and the changes after Mer3 is post-translationally modified, dimerizes, or interacts with other proteins.

6.5. The role of phosphorylation in mediating protein-protein interaction

Although we have established that Mer3 can limit the anti-crossover activity of the Sgs1/Top3/Rmi1 complex in meiotic recombination by competing with Sgs1 for the same binding site and forming the complex with Top3/Rmi1, there are still many questions that arise after the discovery:

- Which processes are required for the interaction to be established? Do the post-translational modifications play any role there?
- Which conditions are required for Mer3 to recognize the Top3/Rmi1 complex?
- Which mechanisms are responsible for the removal of Mer3 from the complex so that the Top3/Rmi1/Sgs1 complex can be reestablished? We know that STR complex activity is required at the late stages of meiosis to remove incorrectly connected and tangled DNA.

One of the possible regulation mechanisms triggering the interaction could be phosphorylation. When only some of the Sgs1 molecules get phosphorylated and thereby the affinity to Top3/Rmi1 weakens, only these molecules can be outcompeted by Mer3. This could be one of the regulation mechanisms in the decision-making process whether a break will be repaired as a crossover or not. Similarly, in later recombination stages, Mer3 could be phosphorylated, and thereby the affinity to Top3/Rmi1 could be weakened. This could enable secondary binding of Sgs1 instead of Mer3, STR complex reassembly and reintroduction of complex activity, which is required for the later stages of meiotic recombination. This could be studied by using phosphomimic mutants of Mer3 and Sgs1 to analyze the affinity changes within the complexes.

6.6. Partners or competitors? – the cooperativity of Mer3 binding to Mlh1/Mlh2 and Top3/Rmi1 complexes

Another part of my project that will require more extensive studies is the nature of the interactions between Mer3, Mlh1/Mlh2, and Top3/Rmi1. Our data suggest that the

simultaneous Mer3 interaction with Top3/Rmi1 and Mlh1/Mlh2 is cooperative, however, the crosslinking data also indicates an overlapping interaction surface. One possible way to study the cooperativity of the binding is to use the SPR (surface plasmon resonance) to check if binding one of the interaction partners still allows the other interaction partner to bind. It would be important to study whether the binding order influences the binding affinity and kinetics. This information could also be insightful when it comes to the prediction of the binding order *in vivo*, which in turn could shed light on the sequence of events that need to take place while making the decision whether the strand invasion intermediate will be directed towards crossover formation or not.

6.7. Other ZMM proteins as potential players in protecting the crossover intermediate from the STR activity

After establishing that both Mer3 and Mlh1/Mlh2 interact with Top3/Rmi1, a natural order would be to check if other ZMM proteins also interact with Top3/Rmi1 or with the Sgs1 helicase. It has been shown that Mer3 localization on chromosomes depends on the location of Zip4 and Msh4 (Pyatnitskaya et al., 2019; Shen et al., 2012), but they don't seem to be interacting directly. One of the possibilities is that the interaction is bridged by the Top3/Rmi1 complex. Also, other ZMM proteins were proven to be critical for promoting crossover formation instead of D-loop dissolution (Pyatnitskaya et al., 2019). Some of them may also be involved in the same interaction network as Mer3. This needs to be tested using e.g. yeast two-hybrid assay and *in vitro* pull-down to detect possible interaction and in case of success add it to the already existing network (Mer3/Top3/Rmi1/Mlh1/Mlh2) to check if the interactions are competitive or cooperative and what effect it causes (*in vivo* and *in vitro*).

6.8. The conservation of the Mer3/Top3/Rmi1 interaction in mammals

According to the results of the yeast two-hybrid experiment presented in Chapter 2 (Supplementary Figure 2.4B), HFM1 (human homolog of Mer3) does not interact with TOP3 α (human homolog of Top3). Although there is a possibility that the interactions between the proteins are yeast-specific, the level of conservation between Mer3 and HFM1 (yeast Mer3 shares 29.8% sequence identity with its human homolog HFM1) and other proteins involved increases the possibility that the mechanism is conserved also in other organisms. One of the

possible explanations is simply that in the yeast two-hybrid setup proteins might not obtain the post-translational modifications that are required for the interaction in the mammalian system. In mammals, the TOP3 α (mammalian homolog of Top3) in complex with the BLM helicase interacts not only with RMI1 but also RMI2. It is possible that without RMI2 the interaction cannot be established. This will need to be further studied, optimally using mammalian cell line or purified mammalian proteins TOP3 α , RMI1, RMI2, BLM, and HFM1.

6.9. The importance of understanding the mechanisms in the context of fertility and cancer

To this date, mutations in the HFM1 gene have mostly been linked to two meiosis-related fertility disorders: premature ovarian failure 9 (J. Wang et al., 2014a, 2014b) and non-obstructive Azoospermia (D. Tang et al., 2021; Xie et al., 2022).

HFM1 is a meiosis-specific protein, which in normal conditions is not expressed in somatic cells. However, an undesirable expression of HFM1 during a normal cell cycle could potentially have catastrophic effects. There is now emerging evidence supporting the concept that activation of meiosis-specific genes involved in homologous recombination template selection, DSB formation, and repair in somatic cells may result in disruption of the mechanisms controlling chromosome maintenance and segregation (McFarlane et al., 2014, 2015).

If aberrantly expressed in somatic cells, human HFM1 could block the activity of the BLM helicase or potentially other RecQ helicases (mammals have more than one RecQ homolog). This could trigger DSB repair using homologous chromosome as a template, which in turn could result in loss of heterozygosity and potentially cause cell malignancy and cancer development.

7. Concluding remarks

To summarize my work and the results obtained during almost 5 years of my research, the biggest success was the discovery of novel interaction partners of Mer3 and a primary understanding of the potential roles of the discovered interactions. Although at the early stages of the project it did not seem that any of the possible partners will interact, we finally found what we were looking for: a novel interaction of Mer3 with Top3/Rmi1. This discovery together with the follow-up experiments, which I conducted with the support of Veronika Altmannová and two very talented and motivated students who I was lucky to supervise allowed me to write the complete paper manuscript that is now ready to be submitted.

Secondly, part of my research included working with collaborating teams on a variety of projects. One of them included *in vitro* studies of Pch2 interaction with the ORC complex. My results were an important part of the project and were also included in the paper manuscript published in 2020 (Villar-Fernández et al., 2020). This and other collaboration projects (which are not mentioned in my thesis due to the variety of the topics) helped me understand the importance of networking in science.

A big part of my work also included theoretical background research. Mer3 is a meiosis-specific helicase, which is not the only helicase that is essential for the regulation of mechanisms in meiotic recombination. Together with my supervisor John Weir, we prepared a review that summarizes what is currently understood about helicases involved in the regulation of meiotic recombination, their interaction partners, and the role of regulatory modifications. Importantly, our review preparation involved creating scientific illustrations, which as I have found out during my PhD work is one of my strengths and gave me a lot of joy. Finally, I also included in my thesis some of the preliminary results that in future can serve as a basis for new projects. This will be my final contribution to the projects in our group. From the experiments included in Chapter 5, those that I conducted to solve the structure of Mer3 were the ones that took most of my work time and that I gained the most from. Although my work was not rewarded with the structure, exactly these experiments allowed me to learn all the new methods that I wanted to learn and taught me how to troubleshoot. Altogether, the variety of methods that I had a chance to learn, explore and apply, combined with me growing as a self-dependant scientist makes me believe that I am ready to take another step on my scientific path.

Bibliography

Introduction

- Absmeier, E., Becke, C., Wollenhaupt, J., Santos, K. F., & Wahl, M. C. (2017). Interplay of cis- and trans-regulatory mechanisms in the spliceosomal RNA helicase Brr2. *Cell Cycle (Georgetown, Tex.)*, *16*(1), 100–112. <https://doi.org/10.1080/15384101.2016.1255384>
- Allers, T., & Lichten, M. (2001). Differential timing and control of noncrossover and crossover recombination during meiosis. *Cell*, *106*(1), 47–57. [https://doi.org/10.1016/S0092-8674\(01\)00416-0](https://doi.org/10.1016/S0092-8674(01)00416-0)
- Bell, G. (1982). *MASTERPIECE OF NATURE: the evolution and genetics of sexuality*. ROUTLEDGE. <https://www.routledge.com/The-Masterpiece-of-Nature-The-Evolution-and-Genetics-of-Sexuality/Bell/p/book/9780367339272>
- Bizard, A. H., & Hickson, I. D. (2014). The dissolution of double Holliday junctions. *Cold Spring Harbor Perspectives in Biology*, *6*(7). <https://doi.org/10.1101/CSHPERSPECT.A016477>
- Boddy, M. N., Gaillard, P. H. L., McDonald, W. H., Shanahan, P., Yates, J. R., & Russell, P. (2001). Mus81-Eme1 are essential components of a Holliday junction resolvase. *Cell*, *107*(4), 537–548. [https://doi.org/10.1016/S0092-8674\(01\)00536-0](https://doi.org/10.1016/S0092-8674(01)00536-0)
- Boguslawski, S. J., Smith, D. E., Michalak, M. A., Mickelson, K. E., Yehle, C. O., Patterson, W. L., & Carrico, R. J. (1986). Characterization of monoclonal antibody to DNA:RNA and its application to immunodetection of hybrids. *Journal of Immunological Methods*, *89*(1), 123–130. [https://doi.org/10.1016/0022-1759\(86\)90040-2](https://doi.org/10.1016/0022-1759(86)90040-2)
- Borgogno, M. v., Monti, M. R., Zhao, W., Sung, P., Argarana, C. E., & Pezza, R. J. (2016). Tolerance of DNA Mismatches in Dmc1 Recombinase-mediated DNA Strand Exchange. *The Journal of Biological Chemistry*, *291*(10), 4928. <https://doi.org/10.1074/JBC.M115.704718>
- Brick, K., Pratto, F., & Camerini-Otero, R. D. (2020). After the break: DSB end processing in mouse meiosis. *Genes & Development*, *34*(11–12), 731. <https://doi.org/10.1101/GAD.339309.120>
- Cardoso da Silva, R., & Vader, G. (2021). Getting there: understanding the chromosomal recruitment of the AAA+ ATPase Pch2/TRIP13 during meiosis. *Current Genetics*, *67*(4), 553–565. <https://doi.org/10.1007/S00294-021-01166-3>
- Cejka, P., & Kowalczykowski, S. C. (2010). The full-length *Saccharomyces cerevisiae* Sgs1 protein is a vigorous DNA helicase that preferentially unwinds holliday junctions. *Journal of Biological Chemistry*, *285*(11), 8290–8301. <https://doi.org/10.1074/jbc.M109.083196>
- Cejka, P., Plank, J. L., Bachrati, C. Z., Hickson, I. D., & Kowalczykowski, S. C. (2010). Rmi1 stimulates decatenation of double Holliday junctions during dissolution by Sgs1-Top3. *Nature Structural and Molecular Biology*, *17*(11), 1377–1382. <https://doi.org/10.1038/nsmb.1919>

- Chari, A., Haselbach, D., Kirves, J. M., Ohmer, J., Paknia, E., Fischer, N., Ganichkin, O., Möller, V., J Frye, J., Petzold, G., Jarvis, M., Tietzel, M., Grimm, C., Peters, J. M., Schulman, B. A., Tittmann, K., Markl, J., Fischer, U., & Stark, H. (2015). ProteoPlex: stability optimization of macromolecular complexes by sparse-matrix screening of chemical space. *Nature Methods* 2015 12:9, 12(9), 859–865. <https://doi.org/10.1038/nmeth.3493>
- Chen, C., Zhang, W., Timofejeva, L., Gerardin, Y., & Ma, H. (2005). The Arabidopsis ROCK-N-ROLLERS gene encodes a homolog of the yeast ATP-dependent DNA helicase MER3 and is required for normal meiotic crossover formation. *The Plant Journal : For Cell and Molecular Biology*, 43(3), 321–334. <https://doi.org/10.1111/J.1365-313X.2005.02461.X>
- Cheng, C. H., Lo, Y. H., Liang, S. S., Ti, S. C., Lin, F. M., Yeh, C. H., Huang, H. Y., & Wang, T. F. (2006). SUMO modifications control assembly of synaptonemal complex and polycomplex in meiosis of *Saccharomyces cerevisiae*. *Genes & Development*, 20(15), 2067–2081. <https://doi.org/10.1101/GAD.1430406>
- Cole, F., Kauppi, L., Lange, J., Roig, I., Wang, R., Keeney, S., & Jasin, M. (2012). Homeostatic control of recombination is implemented progressively in mouse meiosis. *Nature Cell Biology* 2012 14:4, 14(4), 424–430. <https://doi.org/10.1038/ncb2451>
- Costa, Y., & Cooke, H. J. (2007). Dissecting the mammalian synaptonemal complex using targeted mutations. *Chromosome Research*, 15(5), 579–589. <https://doi.org/10.1007/S10577-007-1142-1>
- D'Alessandro, G., Whelan, D. R., Howard, S. M., Vitelli, V., Renaudin, X., Adamowicz, M., Iannelli, F., Jones-Weinert, C. W., Lee, M. Y., Matti, V., Lee, W. T. C., Morten, M. J., Venkitaraman, A. R., Cejka, P., Rothenberg, E., & d'Adda di Fagagna, F. (2018). BRCA2 controls DNA:RNA hybrid level at DSBs by mediating RNase H2 recruitment. *Nature Communications* 2018 9:1, 9(1), 1–17. <https://doi.org/10.1038/s41467-018-07799-2>
- de los Santos, T., Hunter, N., Lee, C., Larkin, B., Loidl, J., & Hollingsworth, N. M. (2003). The Mus81/Mms4 endonuclease acts independently of double-Holliday junction resolution to promote a distinct subset of crossovers during meiosis in budding yeast. *Genetics*, 164(1), 81–94. <https://doi.org/10.1093/GENETICS/164.1.81>
- de Muyt, A., Jessop, L., Kolar, E., Sourirajan, A., Chen, J., Dayani, Y., & Lichten, M. (2012). BLM helicase ortholog Sgs1 is a central regulator of meiotic recombination intermediate metabolism. *Molecular Cell*, 46(1), 43. <https://doi.org/10.1016/J.MOLCEL.2012.02.020>
- de Muyt, A., Pyatnitskaya, A., Andréani, J., Ranjha, L., Ramus, C., Laureau, R., Fernandez-Vega, A., Holoch, D., Girard, E., Govin, J., Margueron, R., Couté, Y., Cejka, P., Guérois, R., & Borde, V. (2018). A meiotic XPF-ERCC1-like complex recognizes joint molecule recombination intermediates to promote crossover formation. <https://doi.org/10.1101/gad.308510.117>
- Drouaud, J., Khademian, H., Giraut, L., Zanni, V., Bellalou, S., Henderson, I. R., Falque, M., & Mézard, C. (2013). Contrasted Patterns of Crossover and Non-crossover at Arabidopsis thaliana Meiotic Recombination Hotspots. *PLOS Genetics*, 9(11), e1003922. <https://doi.org/10.1371/JOURNAL.PGEN.1003922>

- Duroc, Y., Kumar, R., Ranjha, L., line Adam, C., Gué rois, R., Md Muntaz, K., Marsolier-Kergoat, M.-C., Dingli, F., Ile Laureau, R., Loew, D., Llorente, B., Charbonnier, J.-B., Cejka, P., & rie Borde, V. (2017). *Concerted action of the MutLb heterodimer and Mer3 helicase regulates the global extent of meiotic gene conversion*. <https://doi.org/10.7554/eLife.21900.001>
- Egydio De Carvalho, C., & Colaiácovo, M. P. (2006). *SUMO-mediated regulation of synaptonemal complex formation during meiosis*. <https://doi.org/10.1101/gad.1457806>
- Fasching, C. L., Cejka, P., Kowalczykowski, S. C., & Heyer, W.-D. (2015). *Top3-Rmi1 dissolve Rad51-mediated D-loops by a topoisomerase-based mechanism*. <https://doi.org/10.1016/j.molcel.2015.01.022>
- Globus, S. T., & Keeney, S. (2012). The Joy of Six: How to Control Your Crossovers. *Cell*, *149*(1), 11–12. <https://doi.org/10.1016/J.CELL.2012.03.011>
- Goldfarb, T., & Lichten, M. (2010). Frequent and efficient use of the sister chromatid for DNA double-strand break repair during budding yeast meiosis. *PLoS Biology*, *8*(10). <https://doi.org/10.1371/JOURNAL.PBIO.1000520>
- Gravel, S., Chapman, J. R., Magill, C., & Jackson, S. P. (2008). DNA helicases Sgs1 and BLM promote DNA double-strand break resection. *Genes & Development*, *22*(20), 2767–2772. <https://doi.org/10.1101/GAD.503108>
- Guillon, H., Baudat, F., Grey, C., Liskay, R. M., & de Massy, B. (2005). Crossover and Noncrossover Pathways in Mouse Meiosis. *Molecular Cell*, *20*(4), 563–573. <https://doi.org/10.1016/J.MOLCEL.2005.09.021>
- Hassold, T., Hall, H., & Hunt, P. (2007). The origin of human aneuploidy: where we have been, where we are going. *Human Molecular Genetics*, *16 Spec No. 2*(R2). <https://doi.org/10.1093/HMG/DDM243>
- Hodson, C., Low, J. K. K., van Twest, S., Jones, S. E., Swuec, P., Murphy, V., Tsukada, K., Fawkes, M., Bythell-Douglas, R., Davies, A., Holien, J. K., O'Rourke, J. J., Parker, B. L., Glaser, A., Parker, M. W., Mackay, J. P., Blackford, A. N., Costa, A., & Deans, A. J. (2022). Mechanism of Bloom syndrome complex assembly required for double Holliday junction dissolution and genome stability. *Proceedings of the National Academy of Sciences of the United States of America*, *119*(6). https://doi.org/10.1073/PNAS.2109093119/SUPPL_FILE/PNAS.2109093119.SD01.XLSX
- Hollingsworth, N. M., & Brill, S. J. (2004). The Mus81 solution to resolution: generating meiotic crossovers without Holliday junctions. *Genes & Development*, *18*(2), 117–125. <https://doi.org/10.1101/GAD.1165904>
- Hollingsworth, N. M., Ponte, L., & Halsey, C. (1995). MSH5, a novel MutS homolog, facilitates meiotic reciprocal recombination between homologs in *Saccharomyces cerevisiae* but not mismatch repair. *Genes and Development*, *9*(14), 1728–1739. <https://doi.org/10.1101/gad.9.14.1728>

- Humphryes, N., & Hochwagen, A. (2014). A non-sister act: recombination template choice during meiosis. *Experimental Cell Research*, 329(1), 53–60. <https://doi.org/10.1016/J.YEXCR.2014.08.024>
- Hunter, N., & Kleckner, N. (2001). The single-end invasion: an asymmetric intermediate at the double-strand break to double-holliday junction transition of meiotic recombination. *Cell*, 106(1), 59–70. [https://doi.org/10.1016/S0092-8674\(01\)00430-5](https://doi.org/10.1016/S0092-8674(01)00430-5)
- Jeffreys, A. J., & May, C. A. (2004). Erratum: Intense and highly localized gene conversion activity in human meiotic crossover hot spots (Nature Genetics (2004) 36 (151-156)). *Nature Genetics*, 36(4), 427. <https://doi.org/10.1038/NG0404-427A>
- Jessop, L., Rockmill, B., Roeder, G. S., & Lichten, M. (2006). Meiotic chromosome synapsis-promoting proteins antagonize the anti-crossover activity of sgs1. *PLoS Genetics*, 2(9), 1402–1412. <https://doi.org/10.1371/journal.pgen.0020155>
- Jones, G. H., & Franklin, F. C. H. (2006). Meiotic crossing-over: obligation and interference. *Cell*, 126(2), 246–248. <https://doi.org/10.1016/J.CELL.2006.07.010>
- Kaur, H., DeMuyt, A., & Lichten, M. (2015). Top3-Rmi1 DNA single-strand decatenase is integral to the formation and resolution of meiotic recombination intermediates. *Molecular Cell*, 57(4), 583–594. <https://doi.org/10.1016/j.molcel.2015.01.020>
- Keeney, S. (2008). Spo11 and the Formation of DNA Double-Strand Breaks in Meiosis. *Genome Dynamics and Stability*, 2, 81–123. https://doi.org/10.1007/7050_2007_026
- Keskin, H., Shen, Y., Huang, F., Patel, M., Yang, T., Ashley, K., Mazin, A. v., & Storici, F. (2014). Transcript-RNA-templated DNA recombination and repair. *Nature*, 515(7527), 436–439. <https://doi.org/10.1038/NATURE13682>
- Kim, K. P., Weiner, B. M., Zhang, L., Jordan, A., Dekker, J., & Kleckner, N. (2010). Sister cohesion and structural axis components mediate homolog bias of meiotic recombination. *Cell*, 143(6), 924–937. <https://doi.org/10.1016/J.CELL.2010.11.015>
- Klein, F., Mahr, P., Galova, M., Buonomo, S. B. C., Michaelis, C., Nairz, K., & Nasmyth, K. (1999). A central role for cohesins in sister chromatid cohesion, formation of axial elements, and recombination during yeast meiosis. *Cell*, 98(1), 91–103. [https://doi.org/10.1016/S0092-8674\(00\)80609-1](https://doi.org/10.1016/S0092-8674(00)80609-1)
- Kohl, K. P., & Sekelsky, J. (2013). Meiotic and Mitotic Recombination in Meiosis. *Genetics*, 194(2), 327–334. <https://doi.org/10.1534/GENETICS.113.150581>
- Liu, S., Rauhut, R., Vornlocher, H. P., & Lührmann, R. (2006). The network of protein–protein interactions within the human U4/U6.U5 tri-snRNP. *RNA*, 12(7), 1418. <https://doi.org/10.1261/RNA.55406>
- Lu, W. T., Hawley, B. R., Skalka, G. L., Baldock, R. A., Smith, E. M., Bader, A. S., Malewicz, M., Watts, F. Z., Wilczynska, A., & Bushell, M. (2018). Drosha drives the formation of DNA:RNA hybrids around

- DNA break sites to facilitate DNA repair. *Nature Communications* 2018 9:1, 9(1), 1–13. <https://doi.org/10.1038/s41467-018-02893-x>
- Lynn, A., Soucek, R., & Börner, G. V. (2007). ZMM proteins during meiosis: Crossover artists at work. In *Chromosome Research* (Vol. 15, Issue 5, pp. 591–605). <https://doi.org/10.1007/s10577-007-1150-1>
- Mancera, E., Bourgon, R., Brozzi, A., Huber, W., & Steinmetz, L. M. (2008). High-resolution mapping of meiotic crossovers and non-crossovers in yeast. *Nature*, 454(7203), 479–485. <https://doi.org/10.1038/NATURE07135>
- Martini, E., Diaz, R. L., Hunter, N., & Keeney, S. (2006a). Crossover homeostasis in yeast meiosis. *Cell*, 126(2), 285. <https://doi.org/10.1016/J.CELL.2006.05.044>
- Martini, E., Diaz, R. L., Hunter, N., & Keeney, S. (2006b). Crossover homeostasis in yeast meiosis. *Cell*, 126(2), 285–295. <https://doi.org/10.1016/J.CELL.2006.05.044>
- Masson, J. Y., & West, S. C. (2001). The Rad51 and Dmc1 recombinases: a non-identical twin relationship. *Trends in Biochemical Sciences*, 26(2), 131–136. [https://doi.org/10.1016/S0968-0004\(00\)01742-4](https://doi.org/10.1016/S0968-0004(00)01742-4)
- Mazina, O. M., Keskin, H., Hanamshet, K., Storici, F., & Mazin, A. v. (2017). Rad52 Inverse Strand Exchange Drives RNA-Templated DNA Double-Strand Break Repair. *Molecular Cell*, 67(1), 19-29.e3. <https://doi.org/10.1016/J.MOLCEL.2017.05.019>
- Mazina, O. M., Mazin, A. v, Nakagawa, T., Kolodner, R. D., & Kowalczykowski, S. C. (2004). Saccharomyces cerevisiae Mer3 Helicase Stimulates 3-5 Heteroduplex Extension by Rad51: Implications for Crossover Control in Meiotic Recombination Division of Biological Sciences Sections of Microbiology and of Molecular Rad51 and Dmc1 proteins bind to the ssDNA tails to and Cellular Biology form filamentous nucleoprotein structures that promote Center for Genetics and Development a search for homologous DNA (Hong et al junction blunt end 5-overhang, implying that the. In *Cell* (Vol. 117).
- McFarlane, R. J., Feichtinger, J., & Larcombe, L. (2014). Cancer germline gene activation. <https://doi.org/10.4161/Cc.29661>, 13(14), 2151–2152. <https://doi.org/10.4161/CC.29661>
- McFarlane, R. J., Feichtinger, J., & Larcombe, L. (2015). Germline/meiotic genes in cancer: new dimensions. *Cell Cycle*, 14(6), 791. <https://doi.org/10.1080/15384101.2015.1010965>
- Mimitou, E. P., & Symington, L. S. (2008). Sae2, Exo1 and Sgs1 collaborate in DNA double-strand break processing. *Nature*, 455(7214), 770–774. <https://doi.org/10.1038/NATURE07312>
- Moore, D. P., & Orr-Weaver, T. L. (1998). Chromosome segregation during meiosis: building an unambivalent bivalent. *Current Topics in Developmental Biology*, 37(C), 263–299. [https://doi.org/10.1016/S0070-2153\(08\)60177-5](https://doi.org/10.1016/S0070-2153(08)60177-5)
- Nakagawa, T., Flores-Rozas, H., & Kolodner, R. D. (2001). The MER3 Helicase Involved in Meiotic Crossing Over Is Stimulated by Single-stranded DNA-binding Proteins and Unwinds DNA in the 3'

- to 5' Direction. *Journal of Biological Chemistry*, 276(34), 31487–31493. <https://doi.org/10.1074/jbc.M104003200>
- Nakagawa, T., & Kolodner, R. D. (2002). *Saccharomyces cerevisiae* Mer3 Is a DNA Helicase Involved in Meiotic Crossing Over. *Molecular and Cellular Biology*, 22(10), 3281–3291. <https://doi.org/10.1128/mcb.22.10.3281-3291.2002>
- Nakagawa, T., & Ogawa, H. (1999). The *Saccharomyces cerevisiae* MER3 gene, encoding a novel helicase-like protein, is required for crossover control in meiosis. *The EMBO Journal*, 18(20), 5714–5723. <https://doi.org/10.1093/EMBOJ/18.20.5714>
- Ohle, C., Tesorero, R., Schermann, G., Dobrev, N., Sinning, I., & Fischer, T. (2016). Transient RNA-DNA Hybrids Are Required for Efficient Double-Strand Break Repair. *Cell*, 167(4), 1001-1013.e7. <https://doi.org/10.1016/J.CELL.2016.10.001>
- Pena, V., Jovin, S. M., Fabrizio, P., Orłowski, J., Bujnicki, J. M., Lührmann, R., & Wahl, M. C. (2009). Common Design Principles in the Spliceosomal RNA Helicase Brr2 and in the Hel308 DNA Helicase. *Molecular Cell*, 35(4), 454–466. <https://doi.org/10.1016/j.molcel.2009.08.006>
- Perry, J., Kleckner, N., & Börner, G. V. (2005). Bioinformatic analyses implicate the collaborating meiotic crossover/chiasma proteins Zip2, Zip3, and Spo22/Zip4 in ubiquitin labeling. *Proceedings of the National Academy of Sciences of the United States of America*, 102(49), 17594–17599. <https://doi.org/10.1073/pnas.0508581102>
- Pyatnitskaya, A., Borde, V., & de Muyt, A. (2019). Crossing and zipping: molecular duties of the ZMM proteins in meiosis. In *Chromosoma* (Vol. 128, Issue 3, pp. 181–198). Springer Science and Business Media Deutschland GmbH. <https://doi.org/10.1007/s00412-019-00714-8>
- Roeder, G. S., & Bailis, J. M. (2000). The pachytene checkpoint. *Trends in Genetics : TIG*, 16(9), 395–403. [https://doi.org/10.1016/S0168-9525\(00\)02080-1](https://doi.org/10.1016/S0168-9525(00)02080-1)
- Rosenberg, S. C., & Corbett, K. D. (2015). The multifaceted roles of the HORMA domain in cellular signaling. *Journal of Cell Biology*, 211(4), 745–755. <https://doi.org/10.1083/JCB.201509076>
- Ross-Macdonald, P., & Roeder, G. S. (1994). Mutation of a meiosis-specific MutS homolog decreases crossing over but not mismatch correction. *Cell*, 79(6), 1069–1080. [https://doi.org/10.1016/0092-8674\(94\)90037-X](https://doi.org/10.1016/0092-8674(94)90037-X)
- Rosu, S., Libuda, D. E., & Villeneuve, A. M. (2011). Robust crossover assurance and regulated interhomolog access maintain meiotic crossover number. *Science*, 334(6060), 1286–1289. https://doi.org/10.1126/SCIENCE.1212424/SUPPL_FILE/ROSU.SOM.PDF
- Schwacha, A., & Kleckner, N. (1995). Identification of double Holliday junctions as intermediates in meiotic recombination. *Cell*, 83(5), 783–791. [https://doi.org/10.1016/0092-8674\(95\)90191-4](https://doi.org/10.1016/0092-8674(95)90191-4)
- Shen, Y., Tang, D., Wang, K., Wang, M., Huang, J., Luo, W., Luo, Q., Hong, L., Li, M., & Cheng, Z. (2012). ZIP4 in homologous chromosome synapsis and crossover formation in rice meiosis. *Journal of Cell Science*, 125(11), 2581–2591. <https://doi.org/10.1242/jcs.090993>

- Siller, S. (2001). Sexual selection and the maintenance of sex. *Nature* 2001 411:6838, 411(6838), 689–692. <https://doi.org/10.1038/35079578>
- Snowden, T., Acharya, S., Butz, C., Berardini, M., & Fishel, R. (2004). hMSH4-hMSH5 recognizes Holliday Junctions and forms a meiosis-specific sliding clamp that embraces homologous chromosomes. *Molecular Cell*, 15(3), 437–451. <https://doi.org/10.1016/J.MOLCEL.2004.06.040>
- Stark, H. (2010). GraFix: stabilization of fragile macromolecular complexes for single particle cryo-EM. *Methods in Enzymology*, 481(C), 109–126. [https://doi.org/10.1016/S0076-6879\(10\)81005-5](https://doi.org/10.1016/S0076-6879(10)81005-5)
- Sym, M., Engebrecht, J. A., & Roeder, G. S. (1993). ZIP1 is a synaptonemal complex protein required for meiotic chromosome synapsis. *Cell*, 72(3), 365–378. [https://doi.org/10.1016/0092-8674\(93\)90114-6](https://doi.org/10.1016/0092-8674(93)90114-6)
- Szostak, J. W., Orr-Weaver, T. L., Rothstein, R. J., & Stahl, F. W. (1983). The double-strand-break repair model for recombination. *Cell*, 33(1), 25–35. [https://doi.org/10.1016/0092-8674\(83\)90331-8](https://doi.org/10.1016/0092-8674(83)90331-8)
- Tanaka, K., Miyamoto, N., Shouguchi-Miyata, J., & Ikeda, J. E. (2006). HFM1, the human homologue of yeast Mer3, encodes a putative DNA helicase expressed specifically in germ-line cells. *DNA Sequence: The Journal of DNA Sequencing and Mapping*, 17(3), 242–246. <https://doi.org/10.1080/10425170600805433>
- Tang, D., Lv, M., Gao, Y., Cheng, H., Li, K., Xu, C., Geng, H., Li, G., Shan, Q., Wang, C., He, X., & Cao, Y. (2021). Novel Variants in HFM1 Lead to Male Infertility Due to Non-obstructive Azoospermia. <https://doi.org/10.21203/rs.3.rs-431339/v1>
- Tang, S., Wu, M. K. Y., Zhang, R., & Hunter, N. (2015). Pervasive and essential roles of the top3-rmi1 decatenase orchestrate recombination and facilitate chromosome segregation in meiosis. *Molecular Cell*, 57(4), 607–621. <https://doi.org/10.1016/j.molcel.2015.01.021>
- Tock, A. J., & Henderson, I. R. (2018). Hotspots for Initiation of Meiotic Recombination. *Frontiers in Genetics*, 9, 521. <https://doi.org/10.3389/FGENE.2018.00521/BIBTEX>
- Vader, G. (2015). Pch2(TRIP13): controlling cell division through regulation of HORMA domains. *Chromosoma*, 124(3), 333–339. <https://doi.org/10.1007/S00412-015-0516-Y>
- van Nues, R. W., & Beggs, J. D. (2001). Functional contacts with a range of splicing proteins suggest a central role for Brr2p in the dynamic control of the order of events in spliceosomes of *Saccharomyces cerevisiae*. *Genetics*, 157(4), 1451–1467. <https://doi.org/10.1093/GENETICS/157.4.1451>
- Vernekar, D. V., Reginato, G., Adam, C., Ranjha, L., Dingli, F., Marsolier, M. C., Loew, D., Gue´rois, R., Llorente, B., Cejka, P., & Borde, V. (2021). The Pif1 helicase is actively inhibited during meiotic recombination which restrains gene conversion tract length. *Nucleic Acids Research*, 49(8), 4522–4533. <https://doi.org/10.1093/nar/gkab232>
- Villar-Fernández, M. A., da Silva, R. C., Firlej, M., Pan, D., Weir, E., Sarembe, A., Raina, V. B., Bange, T., Weir, J. R., & Vader, G. (2020). Biochemical and functional characterization of a meiosis-specific Pch2/ORC AAA+ assembly. *Life Science Alliance*, 3(11). <https://doi.org/10.26508/LSA.201900630>

- Wang, J., Zhang, W., Jiang, H., & Wu, B.-L. (2014a). Mutations in HFM1 in Recessive Primary Ovarian Insufficiency . *New England Journal of Medicine*, 370(10), 972–974. <https://doi.org/10.1056/NEJMC1310150>
- Wang, J., Zhang, W., Jiang, H., & Wu, B.-L. (2014b). Mutations in HFM1 in Recessive Primary Ovarian Insufficiency . *New England Journal of Medicine*, 370(10), 972–974. https://doi.org/10.1056/NEJMC1310150/SUPPL_FILE/NEJMC1310150_DISCLOSURES.PDF
- Wang, K., Tang, D., Wang, M., Lu, J., Yu, H., Liu, J., Qian, B., Gong, Z., Wang, X., Chen, J., Gu, M., & Cheng, Z. (2009). MER3 is required for normal meiotic crossover formation, but not for presynaptic alignment in rice. *Journal of Cell Science*, 122(12), 2055–2063. <https://doi.org/10.1242/jcs.049080>
- Watanabe, Y., & Nurse, P. (1999). Cohesin Rec8 is required for reductional chromosome segregation at meiosis. *Nature*, 400(6743), 461–464. <https://doi.org/10.1038/22774>
- Wijnker, E., James, G. V., Ding, J., Becker, F., Klasen, J. R., Rawat, V., Rowan, B. A., de Jong, D. F., de Snoo, C. B., Zapata, L., Huettel, B., de Jong, H., Ossowski, S., Weigel, D., Koornneef, M., Keurentjes, J. J. B., & Schneeberger, K. (2013). The genomic landscape of meiotic crossovers and gene conversions in *Arabidopsis thaliana*. *ELife*, 2013(2). <https://doi.org/10.7554/ELIFE.01426>
- Xie, X., Murtaza, G., Li, Y., Zhou, J., Ye, J., Khan, R., Jiang, L., Khan, I., Zubair, M., Yin, H., Jiang, H., Liu, W., Shi, B., Hou, X., Gong, C., Fan, S., Wang, Y., Jiang, X., Zhang, Y., ... Shi, Q. (2022). Biallelic HFM1 variants cause non-obstructive azoospermia with meiotic arrest in humans by impairing crossover formation to varying degrees. *Human Reproduction*. <https://doi.org/10.1093/HUMREP/DEAC092>
- Yang, X., Zhai, B., Wang, S., Kong, X., Tan, Y., Liu, L., Yang, X., Tan, T., Zhang, S., & Zhang, L. (2021). RNA-DNA hybrids regulate meiotic recombination. *Cell Reports*, 37(10). <https://doi.org/10.1016/J.CELREP.2021.110097>
- Yasuhara, T., Kato, R., Hagiwara, Y., Shiotani, B., Yamauchi, M., Nakada, S., Shibata, A., & Miyagawa, K. (2018). Human Rad52 Promotes XPG-Mediated R-loop Processing to Initiate Transcription-Associated Homologous Recombination Repair. *Cell*, 175(2), 558-570.e11. <https://doi.org/10.1016/J.CELL.2018.08.056>
- Youds, J. L., & Boulton, S. J. (2011). The choice in meiosis – defining the factors that influence crossover or non-crossover formation. *Journal of Cell Science*, 124(4), 501–513. <https://doi.org/10.1242/JCS.074427>
- Zakharyevich, K., Tang, S., Ma, Y., & Hunter, N. (2012). Delineation of joint molecule resolution pathways in meiosis identifies a crossover-specific resolvase. *Cell*, 149(2), 334. <https://doi.org/10.1016/J.CELL.2012.03.023>

Preliminary results

- Absmeier, E., Becke, C., Wollenhaupt, J., Santos, K. F., & Wahl, M. C. (2017). Interplay of cis- and trans-regulatory mechanisms in the spliceosomal RNA helicase Brr2. *Cell Cycle (Georgetown, Tex.)*, *16*(1), 100–112. <https://doi.org/10.1080/15384101.2016.1255384>
- Allers, T., & Lichten, M. (2001). Differential timing and control of noncrossover and crossover recombination during meiosis. *Cell*, *106*(1), 47–57. [https://doi.org/10.1016/S0092-8674\(01\)00416-0](https://doi.org/10.1016/S0092-8674(01)00416-0)
- Bell, G. (1982). *MASTERPIECE OF NATURE: the evolution and genetics of sexuality*. ROUTLEDGE. <https://www.routledge.com/The-Masterpiece-of-Nature-The-Evolution-and-Genetics-of-Sexuality/Bell/p/book/9780367339272>
- Bizard, A. H., & Hickson, I. D. (2014). The dissolution of double Holliday junctions. *Cold Spring Harbor Perspectives in Biology*, *6*(7). <https://doi.org/10.1101/CSHPERSPECT.A016477>
- Boddy, M. N., Gaillard, P. H. L., McDonald, W. H., Shanahan, P., Yates, J. R., & Russell, P. (2001). Mus81-Eme1 are essential components of a Holliday junction resolvase. *Cell*, *107*(4), 537–548. [https://doi.org/10.1016/S0092-8674\(01\)00536-0](https://doi.org/10.1016/S0092-8674(01)00536-0)
- Boguslawski, S. J., Smith, D. E., Michalak, M. A., Mickelson, K. E., Yehle, C. O., Patterson, W. L., & Carrico, R. J. (1986). Characterization of monoclonal antibody to DNA.RNA and its application to immunodetection of hybrids. *Journal of Immunological Methods*, *89*(1), 123–130. [https://doi.org/10.1016/0022-1759\(86\)90040-2](https://doi.org/10.1016/0022-1759(86)90040-2)
- Borgogno, M. v., Monti, M. R., Zhao, W., Sung, P., Argarana, C. E., & Pezza, R. J. (2016). Tolerance of DNA Mismatches in Dmc1 Recombinase-mediated DNA Strand Exchange. *The Journal of Biological Chemistry*, *291*(10), 4928. <https://doi.org/10.1074/JBC.M115.704718>
- Brick, K., Pratto, F., & Camerini-Otero, R. D. (2020). After the break: DSB end processing in mouse meiosis. *Genes & Development*, *34*(11–12), 731. <https://doi.org/10.1101/GAD.339309.120>
- Cardoso da Silva, R., & Vader, G. (2021). Getting there: understanding the chromosomal recruitment of the AAA+ ATPase Pch2/TRIP13 during meiosis. *Current Genetics*, *67*(4), 553–565. <https://doi.org/10.1007/S00294-021-01166-3>
- Cejka, P., & Kowalczykowski, S. C. (2010). The full-length *Saccharomyces cerevisiae* Sgs1 protein is a vigorous DNA helicase that preferentially unwinds holliday junctions. *Journal of Biological Chemistry*, *285*(11), 8290–8301. <https://doi.org/10.1074/jbc.M109.083196>
- Cejka, P., Plank, J. L., Bachrati, C. Z., Hickson, I. D., & Kowalczykowski, S. C. (2010). Rmi1 stimulates decatenation of double Holliday junctions during dissolution by Sgs1-Top3. *Nature Structural and Molecular Biology*, *17*(11), 1377–1382. <https://doi.org/10.1038/nsmb.1919>
- Chari, A., Haselbach, D., Kirves, J. M., Ohmer, J., Paknia, E., Fischer, N., Ganichkin, O., Möller, V., J Frye, J., Petzold, G., Jarvis, M., Tietzel, M., Grimm, C., Peters, J. M., Schulman, B. A., Tittmann, K., Markl, J., Fischer, U., & Stark, H. (2015). ProteoPlex: stability optimization of macromolecular complexes

- by sparse-matrix screening of chemical space. *Nature Methods* 2015 12:9, 12(9), 859–865. <https://doi.org/10.1038/nmeth.3493>
- Chen, C., Zhang, W., Timofejeva, L., Gerardin, Y., & Ma, H. (2005). The Arabidopsis ROCK-N-ROLLERS gene encodes a homolog of the yeast ATP-dependent DNA helicase MER3 and is required for normal meiotic crossover formation. *The Plant Journal : For Cell and Molecular Biology*, 43(3), 321–334. <https://doi.org/10.1111/J.1365-313X.2005.02461.X>
- Cheng, C. H., Lo, Y. H., Liang, S. S., Ti, S. C., Lin, F. M., Yeh, C. H., Huang, H. Y., & Wang, T. F. (2006). SUMO modifications control assembly of synaptonemal complex and polycomplex in meiosis of *Saccharomyces cerevisiae*. *Genes & Development*, 20(15), 2067–2081. <https://doi.org/10.1101/GAD.1430406>
- Cole, F., Kauppi, L., Lange, J., Roig, I., Wang, R., Keeney, S., & Jasin, M. (2012). Homeostatic control of recombination is implemented progressively in mouse meiosis. *Nature Cell Biology* 2012 14:4, 14(4), 424–430. <https://doi.org/10.1038/ncb2451>
- Costa, Y., & Cooke, H. J. (2007). Dissecting the mammalian synaptonemal complex using targeted mutations. *Chromosome Research*, 15(5), 579–589. <https://doi.org/10.1007/S10577-007-1142-1>
- D'Alessandro, G., Whelan, D. R., Howard, S. M., Vitelli, V., Renaudin, X., Adamowicz, M., Iannelli, F., Jones-Weinert, C. W., Lee, M. Y., Matti, V., Lee, W. T. C., Morten, M. J., Venkitaraman, A. R., Cejka, P., Rothenberg, E., & d'Adda di Fagagna, F. (2018). BRCA2 controls DNA:RNA hybrid level at DSBs by mediating RNase H2 recruitment. *Nature Communications* 2018 9:1, 9(1), 1–17. <https://doi.org/10.1038/s41467-018-07799-2>
- de los Santos, T., Hunter, N., Lee, C., Larkin, B., Loidl, J., & Hollingsworth, N. M. (2003). The Mus81/Mms4 endonuclease acts independently of double-Holliday junction resolution to promote a distinct subset of crossovers during meiosis in budding yeast. *Genetics*, 164(1), 81–94. <https://doi.org/10.1093/GENETICS/164.1.81>
- de Muyt, A., Jessop, L., Kolar, E., Sourirajan, A., Chen, J., Dayani, Y., & Lichten, M. (2012). BLM helicase ortholog Sgs1 is a central regulator of meiotic recombination intermediate metabolism. *Molecular Cell*, 46(1), 43. <https://doi.org/10.1016/J.MOLCEL.2012.02.020>
- de Muyt, A., Pyatnitskaya, A., Andréani, J., Ranjha, L., Ramus, C., Laureau, R., Fernandez-Vega, A., Holoch, D., Girard, E., Govin, J., Margueron, R., Couté, Y., Cejka, P., Guérois, R., & Borde, V. (2018). A meiotic XPF-ERCC1-like complex recognizes joint molecule recombination intermediates to promote crossover formation. <https://doi.org/10.1101/gad.308510.117>
- Drouaud, J., Khademian, H., Giraut, L., Zanni, V., Bellalou, S., Henderson, I. R., Falque, M., & Mézard, C. (2013). Contrasted Patterns of Crossover and Non-crossover at Arabidopsis thaliana Meiotic Recombination Hotspots. *PLOS Genetics*, 9(11), e1003922. <https://doi.org/10.1371/JOURNAL.PGEN.1003922>
- Duroc, Y., Kumar, R., Ranjha, L., line Adam, C., Gué rois, R., Md Muntaz, K., Marsolier-Kergoat, M.-C., Dingli, F., lle Laureau, R., Loew, D., Llorente, B., Charbonnier, J.-B., Cejka, P., & rie Borde, V. (2017).

- Concerted action of the MutLb heterodimer and Mer3 helicase regulates the global extent of meiotic gene conversion.* <https://doi.org/10.7554/eLife.21900.001>
- Egydio De Carvalho, C., & Colaiácovo, M. P. (2006). *SUMO-mediated regulation of synaptonemal complex formation during meiosis.* <https://doi.org/10.1101/gad.1457806>
- Fasching, C. L., Cejka, P., Kowalczykowski, S. C., & Heyer, W.-D. (2015). *Top3-Rmi1 dissolve Rad51-mediated D-loops by a topoisomerase-based mechanism.* <https://doi.org/10.1016/j.molcel.2015.01.022>
- Globus, S. T., & Keeney, S. (2012). The Joy of Six: How to Control Your Crossovers. *Cell*, *149*(1), 11–12. <https://doi.org/10.1016/J.CELL.2012.03.011>
- Goldfarb, T., & Lichten, M. (2010). Frequent and efficient use of the sister chromatid for DNA double-strand break repair during budding yeast meiosis. *PLoS Biology*, *8*(10). <https://doi.org/10.1371/JOURNAL.PBIO.1000520>
- Gravel, S., Chapman, J. R., Magill, C., & Jackson, S. P. (2008). DNA helicases Sgs1 and BLM promote DNA double-strand break resection. *Genes & Development*, *22*(20), 2767–2772. <https://doi.org/10.1101/GAD.503108>
- Guillon, H., Baudat, F., Grey, C., Liskay, R. M., & de Massy, B. (2005). Crossover and Noncrossover Pathways in Mouse Meiosis. *Molecular Cell*, *20*(4), 563–573. <https://doi.org/10.1016/J.MOLCEL.2005.09.021>
- Hassold, T., Hall, H., & Hunt, P. (2007). The origin of human aneuploidy: where we have been, where we are going. *Human Molecular Genetics*, *16 Spec No.* 2(R2). <https://doi.org/10.1093/HMG/DDM243>
- Hodson, C., Low, J. K. K., van Twest, S., Jones, S. E., Swuec, P., Murphy, V., Tsukada, K., Fawkes, M., Bythell-Douglas, R., Davies, A., Holien, J. K., O'Rourke, J. J., Parker, B. L., Glaser, A., Parker, M. W., Mackay, J. P., Blackford, A. N., Costa, A., & Deans, A. J. (2022). Mechanism of Bloom syndrome complex assembly required for double Holliday junction dissolution and genome stability. *Proceedings of the National Academy of Sciences of the United States of America*, *119*(6). https://doi.org/10.1073/PNAS.2109093119/SUPPL_FILE/PNAS.2109093119.SD01.XLSX
- Hollingsworth, N. M., & Brill, S. J. (2004). The Mus81 solution to resolution: generating meiotic crossovers without Holliday junctions. *Genes & Development*, *18*(2), 117–125. <https://doi.org/10.1101/GAD.1165904>
- Hollingsworth, N. M., Ponte, L., & Halsey, C. (1995). MSH5, a novel MutS homolog, facilitates meiotic reciprocal recombination between homologs in *Saccharomyces cerevisiae* but not mismatch repair. *Genes and Development*, *9*(14), 1728–1739. <https://doi.org/10.1101/gad.9.14.1728>
- Humphries, N., & Hochwagen, A. (2014). A non-sister act: recombination template choice during meiosis. *Experimental Cell Research*, *329*(1), 53–60. <https://doi.org/10.1016/J.YEXCR.2014.08.024>

- Hunter, N., & Kleckner, N. (2001). The single-end invasion: an asymmetric intermediate at the double-strand break to double-holliday junction transition of meiotic recombination. *Cell*, *106*(1), 59–70. [https://doi.org/10.1016/S0092-8674\(01\)00430-5](https://doi.org/10.1016/S0092-8674(01)00430-5)
- Jeffreys, A. J., & May, C. A. (2004). Erratum: Intense and highly localized gene conversion activity in human meiotic crossover hot spots (Nature Genetics (2004) 36 (151-156)). *Nature Genetics*, *36*(4), 427. <https://doi.org/10.1038/NG0404-427A>
- Jessop, L., Rockmill, B., Roeder, G. S., & Lichten, M. (2006). Meiotic chromosome synapsis-promoting proteins antagonize the anti-crossover activity of *sgs1*. *PLoS Genetics*, *2*(9), 1402–1412. <https://doi.org/10.1371/journal.pgen.0020155>
- Jones, G. H., & Franklin, F. C. H. (2006). Meiotic crossing-over: obligation and interference. *Cell*, *126*(2), 246–248. <https://doi.org/10.1016/J.CELL.2006.07.010>
- Kaur, H., DeMuyt, A., & Lichten, M. (2015). Top3-Rmi1 DNA single-strand decatenase is integral to the formation and resolution of meiotic recombination intermediates. *Molecular Cell*, *57*(4), 583–594. <https://doi.org/10.1016/j.molcel.2015.01.020>
- Keeney, S. (2008). Spo11 and the Formation of DNA Double-Strand Breaks in Meiosis. *Genome Dynamics and Stability*, *2*, 81–123. https://doi.org/10.1007/7050_2007_026
- Keskin, H., Shen, Y., Huang, F., Patel, M., Yang, T., Ashley, K., Mazin, A. v., & Storici, F. (2014). Transcript-RNA-templated DNA recombination and repair. *Nature*, *515*(7527), 436–439. <https://doi.org/10.1038/NATURE13682>
- Kim, K. P., Weiner, B. M., Zhang, L., Jordan, A., Dekker, J., & Kleckner, N. (2010). Sister cohesion and structural axis components mediate homolog bias of meiotic recombination. *Cell*, *143*(6), 924–937. <https://doi.org/10.1016/J.CELL.2010.11.015>
- Klein, F., Mahr, P., Galova, M., Buonomo, S. B. C., Michaelis, C., Nairz, K., & Nasmyth, K. (1999). A central role for cohesins in sister chromatid cohesion, formation of axial elements, and recombination during yeast meiosis. *Cell*, *98*(1), 91–103. [https://doi.org/10.1016/S0092-8674\(00\)80609-1](https://doi.org/10.1016/S0092-8674(00)80609-1)
- Kohl, K. P., & Sekelsky, J. (2013). Meiotic and Mitotic Recombination in Meiosis. *Genetics*, *194*(2), 327–334. <https://doi.org/10.1534/GENETICS.113.150581>
- Liu, S., Rauhut, R., Vornlocher, H. P., & Lührmann, R. (2006). The network of protein–protein interactions within the human U4/U6.U5 tri-snRNP. *RNA*, *12*(7), 1418. <https://doi.org/10.1261/RNA.55406>
- Lu, W. T., Hawley, B. R., Skalka, G. L., Baldock, R. A., Smith, E. M., Bader, A. S., Malewicz, M., Watts, F. Z., Wilczynska, A., & Bushell, M. (2018). Drosha drives the formation of DNA:RNA hybrids around DNA break sites to facilitate DNA repair. *Nature Communications* *2018* *9*:1, 9(1), 1–13. <https://doi.org/10.1038/s41467-018-02893-x>

- Lynn, A., Soucek, R., & Börner, G. V. (2007). ZMM proteins during meiosis: Crossover artists at work. In *Chromosome Research* (Vol. 15, Issue 5, pp. 591–605). <https://doi.org/10.1007/s10577-007-1150-1>
- Mancera, E., Bourgon, R., Brozzi, A., Huber, W., & Steinmetz, L. M. (2008). High-resolution mapping of meiotic crossovers and non-crossovers in yeast. *Nature*, *454*(7203), 479–485. <https://doi.org/10.1038/NATURE07135>
- Martini, E., Diaz, R. L., Hunter, N., & Keeney, S. (2006a). Crossover homeostasis in yeast meiosis. *Cell*, *126*(2), 285. <https://doi.org/10.1016/J.CELL.2006.05.044>
- Martini, E., Diaz, R. L., Hunter, N., & Keeney, S. (2006b). Crossover homeostasis in yeast meiosis. *Cell*, *126*(2), 285–295. <https://doi.org/10.1016/J.CELL.2006.05.044>
- Masson, J. Y., & West, S. C. (2001). The Rad51 and Dmc1 recombinases: a non-identical twin relationship. *Trends in Biochemical Sciences*, *26*(2), 131–136. [https://doi.org/10.1016/S0968-0004\(00\)01742-4](https://doi.org/10.1016/S0968-0004(00)01742-4)
- Mazina, O. M., Keskin, H., Hanamshet, K., Storici, F., & Mazin, A. v. (2017). Rad52 Inverse Strand Exchange Drives RNA-Templated DNA Double-Strand Break Repair. *Molecular Cell*, *67*(1), 19–29.e3. <https://doi.org/10.1016/J.MOLCEL.2017.05.019>
- Mazina, O. M., Mazin, A. v, Nakagawa, T., Kolodner, R. D., & Kowalczykowski, S. C. (2004). *Saccharomyces cerevisiae* Mer3 Helicase Stimulates 3-5 Heteroduplex Extension by Rad51: Implications for Crossover Control in Meiotic Recombination Division of Biological Sciences Sections of Microbiology and of Molecular Rad51 and Dmc1 proteins bind to the ssDNA tails to and Cellular Biology form filamentous nucleoprotein structures that promote Center for Genetics and Development a search for homologous DNA (Hong et al junction blunt end 5-overhang, implying that the. In *Cell* (Vol. 117).
- McFarlane, R. J., Feichtinger, J., & Larcombe, L. (2014). Cancer germline gene activation. <https://doi.org/10.4161/Cc.29661>, *13*(14), 2151–2152. <https://doi.org/10.4161/CC.29661>
- McFarlane, R. J., Feichtinger, J., & Larcombe, L. (2015). Germline/meiotic genes in cancer: new dimensions. *Cell Cycle*, *14*(6), 791. <https://doi.org/10.1080/15384101.2015.1010965>
- Mimitou, E. P., & Symington, L. S. (2008). Sae2, Exo1 and Sgs1 collaborate in DNA double-strand break processing. *Nature*, *455*(7214), 770–774. <https://doi.org/10.1038/NATURE07312>
- Moore, D. P., & Orr-Weaver, T. L. (1998). Chromosome segregation during meiosis: building an unambivalent bivalent. *Current Topics in Developmental Biology*, *37*(C), 263–299. [https://doi.org/10.1016/S0070-2153\(08\)60177-5](https://doi.org/10.1016/S0070-2153(08)60177-5)
- Nakagawa, T., Flores-Rozas, H., & Kolodner, R. D. (2001). The MER3 Helicase Involved in Meiotic Crossing Over Is Stimulated by Single-stranded DNA-binding Proteins and Unwinds DNA in the 3' to 5' Direction. *Journal of Biological Chemistry*, *276*(34), 31487–31493. <https://doi.org/10.1074/jbc.M104003200>

- Nakagawa, T., & Kolodner, R. D. (2002). *Saccharomyces cerevisiae* Mer3 Is a DNA Helicase Involved in Meiotic Crossing Over. *Molecular and Cellular Biology*, 22(10), 3281–3291. <https://doi.org/10.1128/mcb.22.10.3281-3291.2002>
- Nakagawa, T., & Ogawa, H. (1999). The *Saccharomyces cerevisiae* MER3 gene, encoding a novel helicase-like protein, is required for crossover control in meiosis. *The EMBO Journal*, 18(20), 5714–5723. <https://doi.org/10.1093/EMBOJ/18.20.5714>
- Ohle, C., Tesorero, R., Schermann, G., Dobrev, N., Sinning, I., & Fischer, T. (2016). Transient RNA-DNA Hybrids Are Required for Efficient Double-Strand Break Repair. *Cell*, 167(4), 1001-1013.e7. <https://doi.org/10.1016/J.CELL.2016.10.001>
- Pena, V., Jovin, S. M., Fabrizio, P., Orłowski, J., Bujnicki, J. M., Lührmann, R., & Wahl, M. C. (2009). Common Design Principles in the Spliceosomal RNA Helicase Brr2 and in the Hel308 DNA Helicase. *Molecular Cell*, 35(4), 454–466. <https://doi.org/10.1016/j.molcel.2009.08.006>
- Perry, J., Kleckner, N., & Börner, G. V. (2005). Bioinformatic analyses implicate the collaborating meiotic crossover/chiasma proteins Zip2, Zip3, and Spo22/Zip4 in ubiquitin labeling. *Proceedings of the National Academy of Sciences of the United States of America*, 102(49), 17594–17599. <https://doi.org/10.1073/pnas.0508581102>
- Pyatnitskaya, A., Borde, V., & de Muyt, A. (2019). Crossing and zipping: molecular duties of the ZMM proteins in meiosis. In *Chromosoma* (Vol. 128, Issue 3, pp. 181–198). Springer Science and Business Media Deutschland GmbH. <https://doi.org/10.1007/s00412-019-00714-8>
- Roeder, G. S., & Bailis, J. M. (2000). The pachytene checkpoint. *Trends in Genetics : TIG*, 16(9), 395–403. [https://doi.org/10.1016/S0168-9525\(00\)02080-1](https://doi.org/10.1016/S0168-9525(00)02080-1)
- Rosenberg, S. C., & Corbett, K. D. (2015). The multifaceted roles of the HORMA domain in cellular signaling. *Journal of Cell Biology*, 211(4), 745–755. <https://doi.org/10.1083/JCB.201509076>
- Ross-Macdonald, P., & Roeder, G. S. (1994). Mutation of a meiosis-specific MutS homolog decreases crossing over but not mismatch correction. *Cell*, 79(6), 1069–1080. [https://doi.org/10.1016/0092-8674\(94\)90037-X](https://doi.org/10.1016/0092-8674(94)90037-X)
- Rosu, S., Libuda, D. E., & Villeneuve, A. M. (2011). Robust crossover assurance and regulated interhomolog access maintain meiotic crossover number. *Science*, 334(6060), 1286–1289. https://doi.org/10.1126/SCIENCE.1212424/SUPPL_FILE/ROSU.SOM.PDF
- Schwacha, A., & Kleckner, N. (1995). Identification of double Holliday junctions as intermediates in meiotic recombination. *Cell*, 83(5), 783–791. [https://doi.org/10.1016/0092-8674\(95\)90191-4](https://doi.org/10.1016/0092-8674(95)90191-4)
- Shen, Y., Tang, D., Wang, K., Wang, M., Huang, J., Luo, W., Luo, Q., Hong, L., Li, M., & Cheng, Z. (2012). ZIP4 in homologous chromosome synapsis and crossover formation in rice meiosis. *Journal of Cell Science*, 125(11), 2581–2591. <https://doi.org/10.1242/jcs.090993>
- Siller, S. (2001). Sexual selection and the maintenance of sex. *Nature* 2001 411:6838, 411(6838), 689–692. <https://doi.org/10.1038/35079578>

- Snowden, T., Acharya, S., Butz, C., Berardini, M., & Fishel, R. (2004). hMSH4-hMSH5 recognizes Holliday Junctions and forms a meiosis-specific sliding clamp that embraces homologous chromosomes. *Molecular Cell*, *15*(3), 437–451. <https://doi.org/10.1016/J.MOLCEL.2004.06.040>
- Stark, H. (2010). GraFix: stabilization of fragile macromolecular complexes for single particle cryo-EM. *Methods in Enzymology*, *481*(C), 109–126. [https://doi.org/10.1016/S0076-6879\(10\)81005-5](https://doi.org/10.1016/S0076-6879(10)81005-5)
- Sym, M., Engebrecht, J. A., & Roeder, G. S. (1993). ZIP1 is a synaptonemal complex protein required for meiotic chromosome synapsis. *Cell*, *72*(3), 365–378. [https://doi.org/10.1016/0092-8674\(93\)90114-6](https://doi.org/10.1016/0092-8674(93)90114-6)
- Szostak, J. W., Orr-Weaver, T. L., Rothstein, R. J., & Stahl, F. W. (1983). The double-strand-break repair model for recombination. *Cell*, *33*(1), 25–35. [https://doi.org/10.1016/0092-8674\(83\)90331-8](https://doi.org/10.1016/0092-8674(83)90331-8)
- Tanaka, K., Miyamoto, N., Shouguchi-Miyata, J., & Ikeda, J. E. (2006). HFM1, the human homologue of yeast Mer3, encodes a putative DNA helicase expressed specifically in germ-line cells. *DNA Sequence: The Journal of DNA Sequencing and Mapping*, *17*(3), 242–246. <https://doi.org/10.1080/10425170600805433>
- Tang, D., Lv, M., Gao, Y., Cheng, H., Li, K., Xu, C., Geng, H., Li, G., Shan, Q., Wang, C., He, X., & Cao, Y. (2021). *Novel Variants in HFM1 Lead to Male Infertility Due to Non-obstructive Azoospermia*. <https://doi.org/10.21203/rs.3.rs-431339/v1>
- Tang, S., Wu, M. K. Y., Zhang, R., & Hunter, N. (2015). Pervasive and essential roles of the top3-rmi1 decatenase orchestrate recombination and facilitate chromosome segregation in meiosis. *Molecular Cell*, *57*(4), 607–621. <https://doi.org/10.1016/j.molcel.2015.01.021>
- Tock, A. J., & Henderson, I. R. (2018). Hotspots for Initiation of Meiotic Recombination. *Frontiers in Genetics*, *9*, 521. <https://doi.org/10.3389/FGENE.2018.00521/BIBTEX>
- Vader, G. (2015). Pch2(TRIP13): controlling cell division through regulation of HORMA domains. *Chromosoma*, *124*(3), 333–339. <https://doi.org/10.1007/S00412-015-0516-Y>
- van Nues, R. W., & Beggs, J. D. (2001). Functional contacts with a range of splicing proteins suggest a central role for Brr2p in the dynamic control of the order of events in spliceosomes of *Saccharomyces cerevisiae*. *Genetics*, *157*(4), 1451–1467. <https://doi.org/10.1093/GENETICS/157.4.1451>
- Vernekar, D. V., Reginato, G., Adam, C., Ranjha, L., Dingli, F., Marsolier, M. C., Loew, D., Gue´rois, R., Llorente, B., Cejka, P., & Borde, V. (2021). The Pif1 helicase is actively inhibited during meiotic recombination which restrains gene conversion tract length. *Nucleic Acids Research*, *49*(8), 4522–4533. <https://doi.org/10.1093/nar/gkab232>
- Villar-Fernández, M. A., da Silva, R. C., Firlej, M., Pan, D., Weir, E., Sarembe, A., Raina, V. B., Bange, T., Weir, J. R., & Vader, G. (2020). Biochemical and functional characterization of a meiosis-specific Pch2/ORC AAA+ assembly. *Life Science Alliance*, *3*(11). <https://doi.org/10.26508/LSA.201900630>

- Wang, J., Zhang, W., Jiang, H., & Wu, B.-L. (2014a). Mutations in HFM1 in Recessive Primary Ovarian Insufficiency . *New England Journal of Medicine*, 370(10), 972–974. <https://doi.org/10.1056/NEJMC1310150>
- Wang, J., Zhang, W., Jiang, H., & Wu, B.-L. (2014b). Mutations in HFM1 in Recessive Primary Ovarian Insufficiency . *New England Journal of Medicine*, 370(10), 972–974. https://doi.org/10.1056/NEJMC1310150/SUPPL_FILE/NEJMC1310150_DISCLOSURES.PDF
- Wang, K., Tang, D., Wang, M., Lu, J., Yu, H., Liu, J., Qian, B., Gong, Z., Wang, X., Chen, J., Gu, M., & Cheng, Z. (2009). MER3 is required for normal meiotic crossover formation, but not for presynaptic alignment in rice. *Journal of Cell Science*, 122(12), 2055–2063. <https://doi.org/10.1242/jcs.049080>
- Watanabe, Y., & Nurse, P. (1999). Cohesin Rec8 is required for reductional chromosome segregation at meiosis. *Nature*, 400(6743), 461–464. <https://doi.org/10.1038/22774>
- Wijnker, E., James, G. V., Ding, J., Becker, F., Klasen, J. R., Rawat, V., Rowan, B. A., de Jong, D. F., de Snoo, C. B., Zapata, L., Huettel, B., de Jong, H., Ossowski, S., Weigel, D., Koornneef, M., Keurentjes, J. J. B., & Schneeberger, K. (2013). The genomic landscape of meiotic crossovers and gene conversions in *Arabidopsis thaliana*. *ELife*, 2013(2). <https://doi.org/10.7554/ELIFE.01426>
- Xie, X., Murtaza, G., Li, Y., Zhou, J., Ye, J., Khan, R., Jiang, L., Khan, I., Zubair, M., Yin, H., Jiang, H., Liu, W., Shi, B., Hou, X., Gong, C., Fan, S., Wang, Y., Jiang, X., Zhang, Y., ... Shi, Q. (2022). Biallelic HFM1 variants cause non-obstructive azoospermia with meiotic arrest in humans by impairing crossover formation to varying degrees. *Human Reproduction*. <https://doi.org/10.1093/HUMREP/DEAC092>
- Yang, X., Zhai, B., Wang, S., Kong, X., Tan, Y., Liu, L., Yang, X., Tan, T., Zhang, S., & Zhang, L. (2021). RNA-DNA hybrids regulate meiotic recombination. *Cell Reports*, 37(10). <https://doi.org/10.1016/J.CELREP.2021.110097>
- Yasuhara, T., Kato, R., Hagiwara, Y., Shiotani, B., Yamauchi, M., Nakada, S., Shibata, A., & Miyagawa, K. (2018). Human Rad52 Promotes XPG-Mediated R-loop Processing to Initiate Transcription-Associated Homologous Recombination Repair. *Cell*, 175(2), 558-570.e11. <https://doi.org/10.1016/J.CELL.2018.08.056>
- Youds, J. L., & Boulton, S. J. (2011). The choice in meiosis – defining the factors that influence crossover or non-crossover formation. *Journal of Cell Science*, 124(4), 501–513. <https://doi.org/10.1242/JCS.074427>
- Zakharyevich, K., Tang, S., Ma, Y., & Hunter, N. (2012). Delineation of joint molecule resolution pathways in meiosis identifies a crossover-specific resolvase. *Cell*, 149(2), 334. <https://doi.org/10.1016/J.CELL.2012.03.023>

Outlook

- Absmeier, E., Becke, C., Wollenhaupt, J., Santos, K. F., & Wahl, M. C. (2017). Interplay of cis- and trans-regulatory mechanisms in the spliceosomal RNA helicase Brr2. *Cell Cycle (Georgetown, Tex.)*, *16*(1), 100–112. <https://doi.org/10.1080/15384101.2016.1255384>
- Allers, T., & Lichten, M. (2001). Differential timing and control of noncrossover and crossover recombination during meiosis. *Cell*, *106*(1), 47–57. [https://doi.org/10.1016/S0092-8674\(01\)00416-0](https://doi.org/10.1016/S0092-8674(01)00416-0)
- Bell, G. (1982). *MASTERPIECE OF NATURE: the evolution and genetics of sexuality*. ROUTLEDGE. <https://www.routledge.com/The-Masterpiece-of-Nature-The-Evolution-and-Genetics-of-Sexuality/Bell/p/book/9780367339272>
- Bizard, A. H., & Hickson, I. D. (2014). The dissolution of double Holliday junctions. *Cold Spring Harbor Perspectives in Biology*, *6*(7). <https://doi.org/10.1101/CSHPERSPECT.A016477>
- Boddy, M. N., Gaillard, P. H. L., McDonald, W. H., Shanahan, P., Yates, J. R., & Russell, P. (2001). Mus81-Eme1 are essential components of a Holliday junction resolvase. *Cell*, *107*(4), 537–548. [https://doi.org/10.1016/S0092-8674\(01\)00536-0](https://doi.org/10.1016/S0092-8674(01)00536-0)
- Boguslawski, S. J., Smith, D. E., Michalak, M. A., Mickelson, K. E., Yehle, C. O., Patterson, W. L., & Carrico, R. J. (1986). Characterization of monoclonal antibody to DNA.RNA and its application to immunodetection of hybrids. *Journal of Immunological Methods*, *89*(1), 123–130. [https://doi.org/10.1016/0022-1759\(86\)90040-2](https://doi.org/10.1016/0022-1759(86)90040-2)
- Borgogno, M. v., Monti, M. R., Zhao, W., Sung, P., Argarana, C. E., & Pezza, R. J. (2016). Tolerance of DNA Mismatches in Dmc1 Recombinase-mediated DNA Strand Exchange. *The Journal of Biological Chemistry*, *291*(10), 4928. <https://doi.org/10.1074/JBC.M115.704718>
- Brick, K., Pratto, F., & Camerini-Otero, R. D. (2020). After the break: DSB end processing in mouse meiosis. *Genes & Development*, *34*(11–12), 731. <https://doi.org/10.1101/GAD.339309.120>
- Cardoso da Silva, R., & Vader, G. (2021). Getting there: understanding the chromosomal recruitment of the AAA+ ATPase Pch2/TRIP13 during meiosis. *Current Genetics*, *67*(4), 553–565. <https://doi.org/10.1007/S00294-021-01166-3>
- Cejka, P., & Kowalczykowski, S. C. (2010). The full-length *Saccharomyces cerevisiae* Sgs1 protein is a vigorous DNA helicase that preferentially unwinds holliday junctions. *Journal of Biological Chemistry*, *285*(11), 8290–8301. <https://doi.org/10.1074/jbc.M109.083196>
- Cejka, P., Plank, J. L., Bachrati, C. Z., Hickson, I. D., & Kowalczykowski, S. C. (2010). Rmi1 stimulates decatenation of double Holliday junctions during dissolution by Sgs1-Top3.

Nature Structural and Molecular Biology, 17(11), 1377–1382.
<https://doi.org/10.1038/nsmb.1919>

- Chari, A., Haselbach, D., Kirves, J. M., Ohmer, J., Paknia, E., Fischer, N., Ganichkin, O., Möller, V., J Frye, J., Petzold, G., Jarvis, M., Tietzel, M., Grimm, C., Peters, J. M., Schulman, B. A., Tittmann, K., Markl, J., Fischer, U., & Stark, H. (2015). ProteoPlex: stability optimization of macromolecular complexes by sparse-matrix screening of chemical space. *Nature Methods* 2015 12:9, 12(9), 859–865. <https://doi.org/10.1038/nmeth.3493>
- Chen, C., Zhang, W., Timofejeva, L., Gerardin, Y., & Ma, H. (2005). The Arabidopsis ROCK-N-ROLLERS gene encodes a homolog of the yeast ATP-dependent DNA helicase MER3 and is required for normal meiotic crossover formation. *The Plant Journal: For Cell and Molecular Biology*, 43(3), 321–334. <https://doi.org/10.1111/J.1365-313X.2005.02461.X>
- Cheng, C. H., Lo, Y. H., Liang, S. S., Ti, S. C., Lin, F. M., Yeh, C. H., Huang, H. Y., & Wang, T. F. (2006). SUMO modifications control assembly of synaptonemal complex and polycomplex in meiosis of *Saccharomyces cerevisiae*. *Genes & Development*, 20(15), 2067–2081. <https://doi.org/10.1101/GAD.1430406>
- Cole, F., Kauppi, L., Lange, J., Roig, I., Wang, R., Keeney, S., & Jasin, M. (2012). Homeostatic control of recombination is implemented progressively in mouse meiosis. *Nature Cell Biology* 2012 14:4, 14(4), 424–430. <https://doi.org/10.1038/ncb2451>
- Costa, Y., & Cooke, H. J. (2007). Dissecting the mammalian synaptonemal complex using targeted mutations. *Chromosome Research*, 15(5), 579–589. <https://doi.org/10.1007/S10577-007-1142-1>
- D’Alessandro, G., Whelan, D. R., Howard, S. M., Vitelli, V., Renaudin, X., Adamowicz, M., Iannelli, F., Jones-Weinert, C. W., Lee, M. Y., Matti, V., Lee, W. T. C., Morten, M. J., Venkitaraman, A. R., Cejka, P., Rothenberg, E., & d’Adda di Fagagna, F. (2018). BRCA2 controls DNA:RNA hybrid level at DSBs by mediating RNase H2 recruitment. *Nature Communications* 2018 9:1, 9(1), 1–17. <https://doi.org/10.1038/s41467-018-07799-2>
- de los Santos, T., Hunter, N., Lee, C., Larkin, B., Loidl, J., & Hollingsworth, N. M. (2003). The Mus81/Mms4 endonuclease acts independently of double-Holliday junction resolution to promote a distinct subset of crossovers during meiosis in budding yeast. *Genetics*, 164(1), 81–94. <https://doi.org/10.1093/GENETICS/164.1.81>
- de Muyt, A., Jessop, L., Kolar, E., Sourirajan, A., Chen, J., Dayani, Y., & Lichten, M. (2012). BLM helicase ortholog Sgs1 is a central regulator of meiotic recombination intermediate metabolism. *Molecular Cell*, 46(1), 43. <https://doi.org/10.1016/J.MOLCEL.2012.02.020>
- de Muyt, A., Pyatnitskaya, A., Andréani, J., Ranjha, L., Ramus, C., Laureau, R., Fernandez-Vega, A., Holoch, D., Girard, E., Govin, J., Margueron, R., Couté, Y., Cejka, P., Guérois, R., & Borde, V. (2018). A meiotic XPF-ERCC1-like complex recognizes joint molecule

recombination intermediates to promote crossover formation.
<https://doi.org/10.1101/gad.308510.117>

- Drouaud, J., Khademian, H., Giraut, L., Zanni, V., Bellalou, S., Henderson, I. R., Falque, M., & Mézard, C. (2013). Contrasted Patterns of Crossover and Non-crossover at Arabidopsis thaliana Meiotic Recombination Hotspots. *PLOS Genetics*, 9(11), e1003922. <https://doi.org/10.1371/JOURNAL.PGEN.1003922>
- Duroc, Y., Kumar, R., Ranjha, L., line Adam, C., Gué rois, R., Md Muntaz, K., Marsolier-Kergoat, M.-C., Dingli, F., Ile Laureau, R., Loew, D., Llorente, B., Charbonnier, J.-B., Cejka, P., & rie Borde, V. (2017). *Concerted action of the MutLb heterodimer and Mer3 helicase regulates the global extent of meiotic gene conversion.* <https://doi.org/10.7554/eLife.21900.001>
- Egydio De Carvalho, C., & Colaiácovo, M. P. (2006). *SUMO-mediated regulation of synaptonemal complex formation during meiosis.* <https://doi.org/10.1101/gad.1457806>
- Fasching, C. L., Cejka, P., Kowalczykowski, S. C., & Heyer, W.-D. (2015). *Top3-Rmi1 dissolve Rad51-mediated D-loops by a topoisomerase-based mechanism.* <https://doi.org/10.1016/j.molcel.2015.01.022>
- Globus, S. T., & Keeney, S. (2012). The Joy of Six: How to Control Your Crossovers. *Cell*, 149(1), 11–12. <https://doi.org/10.1016/J.CELL.2012.03.011>
- Goldfarb, T., & Lichten, M. (2010). Frequent and efficient use of the sister chromatid for DNA double-strand break repair during budding yeast meiosis. *PLoS Biology*, 8(10). <https://doi.org/10.1371/JOURNAL.PBIO.1000520>
- Gravel, S., Chapman, J. R., Magill, C., & Jackson, S. P. (2008). DNA helicases Sgs1 and BLM promote DNA double-strand break resection. *Genes & Development*, 22(20), 2767–2772. <https://doi.org/10.1101/GAD.503108>
- Guillon, H., Baudat, F., Grey, C., Liskay, R. M., & de Massy, B. (2005). Crossover and Noncrossover Pathways in Mouse Meiosis. *Molecular Cell*, 20(4), 563–573. <https://doi.org/10.1016/J.MOLCEL.2005.09.021>
- Hassold, T., Hall, H., & Hunt, P. (2007). The origin of human aneuploidy: where we have been, where we are going. *Human Molecular Genetics*, 16 Spec No. 2(R2). <https://doi.org/10.1093/HMG/DDM243>
- Hodson, C., Low, J. K. K., van Twest, S., Jones, S. E., Swuec, P., Murphy, V., Tsukada, K., Fawkes, M., Bythell-Douglas, R., Davies, A., Holien, J. K., O'Rourke, J. J., Parker, B. L., Glaser, A., Parker, M. W., Mackay, J. P., Blackford, A. N., Costa, A., & Deans, A. J. (2022). Mechanism of Bloom syndrome complex assembly required for double Holliday junction dissolution and genome stability. *Proceedings of the National Academy of Sciences of the United*

States of America, 119(6).
https://doi.org/10.1073/PNAS.2109093119/SUPPL_FILE/PNAS.2109093119.SD01.XLSX

- Hollingsworth, N. M., & Brill, S. J. (2004). The Mus81 solution to resolution: generating meiotic crossovers without Holliday junctions. *Genes & Development*, 18(2), 117–125. <https://doi.org/10.1101/GAD.1165904>
- Hollingsworth, N. M., Ponte, L., & Halsey, C. (1995). MSH5, a novel MutS homolog, facilitates meiotic reciprocal recombination between homologs in *Saccharomyces cerevisiae* but not mismatch repair. *Genes and Development*, 9(14), 1728–1739. <https://doi.org/10.1101/gad.9.14.1728>
- Humphryes, N., & Hochwagen, A. (2014). A non-sister act: recombination template choice during meiosis. *Experimental Cell Research*, 329(1), 53–60. <https://doi.org/10.1016/J.YEXCR.2014.08.024>
- Hunter, N., & Kleckner, N. (2001). The single-end invasion: an asymmetric intermediate at the double-strand break to double-holliday junction transition of meiotic recombination. *Cell*, 106(1), 59–70. [https://doi.org/10.1016/S0092-8674\(01\)00430-5](https://doi.org/10.1016/S0092-8674(01)00430-5)
- Jeffreys, A. J., & May, C. A. (2004). Erratum: Intense and highly localized gene conversion activity in human meiotic crossover hot spots (*Nature Genetics* (2004) 36 (151-156)). *Nature Genetics*, 36(4), 427. <https://doi.org/10.1038/NG0404-427A>
- Jessop, L., Rockmill, B., Roeder, G. S., & Lichten, M. (2006). Meiotic chromosome synapsis-promoting proteins antagonize the anti-crossover activity of *sgs1*. *PLoS Genetics*, 2(9), 1402–1412. <https://doi.org/10.1371/journal.pgen.0020155>
- Jones, G. H., & Franklin, F. C. H. (2006). Meiotic crossing-over: obligation and interference. *Cell*, 126(2), 246–248. <https://doi.org/10.1016/J.CELL.2006.07.010>
- Kaur, H., DeMuyt, A., & Lichten, M. (2015). Top3-Rmi1 DNA single-strand decatenase is integral to the formation and resolution of meiotic recombination intermediates. *Molecular Cell*, 57(4), 583–594. <https://doi.org/10.1016/j.molcel.2015.01.020>
- Keeney, S. (2008). Spo11 and the Formation of DNA Double-Strand Breaks in Meiosis. *Genome Dynamics and Stability*, 2, 81–123. https://doi.org/10.1007/7050_2007_026
- Keskin, H., Shen, Y., Huang, F., Patel, M., Yang, T., Ashley, K., Mazin, A. v., & Storici, F. (2014). Transcript-RNA-templated DNA recombination and repair. *Nature*, 515(7527), 436–439. <https://doi.org/10.1038/NATURE13682>
- Kim, K. P., Weiner, B. M., Zhang, L., Jordan, A., Dekker, J., & Kleckner, N. (2010). Sister cohesion and structural axis components mediate homolog bias of meiotic recombination. *Cell*, 143(6), 924–937. <https://doi.org/10.1016/J.CELL.2010.11.015>

- Klein, F., Mahr, P., Galova, M., Buonomo, S. B. C., Michaelis, C., Nairz, K., & Nasmyth, K. (1999). A central role for cohesins in sister chromatid cohesion, formation of axial elements, and recombination during yeast meiosis. *Cell*, *98*(1), 91–103. [https://doi.org/10.1016/S0092-8674\(00\)80609-1](https://doi.org/10.1016/S0092-8674(00)80609-1)
- Kohl, K. P., & Sekelsky, J. (2013). Meiotic and Mitotic Recombination in Meiosis. *Genetics*, *194*(2), 327–334. <https://doi.org/10.1534/GENETICS.113.150581>
- Liu, S., Rauhut, R., Vornlocher, H. P., & Lührmann, R. (2006). The network of protein–protein interactions within the human U4/U6.U5 tri-snRNP. *RNA*, *12*(7), 1418. <https://doi.org/10.1261/RNA.55406>
- Lu, W. T., Hawley, B. R., Skalka, G. L., Baldock, R. A., Smith, E. M., Bader, A. S., Malewicz, M., Watts, F. Z., Wilczynska, A., & Bushell, M. (2018). Drosha drives the formation of DNA:RNA hybrids around DNA break sites to facilitate DNA repair. *Nature Communications* *2018 9:1*, *9*(1), 1–13. <https://doi.org/10.1038/s41467-018-02893-x>
- Lynn, A., Soucek, R., & Börner, G. V. (2007). ZMM proteins during meiosis: Crossover artists at work. In *Chromosome Research* (Vol. 15, Issue 5, pp. 591–605). <https://doi.org/10.1007/s10577-007-1150-1>
- Mancera, E., Bourgon, R., Brozzi, A., Huber, W., & Steinmetz, L. M. (2008). High-resolution mapping of meiotic crossovers and non-crossovers in yeast. *Nature*, *454*(7203), 479–485. <https://doi.org/10.1038/NATURE07135>
- Martini, E., Diaz, R. L., Hunter, N., & Keeney, S. (2006a). Crossover homeostasis in yeast meiosis. *Cell*, *126*(2), 285. <https://doi.org/10.1016/J.CELL.2006.05.044>
- Martini, E., Diaz, R. L., Hunter, N., & Keeney, S. (2006b). Crossover homeostasis in yeast meiosis. *Cell*, *126*(2), 285–295. <https://doi.org/10.1016/J.CELL.2006.05.044>
- Masson, J. Y., & West, S. C. (2001). The Rad51 and Dmc1 recombinases: a non-identical twin relationship. *Trends in Biochemical Sciences*, *26*(2), 131–136. [https://doi.org/10.1016/S0968-0004\(00\)01742-4](https://doi.org/10.1016/S0968-0004(00)01742-4)
- Mazina, O. M., Keskin, H., Hanamshet, K., Storici, F., & Mazin, A. v. (2017). Rad52 Inverse Strand Exchange Drives RNA-Templated DNA Double-Strand Break Repair. *Molecular Cell*, *67*(1), 19-29.e3. <https://doi.org/10.1016/J.MOLCEL.2017.05.019>
- Mazina, O. M., Mazin, A. v., Nakagawa, T., Kolodner, R. D., & Kowalczykowski, S. C. (2004). *Saccharomyces cerevisiae* Mer3 Helicase Stimulates 3-5 Heteroduplex Extension by Rad51: Implications for Crossover Control in Meiotic Recombination Division of Biological Sciences Sections of Microbiology and of Molecular Rad51 and Dmc1 proteins bind to the ssDNA tails to and Cellular Biology form filamentous nucleoprotein structures that

promote Center for Genetics and Development a search for homologous DNA (Hong et al junction blunt end 5-overhang, implying that the. In *Cell* (Vol. 117).

- McFarlane, R. J., Feichtinger, J., & Larcombe, L. (2014). Cancer germline gene activation. <https://doi.org/10.4161/Cc.29661>, 13(14), 2151–2152.
- McFarlane, R. J., Feichtinger, J., & Larcombe, L. (2015). Germline/meiotic genes in cancer: new dimensions. *Cell Cycle*, 14(6), 791. <https://doi.org/10.1080/15384101.2015.1010965>
- Mimitou, E. P., & Symington, L. S. (2008). Sae2, Exo1 and Sgs1 collaborate in DNA double-strand break processing. *Nature*, 455(7214), 770–774. <https://doi.org/10.1038/NATURE07312>
- Moore, D. P., & Orr-Weaver, T. L. (1998). Chromosome segregation during meiosis: building an unambivalent bivalent. *Current Topics in Developmental Biology*, 37(C), 263–299. [https://doi.org/10.1016/S0070-2153\(08\)60177-5](https://doi.org/10.1016/S0070-2153(08)60177-5)
- Nakagawa, T., Flores-Rozas, H., & Kolodner, R. D. (2001). The MER3 Helicase Involved in Meiotic Crossing Over Is Stimulated by Single-stranded DNA-binding Proteins and Unwinds DNA in the 3' to 5' Direction. *Journal of Biological Chemistry*, 276(34), 31487–31493. <https://doi.org/10.1074/jbc.M104003200>
- Nakagawa, T., & Kolodner, R. D. (2002). Saccharomyces cerevisiae Mer3 Is a DNA Helicase Involved in Meiotic Crossing Over. *Molecular and Cellular Biology*, 22(10), 3281–3291. <https://doi.org/10.1128/mcb.22.10.3281-3291.2002>
- Nakagawa, T., & Ogawa, H. (1999). The Saccharomyces cerevisiae MER3 gene, encoding a novel helicase-like protein, is required for crossover control in meiosis. *The EMBO Journal*, 18(20), 5714–5723. <https://doi.org/10.1093/EMBOJ/18.20.5714>
- Ohle, C., Tesorero, R., Schermann, G., Dobrev, N., Sinning, I., & Fischer, T. (2016). Transient RNA-DNA Hybrids Are Required for Efficient Double-Strand Break Repair. *Cell*, 167(4), 1001-1013.e7. <https://doi.org/10.1016/J.CELL.2016.10.001>
- Pena, V., Jovin, S. M., Fabrizio, P., Orlowski, J., Bujnicki, J. M., Lührmann, R., & Wahl, M. C. (2009). Common Design Principles in the Spliceosomal RNA Helicase Brr2 and in the Hel308 DNA Helicase. *Molecular Cell*, 35(4), 454–466. <https://doi.org/10.1016/j.molcel.2009.08.006>
- Perry, J., Kleckner, N., & Börner, G. V. (2005). Bioinformatic analyses implicate the collaborating meiotic crossover/chiasma proteins Zip2, Zip3, and Spo22/Zip4 in ubiquitin labeling. *Proceedings of the National Academy of Sciences of the United States of America*, 102(49), 17594–17599. <https://doi.org/10.1073/pnas.0508581102>

- Pyatnitskaya, A., Borde, V., & de Muyt, A. (2019). Crossing and zipping: molecular duties of the ZMM proteins in meiosis. In *Chromosoma* (Vol. 128, Issue 3, pp. 181–198). Springer Science and Business Media Deutschland GmbH. <https://doi.org/10.1007/s00412-019-00714-8>
- Roeder, G. S., & Bailis, J. M. (2000). The pachytene checkpoint. *Trends in Genetics : TIG*, *16*(9), 395–403. [https://doi.org/10.1016/S0168-9525\(00\)02080-1](https://doi.org/10.1016/S0168-9525(00)02080-1)
- Rosenberg, S. C., & Corbett, K. D. (2015). The multifaceted roles of the HORMA domain in cellular signaling. *Journal of Cell Biology*, *211*(4), 745–755. <https://doi.org/10.1083/JCB.201509076>
- Ross-Macdonald, P., & Roeder, G. S. (1994). Mutation of a meiosis-specific MutS homolog decreases crossing over but not mismatch correction. *Cell*, *79*(6), 1069–1080. [https://doi.org/10.1016/0092-8674\(94\)90037-X](https://doi.org/10.1016/0092-8674(94)90037-X)
- Rosu, S., Libuda, D. E., & Villeneuve, A. M. (2011). Robust crossover assurance and regulated interhomolog access maintain meiotic crossover number. *Science*, *334*(6060), 1286–1289. https://doi.org/10.1126/SCIENCE.1212424/SUPPL_FILE/ROSU.SOM.PDF
- Schwacha, A., & Kleckner, N. (1995). Identification of double Holliday junctions as intermediates in meiotic recombination. *Cell*, *83*(5), 783–791. [https://doi.org/10.1016/0092-8674\(95\)90191-4](https://doi.org/10.1016/0092-8674(95)90191-4)
- Shen, Y., Tang, D., Wang, K., Wang, M., Huang, J., Luo, W., Luo, Q., Hong, L., Li, M., & Cheng, Z. (2012). ZIP4 in homologous chromosome synapsis and crossover formation in rice meiosis. *Journal of Cell Science*, *125*(11), 2581–2591. <https://doi.org/10.1242/jcs.090993>
- Siller, S. (2001). Sexual selection and the maintenance of sex. *Nature* *2001* *411*:6838, *411*(6838), 689–692. <https://doi.org/10.1038/35079578>
- Snowden, T., Acharya, S., Butz, C., Berardini, M., & Fishel, R. (2004). hMSH4-hMSH5 recognizes Holliday Junctions and forms a meiosis-specific sliding clamp that embraces homologous chromosomes. *Molecular Cell*, *15*(3), 437–451. <https://doi.org/10.1016/J.MOLCEL.2004.06.040>
- Stark, H. (2010). GraFix: stabilization of fragile macromolecular complexes for single particle cryo-EM. *Methods in Enzymology*, *481*(C), 109–126. [https://doi.org/10.1016/S0076-6879\(10\)81005-5](https://doi.org/10.1016/S0076-6879(10)81005-5)
- Sym, M., Engebrecht, J. A., & Roeder, G. S. (1993). ZIP1 is a synaptonemal complex protein required for meiotic chromosome synapsis. *Cell*, *72*(3), 365–378. [https://doi.org/10.1016/0092-8674\(93\)90114-6](https://doi.org/10.1016/0092-8674(93)90114-6)

- Szostak, J. W., Orr-Weaver, T. L., Rothstein, R. J., & Stahl, F. W. (1983). The double-strand-break repair model for recombination. *Cell*, *33*(1), 25–35. [https://doi.org/10.1016/0092-8674\(83\)90331-8](https://doi.org/10.1016/0092-8674(83)90331-8)
- Tanaka, K., Miyamoto, N., Shouguchi-Miyata, J., & Ikeda, J. E. (2006). HFM1, the human homologue of yeast Mer3, encodes a putative DNA helicase expressed specifically in germ-line cells. *DNA Sequence : The Journal of DNA Sequencing and Mapping*, *17*(3), 242–246. <https://doi.org/10.1080/10425170600805433>
- Tang, D., Lv, M., Gao, Y., Cheng, H., Li, K., Xu, C., Geng, H., Li, G., Shan, Q., Wang, C., He, X., & Cao, Y. (2021). *Novel Variants in HFM1 Lead to Male Infertility Due to Non-obstructive Azoospermia*. <https://doi.org/10.21203/rs.3.rs-431339/v1>
- Tang, S., Wu, M. K. Y., Zhang, R., & Hunter, N. (2015). Pervasive and essential roles of the top3-rmi1 decatenase orchestrate recombination and facilitate chromosome segregation in meiosis. *Molecular Cell*, *57*(4), 607–621. <https://doi.org/10.1016/j.molcel.2015.01.021>
- Tock, A. J., & Henderson, I. R. (2018). Hotspots for Initiation of Meiotic Recombination. *Frontiers in Genetics*, *9*, 521. <https://doi.org/10.3389/FGENE.2018.00521/BIBTEX>
- Vader, G. (2015). Pch2(TRIP13): controlling cell division through regulation of HORMA domains. *Chromosoma*, *124*(3), 333–339. <https://doi.org/10.1007/S00412-015-0516-Y>
- van Nues, R. W., & Beggs, J. D. (2001). Functional contacts with a range of splicing proteins suggest a central role for Brr2p in the dynamic control of the order of events in spliceosomes of *Saccharomyces cerevisiae*. *Genetics*, *157*(4), 1451–1467. <https://doi.org/10.1093/GENETICS/157.4.1451>
- Vernekar, D. V., Reginato, G., Adam, C., Ranjha, L., Dingli, F., Marsolier, M. C., Loew, D., Gue´rois, R., Llorente, B., Cejka, P., & Borde, V. (2021). The Pif1 helicase is actively inhibited during meiotic recombination which restrains gene conversion tract length. *Nucleic Acids Research*, *49*(8), 4522–4533. <https://doi.org/10.1093/nar/gkab232>
- Villar-Fernández, M. A., da Silva, R. C., Firlej, M., Pan, D., Weir, E., Sarembe, A., Raina, V. B., Bange, T., Weir, J. R., & Vader, G. (2020). Biochemical and functional characterization of a meiosis-specific Pch2/ORC AAA+ assembly. *Life Science Alliance*, *3*(11). <https://doi.org/10.26508/LSA.201900630>
- Wang, J., Zhang, W., Jiang, H., & Wu, B.-L. (2014a). Mutations in HFM1 in Recessive Primary Ovarian Insufficiency . *New England Journal of Medicine*, *370*(10), 972–974. <https://doi.org/10.1056/NEJMC1310150>
- Wang, J., Zhang, W., Jiang, H., & Wu, B.-L. (2014b). Mutations in HFM1 in Recessive Primary Ovarian Insufficiency . *New England Journal of Medicine*, *370*(10), 972–974.

https://doi.org/10.1056/NEJMC1310150/SUPPL_FILE/NEJMC1310150_DISCLOSURES.PDF

- Wang, K., Tang, D., Wang, M., Lu, J., Yu, H., Liu, J., Qian, B., Gong, Z., Wang, X., Chen, J., Gu, M., & Cheng, Z. (2009). MER3 is required for normal meiotic crossover formation, but not for presynaptic alignment in rice. *Journal of Cell Science*, *122*(12), 2055–2063. <https://doi.org/10.1242/jcs.049080>
- Watanabe, Y., & Nurse, P. (1999). Cohesin Rec8 is required for reductional chromosome segregation at meiosis. *Nature*, *400*(6743), 461–464. <https://doi.org/10.1038/22774>
- Wijnker, E., James, G. V., Ding, J., Becker, F., Klasen, J. R., Rawat, V., Rowan, B. A., de Jong, D. F., de Snoo, C. B., Zapata, L., Huettel, B., de Jong, H., Ossowski, S., Weigel, D., Koornneef, M., Keurentjes, J. J. B., & Schneeberger, K. (2013). The genomic landscape of meiotic crossovers and gene conversions in *Arabidopsis thaliana*. *ELife*, *2013*(2). <https://doi.org/10.7554/ELIFE.01426>
- Xie, X., Murtaza, G., Li, Y., Zhou, J., Ye, J., Khan, R., Jiang, L., Khan, I., Zubair, M., Yin, H., Jiang, H., Liu, W., Shi, B., Hou, X., Gong, C., Fan, S., Wang, Y., Jiang, X., Zhang, Y., ... Shi, Q. (2022). Biallelic HFM1 variants cause non-obstructive azoospermia with meiotic arrest in humans by impairing crossover formation to varying degrees. *Human Reproduction*. <https://doi.org/10.1093/HUMREP/DEAC092>
- Yang, X., Zhai, B., Wang, S., Kong, X., Tan, Y., Liu, L., Yang, X., Tan, T., Zhang, S., & Zhang, L. (2021). RNA-DNA hybrids regulate meiotic recombination. *Cell Reports*, *37*(10). <https://doi.org/10.1016/J.CELREP.2021.110097>
- Yasuhara, T., Kato, R., Hagiwara, Y., Shiotani, B., Yamauchi, M., Nakada, S., Shibata, A., & Miyagawa, K. (2018). Human Rad52 Promotes XPG-Mediated R-loop Processing to Initiate Transcription-Associated Homologous Recombination Repair. *Cell*, *175*(2), 558–570.e11. <https://doi.org/10.1016/J.CELL.2018.08.056>
- Youds, J. L., & Boulton, S. J. (2011). The choice in meiosis – defining the factors that influence crossover or non-crossover formation. *Journal of Cell Science*, *124*(4), 501–513. <https://doi.org/10.1242/JCS.074427>
- Zakharyevich, K., Tang, S., Ma, Y., & Hunter, N. (2012). Delineation of joint molecule resolution pathways in meiosis identifies a crossover-specific resolvase. *Cell*, *149*(2), 334. <https://doi.org/10.1016/J.CELL.2012.03.023>